Bone regeneration based on growth factor releasing polymer composites

D.H.R. Kempen

The research in this thesis was financially supported by grants from The Netherlands Organization for Health Research and Development ZonMW (Agiko 920–03-325), Stichting Anna Fonds and the National Institutes of Health (R01-R45871, R01-AR45871 and R01-EB03060)

Printing of this thesis was financially supported by:

Anna Fonds
Arthrex Nederland B.V.
Astra Tech Benelux B.V.
Bauerfeind Benelux B.V.
Boehringer Ingelheim B.V.
George In der Maur orthopedische schoentechniek
J.E. Jurriaanse Stichting
Link Nederland
Livit Orthopedie
Mathys Orthopaedics B.V.
Nederlandse Orthopaedische Vereniging
Oudshoorn Chirurgische Techniek
Reumafonds
Synthes B.V.

ISBN: 978-90-39356524

Cover: Scanning electron microscopy image of polymer microspheres
Lay-out: with the assistance of Steven Janssen and Steven Kempen
Printed by: GVO drukkers & vormgevers B.V. | Ponsen & Looijen

Bone regeneration based on growth factor releasing polymer composites

Bot regeneratie door middel van groeifactor afgifte uit polymere composieten

(met een samenvatting in het Nederlands)

Proefschrift

ter verkrijging van de graad van doctor
aan de Universiteit Utrecht
op gezag van de rector magnificus, prof. dr. G.J. van der Zwaan,
ingevolge het besluit van het college voor promoties
in het openbaar te verdedigen op woensdag 26 oktober 2011
des middags te 2:30 uur

door

Diederik Hendrik Ruth Kempen
geboren op 12 april 1978 te Delft

Promotoren:	Prof. dr. W.J.A. Dhert
	Prof. dr. M.J. Yaszemski
Co-Promotoren:	Dr. L.B. Creemers
	Dr. L. Lu

This thesis is based upon the following publications:

Controlled release from poly(lactic-co-glycolic acid) microspheres embedded in an injectable, biodegradable scaffold for bone tissue engineering
DHR Kempen, CW Kim, L Lu, WJA Dhert, BL Currier, MJ Yaszemski
Materials Science Forum 2003;426-432: 3151-3156

Development of biodegradable poly(propylene fumarate)/poly(lactic-co-glycolic acid) blend microspheres. I. Preparation and characterization
DHR Kempen, L Lu, X Zhu, CW Kim, E Jabbari, WJA Dhert, BL Currier, MJ Yaszemski
Journal of Biomedical Materials Research 2004;70A: 283-292

Development of biodegradable poly(propylene fumarate)/poly(lactic-co-glycolic acid) blend microspheres. II. Controlled drug release and microsphere degradation
DHR Kempen, L Lu, X Zhu, CW Kim, E Jabbari, WJA Dhert, BL Currier, MJ Yaszemski
Journal of Biomedical Materials Research 2004;70A: 293-302

Controlled drug release from a novel injectable biodegradable microsphere/scaffold composite based on poly(propylene fumarate)
DHR Kempen, L Lu, CW Kim, X Zhu, WJA Dhert, BL Currier, MJ Yaszemski
Journal of Biomedical Material Research, 2006;77A: 103-111

The effect of autologous BMSC seeding and BMP-2 delivery on the ectopic bone formation in a microspheres/poly(propylene fumarate) composite
DHR Kempen, MC Kruyt, L Lu, CE Wilson, AV Florschutz, LB Creemers, MJ Yaszemski, WJA Dhert
Tissue Engineering Part A 2009:15:587-594

Non-invasive screening method for simultaneous evaluation of *in vivo* growth factor release profiles from multiple ectopic bone tissue engineering implants
DHR Kempen, L Lu, KL Classic, TE Hefferan, LB Creemers, A Maran, WJA Dhert, MJ Yaszemski
Journal of Controlled Release 2008:130(1):15-21

Non-invasive monitoring of BMP-2 retention and bone formation in composites for bone tissue engineering using SPECT-CT and scintillation probes
DHR Kempen, MJ Yaszemski, A Heijink, TE Hefferan, LB Creemers, J Britson, A Maran, KL Classic, WJA Dhert, L Lu
Journal of Controlled Release 2009:134:169-176

Retention of *in vitro* and *in vivo* BMP-2 bioactivity in sustained delivery vehicles for bone tissue engineering
DHR Kempen, L Lu, TE Hefferan, LB Creemers, A Maran, KL Classic, WJA Dhert, MJ Yaszemski
Biomaterials 2008:29:3245-3252

Growth factor interactions in bone regeneration
DHR Kempen, LB Creemers, JA Alblas, L Lu, AJ Verbout, MJ Yaszemski, WJA Dhert
Tissue Engineering Part B 2010:16:551-566

Effect of local sequential VEGF and BMP-2 delivery on ectopic and orthotopic bone regeneration
DHR Kempen, L Lu, A Heijink, TE Hefferan, LB Creemers, A Maran, MJ Yaszemski, WJA Dhert
Biomaterials 2008:29:3245-3252

Enhanced BMP-2 induced ectopic and orthotopic bone formation by intermittent PTH(1-34) administration
DHR Kempen, L Lu, TE Hefferan, LB Creemers, A Heijink, A Maran, WJA Dhert, MJ Yaszemski
Tissue Engineering Part A 2010:16:3769-3777

Table of contents

List of abbreviations

µCT	micro-computed tomography
ANOVA	analysis of variance
BAPO	bis(2,4,6-trimethylbenzoyl) phenylphosphine oxide
BMD	bone mineral density
BMP	bone morphogenetic protein
BMSC	bone marrow stromal cells
BP	benzoyl peroxide
CAD	computer-aided design
CFU	colony forming efficiency
CLSM	confocal laser-scanning microscope
DBM	demineralised bone matrix
ddH_2O	distilled, deionized water
DEXA	dual energy X-ray absorptiometry
DMEM	Dulbecco's modified eagle's medium
DMT	N,N dimethyl-p-toluidine
ELISA	enzyme-linked immunosorbent assay
FBS	fetal bovine serum
FGF	fibroblast growth factor
IGF	insulin-like growth factor
IL	interleukins
^{125}I	iodine-125 (radioisotope of iodine)
IPA	isopropanol
Mn	molecular weight
MSC	mesenchymal stem cell
Mw	molecular weight
MWCO	molecular weight cutoff
NVP	N-vinylpyrrolidone
PBS	phosphate-buffered saline
PDGF	platelet-derived growth factor
PI	polydispersity index
PLGA	poly(lactic-co-glycolic acid)
PPF	poly(propylene fumatate)
PRP	platelet rich plasma
PTH	parathyroid hormone
PVA	poly(vinyl alcohol)
R^2	squared correlation coefficient
SD	standard deviations
SEM	scanning electron microscopy
SPECT	single photon emission computed tomography
T½	half-life
TCA	trichloroacetic acid
TGF-β	transforming growth factor-β
TRD	Texas red dextran
VEGF	vascular endothelial growth factor
VOI	volume of interest
W1	internal aqueous phase
W2	external aqueous phase

1

Introduction

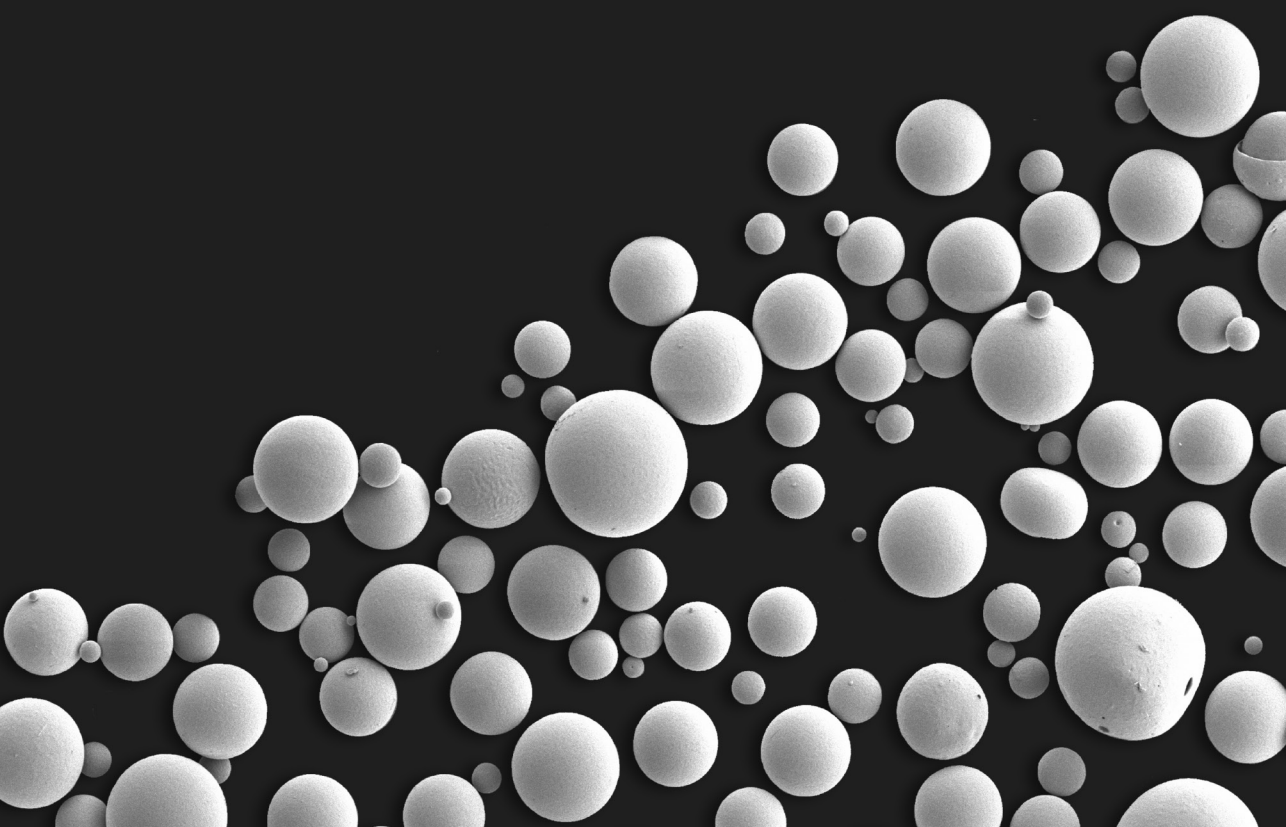

Bone is, after blood, the most commonly transplanted tissue worldwide. The diverse clinical needs for bone regeneration include application after resection of primary and metastatic tumors, bone loss after skeletal trauma, total joint arthroplasty with bone deficiency, spinal arthrodesis, and trabecular voids. To date, close to 2.2 million bone substitution procedures are performed worldwide each year and given our aging population, this number is expected to increase.[1] Autograft and allograft bone are the most frequently used grafts of biological origin and refer to transplantation of bone within the patient or from a donor patient, respectively. However, the weakness of autograft is its limited supply, donor site morbidity and difficulty to be modelled into desired shapes.[2,3] Allograft bone is more readily available than autograft, but has drawbacks including reduced rates of graft incorporation compared to autograft, and the possibility of pathogen transfer from donor to host.[4,5] These disadvantages of autograft and allograft treatments drive the quest for alternative methods to reconstruct large bone defects.

Bone regeneration based on the delivery of bioactive molecules is an emerging field within tissue engineering research, which has evolved tremendously over the past decades. The field was launched more than 4 decades ago by Dr. Marshall Urist who discovered that proteins embedded in the bone matrix can initiate a cellular response resulting in new bone formation when implanted at an ectopic site where bone would not normally form.[6-8] Although this observation was made in 1965, it took approximately 20 years before advances in molecular biology allowed the purification and subsequent cloning of the growth factors involved in bone regeneration.[9-11] Once advances in recombinant DNA technology made their efficient production possible, research started to focus on developing appropriate delivery systems and their clinical applications. So far, this has resulted in two commercially available growth factor-based products: bone morphogenetic protein-2 (BMP-2) and BMP-7. Whereas BMP-7 has received a humanitarian device exemption for revision posterolateral intertransverse lumbar spinal fusion and long bone nonunions, BMP-2 has received a humanitarian device exemption for posterolateral lumbar spine pseudarthrosis and FDA pre-market approval for use in anterior lumbar interbody fusions, acute open tibial shaft fractures and maxillofacial sinus and alveolar ridge augmentations.[12-17] Besides these approved applications, "off-label" use in various procedures has been reported with increased frequency.

Despite the clinical success of these currently available BMP-based products, concerns remain about the implantation of supraphysiological growth factor dosages which override the normal autoregulation of osteoinduction.[18,19] This might result in uncontrolled bony overgrowth. For example, ectopic bone formation extending outside the disc space into the spinal canal or neuroforamina was seen in patients treated with BMP-2 during posterior lumbar interbody fusion.[20,21] Although these cases did not lead to clinical problems, another study reported demanding revision surgery in 3 of 5 patients with similar treatments due to neural complaints caused by ectopic bone formation.[22] Other complications such as neck swelling, hematoma, dysphagia and respiratory problems have been reported with the use of BMP-2 in anterior cervical spinal fusion surgery which required re-operations in severe cases to relieve the symptoms.[23-28] Since these complications were observed less frequently when lower growth factor amounts were implanted, decrease of the BMP dose and improved local growth factor containment have been suggested as key issues to avoid them.[23,24,29]

Due to their local actions and short *in vivo* half-lives, delivery vehicles are required to locally deliver BMPs at the defect site. In current clinical applications, BMPs are locally delivered in collagen-based delivery vehicles. These delivery vehicles should retain the

growth factor for a sufficient period of time to allow migration of osteoprogenitor cells to the target site and elicit their differentiation into osteoblasts. However, animal studies have demonstrated that these collagen delivery vehicles exhibit a large initial BMP burst release with a rapid decline of the released growth factor amounts and a retention of less than 5% after 14 days of implantation.[30,31] Since it takes time before osteoprogenitor cells are migrated to the target site, release of the bulk of the BMPs in the early days of implantation suggests an inefficient use, as large amounts would be lost in the hematoma at the defect site. Furthermore, the rapid release by the collagen delivery vehicle may also be responsible for a significant early transient bone resorption when it is in contact with trabecular bone. The rapid release at the bone surface in contact with the delivery vehicle may create favorable conditions for an early osteoclastic reaction as it is known that BMP-2 stimulates osteoclast formation in a dose-dependent manner.[32,33] This problem was observed in several studies using a BMP-collagen implant in transforaminal lumbar interbody fusion procedures.[34-42] Depending on the resorption area, additional spinal stabilization, and/or patient's activity during the resorption phase, the bone resorption could potentially result in subsidence, loss of correction, graft dislodgment, and failure of spinal fusion. Unlike the collagen sponge, early transient bone resorption was not seen in a distal femoral core defect in nonhuman primates when a slower BMP-2 releasing calcium phosphate matrix was used as a delivery vehicle.[43]

In contrast to the rapid BMP release from the collagen-based delivery vehicles, the *in situ* expression profiles of BMPs known to be associated with ectopical osteoinduction (BMP-2, BMP-4, BMP-6 and BMP-7) show an up-regulation over a prolonged period of time that peaks at/after 21 days during normal bone healing (e.g. fracture healing).[44-46] From a biological point of view, this is not surprising since it takes time to recruit sufficient mesenchymal stem cells which can respond to the differentiation signal and be directed towards the osteoblastic lineage. Due to the short *in vivo* half-lives of the released BMPs, the early and rapidly released amounts will likely be lost in the defect hematoma and surroundings without being able to elicit a response in the target cells. Therefore, the site-specific pharmacological actions of BMPs may be improved by obtaining a release profile that coincides with the normal growth factor expression profile during fracture healing and normal rate of bone formation.

Although tailoring of the pharmacokinetic profile has become less difficult with the newly available drug delivery technologies, designing an appropriate delivery vehicle for BMPs remains complex due to the various biological, mechanical, pharmacological, toxicological and economical aspects associated with biomaterials in bone regeneration. Apart from its delivery role, the vehicle should also provide a biocompatible, biodegradable framework which supports cell adhesion, migration, proliferation, differentiation and ultimately bone formation. Despite the vast choice of materials available for growth factor delivery and bone regeneration, integrating this scaffold and delivery role into one single biomaterial remains challenging. Often, biomaterials appear promising from only one perspective and compromises have to be made with regard to other material characteristics. Furthermore, when the growth factor pharmacokinetics needs to be adjusted, it often requires structural changes to the scaffold matrix, which may also influence the scaffold properties and cell-scaffold interactions. Although the search for a single material with all ideal characteristics for bone regeneration will continue, another way to overcome the material problems is to focus on composite biomaterials, which combine different beneficial characteristics to meet the required design criteria. For example, micro-encapsulating of growth factors in polymeric materials is an effective way to control and tailor the

release profile of the contained substance. These polymer microspheres can be incorporated into a framework with good scaffold properties for bone regeneration, which has less favourable release characteristics. Furthermore, such a composite biomaterial would allow tailoring of the growth factor pharmacokinetics by altering the microsphere composition without having to make changes to the main scaffold material properties.
Apart from optimizing the site-specific pharmacological actions of an individual growth factor, composite biomaterials can also be used to study the effect of multiple growth factor release on the bone regeneration process. So far, most experimental and clinical studies focus on the BMPs with their potent osteoinductive activity. No matter how influential they appear during the process, these exogenously administered BMPs interact with several endogenously produced growth factors, cytokines and hormones to guide tissue formation towards bone. Although none of these molecules are osteoinductive like some BMPs, their chemotactic, angiogenic, mitogenic and/or cell differentiation-related effects have also shown to enhance the bone formation process with varying potency when administered individually. Due to their combined involvement in bone healing, mimicking the natural molecular coordination of the regeneration process by the combined exogenous growth factor administration might be more efficient. Composite biomaterials can play an important role in unravelling this molecular coordination as materials with different release characteristics can be combined to deliver multiple growth factors with different pharmacokinetic profiles. This would result in a better understanding of the actions and interactions of various growth factors and perhaps result in a more efficient use with fewer side effects during clinical applications.

Outline of the thesis

This thesis will focus on using polymeric composite orthopaedic biomaterials for controlled growth factor delivery and subsequent bone regeneration. The central aim of this thesis is to enhance bone formation by tailoring the local growth factor pharmacokinetic profile and investigating growth factor interactions. The three-dimensional biodegradable biomaterial plays a key role in bone regeneration as it provides a three-dimensional framework for tissue formation as well as a delivery vehicle for the release of growth factors and cytokines involved in the coordination of bone regeneration. **Chapter 2** is a literature overview of the different aspects involved in growth factor-based bone regeneration and provides a critical appraisal of the various material-, design- and pharmacokinetic characteristics of growth factor delivery vehicles.
The experimental studies in the first part of this thesis concentrated on the development of a polymeric composite, which can serve as a delivery vehicle for growth factors and a scaffold for bone formation. To avoid compromises in scaffold design and growth factor release, a growth factor delivery system based on polymeric microspheres was integrated into a polymer scaffold for bone regeneration. This would allow adjustment of the growth factor pharmacokinetics without the need to alter the scaffold material properties. In **chapters 3 and 4**, we developed new poly(propylene fumarate) (PPF) and PPF/poly(lactic-co-glycolic acid) (PLGA) blend microspheres and investigated the effects of various processing parameters on the microsphere characteristics and release profiles. **Chapter 5** studied the effect of PPF and PLGA microsphere incorporation on the release of Texas red dextran as a model drug and the mechanical properties of the microsphere/scaffold composite.

Since the composite development was performed using a model drug, the second part of this thesis focused on the release of the osteoinductive growth factor bone morphogenetic protein 2 (BMP-2) from polymeric composites. **Chapter 6** investigated the *in vitro* release of BMP-2 from PLGA microsphere incorporated in a PPF scaffold and subsequent *in vivo* bone forming capacity in combination with autologous bone marrow stromal cells (BMSCs) in a goat ectopic implantation model. Although the obtained *in vitro* release profiles provide valuable information on the growth factor binding capacity and retention/release mechanisms of the delivery vehicle, these data could not be extrapolated to the *in vivo* situation. Therefore, non-invasive screenings methods were required to study the *in vivo* pharmacokinetic profile of the composite. In **chapter 7**, a non-invasive screening method based on the detection of a radioactively labeled growth factor by scintillation probes was developed to evaluate *in vivo* growth factor release profiles of multiple implants in the same animal. The applicability of combined nuclear medicine (scintillation probes or single photon emission computed tomography (SPECT)) and radiological (computed tomography (CT)) techniques to monitor growth factor release profiles and subsequent effects on bone formation were studied in **chapter 8**. To investigate the effect of prolonged growth factor retention on the stability/bioactivity of the protein, **Chapter 9** assessed both the *in vitro* and *in vivo* stability of released BMP-2 from four different sustained delivery vehicles over time.

The third part of this thesis focused on growth factor interactions in bone regeneration. Before exploring these interactions, we first performed a literature study of the growth factor combinations that have been investigated in previous translational studies (**Chapter 10**). In this literature study, growth factor interactions of BMP with vascular endothelial growth factor (VEGF) and parathyroid hormone (PTH) gained our particular interest and were therefore chosen for our next studies. VEGF is a potent angiogenic growth factor inducing vessel formation, which could be important for the local recruitment of osteoprogenitor cells. **Chapter 11** investigated the effect of sequential VEGF and BMP release from a microsphere/PPF/gelatin composite on vessel and bone formation. PTH is one of the major systemic regulators of bone metabolism and its anabolic features upon intermittent administration have made it particularly appealing for the treatment of patients with osteoporosis. In **chapter 12**, effects of local release of BMP-2 from the polymer composite was studied in combination with intermittently administered PTH.

Finally, **chapter 13** discusses the current status and future perspective of clinical growth factor based bone regeneration therapies and **chapter 14** summarizes the results and conclusions of the studies performed for this thesis and their implications for future research.

References

1. Giannoudis, P.V., Einhorn, T.A., and Marsh, D. Fracture healing: a harmony of optimal biology and optimal fixation? Injury 38 Suppl 4, S1, 2007.
2. Damien, C.J., and Parsons, J.R. Bone graft and bone graft substitutes: a review of current technology and applications. J Appl Biomater 2, 187, 1991.
3. Gazdag, A.R., Lane, J.M., Glaser, D., and Forster, R.A. Alternatives to Autogenous Bone Graft: Efficacy and Indications. J Am Acad Orthop Surg 3, 1, 1995.
4. Buck, B.E., Malinin, T.I., and Brown, M.D. Bone transplantation and human immunodeficiency virus. An estimate of risk of acquired immunodeficiency syndrome (AIDS). Clin Orthop Relat Res, 129, 1989.
5. Norman-Taylor, F.H., and Villar, R.N. Bone allograft: a cause for concern? J Bone Joint Surg Br 79, 178, 1997.

6. Urist, M.R. Bone: formation by autoinduction. Science 150, 893, 1965.
7. Urist, M.R., Iwata, H., Ceccotti, P.L., Dorfman, R.L., Boyd, S.D., McDowell, R.M., and Chien, C. Bone morphogenesis in implants of insoluble bone gelatin. Proc Natl Acad Sci U S A 70, 3511, 1973.
8. Urist, M.R., Mikulski, A., and Lietze, A. Solubilized and insolubilized bone morphogenetic protein. Proc Natl Acad Sci U S A 76, 1828, 1979.
9. Sampath, T.K., and Reddi, A.H. Dissociative extraction and reconstitution of extracellular matrix components involved in local bone differentiation. Proc Natl Acad Sci U S A 78, 7599, 1981.
10. Wang, E.A., Rosen, V., Cordes, P., Hewick, R.M., Kriz, M.J., Luxenberg, D.P., Sibley, B.S., and Wozney, J.M. Purification and characterization of other distinct bone-inducing factors. Proc Natl Acad Sci U S A 85, 9484, 1988.
11. Wozney, J.M., Rosen, V., Celeste, A.J., Mitsock, L.M., Whitters, M.J., Kriz, R.W., Hewick, R.M., and Wang, E.A. Novel regulators of bone formation: molecular clones and activities. Science 242, 1528, 1988.
12. United States Food and Drug Administration Humanitarian Device Exemption INFUSE/MASTERGRAFT Posterolateral revision device for symptomatic, posterolateral lumbar spine pseudarthrosis. http://www.accessdata.fda.gov/cdrh_docs/pdf4/H040004b.pdf, 2008.
13. United States Food and Drug Administration Humanitarian Device Exemption OP-1 for recalcitrant long bone nonunions (H010002). http://www.accessdata.fda.gov/cdrh_docs/pdf/H010002b.pdf, 2001.
14. United States Food and Drug Administration Humanitarian Device Exemption OP-1 Putty for revision posterolateral (intertransverse) lumbar spinal fusion (H020008). http://www.accessdata.fda.gov/cdrh_docs/pdf2/H020008b.pdf, 2004.
15. United States Food and Drug Administration Premarket Approval Application INFUSE Bone Graft for acute, open tibial shaft fractures (P000054 & P050053). http://www.accessdata.fda.gov/cdrh_docs/pdf/P000054b.pdf, 2004.
16. United States Food and Drug Administration Premarket Approval Application INFUSE Bone Graft for sinus augmentations and localized alveolar ridge augmentations (P050053). http://www.accessdata.fda.gov/cdrh_docs/pdf5/P050053b.pdf, 2007.
17. United States Food and Drug Administration Premarket Approval Application INFUSE Bone Graft/LT-Cage Lumbar Tapered Fusion Device for anterior lumbar interbody fusion (P000058). http://www.accessdata.fda.gov/cdrh_docs/pdf/P000058b.pdf, 2002.
18. Benglis, D., Wang, M.Y., and Levi, A.D. A comprehensive review of the safety profile of bone morphogenetic protein in spine surgery. Neurosurgery 62, ONS423, 2008.
19. Poynton, A.R., and Lane, J.M. Safety profile for the clinical use of bone morphogenetic proteins in the spine. Spine (Phila Pa 1976) 27, S40, 2002.
20. Haid, R.W., Jr., Branch, C.L., Jr., Alexander, J.T., and Burkus, J.K. Posterior lumbar interbody fusion using recombinant human bone morphogenetic protein type 2 with cylindrical interbody cages. Spine J 4, 527, 2004.
21. McKay, B., and Sandhu, H.S. Use of recombinant human bone morphogenetic protein-2 in spinal fusion applications. Spine (Phila Pa 1976) 27, S66, 2002.
22. Wong, D.A., Kumar, A., Jatana, S., Ghiselli, G., and Wong, K. Neurologic impairment from ectopic bone in the lumbar canal: a potential complication of off-label PLIF/TLIF use of bone morphogenetic protein-2 (BMP-2). Spine J 8, 1011, 2008.
23. Baskin, D.S., Ryan, P., Sonntag, V., Westmark, R., and Widmayer, M.A. A prospective, randomized, controlled cervical fusion study using recombinant human bone morphogenetic protein-2 with the CORNERSTONE-SR allograft ring and the ATLANTIS anterior cervical plate. Spine (Phila Pa 1976) 28, 1219, 2003.
24. Boakye, M., Mummaneni, P.V., Garrett, M., Rodts, G., and Haid, R. Anterior cervical discectomy and fusion involving a polyetheretherketone spacer and bone morphogenetic protein. J Neurosurg Spine 2, 521, 2005.anman, T.H., and Hopkins, T.J. Early findings in a pilot study of anterior cervical interbody fusion in which recombinant human bone morphogenetic protein-2 was used with poly(L-lactide-co-D,L-lactide) bioabsorbable implants. Neurosurg Focus 16, E6, 2004.
25. Perri, B., Cooper, M., Lauryssen, C., and Anand, N. Adverse swelling associated with use of rh-BMP-2 in anterior cervical discectomy and fusion: a case study. Spine J 7, 235, 2007.
26. Shields, L.B., Raque, G.H., Glassman, S.D., Campbell, M., Vitaz, T., Harpring, J., and Shields, C.B. Adverse effects associated with high-dose recombinant human bone morphogenetic protein-2 use in anterior cervical spine fusion. Spine (Phila Pa 1976) 31, 542, 2006.

27. Smucker, J.D., Rhee, J.M., Singh, K., Yoon, S.T., and Heller, J.G. Increased swelling complications associated with off-label usage of rhBMP-2 in the anterior cervical spine. Spine (Phila Pa 1976) 31, 2813, 2006.
28. Dickerman, R.D., Reynolds, A.S., Morgan, B.C., Tompkins, J., Cattorini, J., and Bennett, M. rh-BMP-2 can be used safely in the cervical spine: dose and containment are the keys! Spine J 7, 508, 2007.
29. Committee for Medicinal Products for Human Use, E.M.A. scienfitic discussion for the approval of Osigraft. http://www.emea.europa.eu/humandocs/PDFs/EPAR/osigraft/039301en6.pdf, 2004.
30. Uludag, H., D'Augusta, D., Palmer, R., Timony, G., and Wozney, J. Characterization of rhBMP-2 pharmacokinetics implanted with biomaterial carriers in the rat ectopic model. J Biomed Mater Res 46, 193, 1999.
31. Miyaji, H., Sugaya, T., Kato, K., Kawamura, N., Tsuji, H., and Kawanami, M. Dentin resorption and cementum-like tissue formation by bone morphogenetic protein application. J Periodontal Res 41, 311, 2006.
32. Wutzl, A., Brozek, W., Lernbass, I., Rauner, M., Hofbauer, G., Schopper, C., Watzinger, F., Peterlik, M., and Pietschmann, P. Bone morphogenetic proteins 5 and 6 stimulate osteoclast generation. J Biomed Mater Res A 77, 75, 2006.
33. Burkus, J.K., Sandhu, H.S., Gornet, M.F., and Longley, M.C. Use of rhBMP-2 in combination with structural cortical allografts: clinical and radiographic outcomes in anterior lumbar spinal surgery. J Bone Joint Surg Am 87, 1205, 2005.
34. Hansen, S.M., and Sasso, R.C. Resorptive response of rhBMP2 simulating infection in an anterior lumbar interbody fusion with a femoral ring. J Spinal Disord Tech 19, 130, 2006.
35. Kuklo, T.R., Rosner, M.K., and Polly, D.W., Jr. Computerized tomography evaluation of a resorbable implant after transforaminal lumbar interbody fusion. Neurosurg Focus 16, E10, 2004.
36. Laursen, M., Hoy, K., Hansen, E.S., Gelineck, J., Christensen, F.B., and Bunger, C.E. Recombinant bone morphogenetic protein-7 as an intracorporal bone growth stimulator in unstable thoracolumbar burst fractures in humans: preliminary results. Eur Spine J 8, 485, 1999.
37. Lewandrowski, K.U., Nanson, C., and Calderon, R. Vertebral osteolysis after posterior interbody lumbar fusion with recombinant human bone morphogenetic protein 2: a report of five cases. Spine J 7, 609, 2007.
38. McClellan, J.W., Mulconrey, D.S., Forbes, R.J., and Fullmer, N. Vertebral bone resorption after transforaminal lumbar interbody fusion with bone morphogenetic protein (rhBMP-2). J Spinal Disord Tech 19, 483, 2006.
39. Pradhan, B.B., Bae, H.W., Dawson, E.G., Patel, V.V., and Delamarter, R.B. Graft resorption with the use of bone morphogenetic protein: lessons from anterior lumbar interbody fusion using femoral ring allografts and recombinant human bone morphogenetic protein-2. Spine (Phila Pa 1976) 31, E277, 2006.
40. Vaidya, R., Carp, J., Sethi, A., Bartol, S., Craig, J., and Les, C.M. Complications of anterior cervical discectomy and fusion using recombinant human bone morphogenetic protein-2. Eur Spine J 16, 1257, 2007.
41. Vaidya, R., Weir, R., Sethi, A., Meisterling, S., Hakeos, W., and Wybo, C.D. Interbody fusion with allograft and rhBMP-2 leads to consistent fusion but early subsidence. J Bone Joint Surg Br 89, 342, 2007.
42. Seeherman, H., and Wozney, J.M. Delivery of bone morphogenetic proteins for orthopedic tissue regeneration. Cytokine Growth Factor Rev 16, 329, 2005.
43. Cho, T.J., Gerstenfeld, L.C., and Einhorn, T.A. Differential temporal expression of members of the transforming growth factor beta superfamily during murine fracture healing. J Bone Miner Res 17, 513, 2002.
44. Groeneveld, E.H., and Burger, E.H. Bone morphogenetic proteins in human bone regeneration. Eur J Endocrinol 142, 9, 2000.
45. Niikura, T., Hak, D.J., and Reddi, A.H. Global gene profiling reveals a downregulation of BMP gene expression in experimental atrophic nonunions compared to standard healing fractures. J Orthop Res 24, 1463, 2006.

2

Growth factor delivery vehicles in bone regeneration

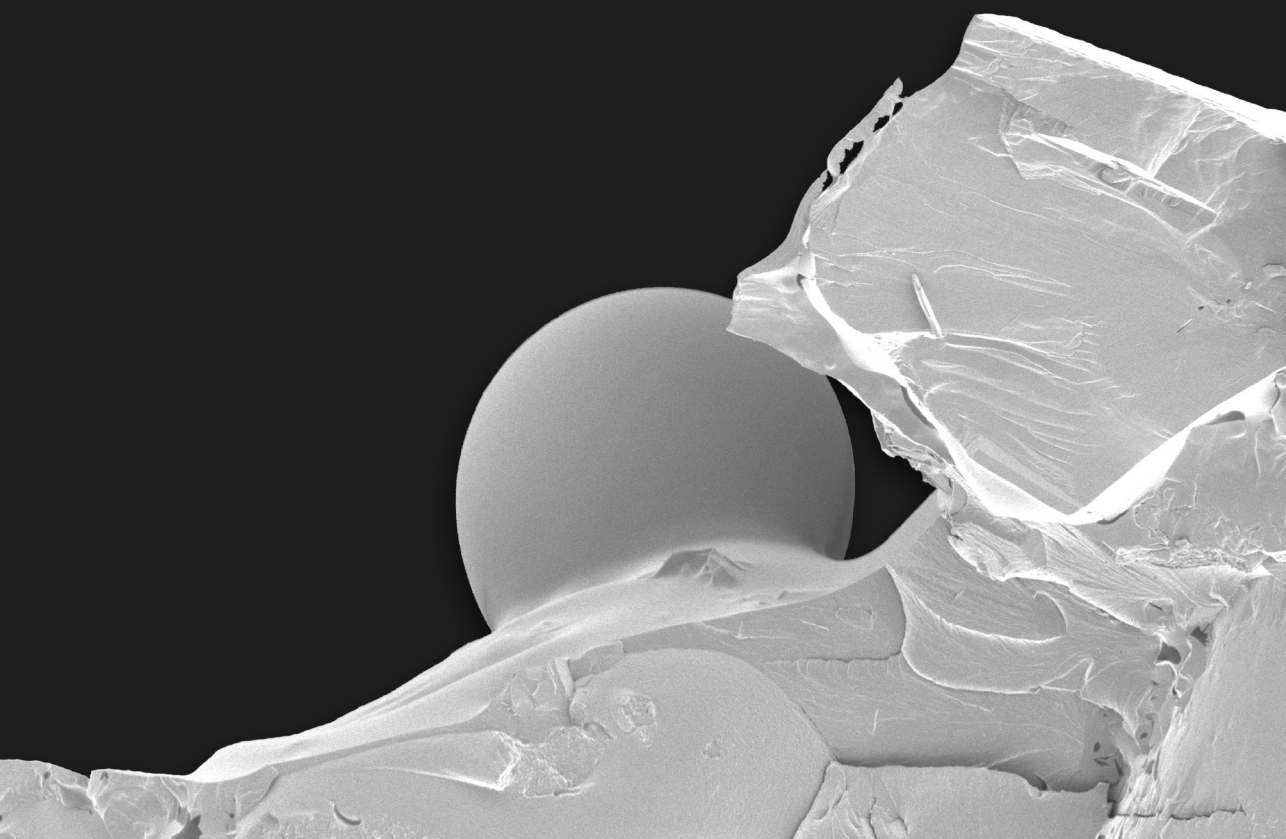

Bone healing

Bone has a tremendous capacity to heal itself, and with proper treatment, most fractures will heal without complication. Primary bone healing rarely occurs and refers to a direct re-establishment of the disrupted continuity without callus formation.[1] It only occurs when the fracture fragments are anatomically reduced and fixated rigidly. Under these conditions, the continuity can be re-established by new Haversian systems crossing the fracture line. The vast majority of bone injuries heal through secondary bone healing which involves the formation of callus.[1,2] The process starts with the formation of a haematoma and a subsequent inflammatory phase in which inflammatory and mesenchymal stem cells are recruited to the injured site. From this phase, it progresses through soft callus formation with the proliferation of osteo- and chondroprogenitor cells, to hard callus formation by intramembranous and endochondral ossification. This transition of soft callus into hard callus results in immature, woven bone, which is subsequently remodelled by osteoclasts and osteoblasts into lamellar bone.

Although the majority heals with proper treatment, some fractures have difficulty healing and result in delayed- or non-unions of the bone.[1] In general, these non-unions can be categorized into atrophic/avascular non-unions and hypertrophic/hypervascular non-unions. Motion at the fracture site due to insufficient fixation, inadequate immobilization or premature weight-bearing may prevent ossification of the callus and lead to hypertrophic non-unions. Since these non-unions maintain their healing potential, proper fracture fixation or immobilization is often sufficient for their treatment. An inadequate biologic reaction due to vascular problems, intermediate necrotic bone fragments, comorbidities or infection may lead to atrophic non-unions. Treatment of atrophic non-unions is more complex and requires debridement of intervening fibrous tissue, stimulation of the biological healing response and stabilization of the fracture fragments.

In contrast to the healing problems occurring in fracture healing, some large bone defects arising from tumor resection (figure 1), skeletal trauma, total joint arthroplasty (figure 2) or spinal fusion, do not stand a chance to heal at all. Even with an adequate biologic reaction, the distance that can be bridged during the normal bone healing process is limited. As a result, bone defects larger than their critical healing size will simply never heal at all.[3] This critical size varies between the different locations and may also be influenced by several patient related factors such as comorbidities and smoking. To enhance healing of these critical size defects, enhancement of the biological healing response is required.

Enhancement of bone regeneration

Enhancement of the bone healing response targets three essential elements of the regeneration process: (1) osteoconduction, (2) osteoinduction and (3) osteogenesis.[4-6] Living osteoprogenitor cells represent the 'osteogenic' potential during the healing process since they are responsible for the bone formation. Osteoinduction is the stimulation of mesenchymal stem cells, which are not committed to the osteogenic lineage to differentiate towards osteoprogenitor cells and bone forming osteoblasts. This process is initiated by 'osteoinductive' growth factors, amongst which some members of the bone morphogenetic protein family belong. The ability to initiate osteogenic differentiation is also recognized for some biomaterials. Osteoconduction refers to the ability of a material or graft to allow spreading of bone tissue from the recipient bed over its surface.

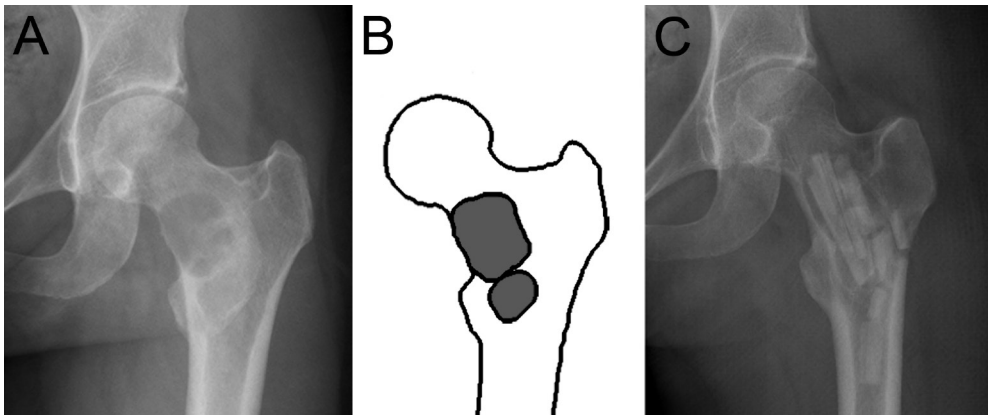

Figure 1: (A) AP-radiograph of left hip showing a central, lytic bone lesion consistent with fibrous dysplasia filling the femoral neck. (B) Schematic drawing of the proximal femur with the location of the lytic bone lesion marked in grey. (C) Radiograph after surgical treatment consisting of curettage and filling of the bone defect with cortical allograft. (courtesy of Dr. I.C.M. van der Geest, UMC St. Radboud)

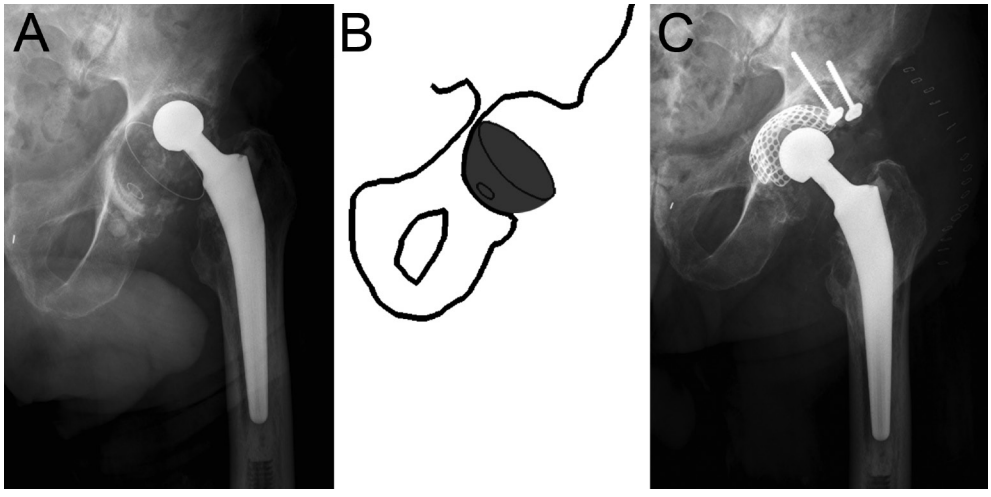

Figure 2: (A) AP-radiograph of left hip showing loosening of the cup of a total hip prosthesis with migration of the cup. (B) Schematic drawing of the acetabulum with the rotated cup position shown in grey. (C) Radiograph after surgical treatment. The upper rim of the acetabulum was reconstructed with a structural allograft and the rest of the acetabulum was reconstructed with a mesh and impacted cancelous allograft. A new cup was cemented into the reconstructed acetabulum. (courtesy of Drs. L.N. Marting, Antonius Ziekenhuis)

Over the past decades, several grafting materials have been used to reconstruct large bone defects. Autograft is considered the "gold standard" graft material and provides all three essential elements to enhance the healing response.[7] Mesenchymal stem cells and osteoprogenitor cells within an autograft may survive during the transplantation

procedure and could potentially proliferate and differentiate into osteoblasts. The bone matrix forms an excellent osteoconductive scaffold for ingrowth of new bone from the surrounding. Furthermore, the hematoma and graft matrix contains various chemotactic, mitogenic, angiogenic and osteoinductive proteins including bone morphogenetic proteins (BMPs), transforming growth factor-beta (TGF-β), fibroblast growth factor (FGF), insulin-like growth factor (IGF), vascular endothelial growth factor (VEGF), platelet-derived growth factor (PDGF) and interleukins (IL).[8,9] Transplanted cells that do not survive due to their large distance from the nutrient supplying capillary bed become hypoxic or apoptotic which also result in the production of growth factors and cytokines (e.g. hypoxia induced factor). These proteins stimulate angiogenesis or cell migration, proliferation and differentiation and direct tissue formation towards bone.[10]
Allograft is the second most commonly used graft material and can be used in fresh, frozen and freeze-dried form. Fresh allograft is no longer used clinically since it might initiate an immune response or transmit diseases.[11,12] To decrease the immunological response, allografts are processed and sterilized before use and therefore in most allografts there are no viable cells. The more aggressive this is done, the less intense the immunologic response will occur. Unfortunately, these processing conditions will also weaken the osteoinductive capabilities of the graft material. Consequently, allograft will provide an osteoconductive matrix with less osteoinductive potential and no osteogenic properties compared to autograft.

Bone tissue engineering strategies

Bone tissue engineering is a challenging field that strives to create alternative methods for current clinical treatments to restore bone defects. The principles of bone regeneration are commonly based on the three elements, consisting of: (1) an osteoconductive scaffold providing a framework for tissue formation, (2) growth factors involved in the molecular coordination of bone formation and (3) osteogenic cells responsible for the bone matrix deposition. Although all three elements are of vital importance during the regeneration process, research in this field can be subdivided into cell-based and growth factor-based strategies. Whereas cell-based strategies focus on the creation of hybrid constructs consisting of harvested cells seeded onto a specially developed scaffold, the growth factor-based strategies focus on the local recruitment of cells.
Mesenchymal stem cells (MSCs), which are capable to differentiate into osteoblasts, play a central role in cell-based strategies.[13] These MSCs can be seeded on osteoinductive biomaterials or scaffolds containing osteoinductive growth factors to guide their differentiation towards osteoblasts. Despite the advances in this field and increased knowledge of cellular behavior and material-cell interactions, the fate of these cells upon implantation of the hybrid construct remains uncertain. In order for these cells to survive *in vivo*, they require vascularization to provide oxygen and nutritional supply. Since the distance for sufficient nutrient supply by diffusion ranges from 100 µm to 5 mm, cells in the center of hybrid constructs with clinically applicable dimensions are unlikely to survive.[14,15] Consequently, these cells may only exhibit a "trophic effect" as a result of their secretion of growth factors and cytokines before apoptosis.[10]
In growth factor-based strategies, bioactive molecules are used for local recruitment of cells to the target site after implantation and induce their differentiation into osteoblasts.[16] In contrast to the cell-based strategies, such a strategy would obviate the logis-

tics and work required to harvest and culture-expand cells before re-implantation. Over the past decades, many growth factors and cytokines involved in the coordination of bone formation have been investigated in growth factor-based strategies and showed an enhancement of the bone regeneration process with varying potency and efficacy. Due to their short *in vivo* half-lives and site-specific actions, many of these bioactive peptides need to be locally delivered at the target site. Therefore, most of the research in this field is focused on developing appropriate delivery vehicles for the controlled release of growth factors.

Multifunctional role of the growth factor delivery vehicle

Shortly after the discovery of BMPs, it was already noticed that a delivery vehicle was essential to enhance the effect of the extracted growth factors. Although the administration of the protein extract itself was sufficient to induce ectopic bone, their reconstitution in a collagenous matrix or synthetic matrix enhanced its osteoinductive potential.[17,18] Also in fracture models, the effect of percutaneous injections of growth factor solutions remained limited to the first few days.[19,20] This limited efficacy of growth factors in fluids is not surprising since their *in vivo* half lives are short and retention at the target site is minimal.[21-25] Since normal bone formation occurs over a longer period of time, a delivery vehicle should retain the growth factor for sufficient time to allow migration of osteoprogenitor cells to the target site and generate their effect.
Apart from its role in retaining the growth factor at the target site and releasing it over a prolonged period of time, the delivery vehicle preferably also has a scaffold role.[26-30] As a scaffold, it should provide a three-dimensional, biocompatible, biodegradable framework to allow cell migration, proliferation and differentiation and serve as a template for extracellular bone matrix deposition. It should also maintain its volume for sufficient space for bone formation by resisting compression from surrounding soft tissue. In some cases, the mechanical strength of the matrix needs to be high enough to provide structural support to the original bony structure. Neither the degradation products nor the scaffold should be toxic or immunogenic and should be excreted through normal metabolic pathways. Furthermore, considerations should be given to the intended clinical use, which includes its cost-efficient production and handling properties for the surgeon. Beyond these essential scaffold demands, numerous other desirable scaffold properties have been described that may differ between the intended application.[27]

Materials

Many different materials have been tested as delivery vehicles for growth factor-assisted bone regeneration. In general, these materials can be grouped into 4 categories consisting of: 1) natural polymers, 2) synthetic polymers, 3) inorganic materials and 4) composites.

Natural polymers

Natural biodegradable polymers are those obtained from animal or plant sources and include collagen, gelatin, hyaluronans, chitosan and alginate. The majority of these poly-

mers are or are derived from proteins or polysaccharides extracted from the extracellular or cellular matrix in which they provide support, contribute to tissue hydrodynamics or interact with cells to regulate anchorage, migration and proliferation. Since normal human enzymes are able to metabolize many of these molecules, scaffolds from natural polymers often require cross-linking to improve their resistance against *in vivo* degradation.[31-33] This modification also improves the mechanical stability of the scaffold.[34] Natural polymer scaffolds absorb water in an aqueous environment and form hydrogels which provide a good physiological environment to support cell growth and facilitate the diffusion of nutrients from the surrounding tissue.[32,34,35] As materials for bone regeneration, their main advantages are their biocompatibility, biodegradability and abundant availability.[36-39] Despite these advantages, the sourcing, processing and possible immunogenicity of natural polymers due to animal and vegetable sourcing or cross-linking remains a concern for their use.[36,40]

Due to the thermic or chemical cross-linking conditions, growth factor solutions are often absorbed into the scaffold matrix after the production of the natural polymer hydrogels.[41-47] This post-manufacturing loading has the advantage that it is straightforward and allows the use of polymer processing conditions which might affect the bioactivity of the growth factor. Furthermore, no growth factor is wasted during the manufacturing process and delivery vehicles can be modulated before loading to further enhance cell functions. Despite these advantages, the limitation is that unbound proteins easily diffuse out of the scaffold matrix upon implantation, which can result a high initial burst release.[46-49]

As a delivery vehicle, natural polymers extend the retention of growth factors at the target site by absorption and electrostatic interactions. The electrostatic interactions may be achieved by using polymer chains with charges opposite to those of the incorporated growth factor.[46] Natural polymeric hydrogels usually have biphasic release profiles consisting of an initial burst phase and subsequent sustained release phase.[23,25,43,46-53] The initial burst is caused by a rapid diffusion of unbound growth factor from the hydrogel by the concentration gradient and ionic environmental changes upon implantation. During the second phase, the growth factors are released in a more sustained fashion, in the course of polymer matrix degradation. By adjusting the polymer cross-linking density and its subsequent degradation rate or by addition of sodium chondroitin sulphate, glutamic acid or citric acid, the burst release and sustained release of growth factors may be varied.[23,25,47,50]

As the major non-mineral component of bone, collagen is probably the most commonly used material for growth factor delivery. It can be derived from bovine and porcine bone, skin or tendon and used in its native form or as denatured gelatin. Collagen delivery vehicles are able to electrostatically bind bone growth factors. For example, at physiologic pH, a negatively charged 'acidic' gelatin was used as a delivery vehicle for positively charged basic fibroblast growth factor (bFGF).[46] Although collagen sponges and powders by themselves provide minimal structural support and function poorly as a graft material, their successful performance in combination with bone morphogenetic proteins in preclinical animal studies has been the primary basis for their clinical use as BMP delivery vehicles.[54-58] Nevertheless, animal-derived collagen may carry potential immunogenicity. Furthermore, animal studies have demonstrated that the clinically available collagen delivery vehicles have a large initial BMP burst release and a retention of less than 5% after 14 days of implantation.[48,59] Since it takes time before osteoprogenitor cells are migrated to the target site, release of the majority of the BMPs in the early days of implantation suggests an inefficient use of the implanted growth factor as large amounts will be lost in

the hematoma at the defect site. Therefore, new delivery vehicles with improved scaffold properties and release profiles that concur better with the rate of bone formation are still being developed.

Synthetic polymers

The majority of synthetic polymers studied for bone regeneration are biodegradable polyesters such as poly(lactic acid), poly(glycolic acid), poly(caprolactone), polyanhydrides, and polyphosphazenes.[26] They are attractive candidates for these applications because of their biocompatibility and degradation by hydrolysis into non-toxic products which can be eliminated or excreted through metabolic pathways.[60,61] Another advantage of synthetic polymers is the possibility of large scale production with well-controlled chemical and physical properties. Furthermore, they have great design flexibility as the polymer composition and structure can be tailored according to the needs. Many copolymers such as poly(lactic-co-glycolic acid), poly(lactide fumarate), poly(propylene fumarate), poly(caprolactone fumarate), poly(ethylene glycol fumarate) and oligo(poly(ethylene glycol) fumarate) have been synthesised and investigated as scaffolds for bone regeneration in an attempt to combine the different valuable characteristics of existing monomers or polymers.[62-68] Due to their different physical properties, the characteristics of synthetic polymer scaffolds vary greatly and range from hydrogels to mechanically strong porous matrices. Although many of these scaffolds appear promising for bone regeneration, synthetic polymers are not osteoinductive and their osteoconductive capacity varies between the different materials and scaffold designs. Extensive foreign body giant cell reactions also may be a disadvantage of some synthetic polymer carriers.

Many synthetic polymers have been studied as growth factor delivery vehicles for bone regeneration. Like natural polymers, synthetic materials can extend the retention of growth factors at the target site by physical absorption and electrostatic interactions.[69] However, since some hydrophobic synthetic polymers remain solid rather than becoming gelatinous in a physiologic environment, growth factors can also be physically entrapped in the polymer matrix.[16] As a result, the dense polymer network surrounding the growth factor prevents its rapid diffusion from the matrix upon immersion in an aqueous environment. This physical entrapment is only applicable when relatively mild scaffold manufacturing conditions are used that do not affect the bioactivity of the growth factor upon incorporation. From a release perspective, this physical entrapment provides additional options to extend the growth factor release. Apart from growth factor absorption and binding, scaffold design features such as macro- and micro-porosity can also be used to influence growth factor release as they dictate the diffusion distance of entrapped proteins from the scaffold matrix. However, since growth factors are exposed to the scaffold fabrication process, loss of growth factor bioactivity is one of the main risks of growth factor entrapment. Furthermore, all residual products after the incorporation process may contain the costly growth factors which may result in a low cost-efficiency of the final product.

Due to the diversity in physiochemical properties of synthetic polymers, growth factor release profiles depend on many factors and vary greatly. For example, polymer hydrophobicity/ hydrophilicity can influence growth factor diffusion from the scaffold as it determines water uptake and swelling ratio of the matrix. Also degradation mechanisms and rates influence the release of entrapped growth factors, as bulk degrading polymers like poly(lactic acid), poly(glycolic acid) will have different release characteristics compared to surface-eroding polymers such as polyanhydrides. Due to this variety of

polymer characteristics and the design flexibility of the scaffold, synthetic polymers are ideal candidates to tailor growth factor release.

Inorganic materials

Inorganic, non-metallic materials used for bone tissue engineering comprise ceramics and cements and can be composed of calcium phosphates, calcium sulfates or silicon dioxide-based bioactive glass. Due to their similarities to the bone mineral phase, these materials have a long history as implant material for bone substitution or reconstruction in clinical applications which already started at the end of the 19th century.[70] As the major non mineral component of bone, calcium phosphates as ceramics or cements are the focus of most research in this field. Compared to most polymers used for bone regeneration, they have excellent osteoconductive properties and are easier to sterilize without damaging the material. Furthermore, some calcium phosphate materials such as hydroxyapatite or biphasic calcium phosphate have shown to be osteoinductive when implanted in muscle tissue.[13,71-73] In general, ceramics and cements have a high compressive strength and resistance to deformation. Unfortunately, they tend to fail because of their brittle nature, which prevents their use in large weight-bearing orthopaedic applications. Another disadvantage is their variable resorption rate, which ranges from weeks to almost non-degradable in case of some sintered calcium phosphate-ceramics.[28,74] Despite their brittleness and variation in degradability, the osteoconductive and osteoinductive properties make these inorganic materials superior scaffold materials for bone regeneration, which has resulted in the approval of several calcium-phosphate products for filling bone defects in orthopaedic applications.[74]

The addition of growth factors to ceramic scaffolds or bioactive glasses is only possible through absorption after manufacturing. Due to the high sintering temperatures normally associated with their manufacturing or their derivation from natural materials (such as coral or bovine bone), entrapment of growth factors into their scaffold matrix is impossible. Since many of the sintered ceramics degrade slowly, release profiles of absorbed growth factors is mainly dictated by the binding affinity of the material.[74] Consequently, the ability to tailor the release in certain materials such as sintered ceramics is limited. Due to strong electrostatic interactions, irreversible binding or inactivation may also occur. For example, mineral-based carriers were found to irreversibly bind 5-10% of a BMP-2 dose.[75] Whether this irreversibly bound protein may still elicit a biological response is unknown. Sintered ceramics typical have a two-phase release profile consisting of an initial burst release of unbound protein and a subsequent sustained release depending on the binding affinity of the material.[48,76] In an attempt to tailor the release from calcium phosphate, scaffolds have been pre-treated with albumin to block the high affinity binding sites, prior to loading them with growth factor.[22] Although this effectively increased the *in vitro* release rate, no significant differences with non-pre-treated scaffolds were seen *in vivo*.[22]

In contrast to ceramics, growth factors can be entrapped in cements, thereby distributing them evenly throughout the calcium phosphate matrix. The relatively low setting temperature and mild precipitation reaction allow the addition of growth factors to the cement components or paste prior to the cementing reaction without risking damage to the protein.[77,78] This entrapment together with the high binding affinity of these materials may further prolong growth factor retention.[33,77] Although some of the growth factor may be released during the setting of the cement, the burst release of cements is less

high compared to the release of growth factors absorbed onto the surface of ceramics.[29] The subsequent sustained release is dictated by growth factor release through cellular resorption/degradation of the cement and diffusion through its micro/macroporous network.[74,78] Therefore, tailoring of the pharmacokinetic profiles from cements remains difficult.

Composites

Although some individual polymeric or ceramic materials appear promising as growth factor delivery vehicles in bone regeneration, no single material meets all the requirements of the ideal scaffold. Therefore, combinations of natural polymers, synthetic polymers and inorganic materials have been used to optimize the benefits offered by each of these materials. For example, the addition of synthetic polymers to ceramics may reduce their brittleness and their ability to tailor growth factor delivery from the composite. On the contrary, the addition of ceramics to polymer scaffolds may improve their compression resistance and biomimetic nature.

Pharmacokinetics

Since growth factors have a limited local retention ($T_{1/2}$ = 0.3 days for ectopically injected BMP-2[22]) and hence efficacy in enhancement of bone formation, the role of the delivery vehicle is to maintain their local concentration within the therapeutic window for a sufficient period of time to allow the migration of bone-forming cells to the area of injury for proliferation and differentiation. Although this seems straightforward, neither the therapeutic window of the growth factors nor the required timing and duration of their release are known. Consequently, a trial and error approach is used for the development of most growth factor delivery vehicles in which their success is usually determined by their *in vivo* osteoinductive capacity.

Over the past years, many new delivery vehicles for bone regeneration have been developed and tested in animal experimental models. Unfortunately, much of the published literature on carrier development only shows *in vitro* release profiles and is deficient in characterisation of *in vivo* pharmacokinetics. Although these *in vitro* profiles provide valuable information on the growth factor binding capacity and retention/release mechanisms of the material, these data cannot be extrapolated to the *in vivo* situation, as release profiles change significantly upon implantation.[22,24,78-80] Depending on the characteristics of the material, various differences could be responsible for these changes. For example, implant degradation may be significantly faster due to cellular and enzymatic actions *in vivo*, or desorption of bound growth factors may be enhanced by extracellular proteins or ionic changes. As the extent of these changes varies between delivery vehicles, characterization of the *in vivo* pharmacokinetic profile is necessary to make correlations between the release rate of the delivery vehicle and the efficacy in bone formation.

Over the past years, the *in vivo* pharmacokinetic profile from collagen-based delivery vehicles has been characterized best. Of the growth factors incorporated in these collagen delivery vehicles (including TGF-β1, bFGF, VEGF, PDGF-BB and IGF-I), the release of BMP has been studied most frequently.[25,43,46,47,49-51,79,81-85] Despite the use of various matrixes, such as suspensions, sponges, hydrogels and minipellets, all collagen-based delivery forms showed the characteristic bi-phasic profile. In general, BMP retention

in the absorbable collagen sponge was higher compared to a simple suspension.[29] For collagen sponges, the BMP pharmacokinetic profile was independent of most *in vitro* determined sponge properties.[53] However, the retention by the sponge was slightly increased by formaldehyde cross-linking and ethylene oxide sterilization.[43] Also in gelatin hydrogels, glutaraldehyde cross-linking elongated the degradation time and increased BMP retention.[25] BMP retention by collagen minipellets could be decreased by the addition of sodium chondroitin sulphate, glutamic acid or citric acid as they disturb the tight arrangement of the collagen fibers and thereby facilitate disintegration of the minipellets.[50,51]

In an attempt to correlate pharmacokinetic profiles to osteoinductive capacity, the release of BMP-2 was compared to plasmin-cleaved BMP-2 which removes the positively charged fraction of the N-terminus giving the protein a lower isoelectric point and thus a lower binding affinity to collagen.[49] The plasmin-cleaved BMP-2 displayed a greater *in vitro* activity than the native protein. However, when incorporated in a collagen sponge and implanted *in vivo*, the burst release of plasmin-cleaved protein was much faster and the osteoinductive capacity was significantly less. A similar observation was done comparing BMP-2 and BMP-4 for *in vivo* osteoinduction.[49,52] Although these BMPs are 92% identical and have similar *in vitro* specific activities, BMP-4 has a lower isoelectric point. *In vivo*, it was released significantly faster from demineralised bone matrix, PLGA and collagen and displayed a lower osteoinductive capacity compared to BMP-2.[49,52] Although both studies suggest that higher retention results in a higher osteoinductive activity, further investigation of the optimal pharmacokinetics using chemically or enzymatically modified BMPs is not possible due to possible effects on their osteoinductive activity.[49,52]

To further study the relationship between growth factor pharmacokinetics and biologic response, release profiles have been adjusted by changing the characteristics of the collagen-based delivery vehicle. Although these adjustments were shown to be effective to tailor growth factor release, the drawback of this approach is that these changes may also alter the scaffold properties and cell-scaffold interactions. For example, 2 studies showed that an increase in the crosslinking density of gelatin hydrogels resulted in a decreased hydrogel degradation time and an increased retention of BMP-2 and TGF-β at the target site.[25,47] Initially, BMP-2-induced osteocalcin in the ectopic ossicles and TGF-β-induced bone mineral density in calvarial defects increased with prolonged growth factor retentions. However, above a certain cross-linking density, osteoinductivity started to decrease and hydrogel residues increase. A possible explanation for this might be that the slower degrading gelatin hydrogel may physically impair bone formation due to the difficulty for cells to infiltrate into the densely cross-linked matrix.[25,47,86] Subsequently, the question remains whether the decreased osteoinductivity at higher protein retentions is the result of inappropriate pharmacokinetics or of physical impairment of bone regeneration due to scaffold properties such as hydrogel degradation/disintegration. The influence of scaffold properties on bone formation was clearly demonstrated in β-TCP/gelatin composites.[84] Whereas incorporation of β-TCP in hydrogels did not affect *in vivo* BMP-2 retention, ectopic osteoinduction decreased as the β-TCP content in the hydrogels increased. This negative influence of β-TCP incorporation was attributed to a decreased stability of the gelatin matrix, which facilitated scaffold deformation and resulted in a reduced pore space for bone ingrowth due to sponge collapse. Overall, these studies clearly demonstrate that correlating growth factor pharmacokinetics to bone formation remains difficult due to additional influences of scaffold characteristics on bone formation. However, when the pharmacokinetic profiles of delivery vehicles are similar, differences in bone

formation can be more clearly attributed to the scaffold characteristics.
Apart from collagen-based delivery vehicles, BMP pharmacokinetics from several other materials or composites have been studied, including hyaluronans, peptide-amphiphile nanofibers, polyglycolic acid, N-isopropylacrylamide-based polymers, biphasic calcium phosphate, calcium phosphate cements, natural hydroxyapatite or composite biomaterials.[21-24,48,52,76,78,80,87-89] Depending on the material or composite formulation, BMP-2 retention varied from 7 days to over 4 weeks. Although these studies provide detailed pharmacokinetic profiles of their delivery vehicles, comparison of the osteoinductive efficiency between the different studies remains impossible due to differences in BMP-2 dosages and the variation in outcome parameters for osteoinductivity. Despite all the research in this field, our knowledge of the therapeutic window and optimal duration of extensively studied growth factors such as BMPs remains limited.

Growth factor bioactivity

Since growth factors often require a complicated higher order of structure to bind and activate target receptors, changes in their conformation such as protein unfolding, cleavage, deamination or disulfide bond reduction may have a large impact on their biological function. Inside the body, growth factors are subjected to harsh physiologic factors such as proteolytic enzymes or low pH, which could lead to alterations in protein structure and their inactivation. Therefore, it is essential that they maintain their native conformation during the retention period. Delivery vehicles could assist in the stabilization of growth factors and subsequently extend their half-lives during the retention period. For example, growth factor binding or entrapment inside the matrix could protect it from enzymatic proteolysis. Furthermore, electrostatic interactions between the growth factor and matrix molecules could also help stabilizing it. In nature, similar interactions occur, for example by forming inactive complexes with binding proteins to extend their biologic half-lives (e.g. TGF-β or IGF).[90,91]
Despite these stabilizing effects of the delivery vehicles, exposure of growth factors to processing conditions during their fabrication or the carrier matrix itself could also result in structural changes and subsequent inactivation of the protein. For example, when alginate was used as delivery vehicle for TGF-β1, irreversible coacervates were formed which resulted in TGF-β1 inactivation. Therefore, polyanions had to be co-incorporated or the delivery vehicle had to be treated with HCl to prevent coacervate formation.[92] Apart from this inactivation by irreversible complexation, prolonged growth factor retention also carries the risk of protein denaturation or degradation over time. When BMP-2, bFGF and VEGF were retained in α-TCP ceramics, neutralized glass ceramics or glass ceramic/PLGA composite delivery vehicles, analysis of the eluted proteins on SDS-PAGE showed that they remained intact during the first couple of days.[93] However, the molecular weight of the released protein decreased dramatically after more than 3 days which could result loss of biologic activity as the protein degrades.
Since various aspects of growth factor delivery could affect their biological functions, the bioactivity of the released protein should be investigated for every newly developed delivery vehicle. *In vitro* assays are able to reliably detect and quantify loss of bioactivity over time. Release medium can be collected and added to cultures of responsive cells to study the growth factor's ability to elicit a biological response, either or not in combination with pharmacokinetic measurements.[80,94-96] Subsequently, the percentage of released

bioactive growth factor can be determined by comparing the biological response to the released growth factor to the response to similar concentrations of the freshly added growth factor.[80] These *in vitro* assays provide valuable information on their stability upon release and are ideal tools to study and compare the stabilizing capacity of different delivery matrices. However, extrapolating the *in vitro* data to the *in vivo* situation remains difficult, since certain *in vivo* biomechanical, physiological, cellular or enzymatic actions affecting growth factor stability cannot be mimicked in the *in vitro* situation.
So far, *in vivo* bioactivity assays such as ectopic and bone defect models have been used most commonly. Ideally, these bone defects should be critical-sized, meaning that they will not heal spontaneously during a defined period. In contrast to the bone defect models, ectopic models (e.g. intramuscular or subcutaneous) have the advantage that paired evaluation of different delivery vehicles is often possible and interfering mechanisms of bone formation are ruled out. Despite their close resemblance to the clinical situation, the use of these *in vivo* bioactivity assays also has drawbacks. In contrast to *in vitro* research, the quantification of the percentage of bioactive growth factor from the total released amount is impossible *in vivo*. Furthermore, the effect of retention time cannot be studied since *in vivo* bone formation may continue long after the growth factor is gone. For instance, Yamamoto et al demonstrated that, although all of the absorbed BMP-2 was released within 15 days from a 99.7% aqueous gelatin hydrogel, alkaline phosphatase activity continued to be elevated till at least 4 weeks post implantation.[25] Due to such a continuing biologic response, *in vivo* assays will never be able to immediately detect loss of growth factor bioactivity in delivery vehicles.
Few studies have focused on the effect of prolonged growth factor retention on protein bioactivity. So far, growth factors such as BMP-2 were shown to be released with preservation of bioactivity for at least 42, 48, 70 and 84 days from gelatin, hyaluronic acid, PLGA and composite delivery vehicles respectively.[80,94] For many of the newly developed delivery vehicles in bone regeneration, *in vitro* bioactivity assessment has mainly focused on the relatively short periods in which the incorporated growth factor is often released. Usually, this is only a small fraction and hence little is known on possible growth factor stabilizing effects of the vehicle matrix. For future comparison of the growth factor stability within the matrix of various materials, extension of these bioactivity assays over a longer period of time is needed.

Design considerations

The architecture of the delivery vehicle plays an important role in bone regeneration as it influences both cell behavior and growth factor release characteristics. To support the regeneration of bone, design features such as porosity, pore interconnectivity and surface texture are considered essential as they enhance cell infiltration and neovascularization into the defect from the surrounding tissue.[27,28,97] In the first generation of scaffold fabrication technologies, control over scaffold design was limited when using techniques such as solvent casting/particulate leaching, fiber bonding or gas-foaming techniques for scaffold fabrication.[98] Nowadays, computer aided design (CAD) and manufacturing techniques such as 3D printing or rapid prototyping technologies allow better control over scaffold design characteristics (figure 3).[98-101]
Despite these advances and the ability to control the design, there is still debate on the essential scaffold demands and therefore design criteria for scaffolds may vary sig-

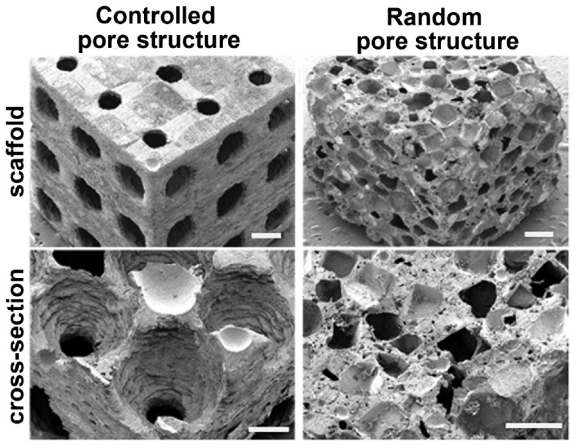

Figure 3: Scanning electron micrographs of scaffolds with controlled internal pore structures produced from computer-aided design (CAD) models using a solid freeform fabrication technique and scaffolds with random pore structures fabricated using a NaCl leaching technique. Scale bars represent 600 µm (top) and 500 µm (bottom). (courtesy of Dr. K.W. Lee[100], Mayo Clinic)

nificantly. For example, interconnected porosity is often mentioned as one of the main design criteria for the delivery vehicle since it dictates the space in which new bone tissue can be formed. However, one of the drawbacks of porous scaffolds is that a major part of the available pore space is often filled with fibrous tissue. Whether this is the result of faster migration of fibroblasts from the surrounding into the defect, or a lack of osteoinductive factors resulting in the cell differentiation towards fibroblasts is unknown. However, converting this fibrous tissue into bone is extremely difficult, if not impossible. To prevent this fibrous tissue formation, researchers also started to experiment with new strategies in which the degradation or resorption of non-porous materials is synchronized with the rate of bone formation.[22,80,102-104] Although some of these non-porous delivery vehicles appear promising, future studies will have to show whether these scaffolds perform better compared to a new generation of porous scaffolds with optimized scaffold design and growth factor pharmacokinetics to enhance the bone regeneration process.

Although the effects of scaffold design on bone formation can be investigated in the absence of growth factors in orthotopic defects, investigating the isolated effects of growth factor pharmacokinetics remains more difficult. Adjustments of the release profile often require changes to the delivery vehicle design or biomaterial composition. Since these changes may also influence the scaffold properties and cell-scaffold interactions, researchers have searched for solutions to independently tailor the release from the scaffold properties of the delivery vehicle. Therefore, composite delivery vehicles have been developed consisting of for example polymeric microspheres embedded into injectable polymeric or ceramic scaffolds.[22,80,83,88,102,105,106] For these delivery vehicles, materials with scaffold properties favourable for bone formation can be used as scaffold component while the growth factor-loaded microspheres serve as controlled delivery vehicles within the scaffold matrix. By tailoring the microsphere characteristics, the pharmacokinetic profile can be adjusted without negative effects on the scaffold matrix. These composite scaffolds may help to correlate growth factor release to bone formation in future studies

which is required to obtain more insight in the appropriate concentrations, timing and duration of a released growth factor in bone regeneration.

Combined growth factor delivery

So far, most of the research in growth factor based bone regeneration focuses on the release of a single growth factor. Although bone formation was enhanced by each of these proteins, bone regeneration will be the final result of a complex interplay between the applied factor and many more endogenously produced growth factors and cytokines. No matter how influential the applied growth factor may appear in the process, its action in isolation may have little effect without interactions with these endogenous factors. Moreover, as various growth factors and cytokines are involved simultaneously in natural bone healing, the combined addition of several factors is likely to be more effective in exogenous stimulation of the healing process. So far, several growth factor combinations have been studied by releasing them from relatively simple delivery vehicles with unknown or simultaneous growth factor release profiles (see Chapter 10[107]). Despite the simplicity of the delivery vehicles, many of the growth factor combinations already showed synergistic enhancements of bone formation compared to release of each individual growth factor.

As drug delivery technologies have improved over the past years, the ability to tailor growth factor release has also increased. This has resulted in delivery vehicles with complex release mechanisms such as dual, intermittent or sequential release of one or multiple growth factors. Many of these complex delivery vehicles are composed of 2 or more biomaterials with different release or degradation characteristics. For example, creation of a composite scaffold containing gelatin loaded VEGF and poly(lactic-co-glycolic acid) loaded BMP-2 resulted in dual release of the angiogenic growth factor at early time-points and a sustained release of the osteogenic growth factor over a prolonged period of time.[83,108,109] Dual release profiles of BMP-2 and dexamethasone or IGF-I were also obtained by using polymer microsphere mixtures or core-shell microspheres.[110-112] Multilayered delivery vehicles of alternating growth factor-loaded and non-loaded surface erodable polymeric materials were used to obtain an intermittent release of simvastatin or parathyroid hormone.[113-117] By alternating layers with different growth factors, these same multilayered delivery vehicles, a sequential alternating release of both molecules was achieved.[118] Although many of these advanced delivery vehicles are still under development, their early results appear promising for further investigation of the optimal ratio, timing and release sequence of growth factors in bone regeneration.

References

1. de Boer, P., Morgan, S.J., and van der Werken, C. AO Handbook: Orthopaedic Trauma Care. Stuttgart: Thieme, 2009.
2. McKibbin, B. The biology of fracture healing in long bones. J Bone Joint Surg Br 60-B, 150, 1978.
3. Einhorn, T.A. Clinically applied models of bone regeneration in tissue engineering research. Clin Orthop Relat Res, S59, 1999.
4. Cypher, T.J., and Grossman, J.P. Biological principles of bone graft healing. J Foot Ankle Surg 35, 413, 1996.
5. Giannoudis, P.V., Dinopoulos, H., and Tsiridis, E. Bone substitutes: an update. Injury 36 Suppl 3, S20, 2005.

6. Lind, M., and Bunger, C. Factors stimulating bone formation. Eur Spine J 10 Suppl 2, S102, 2001.
7. Bauer, T.W., and Muschler, G.F. Bone graft materials. An overview of the basic science. Clin Orthop Relat Res, 10, 2000.
8. Alsousou, J., Thompson, M., Hulley, P., Noble, A., and Willett, K. The biology of platelet-rich plasma and its application in trauma and orthopaedic surgery: a review of the literature. J Bone Joint Surg Br 91, 987, 2009.
9. Einhorn, T.A., Majeska, R.J., Rush, E.B., Levine, P.M., and Horowitz, M.C. The expression of cytokine activity by fracture callus. J Bone Miner Res 10, 1272, 1995.
10. Caplan, A.I., and Dennis, J.E. Mesenchymal stem cells as trophic mediators. J Cell Biochem 98, 1076, 2006.
11. De Long, W.G., Jr., Einhorn, T.A., Koval, K., McKee, M., Smith, W., Sanders, R., and Watson, T. Bone grafts and bone graft substitutes in orthopaedic trauma surgery. A critical analysis. J Bone Joint Surg Am 89, 649, 2007.
12. Keating, J.F., and McQueen, M.M. Substitutes for autologous bone graft in orthopaedic trauma. J Bone Joint Surg Br 83, 3, 2001.
13. Kruyt, M.C., Dhert, W.J., Oner, C., van Blitterswijk, C.A., Verbout, A.J., and de Bruijn, J.D. Optimization of bone-tissue engineering in goats. J Biomed Mater Res B Appl Biomater 69, 113, 2004.
14. Horner, H.A., and Urban, J.P. 2001 Volvo Award Winner in Basic Science Studies: Effect of nutrient supply on the viability of cells from the nucleus pulposus of the intervertebral disc. Spine (Phila Pa 1976) 26, 2543, 2001.
15. Ishaug-Riley, S.L., Crane, G.M., Gurlek, A., Miller, M.J., Yasko, A.W., Yaszemski, M.J., and Mikos, A.G. Ectopic bone formation by marrow stromal osteoblast transplantation using poly(DL-lactic-co-glycolic acid) foams implanted into the rat mesentery. J Biomed Mater Res 36, 1, 1997.
16. Luginbuehl, V., Meinel, L., Merkle, H.P., and Gander, B. Localized delivery of growth factors for bone repair. Eur J Pharm Biopharm 58, 197, 2004.
17. Sampath, T.K., and Reddi, A.H. Homology of bone-inductive proteins from human, monkey, bovine, and rat extracellular matrix. Proc Natl Acad Sci U S A 80, 6591, 1983.
18. Urist, M.R., Lietze, A., and Dawson, E. Beta-tricalcium phosphate delivery system for bone morphogenetic protein. Clin Orthop Relat Res, 277, 1984.
19. Blokhuis, T.J., den Boer, F.C., Bramer, J.A., Jenner, J.M., Bakker, F.C., Patka, P., and Haarman, H.J. Biomechanical and histological aspects of fracture healing, stimulated with osteogenic protein-1. Biomaterials 22, 725, 2001.
20. den Boer, F.C., Bramer, J.A., Blokhuis, T.J., Van Soest, E.J., Jenner, J.M., Patka, P., Bakker, F.C., Burger, E.H., and Haarman, H.J. Effect of recombinant human osteogenic protein-1 on the healing of a freshly closed diaphyseal fracture. Bone 31, 158, 2002.
21. Hosseinkhani, H., Hosseinkhani, M., Khademhosseini, A., and Kobayashi, H. Bone regeneration through controlled release of bone morphogenetic protein-2 from 3-D tissue engineered nanoscaffold. J Control Release 117, 380, 2007.
22. Ruhe, P.Q., Boerman, O.C., Russel, F.G., Mikos, A.G., Spauwen, P.H., and Jansen, J.A. *In vivo* release of rhBMP-2 loaded porous calcium phosphate cement pretreated with albumin. J Mater Sci Mater Med 17, 919, 2006.
23. Seeherman, H., Li, R., and Wozney, J. A review of preclinical program development for evaluating injectable carriers for osteogenic factors. J Bone Joint Surg Am 85-A Suppl 3, 96, 2003.
24. Woo, B.H., Fink, B.F., Page, R., Schrier, J.A., Jo, Y.W., Jiang, G., DeLuca, M., Vasconez, H.C., and DeLuca, P.P. Enhancement of bone growth by sustained delivery of recombinant human bone morphogenetic protein-2 in a polymeric matrix. Pharm Res 18, 1747, 2001.
25. Yamamoto, M., Takahashi, Y., and Tabata, Y. Controlled release by biodegradable hydrogels enhances the ectopic bone formation of bone morphogenetic protein. Biomaterials 24, 4375, 2003.
26. Agrawal, C.M., and Ray, R.B. Biodegradable polymeric scaffolds for musculoskeletal tissue engineering. J Biomed Mater Res 55, 141, 2001.
27. Brekke, J.H., and Toth, J.M. Principles of tissue engineering applied to programmable osteogenesis. J Biomed Mater Res 43, 380, 1998.
28. Khan, Y., Yaszemski, M.J., Mikos, A.G., and Laurencin, C.T. Tissue engineering of bone: material and matrix considerations. J Bone Joint Surg Am 90 Suppl 1, 36, 2008.
29. Seeherman, H., and Wozney, J.M. Delivery of bone morphogenetic proteins for orthopedic tissue regeneration. Cytokine Growth Factor Rev 16, 329, 2005.
30. Yaszemski, M.J., Payne, R.G., Hayes, W.C., Langer, R., and Mikos, A.G. Evolution of bone transplanta-

tion: molecular, cellular and tissue strategies to engineer human bone. Biomaterials 17, 175, 1996.
31. Jorge-Herrero, E., Fernandez, P., Turnay, J., Olmo, N., Calero, P., Garcia, R., Freile, I., and Castillo-Olivares, J.L. Influence of different chemical cross-linking treatments on the properties of bovine pericardium and collagen. Biomaterials 20, 539, 1999.
32. Malafaya, P.B., Silva, G.A., and Reis, R.L. Natural-origin polymers as carriers and scaffolds for biomolecules and cell delivery in tissue engineering applications. Adv Drug Deliv Rev 59, 207, 2007.
33. Seeherman, H., Wozney, J., and Li, R. Bone morphogenetic protein delivery systems. Spine 27, S16, 2002.
34. Geiger, M., Li, R.H., and Friess, W. Collagen sponges for bone regeneration with rhBMP-2. Adv Drug Deliv Rev 55, 1613, 2003.
35. Dang, J.M., and Leong, K.W. Natural polymers for gene delivery and tissue engineering. Adv Drug Deliv Rev 58, 487, 2006.
36. Keefe, J., Wauk, L., Chu, S., and DeLustro, F. Clinical use of injectable bovine collagen: a decade of experience. Clin Mater 9, 155, 1992.
37. Lee, C.H., Singla, A., and Lee, Y. Biomedical applications of collagen. Int J Pharm 221, 1, 2001.
38. Liao, Y.H., Jones, S.A., Forbes, B., Martin, G.P., and Brown, M.B. Hyaluronan: pharmaceutical characterization and drug delivery. Drug Deliv 12, 327, 2005.
39. Prabaharan, M. Review paper: chitosan derivatives as promising materials for controlled drug delivery. J Biomater Appl 23, 5, 2008.
40. United States Food and Drug Administration Premarket Approval Application INFUSE Bone Graft for acute, open tibial shaft fractures (P000054 & P050053). http://www.accessdata.fda.gov/cdrh_docs/pdf/P000054b.pdf, 2004.
41. Burkus, J.K., Transfeldt, E.E., Kitchel, S.H., Watkins, R.G., and Balderston, R.A. Clinical and radiographic outcomes of anterior lumbar interbody fusion using recombinant human bone morphogenetic protein-2. Spine 27, 2396, 2002.
42. Friedlaender, G.E., Perry, C.R., Cole, J.D., Cook, S.D., Cierny, G., Muschler, G.F., Zych, G.A., Calhoun, J.H., LaForte, A.J., and Yin, S. Osteogenic protein-1 (bone morphogenetic protein-7) in the treatment of tibial nonunions. J Bone Joint Surg Am 83-A Suppl 1, S151, 2001.
43. Friess, W., Uludag, H., Foskett, S., Biron, R., and Sargeant, C. Characterization of absorbable collagen sponges as rhBMP-2 carriers. Int J Pharm 187, 91, 1999.
44. Govender, S., Csimma, C., Genant, H.K., Valentin-Opran, A., Amit, Y., Arbel, R., Aro, H., Atar, D., Bishay, M., Borner, M.G., Chiron, P., Choong, P., Cinats, J., Courtenay, B., Feibel, R., Geulette, B., Gravel, C., Haas, N., Raschke, M., Hammacher, E., van der Velde, D., Hardy, P., Holt, M., Josten, C., Ketterl, R.L., Lindeque, B., Lob, G., Mathevon, H., McCoy, G., Marsh, D., Miller, R., Munting, E., Oevre, S., Nordsletten, L., Patel, A., Pohl, A., Rennie, W., Reynders, P., Rommens, P.M., Rondia, J., Rossouw, W.C., Daneel, P.J., Ruff, S., Ruter, A., Santavirta, S., Schildhauer, T.A., Gekle, C., Schnettler, R., Segal, D., Seiler, H., Snowdowne, R.B., Stapert, J., Taglang, G., Verdonk, R., Vogels, L., Weckbach, A., Wentzensen, A., and Wisniewski, T. Recombinant human bone morphogenetic protein-2 for treatment of open tibial fractures: a prospective, controlled, randomized study of four hundred and fifty patients. J Bone Joint Surg Am 84-A, 2123, 2002.
45. Vaccaro, A.R., Anderson, D.G., Patel, T., Fischgrund, J., Truumees, E., Herkowitz, H.N., Phillips, F., Hilibrand, A., Albert, T.J., Wetzel, T., and McCulloch, J.A. Comparison of OP-1 Putty (rhBMP-7) to iliac crest autograft for posterolateral lumbar arthrodesis: a minimum 2-year follow-up pilot study. Spine 30, 2709, 2005.
46. Yamamoto, M., Ikada, Y., and Tabata, Y. Controlled release of growth factors based on biodegradation of gelatin hydrogel. J Biomater Sci Polym Ed 12, 77, 2001.
47. Yamamoto, M., Tabata, Y., Hong, L., Miyamoto, S., Hashimoto, N., and Ikada, Y. Bone regeneration by transforming growth factor beta1 released from a biodegradable hydrogel. J Control Release 64, 133, 2000.
48. Uludag, H., D'Augusta, D., Palmer, R., Timony, G., and Wozney, J. Characterization of rhBMP-2 pharmacokinetics implanted with biomaterial carriers in the rat ectopic model. J Biomed Mater Res 46, 193, 1999.
49. Uludag, H., Gao, T., Porter, T.J., Friess, W., and Wozney, J.M. Delivery systems for BMPs: factors contributing to protein retention at an application site. J Bone Joint Surg Am 83-A Suppl 1, S128, 2001.
50. Maeda, H., Sano, A., and Fujioka, K. Controlled release of rhBMP-2 from collagen minipellet and the relationship between release profile and ectopic bone formation. Int J Pharm 275, 109, 2004.
51. Maeda, H., Sano, A., and Fujioka, K. Profile of rhBMP-2 release from collagen minipellet and induc-

tion of ectopic bone formation. Drug Dev Ind Pharm 30, 473, 2004.
52. Uludag, H., D'Augusta, D., Golden, J., Li, J., Timony, G., Riedel, R., and Wozney, J.M. Implantation of recombinant human bone morphogenetic proteins with biomaterial carriers: A correlation between protein pharmacokinetics and osteoinduction in the rat ectopic model. J Biomed Mater Res 50, 227, 2000.
53. Uludag, H., Friess, W., Williams, D., Porter, T., Timony, G., D'Augusta, D., Blake, C., Palmer, R., Biron, B., and Wozney, J. rhBMP-collagen sponges as osteoinductive devices: effects of *in vitro* sponge characteristics and protein pI on *in vivo* rhBMP pharmacokinetics. Ann N Y Acad Sci 875, 369, 1999.
54. Bostrom, M., Lane, J.M., Tomin, E., Browne, M., Berberian, W., Turek, T., Smith, J., Wozney, J., and Schildhauer, T. Use of bone morphogenetic protein-2 in the rabbit ulnar nonunion model. Clin Orthop Relat Res, 272, 1996.
55. Bouxsein, M.L., Turek, T.J., Blake, C.A., D'Augusta, D., Li, X., Stevens, M., Seeherman, H.J., and Wozney, J.M. Recombinant human bone morphogenetic protein-2 accelerates healing in a rabbit ulnar osteotomy model. J Bone Joint Surg Am 83-A, 1219, 2001.
56. Cook, S.D., Baffes, G.C., Wolfe, M.W., Sampath, T.K., Rueger, D.C., and Whitecloud, T.S., 3rd. The effect of recombinant human osteogenic protein-1 on healing of large segmental bone defects. J Bone Joint Surg Am 76, 827, 1994.
57. Cook, S.D., Wolfe, M.W., Salkeld, S.L., and Rueger, D.C. Effect of recombinant human osteogenic protein-1 on healing of segmental defects in non-human primates. J Bone Joint Surg Am 77, 734, 1995.
58. Hollinger, J.O., Schmitt, J.M., Buck, D.C., Shannon, R., Joh, S.P., Zegzula, H.D., and Wozney, J. Recombinant human bone morphogenetic protein-2 and collagen for bone regeneration. J Biomed Mater Res 43, 356, 1998.
59. United States Food and Drug Administration Humanitarian Device Exemption OP-1 Putty for revision posterolateral (intertransverse) lumbar spinal fusion (H020008). http://www.accessdata.fda.gov/cdrh_docs/pdf2/H020008b.pdf, 2004.
60. Gunatillake, P.A., and Adhikari, R. Biodegradable synthetic polymers for tissue engineering. Eur Cell Mater 5, 1, 2003.
61. Liu, X., and Ma, P.X. Polymeric scaffolds for bone tissue engineering. Ann Biomed Eng 32, 477, 2004.
62. Jabbari, E., and He, X. Synthesis and characterization of bioresorbable *in situ* crosslinkable ultra low molecular weight poly(lactide) macromer. J Mater Sci Mater Med 19, 311, 2008.
63. Jabbari, E., Wang, S., Lu, L., Gruetzmacher, J.A., Ameenuddin, S., Hefferan, T.E., Currier, B.L., Windebank, A.J., and Yaszemski, M.J. Synthesis, material properties, and biocompatibility of a novel self-cross-linkable poly(caprolactone fumarate) as an injectable tissue engineering scaffold. Biomacromolecules 6, 2503, 2005.
64. Shin, H., Quinten Ruhe, P., Mikos, A.G., and Jansen, J.A. *In vivo* bone and soft tissue response to injectable, biodegradable oligo(poly(ethylene glycol) fumarate) hydrogels. Biomaterials 24, 3201, 2003.
65. Tanahashi, K., Jo, S., and Mikos, A.G. Synthesis and characterization of biodegradable cationic poly(propylene fumarate-co-ethylene glycol) copolymer hydrogels modified with agmatine for enhanced cell adhesion. Biomacromolecules 3, 1030, 2002.
66. Tanahashi, K., and Mikos, A.G. Cell adhesion on poly(propylene fumarate-co-ethylene glycol) hydrogels. J Biomed Mater Res 62, 558, 2002.
67. Wang, S., Lu, L., Gruetzmacher, J.A., Currier, B.L., and Yaszemski, M.J. Synthesis and characterizations of biodegradable and crosslinkable poly(epsilon-caprolactone fumarate), poly(ethylene glycol fumarate), and their amphiphilic copolymer. Biomaterials 27, 832, 2006.
68. Wang, S., Lu, L., and Yaszemski, M.J. Bone-tissue-engineering material poly(propylene fumarate): correlation between molecular weight, chain dimensions, and physical properties. Biomacromolecules 7, 1976, 2006.
69. Schrier, J.A., and DeLuca, P.P. Recombinant human bone morphogenetic protein-2 binding and incorporation in PLGA microsphere delivery systems. Pharm Dev Technol 4, 611, 1999.
70. Peltier, L.F. The use of plaster of Paris to fill defects in bone. Clin Orthop 21, 1, 1961.
71. Geuze, R.E., Kruyt, M.C., Verbout, A.J., Alblas, J., and Dhert, W.J. Comparing various off-the-shelf methods for bone tissue engineering in a large-animal ectopic implantation model: bone marrow, allogeneic bone marrow stromal cells, and platelet gel. Tissue Eng Part A 14, 1435, 2008.
72. Kruyt, M.C., de Bruijn, J.D., Wilson, C.E., Oner, F.C., van Blitterswijk, C.A., Verbout, A.J., and Dhert, W.J. Viable osteogenic cells are obligatory for tissue-engineered ectopic bone formation in goats. Tissue Eng 9, 327, 2003.
73. Yuan, H., Fernandes, H., Habibovic, P., de Boer, J., Barradas, A.M., de Ruiter, A., Walsh, W.R., van Blitter-

swijk, C.A., and de Bruijn, J.D. Osteoinductive ceramics as a synthetic alternative to autologous bone grafting. Proc Natl Acad Sci U S A 107, 13614.
74. Habraken, W.J., Wolke, J.G., and Jansen, J.A. Ceramic composites as matrices and scaffolds for drug delivery in tissue engineering. Adv Drug Deliv Rev 59, 234, 2007.
75. Winn, S.R., Uludag, H., and Hollinger, J.O. Carrier systems for bone morphogenetic proteins. Clin Orthop Relat Res, S95, 1999.
76. Louis-Ugbo, J., Kim, H.S., Boden, S.D., Mayr, M.T., Li, R.C., Seeherman, H., D'Augusta, D., Blake, C., Jiao, A., and Peckham, S. Retention of 125I-labeled recombinant human bone morphogenetic protein-2 by biphasic calcium phosphate or a composite sponge in a rabbit posterolateral spine arthrodesis model. J Orthop Res 20, 1050, 2002.
77. Edwards, R.B., 3rd, Seeherman, H.J., Bogdanske, J.J., Devitt, J., Vanderby, R., Jr., and Markel, M.D. Percutaneous injection of recombinant human bone morphogenetic protein-2 in a calcium phosphate paste accelerates healing of a canine tibial osteotomy. J Bone Joint Surg Am 86-A, 1425, 2004.
78. Li, R.H., Bouxsein, M.L., Blake, C.A., D'Augusta, D., Kim, H., Li, X.J., Wozney, J.M., and Seeherman, H.J. rhBMP-2 injected in a calcium phosphate paste (alpha-BSM) accelerates healing in the rabbit ulnar osteotomy model. J Orthop Res 21, 997, 2003.
79. Hori, K., Sotozono, C., Hamuro, J., Yamasaki, K., Kimura, Y., Ozeki, M., Tabata, Y., and Kinoshita, S. Controlled-release of epidermal growth factor from cationized gelatin hydrogel enhances corneal epithelial wound healing. J Control Release, 2006.
80. Kempen, D.H., Lu, L., Hefferan, T.E., Creemers, L.B., Maran, A., Classic, K.L., Dhert, W.J., and Yaszemski, M.J. Retention of *in vitro* and *in vivo* BMP-2 bioactivities in sustained delivery vehicles for bone tissue engineering. Biomaterials 29, 3245, 2008.
81. Erickson, B.P., Pierce, A.R., Simpson, A.K., Nash, J., and Grauer, J.N. 125I-labeled OP-1 is locally retained in a rabbit lumbar fusion model. Clin Orthop Relat Res 466, 210, 2008.
82. Kanematsu, A., Yamamoto, S., Ozeki, M., Noguchi, T., Kanatani, I., Ogawa, O., and Tabata, Y. Collagenous matrices as release carriers of exogenous growth factors. Biomaterials 25, 4513, 2004.
83. Patel, Z.S., Yamamoto, M., Ueda, H., Tabata, Y., and Mikos, A.G. Biodegradable gelatin microparticles as delivery systems for the controlled release of bone morphogenetic protein-2. Acta Biomater 4, 1126, 2008.
84. Takahashi, Y., Yamamoto, M., and Tabata, Y. Enhanced osteoinduction by controlled release of bone morphogenetic protein-2 from biodegradable sponge composed of gelatin and beta-tricalcium phosphate. Biomaterials 26, 4856, 2005.
85. Takahashi, Y., Yamamoto, M., Yamada, K., Kawakami, O., and Tabata, Y. Skull bone regeneration in nonhuman primates by controlled release of bone morphogenetic protein-2 from a biodegradable hydrogel. Tissue Eng 13, 293, 2007.
86. Yamamoto, M., Kato, K., and Ikada, Y. Effect of the structure of bone morphogenetic protein carriers on ectopic bone regeneration. Tissue Eng 2, 315, 1996.
87. Gao, T., and Uludag, H. Effect of molecular weight of thermoreversible polymer on *in vivo* retention of rhBMP-2. J Biomed Mater Res 57, 92, 2001.
88. Ruhe, P.Q., Boerman, O.C., Russel, F.G., Spauwen, P.H., Mikos, A.G., and Jansen, J.A. Controlled release of rhBMP-2 loaded poly(dl-lactic-co-glycolic acid)/calcium phosphate cement composites *in vivo*. J Control Release 106, 162, 2005.
89. Yokota, S., Uchida, T., Kokubo, S., Aoyama, K., Fukushima, S., Nozaki, K., Takahashi, T., Fujimoto, R., Sonohara, R., Yoshida, M., Higuchi, S., Yokohama, S., and Sonobe, T. Release of recombinant human bone morphogenetic protein 2 from a newly developed carrier. Int J Pharm 251, 57, 2003.
90. Conover, C.A. Insulin-like growth factor-binding proteins and bone metabolism. Am J Physiol Endocrinol Metab 294, E10, 2008.
91. Lawrence, D.A. Latent-TGF-beta: an overview. Mol Cell Biochem 219, 163, 2001.
92. Mumper, R.J., Huffman, A.S., Puolakkainen, P.S., Bouchard, L.S., and Gombotz, W.R. Calcium-alginate beads for the oral delivery of transforming growth factor-β1 (TGF-β1): stabilization of TGF-β1 by the addition of polyacrylic acid within acid-treated beads. J Control Release 30, 241, 1994.
93. Ziegler, J., Mayr-Wohlfart, U., Kessler, S., Breitig, D., and Gunther, K.P. Adsorption and release properties of growth factors from biodegradable implants. J Biomed Mater Res 59, 422, 2002.
94. Kim, H.D., and Valentini, R.F. Retention and activity of BMP-2 in hyaluronic acid-based scaffolds *in vitro*. J Biomed Mater Res 59, 573, 2002.
95. Lu, L., Yaszemski, M.J., and Mikos, A.G. TGF-beta1 release from biodegradable polymer microparticles: its effects on marrow stromal osteoblast function. J Bone Joint Surg Am 83-A Suppl 1, S82, 2001.

96. Oldham, J.B., Lu, L., Zhu, X., Porter, B.D., Hefferan, T.E., Larson, D.R., Currier, B.L., Mikos, A.G., and Yaszemski, M.J. Biological activity of rhBMP-2 released from PLGA microspheres. J Biomech Eng 122, 289, 2000.
97. Langer, R., and Vacanti, J.P. Tissue engineering. Science 260, 920, 1993.
98. Sachlos, E., and Czernuszka, J.T. Making tissue engineering scaffolds work. Review: the application of solid freeform fabrication technology to the production of tissue engineering scaffolds. Eur Cell Mater 5, 29, 2003.
99. Fedorovich, N.E., Alblas, J., de Wijn, J.R., Hennink, W.E., Verbout, A.J., and Dhert, W.J. Hydrogels as extracellular matrices for skeletal tissue engineering: state-of-the-art and novel application in organ printing. Tissue Eng 13, 1905, 2007.
100. Lee, K.W., Wang, S., Dadsetan, M., Yaszemski, M.J., and Lu, L. Enhanced cell ingrowth and proliferation through three-dimensional nanocomposite scaffolds with controlled pore structures. Biomacromolecules 11, 682, 2010.
101. Lee, K.W., Wang, S., Lu, L., Jabbari, E., Currier, B.L., and Yaszemski, M.J. Fabrication and characterization of poly(propylene fumarate) scaffolds with controlled pore structures using 3-dimensional printing and injection molding. Tissue Eng 12, 2801, 2006.
102. Habraken, W.J., Wolke, J.G., Mikos, A.G., and Jansen, J.A. PLGA microsphere/calcium phosphate cement composites for tissue engineering: *in vitro* release and degradation characteristics. J Biomater Sci Polym Ed 19, 1171, 2008.
103. Seeherman, H.J., Azari, K., Bidic, S., Rogers, L., Li, X.J., Hollinger, J.O., and Wozney, J.M. rhBMP-2 delivered in a calcium phosphate cement accelerates bridging of critical-sized defects in rabbit radii. J Bone Joint Surg Am 88, 1553, 2006.
104. Simon, C.G., Jr., Khatri, C.A., Wight, S.A., and Wang, F.W. Preliminary report on the biocompatibility of a moldable, resorbable, composite bone graft consisting of calcium phosphate cement and poly(lactide-co-glycolide) microspheres. J Orthop Res 20, 473, 2002.
105. Hedberg, E.L., Tang, A., Crowther, R.S., Carney, D.H., and Mikos, A.G. Controlled release of an osteogenic peptide from injectable biodegradable polymeric composites. J Control Release 84, 137, 2002.
106. Patel, Z.S., Ueda, H., Yamamoto, M., Tabata, Y., and Mikos, A.G. *In vitro* and *in vivo* release of vascular endothelial growth factor from gelatin microparticles and biodegradable composite scaffolds. Pharm Res 25, 2370, 2008.
107. Kempen, D.H., Creemers, L.B., Alblas, J., Lu, L., Verbout, A.J., Yaszemski, M.J., and Dhert, W.J. Growth factor interactions in bone regeneration. Tissue Eng Part B Rev 16, 551, 2010.
108. Kempen, D.H., Lu, L., Heijink, A., Hefferan, T.E., Creemers, L.B., Maran, A., Yaszemski, M.J., and Dhert, W.J. Effect of local sequential VEGF and BMP-2 delivery on ectopic and orthotopic bone regeneration. Biomaterials 30, 2816, 2009.
109. Patel, Z.S., Young, S., Tabata, Y., Jansen, J.A., Wong, M.E., and Mikos, A.G. Dual delivery of an angiogenic and an osteogenic growth factor for bone regeneration in a critical size defect model. Bone, 2008.
110. Chen, F.M., Chen, R., Wang, X.J., Sun, H.H., and Wu, Z.F. *In vitro* cellular responses to scaffolds containing two microencapulated growth factors. Biomaterials 30, 5215, 2009.
111. Choi, D.H., Park, C.H., Kim, I.H., Chun, H.J., Park, K., and Han, D.K. Fabrication of core-shell microcapsules using PLGA and alginate for dual growth factor delivery system. J Control Release 147, 193, 2010.
112. Yilgor, P., Hasirci, N., and Hasirci, V. Sequential BMP-2/BMP-7 delivery from polyester nanocapsules. J Biomed Mater Res A 93, 528, 2010.
113. Jeon, J.H., Piepgrass, W.T., Lin, Y.L., Thomas, M.V., and Puleo, D.A. Localized intermittent delivery of simvastatin hydroxyacid stimulates bone formation in rats. J Periodontol 79, 1457, 2008.
114. Jeon, J.H., and Puleo, D.A. Formulations for intermittent release of parathyroid hormone (1-34) and local enhancement of osteoblast activities. Pharm Dev Technol 13, 505, 2008.
115. Jeon, J.H., Thomas, M.V., and Puleo, D.A. Bioerodible devices for intermittent release of simvastatin acid. Int J Pharm 340, 6, 2007.
116. Jiang, H.L., and Zhu, K.J. Pulsatile protein release from a laminated device comprising polyanhydrides and pH-sensitive complexes. Int J Pharm 194, 51, 2000.
117. Liu, X., Pettway, G.J., McCauley, L.K., and Ma, P.X. Pulsatile release of parathyroid hormone from an implantable delivery system. Biomaterials 28, 4124, 2007.
118. Jeon, J.H., and Puleo, D.A. Alternating release of different bioactive molecules from a complexation polymer system. Biomaterials 29, 3591, 2008.

3

Development of biodegradable PPF/PLGA blend microspheres Part 1: Preparation and characterization

Journal of Biomedical Materials Research 2004;70A:283-292

D.H.R. Kempen
L. Lu
X. Zhu
C. Kim
E. Jabbari
W.J.A. Dhert
B.L. Currier
M.J. Yaszemski

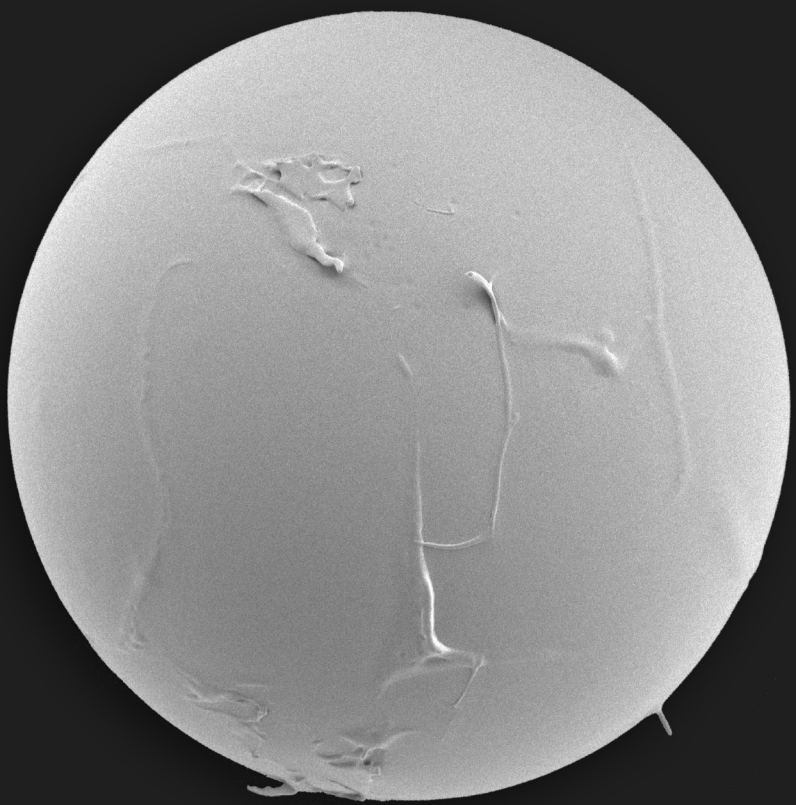

Abstract

We developed poly(propylene fumarate)/poly(lactic-co-glycolic acid) (PPF/PLGA) blend microspheres and investigated the effects of various processing parameters on the characteristics of these microspheres. The advantage of these blend microspheres is that the carbon-carbon double bonds along the PPF backbone could be used for their immobilization in a PPF scaffold. Microspheres containing the model drug Texas red dextran were fabricated using a double emulsion-solvent extraction technique. The effects of the following six processing parameters on the microsphere characteristics were investigated: PPF/PLGA ratio, polymer viscosity, vortex speed during emulsification, amount of internal aqueous phase, use of poly(vinyl alcohol) (PVA) in the internal aqueous phase, and PVA concentration in the external aqueous phase. Our results showed that the microsphere surface morphology was affected most by the viscosity of the polymer solution. Microspheres fabricated with a kinematic viscosity of 39 centistokes had a smooth, nonporous surface. In most microsphere formulations, the model drug was dispersed uniformly in the polymer matrix. For all fabricated formulations, the average microsphere diameter ranged between 19.0 and 76.9 μm. The external PVA concentration and vortex speed had most effect on the size distribution. Entrapment efficiencies varied from 60 to 98% and were most affected by the amount of internal aqueous phase, vortex speed and polymer viscosity. Overall, we demonstrated the ability to fabricate PPF/PLGA blend microspheres with similar surface morphology, entrapment efficiency and size distribution as conventional PLGA microspheres.

Introduction

Controlled release of bioactive molecules such as cytokines and growth factors has become an important aspect of tissue engineering because it allows modulation of cellular function and tissue formation at the afflicted site.[1] The encapsulation of drugs, proteins and other bioactive molecules within degradable materials has long been known to be an effective way to control the release profile of the contained substance. More recently, microencapsulation has been found to have similar effects, and has been used for the controlled delivery of these molecules. In the past, this technique was successfully applied to encapsulate growth factors such as transforming growth factor-β, bone morphogenetic protein-2 and basic fibroblast growth factor in poly(lactic-co-glycolic acid) (PLGA) microspheres.[2-8]

An injectable, *in situ* polymerizable, biodegradable poly(propylene fumarate) (PPF) scaffold for bone regeneration is under development in our laboratory.[9] PPF is a linear polyester that can be cross-linked through unsaturated double bonds along its backbone. The PPF scaffold can be shaped into the desired structure either in an *ex vivo* mold or *in situ*. PPF hardens within 5-15 minutes to attain mechanical properties similar to cancellous bone.[10] Because of the injectability of the formulation, the surgical intervention required for the implantation of this scaffold can be minimized. The addition of growth factors within the PPF scaffold results in a composite biomaterial that could serve both a structural and a drug-delivery role.

The most extensively studied bioabsorbable microsphere is made from PLGA. In a recent study PLGA microspheres were embedded in PPF scaffolds and successfully released the osteogenic peptide TP508.[11] However, these conventional PLGA microspheres could only be physically trapped in the PPF scaffold, and could move away from the scaffold site during degradation. Mechanical testing also showed that incorporation of PLGA microspheres resulted in decreased compressive modulus of the PPF-based scaffold.[12]

The objective of this work was to develop blend microspheres of PPF and PLGA. Because of the presence of carbon-carbon double bonds on the surface of microspheres containing PPF, these microspheres could be covalently bound to an injectable PPF scaffold. In addition to better immobilization, the interface covalent bonding between the microspheres and scaffold could lead to enhanced overall mechanical strength of the composite material. Because a wider range of properties affecting drug-release profiles and degradation time could be achieved by these blend microspheres, they could also be used alone as delivery vehicles. In this study we investigated the effects of various processing parameters on the microsphere characteristics including PPF/PLGA ratio, polymer viscosity, vortex speed during emulsification, internal aqueous phase volume, use of poly(vinyl alcohol) (PVA) in the internal aqueous phase, and PVA concentration in the external aqueous phase.

Materials and methods

Experimental design

We investigated the effects of six fabrication parameters on the microsphere characteristics. The following parameters investigated were: 1. PPF/PLGA ratio; 2. viscosity of polymer solutions; 3. vortex speed; 4. volume of the internal phase (W1 phase); 5. PVA

in internal water phase; and 6. PVA amount in external water phase. The microsphere characteristics evaluated were surface morphology, drug distribution, polymer blending, size distribution and entrapment efficiency of a model drug. The model drug Texas red dextran (TRD) (Molecular Probes, Leiden, The Netherlands) with a molecular weight of 40,000 Dalton was chosen for encapsulation because of its similar molecular weight to a bone morphogenetic protein. We also quantified the viscosity of polymer solutions used for microsphere fabrication.

The first part of the experiments was based on a Resolution III two-level factorial design (2_{III}^{6-3}) varying all six parameters.[13] High and low values were chosen based on our preliminary studies and published literature for each parameter, and these levels were combined according to the fractional factorial design to create eight composite formulations.[14] The values for all parameters are presented in Table 1. The effects of the six parameters on the surface morphology, the drug distribution, the drug entrapment efficiency and the size distribution of the microspheres were evaluated. The results from each experiment were examined to determine the main effects of each parameter on the measured property. The factorial design demonstrates the main effect of each parameter on the measured microparticle characteristic whereas minimizing the number of trails. This design does not confound main effects with one another but does confound main effects with two-factor interactions. Three experimental runs were performed and the results on main effects were reported as means ± standard errors.

The effects of PPF/PLGA ratio, polymer viscosity, vortex speed and the volume of the W1 phase were further investigated in the second part of this study by increasing the range of these parameters. The effect of the PPF/PLGA ratio in the fabrication process was investigated by keeping the amount of polymer at 250 mg per ml of dichloromethane. The values for the fixed parameters are indicated in Table 1 except for the viscosity, which was kept at approximately 39 centistokes (cSt). All measurements were performed in triplicates and the data were expressed as means ± standard deviations (SD).

Table 1

A. High and low levels for parameters in a resolution III two level fractional factorial design (2_{III}^{6-3})

Level	PPF/PLGA Ratio (%)	Polymer Viscosity[a] (cSt)	Vortex Speed[b]	W1 Volume (μL)	Internal PVA (%)	External PVA (%)
+	100/0	50	8	250	1	2[a]
-	50/50[a]	25	4[a]	50[a]	0[a]	0.2

B. Combinations of the Experimental Variables in the 2_{III}^{6-3} Fractional Factorial Design (n=3)

Formulation	PPF/PLGA Ratio	Polymer Viscosity	Vortex Speed	W1 Volume	Internal PVA	External PVA
1	+	+	+	+	+	+
2	+	+	-	+	-	-
3	+	-	+	-	+	-
4	+	-	-	-	-	+
5	-	+	+	-	-	+
6	-	+	-	-	+	-
7	-	-	+	+	-	-
8	-	-	-	+	+	+

[a] Values in fabrication process used if parameters were isolated. The polymer viscosity was kept constant at approximately 39 cSt for the single-factor experiment involving the PPF/PLGA ratio

[b] Vortex speed as indicated on the Daigger Vortex Genie II instrument dial. The corresponding rotation speeds are given in the section Vortexer Calibration.

Materials

PLGA (Medisorb, Alkemers, Cincinnati, OH), with a 50:50 lactic to glycolic acid ratio and a weight-average molecular weight (Mw) of 46,000, was used for the microsphere preparation. PPF (donated by Dr. Antonios G. Mikos, Department of Bioengineering, Rice University, Houston, TX), with a number-average molecular weight (Mn) of 4,800 and a Mw of 8,200 was synthesized by a two-step reaction process as described previously.[15] PVA (87-89% mole hydrolyzed, (Mw=13,000-23,000) and isopropanol were used as received.

Viscosity measurements

The kinematic viscosity of various concentrations of polymer solutions in dichloromethane was measured using an Ubbelohde viscometer (International Research Glassware, Kenilworth, NJ). The polymer solution, consisting of either pure PPF, a 50:50 PPF/PLGA blend, or pure PLGA dissolved in dichloromethane, was poured in the lower reservoir of the viscometer. The viscometer was placed vertically in a constant ambient temperature bath for 20 minutes. The time for the meniscus to pass from one mark to another was measured. To measure the kinematic viscosity at different concentrations of polymer in the organic solvent, the polymer solution was diluted by addition of 1 ml of dichloromethane to the reservoir. Each time after dilution, the solution was vortexed and the measurement was repeated. To obtain the kinematic viscosity in centistokes, the efflux time in seconds was multiplied by the viscometer constant.

Vortexer calibration

The vortex speed as indicated on the Daigger Vortex Genie II (Fisher, Pittsburgh, PA) instrument dial was calibrated using a combination contact/photo tachometer (Model 461895, Extech Instruments, Waltham, MA). At each vortexer setting, a 12 mm square piece of reflective tape was mounted on the vortexer plate. The tachometer was held approximately 15 cm from the plate and the rotation speed measurement was made in triplicates in photo mode in low ambient light conditions. The mean values of the rotation speeds were 950 rpm (setting 1), 1200 rpm (setting 2), 2000 rpm (setting 3), 2550 rpm (setting 4), 2800 rpm (setting 5), 2950 rpm (setting 6), 3050 rpm (setting 7), and 3100 rpm (setting 8). The standard deviations of the measurements were less than 4% of the average values. The vortex speeds within settings 3 and 8 were investigated in this study.

Microparticle fabrication

A water-in-oil-in-water (W1-O-W2) double emulsion-solvent extraction technique was used for the preparation of microspheres.[2,3] Briefly, 500 mg of polymer (PLGA, PPF, or PPF/PLGA blend) was dissolved in 0.75 to 1.75 ml of dichloromethane in a glass test tube. The corresponding viscosity of the polymer solution ranged from 20.6 to 153.9 cSt. While continuously vortexing the polymer solution at a speed ranging from 950 to 3100 rpm, 1.0 mg of TRD dissolved in distilled, deionized water (W1 phase, 50 – 150 µL) was injected to create the first emulsion. The entire mixture was re-emulsified for 30 seconds in 4 mL

of an aqueous PVA solution (0% or 1% w/v) to create the double emulsion. The contents of the test tube were then poured into a 250-mL glass beaker containing 100 mL of an aqueous PVA solution (0.2% or 2% w/v). The beaker was placed on a magnetic stirrer (Corning, Acton, MA) and 100 mL of a 2% aqueous isopropanol solution (w/v) was added. The extraction of the dichloromethane to the external alcoholic phase resulted in precipitation of the dissolved polymers and subsequently the formation of the microspheres. The microspheres were then collected by centrifugation, washed with distilled, deionized water, and finally vacuum-dried (Savant Speedvac systems, Holbrook, NY). This method produced a free flowing powder that could be easily handled and stored at -20 ℃ before to use.

Microparticle characterization

Surface morphology

The surface morphology of the microspheres was observed by scanning electron microscopy (SEM) at 2 kV. Dry microspheres were mounted onto metal stubs using double-sided adhesive tape and sputter coated for 1 min with a 50:50 gold/platinum mixture. The particles were examined with a Hitachi S4700 Field Emission Scanning Microscope (San Jose, CA) set at 2 kV.

Drug distribution and polymer blending

A confocal laser-scanning microscope (CLSM) (Zeiss LSM510, Carl Zeiss, Oberkochen, Germany), equipped with filters for 364 nm (blue) and 543 nm (red) excitation wavelengths was used to observe the PPF in the blend and the TRD distribution within the microspheres, respectively. Dry microspheres were dispersed on coverslips and representative fluorescence images of microparticle cross-sections were taken through optical sectioning. Depth projection micrographs were obtained with a thickness of 20 μm, comparable to the mean microsphere diameter. Thus the confocal images represent the distribution of PPF or TRD through the whole microspheres. By adjusting the wavelength, the filters, and the pinhole, the presence of PPF could be shown because of its stronger blue fluorescence than PLGA.

Size distribution

The size distribution was determined by microsphere counts using the SEM pictures. The diameter of the microspheres and the dimension of the scale bar were measured on micrographs with 100x and 300x magnifications using CorelDRAW! 8 (Corel, Ottawa, Ontario, Canada). The mean microsphere diameter in microns was reported from at least three micrographs each containing 100-3000 microspheres.

Entrapment efficiency

The entrapment efficiency of the model drug in the microspheres was determined by comparing the starting amount of TRD with the quantity contained by the microspheres after the double emulsion-solvent extraction technique. Encapsulated TRD in the microspheres was determined by dissolving 10 mg of microspheres in 1.5 mL of 1M sodium hydroxide. The TRD concentration was determined by absorption at 496 nm in a spec-

trophotometer (SpectraMax plus, Molecular Devices Corporation, Sunnyvale, CA). The background absorption at 496 nm of degradation products from PPF, PLGA and PPF/PLGA blend microspheres was measured by repeating this procedure using microspheres loaded with distilled, deionized water.

Statistical analysis

All data on single-factor effects on mean microsphere diameter and entrapment efficiency are reported as means ± standard deviations (SD) for n = 3. Single-factor analysis of variance was used to assess the statistical significance of the results. Scheffé's method was used for multiple comparison tests at significance levels of 95%.

Results and discussion

Viscosity measurements

Because of the use of two polymers with different properties and unequal molecular weights, the effect of parameter changes in the oil phase could not be simply expressed by polymer concentration and PPF/PLGA ratio. Therefore, we measured the effect of these two parameters on the viscosity of the polymer solution (figure 1). The molecular weights of PPF and PLGA, also known to have a large influence on the viscosity of the polymer solution, were kept constant. Our results demonstrated that a much higher concentration of pure PPF was needed to achieve the same viscosity as pure PLGA and small changes in PPF concentration resulted in less dramatic changes in viscosity compared with PLGA. This was not surprising because the molecular weight of PPF is much lower than the PLGA used in this study. It is also the specific polymer characteristic of PPF that makes it a good candidate for use as an injectable biomaterial. The curve of the PPF/PLGA blend was between the two curves of the pure polymers. These effects of PPF/PLGA ratio and polymer concentration on the oil-phase viscosity will help us gain insight on their effects

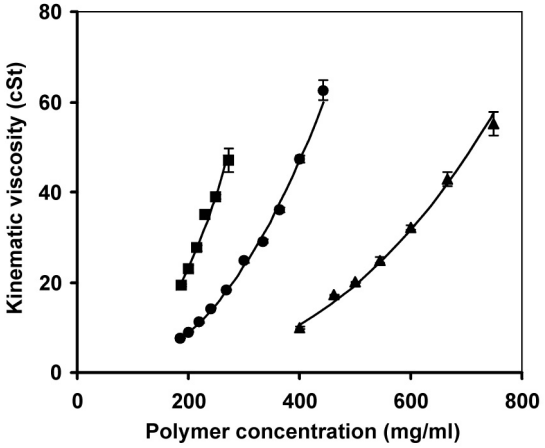

Figure 1: Kinematic viscosity of pure PLGA, a 50:50 ratio PPF/PLGA blend, and PPF solutions in dichloromethane as a function of polymer concentration. Error bars represent means ± SD for n = 3.

on the microsphere characteristics.

Fractional factorial design

The first part of the experiments, a fractional factorial design was used to determine the effects of the different processing parameters on the microsphere characteristics. SEM revealed that microparticles were produced from all formulations (figure 2). There was a wide variation in cracks, dents, porosity and surface smoothness between the different formulations. Overall, PPF/PLGA blend microspheres (formulations 5-8) had a smooth surface, whereas those made with pure PPF (formulations 1-4) had more dents and cracks. Some of the PPF microspheres were broken open and revealed the inner honeycomb-like structure. The majority of microspheres fabricated with a low viscosity of the polymer solution (formulations 3, 4, 7 and 8) had a very porous surface.

The distribution of TRD in the microspheres was shown by confocal light microscopy (figure 3). At a larger W1 volume (formulation 1, 2, 7 and 8), TRD was distributed uniformly throughout the polymer matrix within the microspheres. Lower W1 volumes resulted in accumulations of dextran in small drops. When microspheres were produced with less W1 phase and internal PVA, the aggregation of dextran into drops became more apparent (formulations 4 and 5).

All fabricated microspheres were between 1.7 and 197.8 µm in diameter and the average sizes for the 8 microsphere formulations ranged from 19.0 to 76.9 µm. The microsphere size was most affected by the amount of the W1 phase and the percent external PVA phase (figure 4). Increasing the W1 phase volume and the external PVA phase increased microsphere size. Varying all other parameters showed a minimal effect on microsphere size.

The entrapment efficiency of the microspheres showed a variation for the different formulations ranging from 71.9% to 91.6% entrapped drug and was affected by all six parameters (figure 4). The volume of the internal aqueous phase containing TRD had the highest effect. In addition, an increase in vortex speed, internal PVA phase, and external PVA phase increased the amount of entrapped drug. In contrast, increases in either the

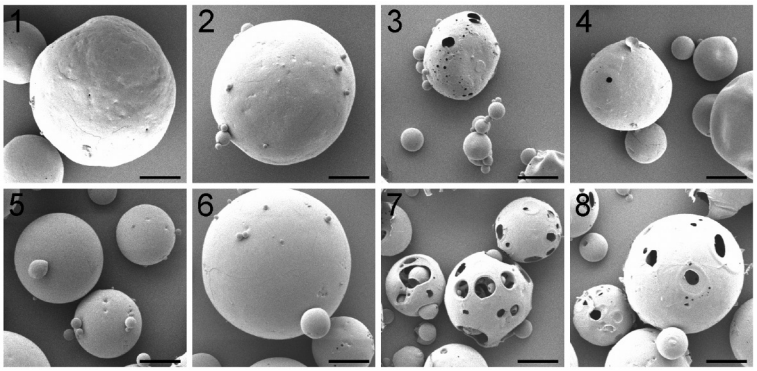

Figure 2: SEM pictures showing the surface morphology of the eight formulations of microspheres fabricated for the fractional factorial design. The number of the picture corresponds to the formulation in Table 1(B), which indicates the values used in the fabrication process.

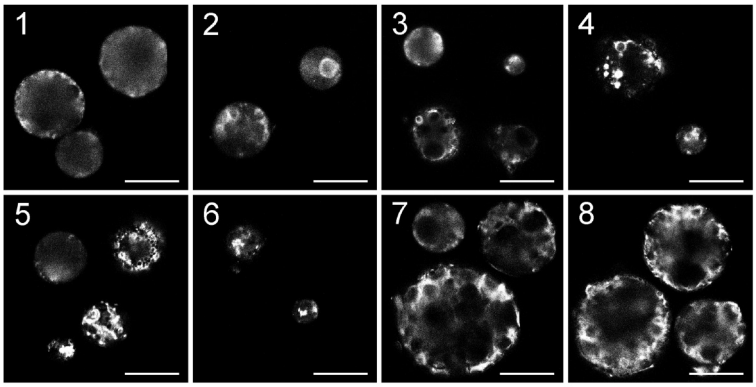

Figure 3: CLSM images showing the distribution of TRD in the microspheres at an excitation wavelength of 543 nm of the eight formulations fabricated for the fractional factorial design. The number of the picture corresponds to the formulation in Table 1(B).

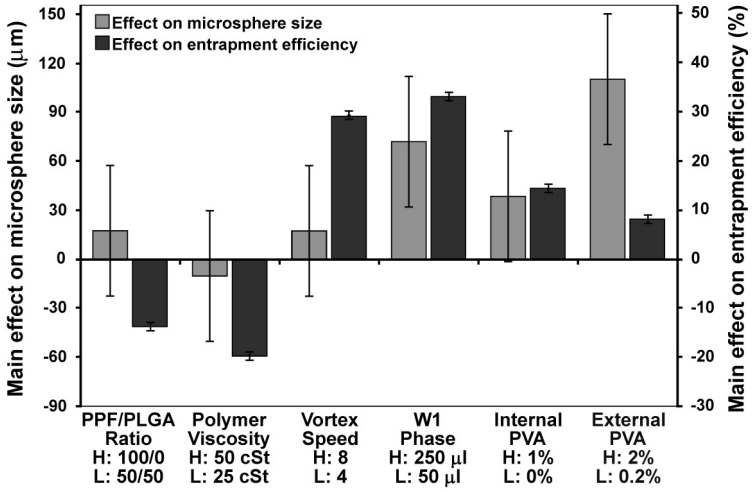

Figure 4: Main effects of PPF/PLGA ratio, polymer viscosity, vortex speed, W1 phase, internal PVA, and external PVA on the microsphere size and entrapment efficiency of TRD. A positive number indicates that the particular parameter had an increasing effect on the mean diameter of the microspheres or entrapment efficiency of TRD as the value was changed from a low (L) level (-) to a high (H) level (+) [see Table 1(A)]. A negative number indicates a decrease in mean microsphere diameter or entrapment efficiency of TRD as the parameter was changed from a low (L) level (-) to a high (H) level (+). Error bars represent the standard errors of the effect and were calculated to be 39.9 for the microsphere size and 2.1 for the TRD entrapment efficiency in this experiment.

PPF/PLGA polymer ratio or the polymer viscosity decreased the entrapment efficiency (figure 4).

The higher entrapment efficiency achieved using a higher PVA concentration in the external phase during fabrication could be explained by its stabilizing effect on the emulsions, thereby preventing mass transfer of the drug to the surroundings. The effect of PVA on the microsphere size distribution is more complex and previous studies have reported two opposite effects. PVA was shown to stabilize the emulsions resulting in a smaller particle size.[16-20] However, the presence of high Mw PVA in the external water phase also increases the viscosity of the double emulsion, leading to an increasing difficulty in breaking up the emulsion into smaller droplets and therefore a larger particle size.[19-21] In this study an increase of 110 μm in microsphere diameter was seen when the PVA concentration was increased from 0.2% to 2% (figure 3), probably due to the increase in the viscosity of the external aqueous phase.

The fractional factorial design presented in this study helps to determine the relative effects of a large number of processing parameters on the specific microsphere characteristics. Other important parameters identified, such as the PPF/PLGA ratio, the polymer viscosity, the vortex speed and the volume of the W1 phase were then varied in a wider range in the second part of the study to determine their effects on the fabricated microspheres.

Effects of PPF/PLGA ratio

To evaluate the effect of incorporating PPF into microspheres during the fabrication process, 0, 25, 50, 75, and 100% of the weight of the PLGA was replaced by PPF in a constant 1-mL volume of dichloromethane. The microspheres fabricated from PLGA had a smooth surface with very few pores. Raising the percentage of PPF resulted in an increasing irregularity and porosity of the surface and an increasing size of pores (data not shown). Because of the difference in blue fluorescence between PLGA and PPF, the confocal images (figure 5) showed that PPF was blended uniformly throughout the microspheres. As the percent of PPF in the microspheres was increased, the specific fluorescence at an excitation wavelength of 364 nm increased. The uniform blending is required since our intent is to use the carbon-carbon double bonds along the PPF backbone to covalently bind the PPF/PLGA blend microspheres to a PPF scaffold or immobilize them to a PPF substrate. The composite microsphere/scaffold system would serve as a delivery vehicle for controlled drug release at a desired treatment location.

The entrapment efficiency of all five formulations varied from 77.4% to 98.0% (figure 6). At a constant volume of dichloromethane, an increase in PPF percentage in the PPF/PLGA blend yielded a decrease in the viscosity of the polymer solution (figure 1). Because it is easier to break up the second emulsion into smaller droplets at lower viscosities, smaller microspheres were obtained at higher PPF contents (figure 6). The average size of PLGA microspheres was significantly ($p < 0.05$) larger than those of blend microspheres containing 50, 75, or 100% PPF.

Effects of polymer viscosity

Polymer solutions with a kinematic viscosity of 20.6, 29.6, 45.7, 77.7, and 153.9 cSt were prepared by dissolving 500 mg of 50:50 PPF/PLGA in 1.75, 1.50, 1.25, 1.00, and 0.75 ml

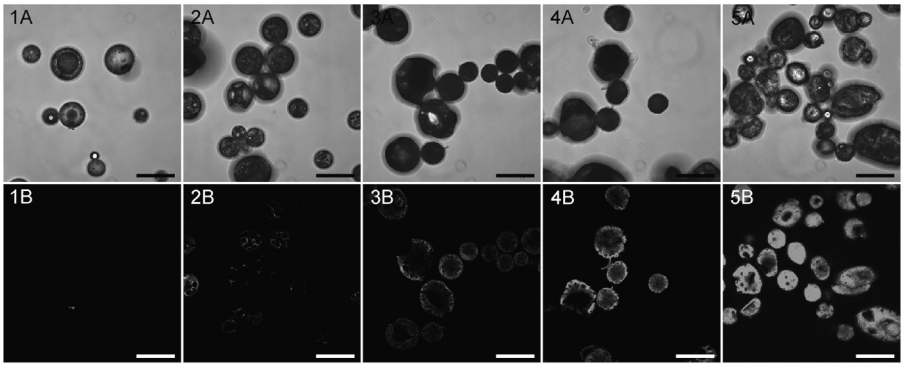

Figure 5: CLSM images of PPF/PLGA blend microspheres containing 0, 25, 50, 75 and 100% PPF, as indicated by numbers 1-5 on the images, respectively. Each image is originated from one picture that is split into (A) a light microscopy image and (B) a fluorescence image at an excitation wavelength of 364 nm to show the presence of PPF. Since PLGA is non-fluorescent, these images indicate the uniform blending of PPF throughout the blend microspheres.

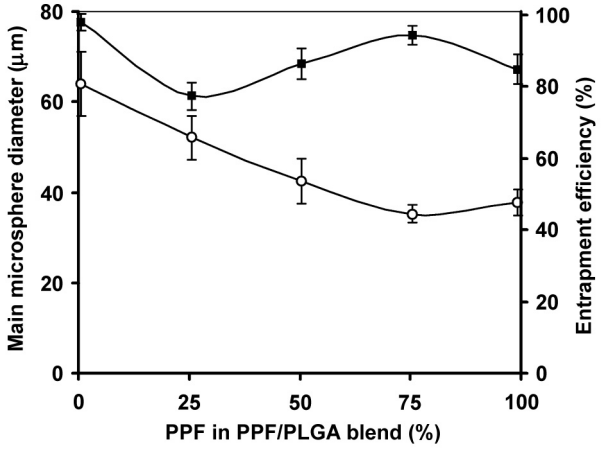

Figure 6: Effects of PPF percentage in the PPF/PLGA blend on average microsphere size (circles) and entrapment efficiency (squares) of TRD within PPF/PLGA blend microspheres. Error bars represent means ± SD for n = 3.

of dichloromethane, respectively. The surface morphology of the corresponding microspheres, along with the ones fabricated from 39.0 cSt solution and used for the remainder of the experiments, was shown to be strongly dependent on the initial viscosity of the polymer solution (figure 7). The microspheres created with solutions of 39.0 and 45.7 cSt had smooth surfaces with very few pores whereas those fabricated with higher or lower viscosities had porous surfaces. Therefore, the concentrations of the polymer solutions need to be adjusted for different PPF/PLGA blend ratios in order to obtain the same viscosity (according to figure 1), thus a similar surface morphology after microsphere fabrication. The surface porosity was found to correlate well with the initial burst release of a model drug from these microspheres.[22]

As shown in Figure 8, there exists a polymer solution viscosity between upper and lower extremes that would result in a maximum average microsphere diameter. Our results showed that a maximal mean diameter of approximately 35 μm was obtained from a 30 cSt solution. One explanation for this phenomenon is that at lower viscosities, it is easier to break up the polymer solution into smaller droplets during fabrication thus creating smaller sized microspheres. At very high viscosities, it is more difficult for the aqueous phase to cut through the droplets. However, tearing off of small droplet parts can cause a wider size distribution with a lot of very small particles and some very large particles varying from 0.6 to 190 μm. The average microsphere size is thus lower due to the presence of the large number of small particles. In our experiments, microspheres prepared from viscosities of 77.7 and 153.9 cSt were significantly ($p < 0.05$) smaller than those prepared from lower viscosities.

Similar to the size distribution, our results show that the entrapment efficiency is also maximized at a viscosity of approximately 30 cSt (figure 8). The organic solution initially serves as a diffusion barrier for the drug between the two aqueous phases. At high viscosities, polymer precipitation occurs much earlier, resulting in lower entrapment efficiencies because of difficulty in forming emulsions and more diffusion.[23,24] The entrapment efficiency at 153.9 cSt was significantly ($p < 0.05$) lower than other viscosity conditions. At low viscosities the double emulsion is less stable. The high surface energy of water (72.8 mJ/m^2) causes internal water droplets to coalesce and mix with the external aqueous phase, resulting in drug loss and lower entrapment efficiency.[19,25]

Effects of vortex speed

For this experiment, 50:50 PPF/PLGA microspheres were fabricated at varying vortex speeds while keeping the other parameters constant (see Table 1). The viscosity was chosen at 39 cSt, the same as the pure PLGA solution at a concentration of 250 mg/mL. SEMs revealed that all microspheres had a smooth surface regardless of the vortex speed used (data not shown).

The stirring speed is considered to have a large effect on microsphere size since it provides the energy to disperse the oil phase in the second aqueous phase.[19] An increase in vortex speed not only resulted in significantly ($p < 0.05$) decreased average microsphere size compared to vortex speed 3, but also a narrower size distribution (figure 9). At a vortex speed of 3, the microsphere size varied form 5 to 370 μm, which narrowed down to sizes between 2 and 90 μm at a vortex speed of 8. The smaller size may be attributed to the breaking up of the second water emulsion into smaller droplets at higher input power. The narrower size distribution at increased vortex speeds is likely caused by a minimum

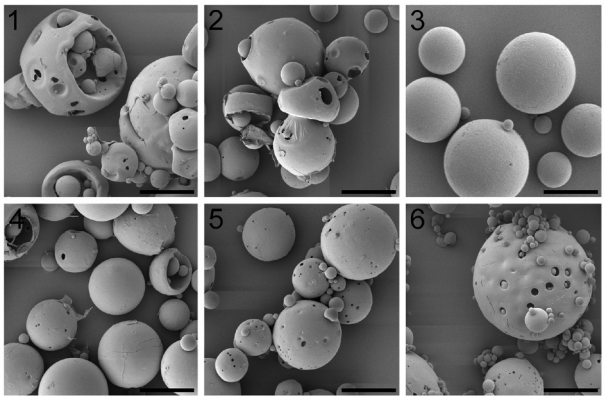

Figure 7: SEM pictures showing the surface morphology of 50:50 PPF/PLGA microspheres fabricated with different viscosities of the polymer solution: (A) 20.6, (B) 29.6, (C) 39.0, (D) 45.7, (E) 77.7, and (F) 153.9 cSt.

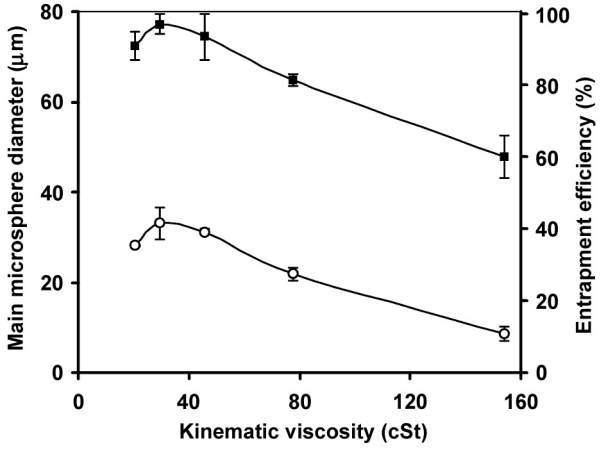

Figure 8: Effects of the polymer solution viscosity on average microsphere size (circles) and entrapment efficiency (squares) of TRD within 50:50 PPF/PLGA blend microspheres. Error bars represent means ± SD for n = 3.

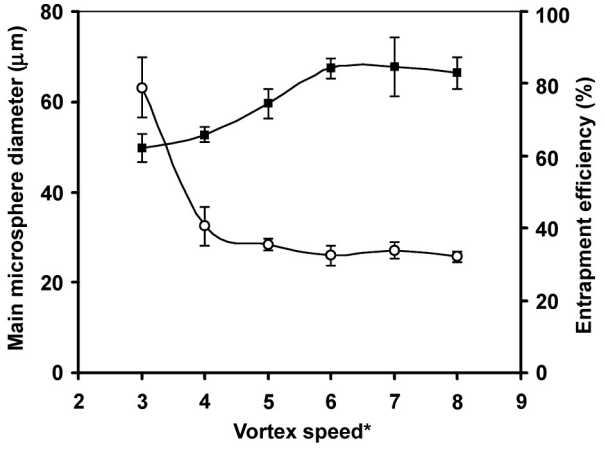

Figure 9: Effects of vortex speed on average microsphere size (circles) and entrapment efficiency (squares) of TRD within 50:50 PPF/PLGA blend microspheres. Error bars represent means ± SD for n = 3. *Vortex speed as indicated on Daigger Vortex Genie II instrument dail. The corresponding rotation speeds are given in the section Vortexer calibration.

drop size that could not be further broken up. The entrapment efficiency of the model drug TRD in the microspheres was similar (p> 0.05) at all vortex speeds tested (figure 9). Because vortexing also provides the energy for the dispersion of the aqueous drug solution into the oil phase, a fine dispersion at high speed typically results in slightly higher entrapment efficiency.[25]

The results obtained by isolating the parameter and varying it in a wider range complement the results obtained from the fractional factorial design. For instance, the vortex speed was not seen as a dominant factor affecting microsphere size (figure 4) because the two levels chosen (vortex speeds 4 and 8) resulted in similar sizes in Figure 9. However, increasing the speed from 4 to 8 significantly increased the entrapment efficiency (figure 9) and thus it was shown as a dominant factor in Figure 4.

Effects of the internal aqueous phase

The effects of the internal aqueous phase (W1) was assessed by fabricating microspheres using 50, 150, 250, 350 and 450 µL of aqueous solution containing 1.0 mg of TRD. All microspheres were spherical with a smooth surface as assessed by SEM (data not shown). Both average microsphere diameter and entrapment efficiency were similar (p > 0.05) for the different W1 volumes tested (figure 10). Previous studies indicated two possible mechanisms of the effect of W1 volume on entrapment efficiency. Because lower W1 volumes result in more concentrated drug solutions, the entrapment efficiency decreases because of higher drug diffusion controlled by an increased concentration gradient.[25] At higher aqueous loadings, the entrapment efficiency decreases as well because the increasing proportion of droplets at the surface of the emulsion enhances drug loss to the external water phase.[25,26]

Conclusion

In this study, we demonstrated that biodegradable PPF/PLGA blend microspheres loaded with the model drug TRD could be fabricated using the established double emulsion-sol-

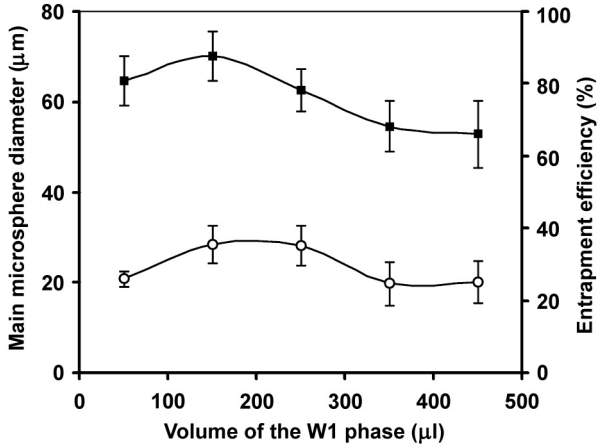

Figure 10: Effects of the volume of the W1 phase on average microsphere size (circles) and entrapment efficiency (squares) of TRD within 50:50 PPF/PLGA blend microspheres. Error bars represent means ± SD for n = 3

vent extraction technique. Polymer viscosity was shown to be the most important factor affecting the surface morphology of the blend microspheres. Spherical microspheres with a smooth surface were fabricated at a viscosity of approximately 39 cSt. We have shown a uniform blending of PPF with PLGA throughout the microsphere matrix, which is an important characteristic for future studies. The microsphere size can be tailored by varying the percent of PVA in the external aqueous phase, the viscosity of the oil phase, and the vortex speed. Important parameters affecting the entrapment efficiency of the model drug are the viscosity of the oil phase, the vortex speed, and the volume of the internal aqueous phase. In subsequent studies we have also investigated the release kinetics of TRD from these PPF/PLGA microspheres and after their incorporation in a PPF scaffold.[22,27]

References

1. Agrawal, C.M., and Ray, R.B. Biodegradable polymeric scaffolds for musculoskeletal tissue engineering. J Biomed Mater Res 55, 141, 2001.
2. Elisseeff, J., McIntosh, W., Fu, K., Blunk, B.T., and Langer, R. Controlled-release of IGF-I and TGF-beta1 in a photopolymerizing hydrogel for cartilage tissue engineering. J Orthop Res 19, 1098, 2001.
3. Lu, L., Stamatas, G.N., and Mikos, A.G. Controlled release of transforming growth factor beta1 from biodegradable polymer microparticles. J Biomed Mater Res 50, 440, 2000.
4. Lu, L., Yaszemski, M.J., and Mikos, A.G. TGF-beta1 release from biodegradable polymer microparticles: its effects on marrow stromal osteoblast function. J Bone Joint Surg Am 83-A Suppl 1, S82, 2001.
5. Oldham, J.B., Lu, L., Zhu, X., Porter, B.D., Hefferan, T.E., Larson, D.R., Currier, B.L., Mikos, A.G., and Yaszemski, M.J. Biological activity of rhBMP-2 released from PLGA microspheres. J Biomech Eng 122, 289, 2000.
6. Peter, S.J., Lu, L., Kim, D.J., Stamatas, G.N., Miller, M.J., Yaszemski, M.J., and Mikos, A.G. Effects of transforming growth factor beta1 released from biodegradable polymer microparticles on marrow stromal osteoblasts cultured on poly(propylene fumarate) substrates. J Biomed Mater Res 50, 452, 2000.
7. Schrier, J.A., and DeLuca, P.P. Recombinant human bone morphogenetic protein-2 binding and incorporation in PLGA microsphere delivery systems. Pharm Dev Technol 4, 611, 1999.
8. Yuksel, E., Weinfeld, A.B., Cleek, R., Wamsley, S., Jensen, J., Boutros, S., Waugh, J.M., Shenaq, S.M., and Spira, M. Increased free fat-graft survival with the long-term, local delivery of insulin, insulin-like growth factor-I, and basic fibroblast growth factor by PLGA/PEG microspheres. Plast Reconstr Surg 105, 1712, 2000.
9. Porter, B.D., Oldham, J.B., He, S.L., Zobitz, M.E., Payne, R.G., An, K.N., Currier, B.L., Mikos, A.G., and Yaszemski, M.J. Mechanical properties of a biodegradable bone regeneration scaffold. J Biomech Eng 122, 286, 2000.
10. Peter, S.J., Kim, P., Yasko, A.W., Yaszemski, M.J., and Mikos, A.G. Crosslinking characteristics of an injectable poly(propylene fumarate)/beta-tricalcium phosphate paste and mechanical properties of the crosslinked composite for use as a biodegradable bone cement. J Biomed Mater Res 44, 314, 1999.
11. Hedberg, E.L., Tang, A., Crowther, R.S., Carney, D.H., and Mikos, A.G. Controlled release of an osteogenic peptide from injectable biodegradable polymeric composites. J Control Release 84, 137, 2002.
12. Kempen, D.H.R., Kim, C.W., Lu, L., Dhert, W.J.A., Currier, B.L., and Yaszemski, M.J. Controlled release from poly(lactic-co-glycolic acid) microspheres embedded in an injectable, biodegradable scaffold for bone tissue engineering. Materials Science Forum, 3151, 2003.
13. Box, G., Hunter, W., and Hunter, J.S. Statistics for experimenters. New York: John Wiley & Sons Inc., 1978.
14. Jain, R.A. The manufacturing techniques of various drug loaded biodegradable poly(lactide-co-glycolide) (PLGA) devices. Biomaterials 21, 2475, 2000.
15. Peter, S.J., Suggs, L.J., Yaszemski, M.J., Engel, P.S., and Mikos, A.G. Synthesis of poly(propylene fumarate) by acylation of propylene glycol in the presence of a proton scavenger. J Biomater Sci Polym Ed 10, 363, 1999.

16. Jeffery, H., Davis, S.S., and O'Hagan, D.T. The preparation and characterization of poly(lactide-co-glycolide) microparticles. II. The entrapment of a model protein using a (water-in-oil)-in-water emulsion solvent evaporation technique. Pharm Res 10, 362, 1993.
17. Jeong, Y.I., Song, J.G., Kang, S.S., Ryu, H.H., Lee, Y.H., Choi, C., Shin, B.A., Kim, K.K., Ahn, K.Y., and Jung, S. Preparation of poly(DL-lactide-co-glycolide) microspheres encapsulating all-trans retinoic acid. Int J Pharm 259, 79, 2003.
18. Sun, S.W., Jeong, Y.I., Jung, S.W., and Kim, S.H. Characterization of FITC-albumin encapsulated poly(DL-lactide-co-glycolide) microspheres and its release characteristics. J Microencapsul 20, 479, 2003.
19. Yang, Y.Y., Chung, T.S., and Ng, N.P. Morphology, drug distribution, and *in vitro* release profiles of biodegradable polymeric microspheres containing protein fabricated by double-emulsion solvent extraction/evaporation method. Biomaterials 22, 231, 2001.
20. Yang, Y.Y., Wan, J.P., Chung, T.S., Pallathadka, P.K., Ng, S., and Heller, J. POE-PEG-POE triblock copolymeric microspheres containing protein. I. Preparation and characterization. J Control Release 75, 115, 2001.
21. Vandervoort, J., and Ludwig, A. Preparation factors affecting the properties of polylactide nanoparticles: a factorial design study. Pharmazie 56, 484, 2001.
22. Kempen, D.H., Lu, L., Zhu, X., Kim, C., Jabbari, E., Dhert, W.J., Currier, B.L., and Yaszemski, M.J. Development of biodegradable poly(propylene fumarate)/poly(lactic-co-glycolic acid) blend microspheres. II. Controlled drug release and microsphere degradation. J Biomed Mater Res A 70A, 293, 2004.
23. Bodmeier, R., and McGinity, J.W. Solvent selection in the preparation of poly(DL-lactide) microspheres prepared by the solvent evaporation method. Int J Pharm 43, 179, 1988.
24. Schugens, C., Laruelle, N., Nihant, N., Grandfils, C., Jérome, R., and Teyssié, P. Effect of the emulsion stability on the morphology and porosity of semicrystalline poly L-lactide microparticles prepared by w/o/w double emulsion-evaporation. J Control Release 32, 161, 1994.
25. Alex, R., and Bodmeier, R. Encapsulation of water-soluble drugs by a modified solvent evaporation method. I. Effect of process and formulation variables on drug entrapment. J Microencapsul 7, 347, 1990.
26. Freytag, T., Dashevsky, A., Tillman, L., Hardee, G.E., and Bodmeier, R. Improvement of the encapsulation efficiency of oligonucleotide-containing biodegradable microspheres. J Control Release 69, 197, 2000.
27. Kempen, D.H., Lu, L., Kim, C., Zhu, X., Dhert, W.J., Currier, B.L., and Yaszemski, M.J. Controlled drug release from a novel injectable biodegradable microsphere/scaffold composite based on poly(propylene fumarate). J Biomed Mater Res A 77, 103, 2006.

4

Development of biodegradable PPF/PLGA blend microspheres Part 2: Controlled drug release and microsphere degradation

Journal of Biomedical Materials Research 2004;70A:293-302

D.H.R. Kempen
L. Lu
X. Zhu
C. Kim
E. Jabbari
W.J.A. Dhert
B.L. Currier
M.J. Yaszemski

Abstract

This article describes the effects of six processing parameters on the release kinetics of a model drug Texas red dextran (TRD) from poly(propylene fumarate)/poly(lactic-co-glycolic acid) (PPF/PLGA) blend microspheres as well as the degradation of these microspheres. The microspheres were fabricated using a double emulsion-solvent extraction technique in which the following 6 parameters were varied: PPF/PLGA ratio, polymer viscosity, vortex speed during emulsification, amount of internal aqueous phase, use of poly(vinyl alcohol) in the internal aqueous phase and poly(vinyl alcohol) concentration in the external aqueous phase. We have previously characterized these microspheres in terms of microsphere morphology, size distribution, and TRD entrapment efficiency. In this work, the TRD release profiles in phosphate-buffered saline were determined and all formulations showed an initial burst release in the first 2 days followed by a decreased sustained release over a 38-day period. The initial burst release varied from 5.1 (± 1.1) to 67.7 (± 3.4) % of the entrapped TRD, and was affected most by the viscosity of the polymer solution used for microsphere fabrication. The sustained release between day 2 and day 38 ranged from 7.9 (± 0.8) to 27.2 (± 3.1) % of the entrapped TRD. During 11 weeks of *in vitro* degradation, the mass of the microspheres remained relatively constant for the first 3 weeks after which it decreased dramatically, whereas the molecular weight of the polymers decreased immediately upon placement in phosphate-buffered saline. Increasing the PPF content in the PPF/PLGA blend resulted in slower microsphere degradation. Overall, this study provides further understanding of the effects of various processing parameters on the release kinetics from PPF/PLGA blend microspheres thus allowing modulation of drug release to achieve a wide spectrum of release profiles.

Introduction

Protein delivery has become an important area of research, as a large number of recombinant proteins are being investigated for therapeutic applications. Microencapsulation of these bioactive molecules into a polymer matrix has been used as one of the methods to locally deliver them in a controlled manner, over a prolonged period of time. In the past multiple proteins with molecular weights varying from approximately 25,000 Daltons (transforming growth factor (TGF)-β) to 150,000 Daltons (rabbit gamma immunoglobulin) have been released from poly(lactic-co-glycolic acid) (PLGA) microspheres.[1-4] These polymer microspheres protect proteins with short *in vivo* half-lives, thus reducing the need for multiple doses during prolonged therapy. Controlled local delivery potentially optimizes local therapeutic responses, thereby reducing the incidents of peak-related side effects and systemic toxic effects.

An injectable, *in situ* polymerizable, biodegradable poly(propylene fumarate) (PPF) scaffold for bone regeneration is under development in our laboratory.[5] The addition of bioactive molecules such as bone morphogenetic proteins or TGF-β to this scaffold can result in a composite biomaterial that could be used as an alternative to bone graft for the treatment of skeletal defects. Verhof et al. used radiofrequency glow discharge to coat PPF scaffolds with TGF-β1 and showed a significant increase in bone formation after implanting the scaffolds in rabbit cranial defects.[6] However, this technique is only applicable to preformed scaffolds and the loaded doses were completely released after one week. Encapsulation of bioactive molecules within biodegradable microspheres, which can then be impregnated into the scaffold, allows controlled release over a longer period of time.[7] In a previous study, we fabricated PPF/PLGA blend microspheres and demonstrated the effects of various processing parameters on the microsphere characteristics.[8] Compared to conventional PLGA microspheres, a wider range of microsphere properties could be achieved by varying the PPF/PLGA ratio in the blend. In addition, these microspheres have the potential capacity to covalently bind to a PPF scaffold through carbon-carbon double bonds along the PPF backbone, thus achieving better immobilization of the microspheres and improved mechanical properties of the microsphere/scaffold composite. In this study, we investigated the effects of various parameters on the release kinetics of the model drug Texas red dextran (TRD) from these blend microspheres and their *in vitro* degradation in simulated body fluids.

Materials and methods

Experimental design

In a previous study we investigated the effects of six fabrication parameters on the microsphere characteristics.[8] In the first part of this study, these parameters were investigated for their effect upon the release profiles of the model drug Texas Red dextran (TRD, Molecular Probes Inc., Leiden, The Netherlands) from the microspheres. The following parameters were investigated: 1. PPF/PLGA ratio; 2. viscosity of polymer solutions; 3. vortex speed; 4. amount of internal phase (W1 phase); 5. poly(vinyl alcohol) (PVA) in internal water phase; and 6. PVA amount in external water phase (W2 phase). We used TRD with a molecular weight of 40,000 Daltons to mimic the molecular weight of a bioactive protein, bone morphogenetic protein, which is a candidate for use in musculoskeletal applications.

To study the main effects of each parameter on the release, we used a Resolution III two-level fractional factorial design (2_{III}^{6-3}) as previously described chapter 3.[8,9] The high and low values for each parameter are represented in chapter 3 in Table 1(A), and the formulation combinations according to this design are presented in Table 1(B). The main effect of each parameter was determined for normalized release over two periods (days 0-2 and days 2-38). The effects of PPF/PLGA ratio, polymer viscosity, vortex speed, and the amount of internal aqueous phase (W1 phase) were then studied in more detail by isolating them and increasing the range. Unless specified, the studies were performed with the values indicated in Table 1. The effect of PPF/PLGA ratio was investigated using a polymer concentration of 250 mg/ml dichloromethane. The other isolated parameters were studied at a viscosity of 39 centistokes (cSt).
In the second part of this study, we investigated the degradation of microspheres containing different PPF/PLGA ratios. All measurements were performed in triplicate and the data were expressed as means ± standard deviations (SD), except for the main effect results where standard errors were reported for three experimental runs.

Microparticle fabrication

The materials, vortex calibration and double emulsion-solvent extraction technique for the preparation of the microspheres were reported in chapter 3.[8,11]

Release kinetics

For the release study, 25 mg of microspheres was suspended in 1 mL of phosphate-buffered saline (PBS) in a small Eppendorf tube. The tubes were sealed and placed in a plastic box in a 37℃ incubator on an orbital shaker set at 100 rpm to ensure continuous mixing. At certain time points the tubes were centrifuged for a few seconds and the supernatant was collected and replaced with 1 mL of fresh PBS. The supernatant was stored at -20 ℃. After all the samples were collected, the absorption at 496 nm was measured using a spectrophotometer (SpectraMax plus; Molecular Devices Corporation, Sunnyvale, CA) to determine the amount of released TRD. This amount was normalized to the amount of entrapped TRD.

Microsphere degradation

To study the different aspects of microsphere degradation, PPF/PLGA microspheres with 0, 25, 50, 75, and 100% PPF were fabricated. No model drug was added to the internal aqueous phase and all other variables were kept constant: viscosity 39 cSt, vortex speed 4, internal water phase 100 µL, no internal PVA and 2% external PVA. Mesh bags, made from a nylon mesh sheet (10 µm mesh size, Spectrum, Houston TX), were filled with 15 mg of microspheres and sealed. Three bags for each time point were placed in a centrifuge tube filled with 50 ml of PBS (pH 7.4) and incubated at 37℃. The medium was changed every week to maintain a constant pH. At pre-determined time points up to 38 days, one tube of each microsphere type was collected, washed 3 times with ddH_2O and freeze-dried before analysis.

Mass loss

To determine the mass loss of the microspheres over time, the initial weights of the filled nylon bags were measured to a precision of 0.01 mg using an analytical balance (model M-220D, Denver Instrument, Denver, CO). Upon sample harvest, the bags were lyophilized and their weight was measured again. Results from a previous study by Yoon et al. demonstrated that the phosphate salts in PBS had insignificant effect on weight loss of PLGA porous scaffolds.[12] It should also be noted that the PBS used in our degradation experiments contained no sodium chloride or magnesium chloride salts. Degrading samples were characterized for mass loss by normalizing the initial mass of the mesh bags to the mass after collection.

Molecular weight loss

The Mw of the initial microspheres and degrading samples were determined by gel permeation chromatography system (Waters, Milford, MA) equipped with a differential refractometer and an absorbance detector. The samples were dissolved in chloroform and eluted through a Phenogel 5 guard column (model 1063376, 50 x 7.8 mm, 5 µm particle diameter, Phenomenex, Torrance, CA) and a Phenogel 5 linear column (Model 106338, 300x 7.8 mm, 5 µm particle diameter, Phenomenex) at a flow rate of 1 mL/min. Polystyrene standards (Polysciences, Warrington, PA) were used to obtain a primary calibration curve.

Surface morphology during degradation

The morphology of the microspheres after 0, 14, and 28 days of degradation was assessed by scanning electron microscopy (SEM). The freeze-dried microspheres were removed from the mesh bags and mounted onto metal stubs using double-sided carbon adhesive tape. The particles were coated for 1 min. with a 50:50 gold:platinum mixture and examined with a Hitachi S4700 Field Emission (San Jose, CA) set at 2 kV.

Results and discussion

Main effects on TRD release from microspheres

In the first part of the release experiments, a fractional factorial design was used to study the effect of the different processing parameters on the release kinetics of TRD. Figure 1 shows the cumulative release profiles of TRD from PPF/PLGA blend microspheres. All eight microsphere formulations exhibited a sustained release of the model drug for at least 38 days and showed a biphasic profile: a burst phase (days 0-2) and a sustained release phase (days 2-38).

The release profiles showed a large variation in the initial burst, varying from 24.9 (± 2.4) to 67.7 (± 3.4) % of the entrapped TRD, released within the first 2 days (Table 2). The burst release is known to depend on the rapid water penetration into the polymer matrix. Encapsulated molecules that are immediately accessible at the periphery of the microspheres and/or in the aqueous channels inside the microspheres are rapidly released upon contact with the release medium.[13] All investigated parameters were shown to affect this initial burst release (figure 2), with the polymer solution viscosity having the largest effect. An increase in polymer solution viscosity, vortex speed and internal PVA all

decreased the amount of TRD released during the first two day. In contrast, an increase in PPF in the PPF/PLGA blend, the first water phase volume and the amount of the external PVA phase all increased the burst release.

After day 2, the profiles showed a decrease in the amount of TRD released over time and obtained an approximately zero-order release until day 38 (figure 1). The release rates varied from 8.4 (±1.5) to 20.0 (±1.6) % of entrapped TRD (Table 2). Typically, the release rate is decreased with time due to a decreased driving force, as the drug is depleted from the surface matrix. Wang et al. also demonstrated that surface morphology changes increased the difficulty of drug diffusion through the water-filled pores.[13] These surface changes, such as a decrease in surface porosity and the formation of a dense outer "skin" layer, are the result of the rearrangement of the polymer matrix. Because of these processes, the burst release is diminished and followed by a zero-order release. During this phase, the release depends upon various other chemical and physical processes, such as 1. polymer chain cleavage; 2. diffusion of the drug and of polymer degradation products out of the microspheres; 3. the creation of new water-filled pores; and 4. the breakdown of the polymeric structure.[14]

The use of internal PVA had no effect on this release phase, and the effect of the vortex speed and percent of external PVA were minimal (figure 2). PVA was added to the aqueous phases during the fabrication process to enhance the emulsion stability. In the internal aqueous phase, PVA stabilizes inner water droplets against coalescence thereby preventing the formation of interconnected water channels.[15] Because of the rearrangement of the polymer chains and depletion of easily accessible drug, no effect of internal PVA was seen on the zero-order release phase. In contrast, a large effect was seen for the PPF/PLGA ratio, the viscosity of the polymer solution and the internal water phase volume. An increase in polymer viscosity resulted in increased release, whereas higher PPF/PLGA ratio and larger internal water phase decreased TRD release. The effects of PPF/PLGA ratio, polymer solution viscosity, vortex speed and the amount of W1 phase were further studied in the second part of this study by increasing the range of these parameters.

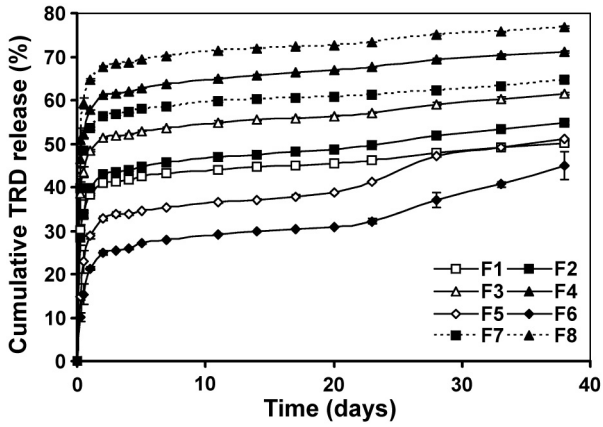

Figure 1: Cumulative release kinetics of TRD from the 8 microsphere formulations in the fractional factorial design (see Table 1B in chapter 3). Error bars represent means ± SD for n = 3.

Table 2
Percent of TRD release during the two phases from the 8 microsphere formulations in the fractional factorial design (means + SD for n = 3)

Formulation	*Day 0-2*	*Day 2-38*
F1	40.9 ± 1.4	9.1 ± 0.7
F2	43.0 ± 2.9	11.8 ± 1.0
F3	51.3 ± 2.5	10.1 ± 1.7
F4	61.1 ± 2.5	9.9 ± 0.3
F5	32.8 ± 1.8	18.2 ± 1.2
F6	24.9 ± 2.4	20.0 ± 1.6
F7	56.3 ± 1.5	8.4 ± 1.1
F8	67.7 ± 3.4	9.0 ± 0.5

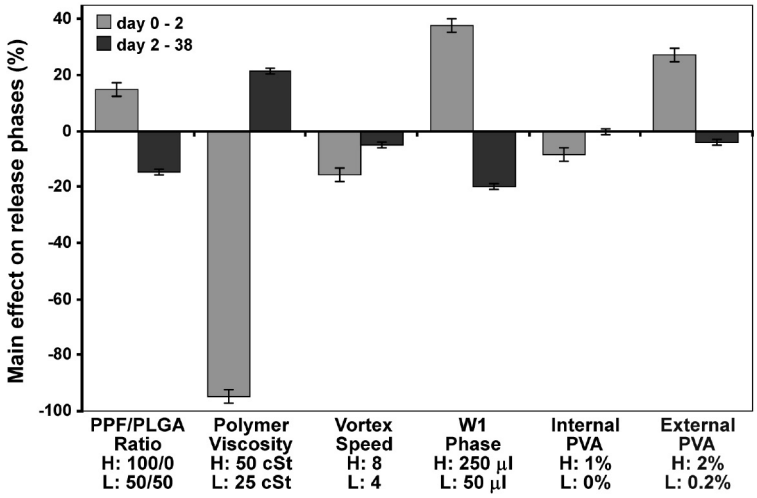

Figure 2: Main effects of PPF/PLGA ratio, polymer viscosity, vortex speed, W1 phase, internal and external PVA on the normalized release of TRD over two time periods. A positive number indicates that the particular parameter had an increasing effect on TRD release over that period as the value was changed from a low (L) level (-) to a high (H) level (+) (see Table 1A in chapter 3). A negative number indicates a decrease in TRD release as the parameter was changed from a low to a high level. Error bars represent the standard errors of the effect and were calculated to be 2.3 and 1.0 for day 0-2 and day 2-38, respectively.

Effects of PPF/PLGA ratio

The effect of PPF incorporation into the PLGA microspheres on TRD release was evaluated by replacing a fraction of PLGA by PPF in a constant 1-mL volume of dichloromethane during the microsphere fabrication process. As the PPF percentage increased from 0 to 75%, the initial burst in the first 2 days increased from 21.9 (± 0.9) to 65.3 (± 2.7) % of the entrapped TRD (figure 3). Pure PPF microspheres had a slightly lower burst of 64.2 (± 1.5) %. We have previously shown that increasing the PPF percentage in the blend microspheres resulted in decreased average microsphere size and increased surface porosity.[8] The larger burst release observed at higher PPF percentage may be due to the larger total surface area available for release.

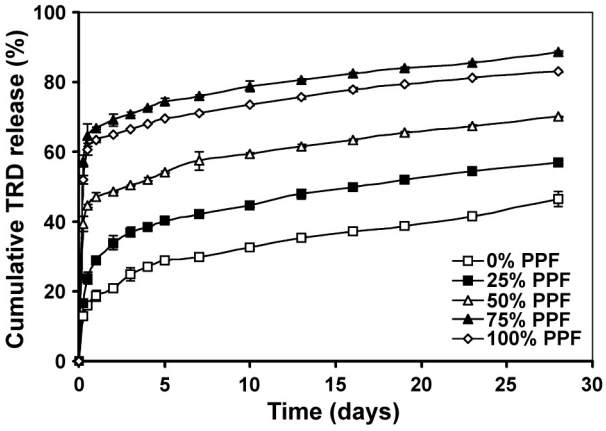

Figure 3: Cumulative release kinetics of TRD from microspheres fabricated with different PPF/PLGA ratios. Error bars represent means ± SD for n = 3.

The results of the subsequent phase were consistent with the effect shown in the fractional factorial design and were the opposite of the burst release. The zero-order release phase showed a decrease in TRD release from 24.5 (± 1.7) % to 11.9 (± 0.5) % as the PPF percentage was increased. The effect could be due to a decrease in concentration gradient as TRD is depleted from the microspheres in the burst phase or due to the slower degradation of PPF containing microspheres.

Effects of polymer viscosity

The results from the fractional factorial design showed that the polymer solution viscosity had a dominant effect on the burst release of TRD during the first 2 days. The cumulative release profiles obtained by isolating this parameter and varying it in a wider range were similar in shape to those in Figure 1. To better illustrate the correlation between burst release and initial microsphere characteristics, the release profiles were plotted against polymer viscosity (figure 4). The initial burst release varied from 13.4 (± 4.2) to 55.1 (± 5.0) % of the entrapped TRD by day 2, with a minimum obtained at a kinematic viscosity of 39 cSt. The release rates for the subsequent zero-order release phase were similar for different viscosities.

We have previously demonstrated that microspheres fabricated with a PPF/PLGA solution of 39 cSt were rounded with smooth surfaces and very few pores whereas those fabricated with higher or lower viscosities had porous surfaces.[8] In addition, maximal microsphere sizes were obtained at this viscosity. Figure 4 therefore correlates well with these previous observations: the burst release is minimized for microspheres with larger size and smooth, non-porous surfaces. At higher or lower viscosities, more TRD is available for rapid release due to decreased diffusion path length and increased effective surface area of porous or small sized microspheres. Our results are also consistent with previous studies that described a relation between the initial burst and the surface area of the microspheres, based on observations of an increased drug release as the microsphere size decreased.[16-20] Our results also suggest that by simply changing the PPF content in the PPF/PLGA blend (thus the viscosity of the polymer solution), the burst release could be modulated.

Effects of vortex speed

Figure 5 summarizes the normalized cumulative release profiles of 50:50 PPF/PLGA microspheres fabricated at different vortex speeds. All microsphere formulations exhibited a sustained release of the model drug for at least 38 days. The initial burst release was the lowest for the larger microspheres fabricated at vortex speed 3. However, no clear correlation between the stirring speed and the burst release was seen for the rest of the results, probably because its effects on the blend microspheres were more pronounced in size distribution than on average size.[8] The zero order release phase showed a decrease from 24.5 (± 1.7) to 18.0 (± 1.7) % in TRD release as the vortex speed increased from 3 to 8.

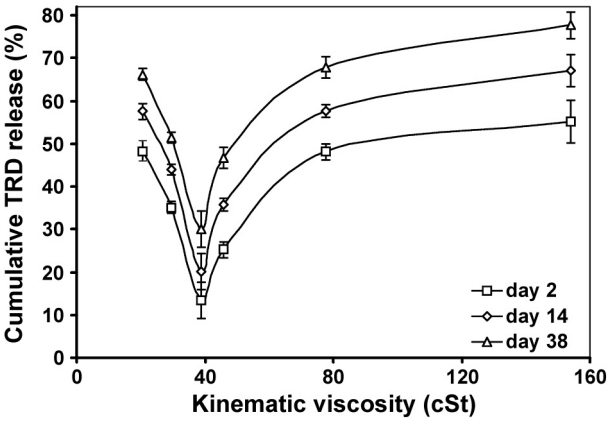

Figure 4: Effect of the viscosity of the polymer solution on the cumulative TRD release at 2, 14, and 38 days from 50/50 PPF/PLGA blend microspheres. Error bars represent means ± SD for n = 3.

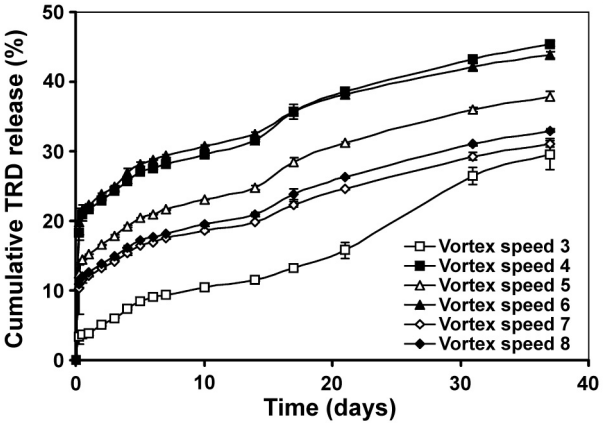

Figure 5: Cumulative release kinetics of TRD from 50/50 PPF/PLGA blend microspheres fabricated at different vortex speeds as indicated on Daigger Vortex Genie II instrument dial. The corresponding rotation speeds are given in Section 2.2. Error bars represent means ± SD for n = 3.

Effects of W1 phase

The effects of the amount of the internal water phase ranging from 50 to 450 µL on TRD release at day 2, 14, and 38 are shown in Figure 6. A maximal burst release of 35.7 (± 6.6) % of the entrapped TRD within the first 2 days was observed for PPF/PLGA microspheres fabricated at a W1 volume of 150 µL. Both an increase and a decrease of the volume led to a decreased TRD release during this phase. The effect of the internal aqueous volume on the burst release is determined by two mechanisms resulting in this maximum: inner matrix porosity and concentration gradient. Low volumes of the internal water result in a minimal microporosity of the polymer matrix, whereas high volumes result in increased micropores and channels thereby facilitating the rapid initial diffusion of TRD. However, our previous results showed that increasing the W1 volume resulted in slightly decreased entrapment efficiency, leading to decreased concentration gradient and therefore lower driving force for the burst release.[15,21] The subsequent zero-order phase release was similar for all formulations with TRD release ranged from 21.3 (± 0.6) to 27.1 (± 3.1) % between day 2 and day 38.

Microsphere degradation

The degradation of PPF and PLGA involves chain scissions of ester bond linkages in the polymer backbone by hydrolytic attack of water molecules.[10,22,23] The degradation products of PPF networks have been previously characterized to be propylene glycol, poly(acrylic acid-co-fumaric acid), and fumaric acid, a substance which occurs naturally as part of the Kreb's cycle.[23] PLGA has been known to degrade into lactic and glycolic acid, which are removed from the body by normal metabolic pathways.[22]

To study the aspects of microsphere degradation, five PPF/PLGA microsphere formulations containing 0, 25, 50, 75, and 100% PPF were fabricated using the W1/O/W2 double emulsion method. Figure 7 shows the mass loss profiles of various PPF/PLGA blend microspheres during 11 weeks of degradation in PBS. Initially, the weight remained relatively constant during the first 21 days. Then the PLGA microsphere weight started to decrease rapidly, losing 88.3% of its initial mass by day 77. In contrast, the PPF microsphere weight

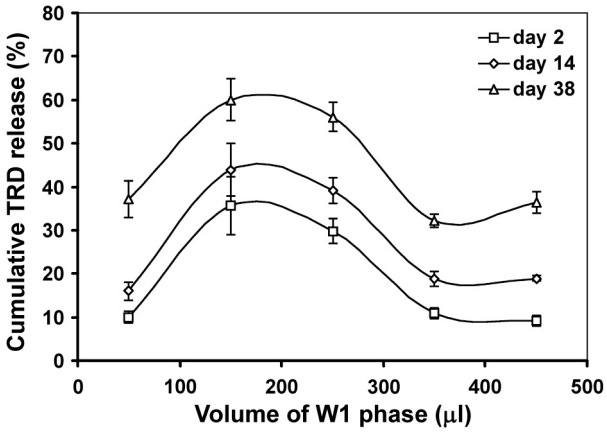

Figure 6: Effect of the amount of internal aqueous phase on the cumulative TRD release at 2, 14, and 38 days from 50/50 PPF/PLGA blend microspheres. Error bars represent means ± SD for n = 3.

dropped only 14.0% during this period. The mass loss profiles of the blend microspheres were in-between the two pure polymer formulations. As the percent of PPF in the blends increased, the remaining mass of the microspheres after 77 days of degradation also increased, indicating slower degradation. The weight of the microspheres consisting of 25, 50, and 75% PPF was reduced to 22.6, 48.6 and 74.7% of their initial mass at the end of the time course.

The molecular weight loss profiles over time for these same microspheres are shown in Figure 8. Unlike mass loss, the molecular weight of all formulations decreased immediately after placement in PBS. The most significant Mw loss was observed for the initial 28 days followed by slower decrease up to day 77. The Mw loss profiles followed a similar trend to the mass loss. Increasing the PPF percentage from 0 to 100% in the microspheres resulted in slower degradation and higher Mw at the end of the time course. The Mw of microspheres containing 0, 25, 50, 75, and 100% PPF was decreased to 7.5, 27.1, 30.7, 43.6, and 71.9% of the initial values after 77 days, respectively.

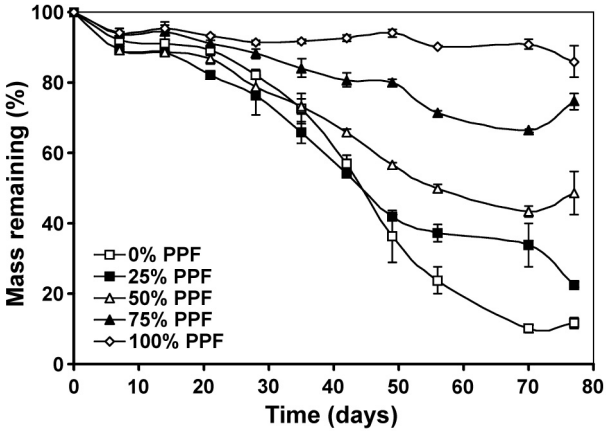

Figure 7: Normalized mass of various PPF/PLGA blend microspheres as a function of time. Error bars represent means ± SD for n = 3.

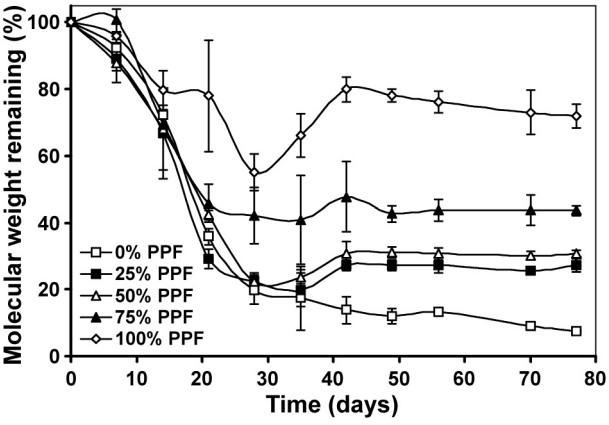

Figure 8: Normalized weight average molecular weight (Mw) of polymers in various PPF/PLGA blend microspheres as a function of time. Error bars represent means ± SD for n = 3.

The surface morphology of all microspheres during degradation was evaluated by SEM (figure 9). All formulations were initially spherical and had smooth surfaces with no visible external pores. However, the microspheres became more irregularly shaped after 14 and 28 days of degradation. As the percentage of PPF increased, the PPF/PLGA blend microspheres showed an increased coalescence and loss in spherical shape. In addition, the microspheres containing higher amounts of PPF developed numerous pores and dents upon degradation. These morphological changes correlated well with the TRD release profiles shown in Figure 3. For instance, although the blend microspheres containing 25% PPF degraded slower than PLGA microspheres, the higher surface area available for release due to the presence of pores throughout the microspheres led to higher burst release and higher overall TRD release.

Our results indicate that bulk degradation is the main degradation pathway for the PPF/PLGA blend microspheres. Because the diffusion rate of water into the system is much higher than the degradation rate of the polymer, the entire polymer matrix is rapidly hydrated and the polymer chains are cleaved throughout the microspheres. This bulk degradation mechanism is characterized by observations that molecular weight starts to

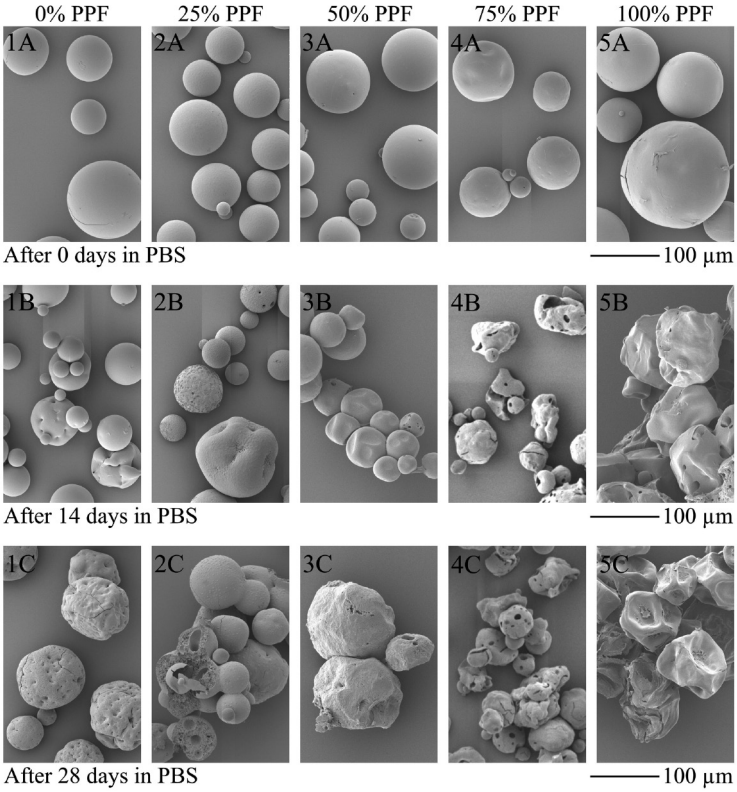

Figure 9: SEM pictures showing the surface morphology of degrading PPF/PLGA blend microspheres containing 0, 25%, 50%, 75%, and 100% PPF, as indicated by numbers 1, 2, 3, 4 and 5 on the images, respectively. The letters A, B and C correspond to the microspheres after 0, 14, and 28 days of degradation, respectively.

decrease immediately upon placement in PBS, whereas the microspheres did not start to lose weight until a critical molecular weight was reached. The bulk degradation mechanism has been previously shown for PLGA matrices and crosslinked PPF networks.[24-28]
In our study, PPF microspheres exhibited a slower degeneration rate as compared to PLGA. PPF has been noticed to be a more hydrophobic polymer[6,10], which results in less accessible hydrolysis-labile ester linkages and therefore slow degradation. The faster degradation of PLGA may be atributed to its higher reactivity with water and/or its greater hydrophilicity. It is also known that the ester bonds of PLGA copolymers linked with the glycolic acid unit (glycolic-glycolic, or glycolic-lactic) may be preferentially cleaved, as compared to those of lactic-lactic acid linked ester.[13-15,24]

Conclusion

In this study we demonstrated the effects of various processing parameters on the release kinetics of TRD from PPF/PLGA blend microspheres. The release studies showed that the viscosity of the oil phase was the most important factor affecting the burst release of the model drug. A clear correlation was seen between the total surface area of the microspheres and the burst release of the model drug. Other factors affecting the burst release were PPF/PLGA ratio (because of its effect on the viscosity of the oil phase) and the volume of the internal aqueous phase. The burst release was followed by a zero order-release phase that lasted for at least 38 days. The PPF/PLGA blend microspheres were shown to degenerate by a bulk degradation mechanism. An increase in PPF/PLGA ratio resulted in increased coalescence and loss in spherical shape of the microspheres. Increasing the percentage of PPF also resulted in slower mass and molecular weight loss profiles and therefore slower overall degradation.

References

1. Cao, X., and Schoichet, M.S. Delivering neuroactive molecules from biodegradable microspheres for application in central nervous system disorders. Biomaterials 20, 329, 1999.
2. Cleek, R.L., Ting, K.C., Eskin, S.G., and Mikos, A.G. Microparticles of poly(DL-lactic-co-glycolic acid)/poly(ethylene glycol) blends for controlled drug delivery. J Control Release 48, 259, 1997.
3. King, T.W., and Patrick, C.W., Jr. Development and *in vitro* characterization of vascular endothelial growth factor (VEGF)-loaded poly(DL-lactic-co-glycolic acid)/poly(ethylene glycol) microspheres using a solid encapsulation/single emulsion/solvent extraction technique. J Biomed Mater Res 51, 383, 2000.
4. Lu, L., Yaszemski, M.J., and Mikos, A.G. TGF-beta1 release from biodegradable polymer microparticles: its effects on marrow stromal osteoblast function. J Bone Joint Surg Am 83-A Suppl 1, S82, 2001.
5. Porter, B.D., Oldham, J.B., He, S.L., Zobitz, M.E., Payne, R.G., An, K.N., Currier, B.L., Mikos, A.G., and Yaszemski, M.J. Mechanical properties of a biodegradable bone regeneration scaffold. J Biomech Eng 122, 286, 2000.
6. Vehof, J.W., Fisher, J.P., Dean, D., van der Waerden, J.P., Spauwen, P.H., Mikos, A.G., and Jansen, J.A. Bone formation in transforming growth factor beta-1-coated porous poly(propylene fumarate) scaffolds. J Biomed Mater Res 60, 241, 2002.
7. Hedberg, E.L., Tang, A., Crowther, R.S., Carney, D.H., and Mikos, A.G. Controlled release of an osteogenic peptide from injectable biodegradable polymeric composites. J Control Release 84, 137, 2002.
8. Kempen, D.H., Lu, L., Zhu, X., Kim, C., Jabbari, E., Dhert, W.J., Currier, B.L., and Yaszemski, M.J. Development of biodegradable poly(propylene fumarate)/poly(lactic-co-glycolic acid) blend microspheres. I. Preparation and characterization. J Biomed Mater Res A 70A, 283, 2004.

9. Box, G., Hunter, W., and Hunter, J.S. Statistics for experimenters. New York: John Wiley & Sons Inc., 1978.
10. Timmer, M.D., Ambrose, C.G., and Mikos, A.G. *In vitro* degradation of polymeric networks of poly(propylene fumarate) and the crosslinking macromer poly(propylene fumarate)-diacrylate. Biomaterials 24, 571, 2003.
11. Lu, L., Stamatas, G.N., and Mikos, A.G. Controlled release of transforming growth factor beta1 from biodegradable polymer microparticles. J Biomed Mater Res 50, 440, 2000.
12. Yoon, J.J., and Park, T.G. Degradation behaviors of biodegradable macroporous scaffolds prepared by gas foaming of effervescent salts. J Biomed Mater Res 55, 401, 2001.
13. Wang, J., Wang, B.M., and Schwendeman, S.P. Characterization of the initial burst release of a model peptide from poly(D,L-lactide-co-glycolide) microspheres. J Control Release 82, 289, 2002.
14. Siepmann, J., Faisant, N., and Benoit, J.P. A new mathematical model quantifying drug release from bioerodible microparticles using Monte Carlo simulations. Pharm Res 19, 1885, 2002.
15. Yang, Y.Y., Chung, T.S., and Ng, N.P. Morphology, drug distribution, and *in vitro* release profiles of biodegradable polymeric microspheres containing protein fabricated by double-emulsion solvent extraction/evaporation method. Biomaterials 22, 231, 2001.
16. Akbuga, J. Effect of microsphere size and formulation factors on drug release from controlled release furosemide microspheres. Drug Dev Ind Pharm 17, 593, 1991.
17. Berkland, C., King, M., Cox, A., Kim, K., and Pack, D.W. Precise control of PLG microsphere size provides enhanced control of drug release rate. J Control Release 82, 137, 2002.
18. Cheng, Y.H., Illum, L., and Davis, S.S. A poly(D,L-lactide-co-glycolide) microsphere depot system for delivery of haloperidol. J Control Release 55, 203, 1998.
19. Obeidat, W.M., and Price, J.C. Viscosity of polymer solution phase and other factors controlling the dissolution of theophylline microspheres prepared by the emulsion solvent evaporation method. J Microencapsul 20, 57, 2003.
20. Roy, S., Pal, M., and Gupta, B.K. Indomethacin-loaded microspheres: design and preparation by a multiple-emulsification technique and their *in vitro* evaluation. Pharm Res 9, 1132, 1992.
21. Cohen, S., Yoshioka, T., Lucarelli, M., Hwang, L.H., and Langer, R. Controlled delivery systems for proteins based on poly(lactic/glycolic acid) microspheres. Pharm Res 8, 713, 1991.
22. Gopferich, A. Mechanisms of polymer degradation and erosion. Biomaterials 17, 103, 1996.
23. He, S., Timmer, M.D., Yaszemski, M.J., Yasko, A.W., Engel, P.S., and Mikos, A.G. Synthesis of biodegradable poly(propylene fumarate) networks with poly(propylene fumarate)-diacrylate macromers as crosslinking agents and characterization of their degradation products. Polymer 42, 1251, 2001.
24. Kenley, R.A., Lee, M.O., Mahoney, R., and Sanders, L.M. Poly(lactide-co-glycolide) decomposition kinetics *in vivo* and *in vitro*. Macromolecules 20, 2398, 1987.
25. Lu, L., Garcia, C.A., and Mikos, A.G. *In vitro* degradation of thin poly(DL-lactic-co-glycolic acid) films. J Biomed Mater Res 46, 236, 1999.
26. Lu, L., Peter, S.J., Lyman, M.D., Lai, H.L., Leite, S.M., Tamada, J.A., Vacanti, J.P., Langer, R., and Mikos, A.G. *In vitro* degradation of porous poly(L-lactic acid) foams. Biomaterials 21, 1595, 2000.
27. Makino, K., Ohshima, H., and Kondo, T. Mechanism of hydrolytic degradation of poly(L-lactide) microcapsules: effects of pH, ionic strength and buffer concentration. J Microencapsul 3, 203, 1986.
28. Park, T.G. Degradation of poly(lactic-co-glycolic acid) microspheres: effect of copolymer composition. Biomaterials 16, 1123, 1995.

5

Controlled drug release from a novel injectable biodegradable microsphere/ scaffold composite based on PPF

Journal of Biomedical Materials Research 2006;77A:103-111

D.H.R. Kempen
L. Lu
C. Kim
X. Zhu
W.J.A. Dhert
B.L. Currier
M.J. Yaszemski

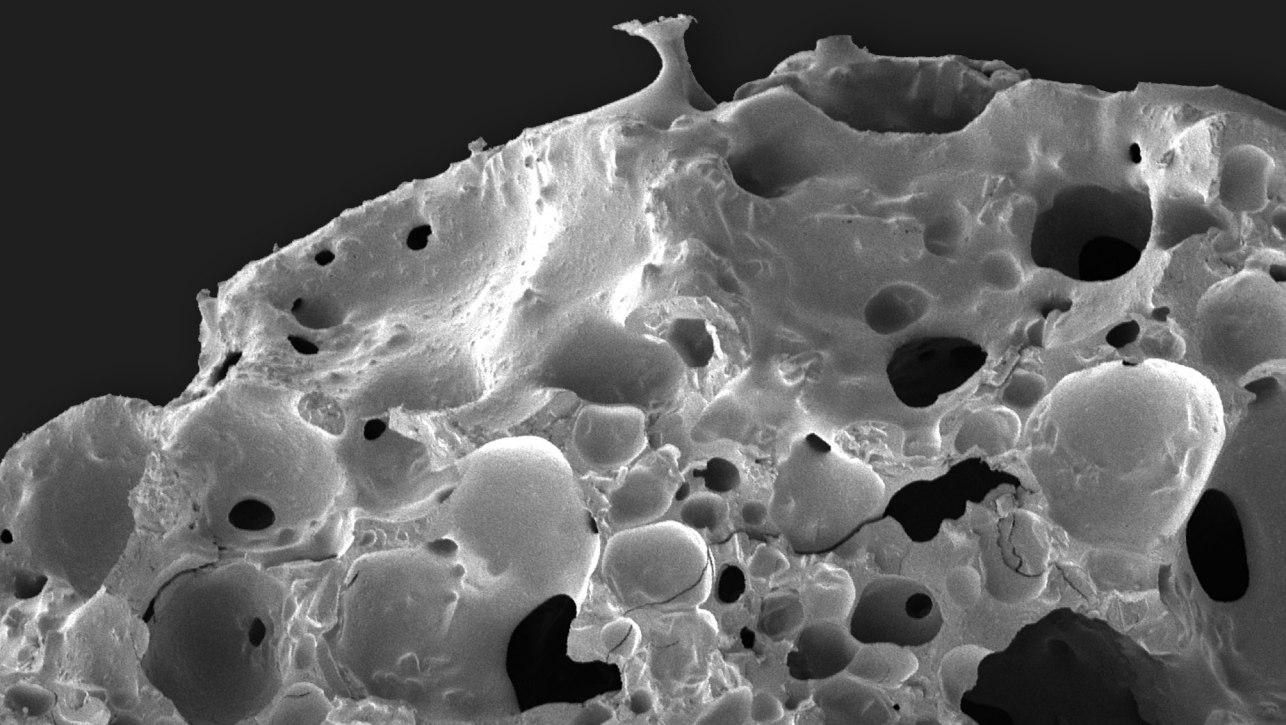

Abstract

The ideal biomaterial for the repair of bone defects is expected to have good mechanical properties, be fabricated easily into a desired shape, support cell attachment, allow controlled release of bioactive factors to induce bone formation, and biodegrade into nontoxic products to permit natural bone formation and remodeling. The synthetic polymer poly(propylene fumarate) (PPF) holds great promise as such a biomaterial. In previous work we developed poly(DL-lactic-co-glycolic acid) (PLGA) and PPF microspheres for the controlled delivery of bioactive molecules. This study presents an approach to incorporate these microspheres into an injectable, porous PPF scaffold. Model drug Texas red dextran (TRD) was encapsulated into biodegradable PLGA and PPF microspheres at 2 μg/mg microsphere. Five porous composite formulations were fabricated via a gas foaming technique by combining the injectable PPF paste with the PLGA or PPF microspheres at 100 or 250 mg microsphere per composite formulation, or a control aqueous TRD solution (200 μg per composite). All scaffolds had an interconnected pore network with an average porosity of 64.8 ± 3.6%. The presence of microspheres in the composite scaffolds was confirmed by scanning electron microscopy and confocal microscopy. The composite scaffolds exhibited a sustained release of the model drug for at least 28 days and had minimal burst release during the initial phase of release, as compared to drug release from microspheres alone. The compressive moduli of the scaffolds were between 2.4 and 26.2 MPa after fabrication, and between 14.9 and 62.8 MPa after 28 days in PBS. The scaffolds containing PPF microspheres exhibited a significantly higher initial compressive modulus than those containing PLGA microspheres. Increasing the amount of microspheres in the composites was found to significantly decrease the initial compressive modulus. The novel injectable PPF-based microsphere/scaffold composites developed in this study are promising to serve as vehicles for controlled drug delivery for bone tissue engineering.

Introduction

Bone injuries, genetic malformations and diseases often require the implantation of bone grafts. To date, autograft and allograft bone are the most frequently used grafts with a biological origin. Although autograft bone is the gold standard graft material, it is limited in supply, difficult to form into desired shapes and necessitates traumatic harvesting procedures.[1-3] Allograft bone is more readily available than autograft, but tends to be expensive. In addition, allografts have risks of rejection and/or disease transmission.[4,5] Materials such as metals or bone cement have also been used to fill bony defects but they are limited by stress shielding to the surrounding bone or fatigue failure of the implant.[6] Bone tissue engineering may potentially provide alternative solutions for creating completely natural living tissue and replace failing or malfunctional bone. Synthetic polymers have been used as scaffolds in many tissue engineering applications. The use of these polymers in bone tissue engineering strategies must address certain demands.[7] The mechanical properties must be similar to the bone tissue that is to be regenerated, to provide proper support in the early stages of healing. The material or its degradation products must be biocompatible to prevent an excessive inflammatory response or extreme immunogenecity or cytotoxicity. For proper bone formation, the material must be porous, osteoconductive and osteoinductive to allow cell migration and metabolism. Finally, the material must be sterilizable and the surgeon must be able to manipulate the material easily into a desired size and shape.

Our laboratory is investigating an injectable, biodegradable composite based on the synthetic polymer poly(propylene fumarate) (PPF). When combined with a cross-linker N-vinylpyrrolidone (NVP), an initiator benzoyl peroxide (BP), and an accelerator N,N-dimethyl-p-toluidine (DMT), PPF forms an injectable paste that can be polymerized *in situ*. PPF is biocompatible and osteoconductive, however, like most synthetic materials used for bone tissue engineering PPF is not osteoinductive.[8-10] A continuing challenge is the incorporation of bioactive factors into this material to render it osteoinductive. Several approaches are under investigation, for example, Payne and colleagues developed a technique whereby osteogenic cells could be incorporated into the polymer scaffold.[11-13] Another approach involved the modification of PPF with Gly-Arg-Gly-Asp (GRGD) peptide sequences to encourage host cell attachment and migration after injection of the construct.[14]

An alternative strategy is the incorporation of osteoinductive molecules, such as bone morphogenetic proteins (BMPs) or transforming growth factor-β (TGF-β), within the scaffold. For instance, Vehof and colleagues used radio frequency glow discharge to coat PPF scaffolds with TGF-β1.[15] This study demonstrated the potency of this molecule to stimulate bone formation by implanting these scaffolds in rabbit cranial defects. However, this technique is only applicable to preformed scaffolds. *In vitro* release studies also showed 100% of the protein was released within 1 week from the scaffolds by using this technique. These osteoinductive molecules can also be incorporated in biodegradable microspheres. Therefore, another approach to incorporate osteoinductive molecules into the scaffolds is using biodegradable microspheres.[16,17] These microspheres can be used as local delivery vehicles while maintaining the injectability of the PPF composite. Incorporating osteoinductive molecules in microspheres has the added advantage of controlled release over a longer period of time.

In previous studies, poly(lactic-co-glycolic acid) (PLGA) microspheres have been incorporated into a PPF scaffold.[16,17] However, the incorporation of PLGA microspheres re-

sulted in a decreased compressive modulus of the PPF scaffold.[17] In order to enhance the bonding between the particulate and the continuous phases of the composite scaffold, we have developed PPF-containing microspheres.[18,19] These microspheres are expected to covalently bind to the PPF matrix through the carbon-carbon double bonds along the polymer backbone on the microsphere surface. In the present study, we focused on the incorporation of these microspheres within an injectable, biodegradable PPF scaffold. We then evaluated the effects of microsphere incorporation (PLGA or PPF) and microsphere loading (100 or 250 mg per composite formulation) on the scaffold properties and release kinetics of a model drug.

Materials and methods

Materials

Polymer preparation and composite scaffold fabrication: Propylene glycol, fumaryl chloride, N-vinyl pyrrolidinone, potassium carbonate, and benzoyl peroxide were purchased from Acros (Pittsburgh, PA). Fumaryl chloride was purified through distillation at 1 atm with a boiling point range of 161 to 164 ℃. Potassium carbonate was ground to a fine powder with mortar and pestle. Chloroform and petroleum ether for polymer purification were purchased from Fisher (Pittsburgh, PA). Citric acid and sodium bicarbonate for the gas foaming process were purchased from Sigma–Aldrich (St. Louis, MO). The remaining chemicals were used as received.

Microsphere fabrication: Poly(lactic-co-glycolic acid) with a 50:50 lactic to glycolic acid ratio and a weight-average molecular weight (Mw) of 46,000 was purchased from Alkemers (Medisorb Cincinnati, OH). Poly(vinyl alcohol) (PVA, 87-89% mole hydrolyzed, Mw=13,000-23,000) and isopropanol (IPA) were obtained from Sigma-Aldrich. The model drug Texas red dextran (TRD) (Molecular Probes, Leiden, The Netherlands) with a molecular weight of 40,000 Dalton was chosen for encapsulation because of its similar molecular weight to a bone morphogenetic protein.

Experimental design

In the present study we varied the microsphere type (PLGA or PPF) and microsphere loading (100 or 250 mg per composite formulation) in the fabrication of microsphere/scaffold composite. As a control, pure TRD was incorporated as an aqueous solution to create a homogeneous mixture of the model drug throughout the scaffold. A total of five composite formulations were fabricated as described in Table 1. The composites were characterized for porosity, surface morphology, particle/TRD distribution, compressive modulus and release kinetics of the model drug. All measurements were performed in triplicates and the data were expressed as means ± standard deviations (SD).

Poly(propylene fumarate) synthesis

PPF was synthesized using established techniques described previously.[20] Briefly, a fumaryl chloride (FuCl) solution in chloroform (2:1 v/v) was added dropwise to a mixture of propylene glycol (PG), potassium carbonate (K_2CO_3), and chloroform with 1:3 FuCl:PG

Table I
Five formulations of composite scaffold used in the experiment

Formulations	*TRD loading*	*Microsphere loading in composite*	*TRD loading per composite*	*Entrapment Efficiency*	*TRD amount per composite*
PLG-L	1 mg per 500 mg PLGA microspheres	100 mg	200 μg	79.8 ± 4.2%	160 mg
PLG-H	1 mg per 500 mg PLGA microspheres	250 mg	500 μg	79.8 ± 4.2%	399 mg
PPF-L	1 mg per 500 mg PPF microspheres	100 mg	200 μg	78.9 ± 5.3%	158 mg
PPF-H	1 mg per 500 mg PPF microspheres	250 mg	500 μg	78.9 ± 5.3%	395 mg
TRD-L	20 μl of a 10 mg/ml solution in composite	None	200 μg	100%	200 mg

and 1:1.5 FuCl:K_2CO_3 molar ratios to form a short chain oligomer. The resulting oligomer solution was centrifuged to remove the K_2CO_3, and then purified through solution precipitation in chloroform and petroleum ether. The oligomer was then subjected to a transesterification reaction at 160 ℃ and 100-110 mmHg. Upon termination of the reaction, the product was dissolved in chloroform. Precipitation into petroleum ether and subsequent drying on a rotoevaporator produced a viscous, amber-colored polymer. The PPF used for microsphere fabrication and scaffold fabrication had number average molecular weights of 4,800 and 2,500 Daltons and polydispersity indices of 1.7 and 1.8, respectively.

Microsphere fabrication

A water-in-oil-in water (W1-O-W2) double-emulsion-solvent-extraction technique was used for microsphere preparation.[21] Briefly, 500 mg of polymer (PLGA or PPF) was dissolved in a certain amount of dichloromethane (2 ml or 0.8 ml, respectively) in a glass test tube. The resulting viscosity of the polymer solution was approximately 39 centistokes. While continuously vortexing the polymer solution at 3050 rpm (speed 7, Daigger Vortex Genie 2, Fisher, Pittsburg, PA), 1.0 mg of TRD dissolved in 100 μl distilled, deionized water (ddH_2O) was injected to create the first emulsion. The entire mixture was re-emulsified for 30 seconds in 4 ml of 1% w/v aqueous PVA solution to create the double emulsion. The content of the test tube was then poured into a 250 ml glass beaker containing 100 ml of a 0.3 % w/v aqueous PVA solution and 100 ml of a 2% w/v aqueous IPA solution. The beaker was placed on a magnetic stirrer (Corning, Acton, MA) for 1 hour. The microspheres were then collected by centrifugation, washed with ddH_2O, finally vacuum-dried (Savant Speedvac systems, Holbrook, NY) and stored at -20℃ prior to use.

Microsphere characterization

Prior to incorporation of the microspheres in the scaffold, the surface morphology, size distribution and entrapment efficiency of the model drug were investigated as previously described in chapter 3.

Scaffold fabrication

Porous PPF scaffolds with incorporated microspheres or an aqueous TRD solution were fabricated using the foaming technique described by Lewandrowski and colleagues, with minor modifications.[22] Briefly, 1.0 g of PPF was dissolved overnight in 0.7 ml of NVP in a small glass vial. The PPF/NVP mixture was transferred to a 10 ml disposable syringe with a 14 gauge needle. First, 200 mg of dry $NaHCO_3$ and 5 mg BP was added and mixed well with a spatula. Second, 100 or 250 mg of microspheres containing TRD as described above were added and mixed. To assess TRD release from the scaffold without microspheres, 20 µl of a 10 mg/ml aqueous TRD solution was added directly to the PPF scaffold. Subsequently, 100 µl concentrated (6.9M) citric acid solution containing 4 µl DMT was added to the PPF/NVP/$NaHCO_3$/BP/microsphere mixture and rapidly stirred. During stirring the foaming reaction could be observed immediately. The plunger was inserted and the composite was injected into a 6-well Teflon-coated mold to create multiple scaffolds. The composite was allowed to polymerize at room temperature for approximately 1 hr then lyophilized overnight. The next day the scaffolds were removed from the wells and the tops and bottoms were cropped to create uniform cylinders of approximately 5 mm in diameter and 15 mm in length.

Scaffold characterization

To determine the porosity of the composite scaffolds, the weight (W), diameter, and height of the lyophilized scaffolds were measured. Total volume of the composites (V) was calculated from the measured dimensions. The scaffold porosity was calculated from the following equation similar to that described by Goldstein and colleagues:[23]

$$\text{Porosity} = \left[1 - \frac{W_{composite} / \rho_{solid}}{V_{composite}} \right] \times 100\%$$

where is calculated based on the weight fraction of PLGA and PPF in the composite formulations according to table 1 using = 1.374 g/ml and = 1.244 g/ml.

A confocal laser scanning microscope (CLSM, Zeiss LSM510, Carl Zeiss, Germany), equipped with filters for 364 nm and 543 nm excitation wavelengths was used to observe the PPF scaffold and TRD drug distribution, respectively. Thin slices cut from dry scaffolds were placed on coverslips and depth projection micrographs were taken through optical sectioning.

The elastic modulus was determined in a non-destructive fashion using a dynamic mechanical analyzer (DMA 2980, TA Instruments, New Castle, DE). All cylinders were tested on the DMA machine under unconfined compression at a rate of 10 N/min to a maximum compression of 18 N. The slope of the stress-strain rate was used to calculate the compression moduli.

In vitro TRD release

Scaffolds with embedded microspheres or dispersed TRD were placed in microcentrifuge tubes containing 1.5 ml of pH 7.4 phosphate buffered saline (PBS) and maintained at 37℃ with orbital shaking for 28 days. At the end of 0.5, 1, 2, 3, 5, 8, 11, 14, 18, 23 and 28 days, the supernatant was collected and replaced by fresh PBS. The samples were assayed for TRD concentration using spectophotometry.

Statistical analysis

All data on entrapment efficiency, porosity, TRD release, and mechanical testing are reported as means ± standard deviations (SD) for n = 3. Single factor analysis of variance (ANOVA) was used to assess the statistical significance of the results. Scheffé's method was employed for multiple comparison tests at significance levels of 95%.

Results and discussion

Microsphere characterization

Using a double emulsion-solvent extraction technique, microspheres were fabricated from biodegradable polymers PLGA and PPF. The entrapment efficiency of TRD in the PLGA and PPF microspheres was 79.8 ± 4.2 % and 78.9 ± 5.4 %, respectively. The PLGA microspheres had a diameter varying between 4 and 121 µm, with an average of 33.3 ± 29.1 µm. The diameter of the PPF microspheres ranged from 1 to 110 µm with an average of 43.4 ± 28.3 µm. The size of these microspheres renders them suitable for injection through a 14 gauge needle to fabricate microsphere/scaffold composites.
Scanning electron microscopy revealed spherical microspheres with varied surface morphologies (figure 1). The PPF microspheres had small pores on their surfaces. Some of the PPF microspheres had cracks in their surface or were broken open to reveal the inner honeycomb like structure. The PLGA microspheres with a diameter of approximately 60 µm or less had smooth surfaces, whereas most of the larger particles had a slightly irregular or porous surface.

Scaffold characterization

The porous cylindrical scaffolds fabricated in this study had a diameter of 5.5 ± 0.2 mm, a length of 14.6 ± 0.9 mm and a weight of 158.8 ± 37.7 mg. The polymeric materials were easy to handle during the fabrication process and the gas foaming technique was reproducible. The ease of handling is of great importance for clinical use of any biomaterial.

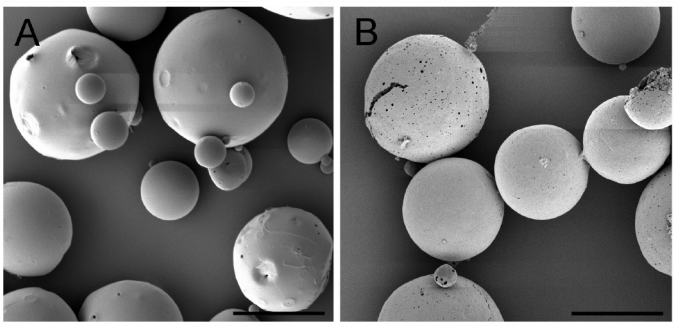

Figure 1: Scanning electron micrographs showing the surface morphology of (A) PLGA and (B) PPF microspheres before incorporation into the PPF scaffold.

The fabrication technique and material properties gave us the ability to easily manipulate the placement of the material because of the effortless injection through a small needle. Mixing the components in a syringe takes approximately 5 minutes and after injection and an additional 5 to 15 minutes are needed for the composite to polymerize. This will give sufficient time to place the material before hardening while also minimizing the length of the procedure.

Composite scaffolds incorporating PLGA and PPF microspheres were highly porous as revealed by SEM (figure 2A and figure 2B, respectively). Partially or fully embedded PLGA microspheres were clearly seen in the PPF polymer matrix (figure 2C). The embedded PPF microspheres were more difficult to distinguish in the composite probably due to covalent bonding between the PPF microspheres and the PPF scaffold. Confocal micrographs showed that PLGA and PPF microspheres were dispersed within the PPF matrix (figure 3A and figure 3B, respectively). Scaffolds fabricated with the aqueous TRD solution also showed TRD distribution throughout the scaffold matrix.

Both SEM and confocal microscopy revealed interconnected pores with a wide variation in pore sizes. Scaffold porosity is important in tissue engineering since it provides space for cells to migrate into the construct and space for intracellular matrix formation.

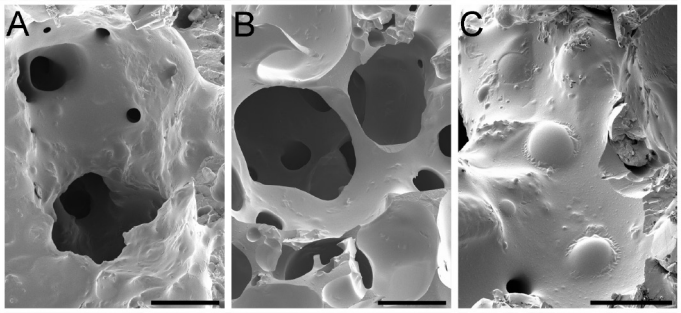

Figure 2: Scanning electron micrographs showing an interconnected pore structure of (A) PPF scaffold containing PLGA microspheres and (B) PPF scaffold containing PPF microspheres. The embedded PLGA microspheres in the PPF matrix could be clearly seen in (C). The PPF microspheres were not visible probably due to covalent bonding at the microsphere-scaffold interface. The microsphere loading in both scaffolds was 250 mg per composite.

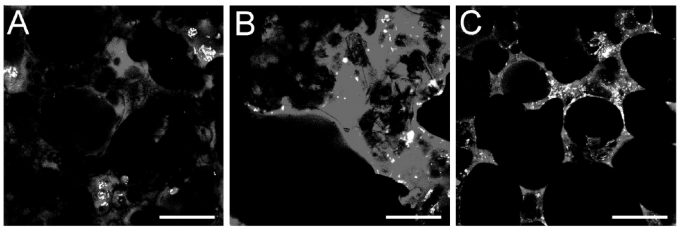

Figure 3: Confocal micrographs showing the distribution of Texas red dextran (white) in the PPF scaffolds (grey) containing (A) PLGA microspheres (PLG-L), (B) PPF microspheres (PPF-L), and (C) the aqueous TRD solution embedded in the scaffold matrix (TRD-L). The different formulations are given in Table 1.

Interconnectivity of the pores provides better permeability for inflow of nutrients and elution of metabolic waist products and degradation products out of the scaffold. The porosity of the scaffolds varied between 61.8 ± 2.0 % and 70.7 ± 3.6 %. Figure 4 shows the average porosity of the five different composite formulations. There was no significant difference ($p > 0.05$) in porosity between these composites containing either PLGA microspheres, PPF microspheres, or the TRD solution. By varying the foaming parameters such as $Na\ HCO_3$ and citric acid amounts in future studies, the extent of gas foaming could be altered thereby controlling the porosity of the scaffold.[24-26] This provides an alternative method of easily adjusting the scaffold porosity in a clinical setting.

To study the effect of microsphere incorporation on the compressive modulus, the foaming parameters ($NaHCO_3$ and citric acid) were kept at a constant level in the present study. The scaffold strength is also known to vary according to the synthetic method, crosslinking agents used and the addition of other components such as particulates or fibers.[7] The initial compressive modulus of the composite scaffolds varied between 3.6 ± 1.0 and 13.9 ± 2.5 MPa (figure 5). Scaffolds containing PPF microspheres had significantly higher ($p < 0.05$) compressive modulus than those containing PLGA microspheres, at both microsphere loading densities. This higher modulus was attributed to the interfacial

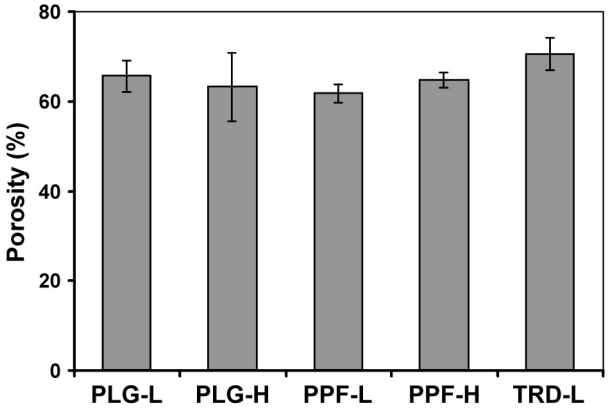

Figure 4: Porosity of the PPF composites containing 100 mg or 250 mg of PLGA or PPF microspheres and the composite containing an aqueous TRD solution. The different formulations are given in Table 1.

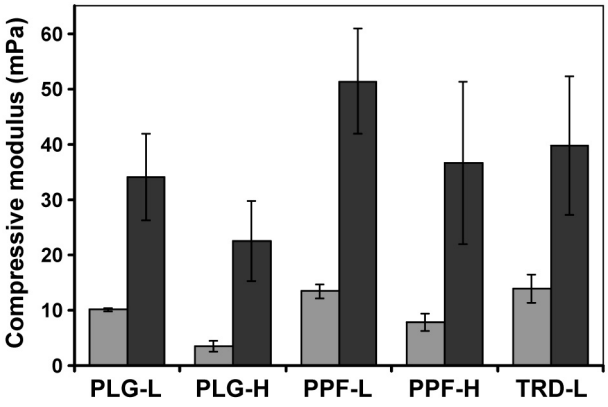

Figure 5: The compressive modulus of PPF composites containing PLGA microspheres, PPF microspheres or containing an aqueous TRD solution before and after 28 days of degradation in PBS. The different formulations are given in Table 1.

covalent bonding between PPF microspheres and the PPF matrix. The PLGA microspheres were simply dispersed and physically trapped in the matrix without covalent bonding. For both PLGA and PPF microspheres, increasing the microsphere loading from 100 to 250 mg resulted in significant decrease ($p < 0.05$) in the overall composite modulus.
After 28 days of incubation in PBS, all scaffolds showed a significant increase ($p < 0.05$) in compressive modulus with values ranging from 22.5 ± 7.3 to 51.3 ± 9.5 MPa. No significant difference ($p > 0.05$), however, was observed between the five composite formulations. Although PPF undergoes bulk degradation during this time period, the continued crosslinking of the double carbon-carbon bonds along the PPF backbone actually results in increased mechanical properties. This phenomenon has been previously reported for other PPF scaffold formulations.[27]

In vitro TRD release kinetics

The release kinetics of TRD from the different composites was determined following their immersion in PBS at 37℃. Figure 6 shows the TRD release profiles from the PLG-L, PPF-L and TRD-L composites (figure 6A) and the PLG-H and PPF-H composites (figure 6B). All scaffolds exhibited a sustained release of the model drug for at least 28 days. After a few days in PBS, the initially floating scaffolds settled on the bottom of the tubes. The TRD is released from the scaffolds in two phases: (1) an initial burst release, and (2) a sustained release phase. The burst phase, lasting approximately 5 days, ranged from 15.8 ± 1.2 to 30.2 ± 4.1 μg TRD/g scaffold. After 28 days the release varied between 37.6 ± 1.5 % and 68.2 ± 7.8. μg TRD/g scaffold.
The PPF-L and TRD-L scaffolds had a similar amount of released TRD over the 28-day period (figure 6A), which was significantly lower ($p < 0.05$) than the release from PLG-L scaffolds. The model drug is expected to diffuse through three layers of matrix in order to be released from the microsphere/scaffold composites: (1) the microsphere matrix, (2) the microsphere/scaffold interface, and (3) the crosslinked PPF scaffold. Incorporation of PLGA microspheres results in relatively fast release as drug diffusion goes through the PLGA microsphere matrix, an un-crosslinked interface, and scaffold matrix. The release from scaffolds containing PPF microspheres is much slower, as the PPF microsphere phase is more hydrophobic and the microsphere/scaffold is crosslinked due to interfacial covalent bonding. In the control TRD-L scaffolds, the drug needs to diffuse entirely through the tightly crosslinked PPF matrix, leading to a slower release.
The influence of the type of scaffold matrix on TRD release seemed to diminish when the microsphere loading was increased from 100 to 250 mg/g composite scaffold. As shown in Figure 6B, TRD release from PLG-H and PPF-H composites was similar ($p > 0.05$), reaching a cumulative release of approximately 60 μg/g composite after 28 days. In addition, increasing the microsphere loading significantly ($p < 0.05$) increased the released TRD amount from PPF-H composites as compared to PPF-L composites. However, no significant ($p > 0.05$) difference was found between the PLG-L and PLG-H groups.
Although the release kinetics from the composite scaffolds showed a similar biphasic pattern as PLGA or PPF microspheres previously reported from our group, the burst release phase was significantly lower from the scaffolds resulting in a more linear and sustained release.[16-19] For PLGA microspheres, the initial burst release lasted 5 days when imbedded in scaffolds instead of 2 days for microspheres only, which was caused by rapid release of TRD at or near the surface. After 5 days, approximately 11.8 ± 1.6 % and 28.8 ± 1.0 % of entrapped TRD were released from PLG-H scaffolds and PLGA mi-

crospheres alone, respectively. Similarly, the burst release was significantly lower for PPF microspheres after embedding in the scaffold. Approximately 11.3 ± 0.9 % was released from PPF-H scaffolds as compared to 69.7 ± 1.9 % from PPF microspheres alone. The slower, more sustained release observed from the scaffold composites were due to the slower penetration of PBS into PPF scaffolds and an additional layer for diffusion caused by the scaffold matrix surrounding the microspheres. The slowest burst release during the first 5 days was seen in the scaffolds containing the aqueous TRD solution (10.8 ± 0.8 %). The slow diffusion may be attributed to the tightly crosslinked PPF network surrounding the aqueous droplets.

In previous studies PLGA microspheres have been incorporated into injectable PPF and calcium phosphate scaffolds and showed similar decreased release phases of encapsulated osteoinductive molecules.[16,28] However, incorporation of these PLGA microspheres resulted in a decreased mechanical strength of the composite scaffolds.[17,28] Direct encapsulation of molecules in polymer networks is also a promising method for their controlled release. In arthroplasty surgery antibiotics could be mixed within an injectable polymethylmethacrylate bone cement to prevent infections and reduce possible systemic toxicity of the antibiotics.[29,30] Although our results of direct incorporation of TRD in the PPF scaf-

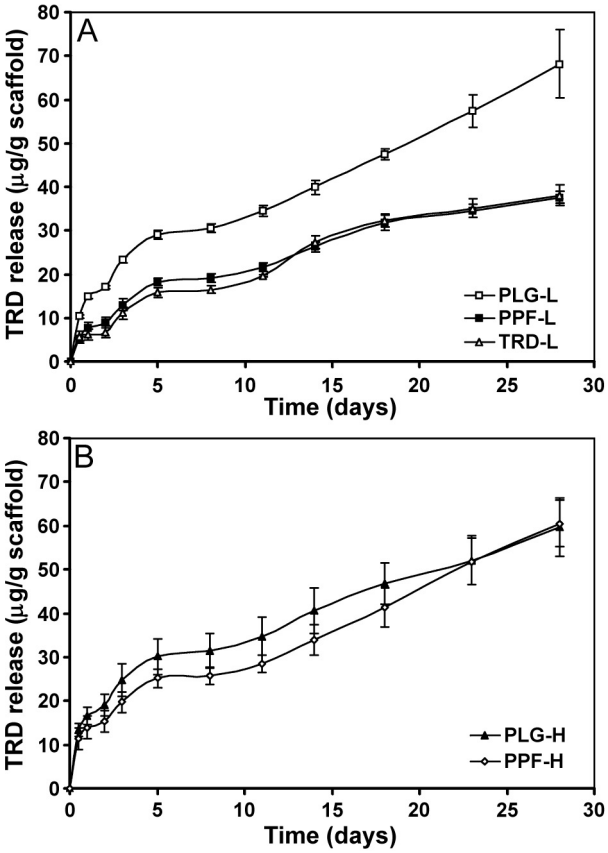

Figure 6: Release kinetics of TRD from the PPF composites containing (A) 100 mg of PLGA or PPF microspheres or the aqueous TRD solution; or (B) 250 mg of PLGA or PPF microspheres. The different formulations are given in Table 1.

fold also looked promising, we do not yet expect it to be applicable for growth factors. Previous studies have shown no cell survival of marrow stromal osteoblasts when exposed directly to the crosslinking reaction.[11] Free radicals and reactive PPF and NVP groups may react directly with BMP molecules resulting in a decreased bioactivity. Microspheres are expected to protect the encapsulated growth factors from the initial unfavorable condition of the polymerization reaction and thereby preserve their bioactivity. However, molecules that can withstand these conditions could be directly incorporated in the scaffold for controlled release. PPF polymerization reaction is slightly exothermic and previous studies have shown that the temperatures never reach above 48 ℃.[31] These temperatures are not likely to be deleterious to BMP molecules.[32]

Conclusion

PPF holds great promise for use as an injectable, biodegradable composite for filling skeletal defects. The ability to mix the prefabricated components in a syringe and the effortless injection of the composite through a small needle indicated good handling properties of PPF. The incorporation of PLGA microspheres in the PPF scaffolds resulted in a significant decrease in the initial compressive modulus of the composite. By replacing the PLGA microspheres with PPF ones, the mechanical properties could be increased due to covalent bonding of these microspheres to the PPF scaffold. Our results also showed that microspheres incorporated within the PPF composite could be used as a local delivery system. Compared to drug release from PLGA and PPF microsphere alone, the microsphere/scaffold composites had a significantly lower burst release thereby releasing the TRD in a controlled fashion over a longer period of time.

References

1. Coventry, M.B., and Tapper, E.M. Pelvic instability: a consequence of removing iliac bone for grafting. J Bone Joint Surg Am 54, 83, 1972.
2. Damien, C.J., and Parsons, J.R. Bone graft and bone graft substitutes: a review of current technology and applications. J Appl Biomater 2, 187, 1991.
3. Gazdag, A.R., Lane, J.M., Glaser, D., and Forster, R.A. Alternatives to Autogenous Bone Graft: Efficacy and Indications. J Am Acad Orthop Surg 3, 1, 1995.
4. Buck, B.E., Malinin, T.I., and Brown, M.D. Bone transplantation and human immunodeficiency virus. An estimate of risk of acquired immunodeficiency syndrome (AIDS). Clin Orthop Relat Res, 129, 1989.
5. Norman-Taylor, F.H., and Villar, R.N. Bone allograft: a cause for concern? J Bone Joint Surg Br 79, 178, 1997.
6. Masuda, T., Yliheikkila, P.K., Felton, D.A., and Cooper, L.F. Generalizations regarding the process and phenomenon of osseointegration. Part I. *In vivo* studies. Int J Oral Maxillofac Implants 13, 17, 1998.
7. Temenoff, J.S., and Mikos, A.G. Injectable biodegradable materials for orthopedic tissue engineering. Biomaterials 21, 2405, 2000.
8. Fisher, J.P., Vehof, J.W., Dean, D., van der Waerden, J.P., Holland, T.A., Mikos, A.G., and Jansen, J.A. Soft and hard tissue response to photocrosslinked poly(propylene fumarate) scaffolds in a rabbit model. J Biomed Mater Res 59, 547, 2002.
9. Peter, S.J., Lu, L., Kim, D.J., and Mikos, A.G. Marrow stromal osteoblast function on a poly(propylene fumarate)/beta-tricalcium phosphate biodegradable orthopaedic composite. Biomaterials 21, 1207, 2000.
10. Peter, S.J., Miller, S.T., Zhu, G., Yasko, A.W., and Mikos, A.G. *In vivo* degradation of a poly(propylene fumarate)/beta-tricalcium phosphate injectable composite scaffold. J Biomed Mater Res 41, 1, 1998.

11. Payne, R.G., McGonigle, J.S., Yaszemski, M.J., Yasko, A.W., and Mikos, A.G. Development of an injectable, *in situ* crosslinkable, degradable polymeric carrier for osteogenic cell populations. Part 2. Viability of encapsulated marrow stromal osteoblasts cultured on crosslinking poly(propylene fumarate). Biomaterials 23, 4373, 2002.
12. Payne, R.G., McGonigle, J.S., Yaszemski, M.J., Yasko, A.W., and Mikos, A.G. Development of an injectable, *in situ* crosslinkable, degradable polymeric carrier for osteogenic cell populations. Part 3. Proliferation and differentiation of encapsulated marrow stromal osteoblasts cultured on crosslinking poly(propylene fumarate). Biomaterials 23, 4381, 2002.
13. Payne, R.G., Yaszemski, M.J., Yasko, A.W., and Mikos, A.G. Development of an injectable, *in situ* crosslinkable, degradable polymeric carrier for osteogenic cell populations. Part 1. Encapsulation of marrow stromal osteoblasts in surface crosslinked gelatin microparticles. Biomaterials 23, 4359, 2002.
14. Jo, S., Engel, P.S., and Mikos, A.G. Synthesis of poly(ethylene glycol)-tethered poly(propylene-co-fumarate) and its modification with GRGD peptide. Polymer 41, 7595, 2001.
15. Vehof, J.W., Fisher, J.P., Dean, D., van der Waerden, J.P., Spauwen, P.H., Mikos, A.G., and Jansen, J.A. Bone formation in transforming growth factor beta-1-coated porous poly(propylene fumarate) scaffolds. J Biomed Mater Res 60, 241, 2002.
16. Hedberg, E.L., Tang, A., Crowther, R.S., Carney, D.H., and Mikos, A.G. Controlled release of an osteogenic peptide from injectable biodegradable polymeric composites. J Control Release 84, 137, 2002.
17. Kempen, D.H.R., Kim, C.W., Lu, L., Dhert, W.J.A., Currier, B.L., and Yaszemski, M.J. Controlled release from poly(lactic-co-glycolic acid) microspheres embedded in an injectable, biodegradable scaffold for bone tissue engineering. Materials Science Forum, 3151, 2003.
18. Kempen, D.H., Lu, L., Zhu, X., Kim, C., Jabbari, E., Dhert, W.J., Currier, B.L., and Yaszemski, M.J. Development of biodegradable poly(propylene fumarate)/poly(lactic-co-glycolic acid) blend microspheres. I. Preparation and characterization. J Biomed Mater Res A 70A, 283, 2004.
19. Kempen, D.H., Lu, L., Zhu, X., Kim, C., Jabbari, E., Dhert, W.J., Currier, B.L., and Yaszemski, M.J. Development of biodegradable poly(propylene fumarate)/poly(lactic-co-glycolic acid) blend microspheres. II. Controlled drug release and microsphere degradation. J Biomed Mater Res A 70A, 293, 2004.
20. Peter, S.J., Suggs, L.J., Yaszemski, M.J., Engel, P.S., and Mikos, A.G. Synthesis of poly(propylene fumarate) by acylation of propylene glycol in the presence of a proton scavenger. J Biomater Sci Polym Ed 10, 363, 1999.
21. Lu, L., Stamatas, G.N., and Mikos, A.G. Controlled release of transforming growth factor beta1 from biodegradable polymer microparticles. J Biomed Mater Res 50, 440, 2000.
22. Lewandrowski, K.U., Cattaneo, M.V., Gresser, J.D., Wise, D.L., White, R.L., Bonassar, L., and Trantolo, D.J. Effect of a poly(propylene fumarate) foaming cement on the healing of bone defects. Tissue Eng 5, 305, 1999.
23. Goldstein, A.S., Zhu, G., Morris, G.E., Meszlenyi, R.K., and Mikos, A.G. Effect of osteoblastic culture conditions on the structure of poly(DL-lactic-co-glycolic acid) foam scaffolds. Tissue Eng 5, 421, 1999.
24. Kim, C.W., Talac, R., Lu, L., Moore, M.J., Currier, B.L., and Yaszemski, M.J. Characterization of porous injectable poly-(propylene fumarate)-based bone graft substitute. J Biomed Mater Res A 85, 1114, 2008.
25. Nam, Y.S., Yoon, J.J., and Park, T.G. A novel fabrication method of macroporous biodegradable polymer scaffolds using gas foaming salt as a porogen additive. J Biomed Mater Res 53, 1, 2000.
26. Yoon, J.J., and Park, T.G. Degradation behaviors of biodegradable macroporous scaffolds prepared by gas foaming of effervescent salts. J Biomed Mater Res 55, 401, 2001.
27. Peter, S.J., Nolley, J.A., Widmer, M.S., Merwin, J.E., Yaszemski, M.J., Yasko, A.W., Engel, P.S., and Mikos, A.G. *In vitro* degradation of a poly(propylene fumarate)/beta-tricalcium phosphate composite orthopedic scaffold. Tissue Eng 3, 207, 1997.
28. Ruhe, P.Q., Hedberg, E.L., Padron, N.T., Spauwen, P.H., Jansen, J.A., and Mikos, A.G. rhBMP-2 release from injectable poly(DL-lactic-co-glycolic acid)/calcium-phosphate cement composites. J Bone Joint Surg Am 85-A Suppl 3, 75, 2003.
29. Espehaug, B., Engesaeter, L.B., Vollset, S.E., Havelin, L.I., and Langeland, N. Antibiotic prophylaxis in total hip arthroplasty. Review of 10,905 primary cemented total hip replacements reported to the Norwegian arthroplasty register, 1987 to 1995. J Bone Joint Surg Br 79, 590, 1997.
30. van de Belt, H., Neut, D., Schenk, W., van Horn, J.R., van der Mei, H.C., and Busscher, H.J. Infection of orthopedic implants and the use of antibiotic-loaded bone cements. A review. Acta Orthop Scand 72, 557, 2001.

31. Peter, S.J., Kim, P., Yasko, A.W., Yaszemski, M.J., and Mikos, A.G. Crosslinking characteristics of an injectable poly(propylene fumarate)/beta-tricalcium phosphate paste and mechanical properties of the crosslinked composite for use as a biodegradable bone cement. J Biomed Mater Res 44, 314, 1999.
32. Sato, T., Iwata, H., Takahashi, M., and Miura, T. Heat tolerance of activity toward ectopic bone formation by rabbit bone matrix protein. Ann Chir Gynaecol Suppl 207, 37, 1993.

6

Effect of autologous bone marrow stromal cell seeding and BMP-2 delivery on ectopic bone formation in a microsphere/PPF composite

Tissue Engineering Part A 2009;15:587-594

D.H.R. Kempen
M.C. Kruyt
L. Lu
C.E. Wilson
A.V. Florschutz
L.B. Creemers
M.J. Yaszemski
W.J.A. Dhert

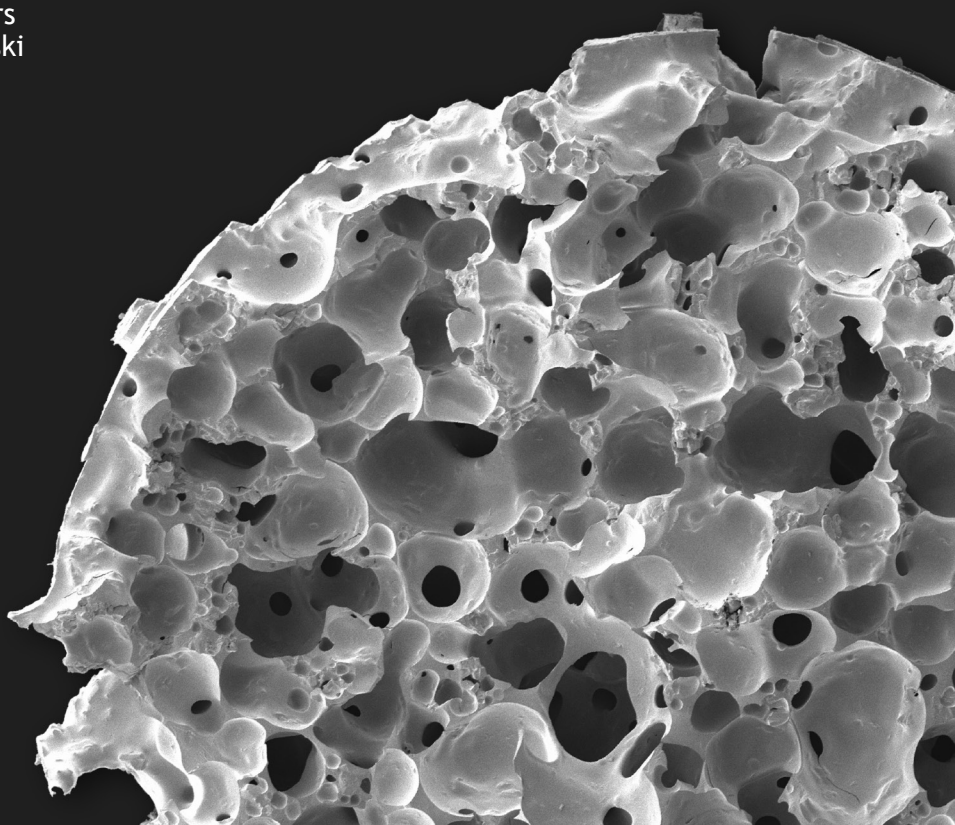

Abstract

A biodegradable microsphere/scaffold composite based on the synthetic polymer poly(propylene fumarate) holds promise as a scaffold for cell growth and sustained delivery vehicle for growth factors for bone regeneration. The objective of the current work was to investigate the *in vitro* release and *in vivo* bone forming capacity of this microsphere/scaffold composite containing bone morphogenetic protein 2 (BMP-2) in combination with autologous bone marrow stromal cells (BMSCs) in a goat ectopic implantation model. Three composites consisting of 0, 0.08 or 8 μg BMP-2 per mg of poly(lactic-co-glycolic acid) (PLGA) microspheres, embedded in a porous poly(propylene fumarate) (PPF) scaffold, were combined with either plasma (no cells) or culture-expanded BMSCs. PPF scaffolds impregnated with a BMP-2 solution and combined with BMSCs as well as empty PPF scaffolds were also tested. The 8 different composites were implanted subcutaneously in the dorsal thoracolumbar area of goats. Incorporation of BMP-2 loaded microspheres in the PPF scaffold resulted in a more sustained *in vitro* release with a lower burst phase, as compared to BMP-2 impregnated scaffolds. Histological analysis after 9 weeks of implantation showed bone formation in the pores of 11/16 composites containing 8 μg/mg BMP-2 loaded microspheres with no significant difference between composites with or without BMSCs (6/8 and 5/8, respectively). Bone formation was also observed in 1/8 of the BMP-2 impregnated scaffolds. No bone formation was observed in the other conditions. Overall, this study shows the feasibility of bone induction by BMP-2 release from microspheres/scaffold composites.

Introduction

Bone tissue engineering is a challenging field that strives to create alternative methods for current autograft and allograft treatments to restore bone defects or reinforce existing malfunctioning bone. Current strategies are mainly based on three components: (1) scaffolds, (2) (progenitor) cells and (3) growth and differentiation factors. A three-dimensional biodegradable scaffold is the starting point for most regenerative strategies, providing initial mechanical strength and a framework for attachment and proliferation of cells. The cells are responsible for the matrix deposition that precedes ossification and can be locally recruited after implantation or seeded before implantation. Growth factors can be added to the scaffold to induce cell differentiation towards the osteogenic lineage. These tissue engineering strategies have proven to be successful in many studies; however, up-scaling bone tissue engineering towards clinical applications remains challenging.

The ideal biomaterial for bone regeneration should have good mechanical properties, support cell attachment and differentiation, and allow controlled release of bioactive factors for the modulation of cellular function. Furthermore, the scaffold must biodegrade into non-toxic products to permit natural bone formation and remodelling. Poly(propylene fumarate) (PPF) based materials are promising as biodegradable scaffolds for filling skeletal defects.[1-3] Crosslinking of the linear polyester PPF through double bonds along its polymer backbone, results in a biocompatible, biodegradable scaffold with mechanical properties similar to human trabecular bone.[4-6] The injectable nature of the material makes it easy to shape the scaffold into a desired interconnected porous structure.[7,8] Crosslinked PPF scaffolds have shown to be suitable substrates for the *in vitro* proliferation and osteoblastic differentiation of bone marrow stromal cells (BMSCs).[9,10] Although these material characteristics are favorable for bone regeneration, PPF scaffolds are not osteoinductive. Making PPF scaffolds osteoinductive by adding the appropriate growth factors would be an improvement.

Bone morphogenetic protein-2 (BMP-2) is a very potent growth factor capable of inducing bone formation in both orthotopic and ectopic implantation sites.[11-14] However, due to its short *in vivo* half live and localized actions, BMP-2 requires a delivery vehicle to sustain its release at the implantation site. Biodegradable poly(lactic-co-glycolic acid) (PLGA) microspheres are ideal candidates for such a sustained release of BMP-2.[1] Previous studies have shown that BMP-2 can be successfully encapsulated into PLGA microspheres with retention of its bioactivity.[15] Furthermore, the PLGA microspheres could be incorporated into PPF scaffolds to form microsphere/scaffold composites with a decreased burst release of loaded molecules.[1]

The purpose of this study was to investigate the effect of the incorporation of BMP-2 loaded microspheres in PPF scaffolds in a goat ectopic implantation model. In order to test whether the addition of progenitor cells would influence the bone regeneration capacity of the composite, some of the scaffolds were combined with autologous BMSCs before implantation.

Materials and methods

Experimental design

Five different porous PPF scaffolds were prepared consisting of: scaffolds alone (Blank) , scaffolds impregnated with a solution containing 50 µg BMP-2 ($BMP^{impregnated}$) and scaffolds with incorporated PLGA microspheres containing 0, 0.08 or 8.0 µg BMP-2/mg PLGA (Mps^{empty}, Mps-BMP^{low} and Mps-BMP^{high}, respectively - Table 1). A 50 µg dose of BMP-2 was used for the $BMP^{impregnated}$ scaffolds since this was approximately the initial amount used for the fabrication of the Mps-BMP^{high} scaffolds. The *in vitro* BMP-2 release profile from the scaffolds was determined in PBS. The composites were combined with autologous plasma containing either no cells or autologous BMSCs and implanted ectopically in goats. After 9 weeks, the composites were harvested and characterized for tissue ingrowth, bone formation and porosity by histology and histomorphometry.

Materials

PLGA (75:25 lactic to glycolic ratio, Mw=62 kDa, Medisorb®, Lakeshore Biomaterials, Birmingham, AL), poly(vinyl alcohol) (PVA, 87-89% mole hydrolyzed, Mw=13,000-23,000, Sigma-Aldrich, St. Louis, MO) and isopropanol (IPA, Sigma-Aldrich) were used for the microsphere preparation. PPF with a molecular weight of 3,100 and a polydispersity index of 2.7 was synthesized by a two-step reaction process as previously described.[2] N-vinylpyrrolidinone (NVP, Acros, Pittsburgh, PA) and bis(2,4,6-trimethylbenzoyl) phenylphosphine oxide (BAPO, Ciba Specialty Chemicals, Tarrytown, NY) were used for the scaffold fabrication. BMP-2 (kindly provided by Wyeth Pharmaceuticals, Madison, NJ) was concentrated by centrifuging at 5000 G in a Centricon-10 filter unit (Amicon, Beverly, MA) and reconstituted to the appropriate concentrations in an aqueous buffer (pH 4.5) consisting of 5 mM glutamate, 5 mM NaCl, 0.5% sucrose, 2.5% glycine and 0.01% polysorbate 80 (all Sigma-Aldrich). An enzyme-linked immunosorbent assay (ELISA, Quantikine BMP-2 Immunoassay®, R&D Systems, Minneapolis, MN) was used for the entrapment efficiency and release assay.

Table 1
Experimental groups and implant composition

	PPF Scaffold	*Cells*	*Initial mps loading (µg BMP/mg PLGA)*	*Composite (Mps/PPF/porogen) (%)*	*BMP/ scaffold (µg)*	*Number of Scaffolds*
1	Blank	No cells	No mps	0/30/70	0	4
2	$BMP^{impregnated}$	BMSCs	No mps	0/30/70	50	8
3	Mps^{empty}	No cells	0	6/24/70	0	8
4	Mps^{empty}	BMSCs	0	6/24/70	0	8
5	Mps-BMP^{low}	No cells	0.08	6/24/70	0.04-0.38	8
6	Mps-BMP^{low}	BMSCs	0.08	6/24/70	0.04-0.38	8
7	Mps-BMP^{high}	No cells	8.0	6/24/70	39	8
8	Mps-BMP^{high}	BMSCs	8.0	6/24/70	39	8

Mps = microparticles; PLGA = poly(lactic-co-glycolic acid); BMP = bone morphogenetic protein-2; PPF = poly(propylene fumara
BMSCs = bone marrow stromal cells

Microsphere fabrication

A water-in-oil-in water (W1-O-W2) double-emulsion-solvent-extraction technique was used for microsphere preparation.[15] Briefly, 50 µl of a 0, 0.40 or 40 mg/ml BMP-2 solution was emulsified in a solution of 250 mg PLGA in 1 ml dichloromethane using a vortexer at 3050 rpm. The entire mixture was re-emulsified for 30 seconds in 2 ml of 1% w/v aqueous PVA solution to create the double emulsion. The content was then added to 100 ml of 0.3 % w/v aqueous PVA solution and 100 ml of 2% w/v aqueous IPA solution with stirring for one hour. The extraction of the dichloromethane to the external alcohol phase resulted in precipitation of the dissolved polymers and subsequently the formation of microspheres. The microspheres were collected by centrifugation, washed twice with ddH_2O, and finally vacuum-dried. The resulting powder was stored at -20℃ prior to use.

Scaffold fabrication

Porous PPF scaffolds were fabricated using a salt leaching technique. Sodium chloride particles sieved to a size range of 300-500 µm were used as porogen. Briefly, 60 µl of an initiator solution (100 mg/ml of BAPO in dichloromethane) was added to a solution of 0.9 g of PPF in 0.27 ml NVP and mixed well with a spatula. The PPF/NVP/BAPO paste was then combined with the appropriate microsphere formulation (0 or 6 % w/w) and 70 % w/w NaCl particles as indicated in Table 1. The mixture was forced into glass cylindrical vials with a diameter of 6 mm and placed under UV-light (PS135, Matcon, the Netherlands) for 30 minutes for photo-crosslinking. The cylindrical scaffolds were then cut into 3-mm thick disks and sterilized by ethanol evaporation. Finally, the disks were placed in phosphate buffered saline (PBS) for 12 hours to leach out the NaCl particles. Eight blank PPF scaffolds were impregnated with 19 µl of a solution containing 50 µg BMP-2. All implants were cryopreserved at –20℃ until use.

Microsphere and scaffold characterization

The entrapment efficiency of BMP-2 in the PLGA microspheres was determined by normalizing the actual amount of entrapped BMP-2 to the starting amount. Approximately 10 mg of microspheres was dissolved in 0.75 ml of dichloromethane and 0.75 ml of a strong desorption buffer consisting of 0.5 M arginine, 0.5 M NaCl and 50 mM K_2HPO_4. The BMP-2 was extracted over a period of 48 hours with a buffer change after 24 hours. The concentration of the extracted BMP-2 was analyzed by ELISA following the manufacturer's instruction. To determine the *in vitro* BMP-2 release profile, the scaffolds were placed in microcentrifuge tubes containing 1.0 ml of pH 7.4 PBS and maintained at 37℃ on an orbital shaker set at 100 rpm to ensure continuous mixing. At day 0.5, 1, 2, 3, 5, 7, 9, 13, 17, 21 and 24, the supernatant was collected, stored at -20°C and replaced with fresh PBS. The samples were assayed for BMP-2 concentration using the BMP-2 ELISA.

BMSC culture and seeding conditions

The animal experiments were approved by the Institutional Animal Care and Use Committee. Ten adult Dutch milk goats were obtained from a professional stockbreeder at least four weeks prior to surgery. Autologous BMSCs were derived and expanded three

weeks preoperatively. Briefly, bone marrow aspirates were taken from both iliac wings under general anesthesia. The BMSCs in the aspirates were culture-expanded in standard culture medium containing 15% fetal bovine serum (FBS, Gibco, Paisly, Scotland) and antibiotics (100 U/ml penicillin and 100 µg/ml streptomycin, Gibco, Paisly, Scotland) with media changes every 3 days. The proportion of BMSCs in the bone marrow aspirates was determined by a colony forming efficiency (CFU) assay in which nucleated cells from the aspirate were plated in two 25 cm^2 flasks at a density of 1 x 10^5 cells/cm^2. After 8 or 9 days, the colonies were washed with PBS, fixed in 8% formalin, stained with methylene blue and counted under an inverted microscope. The rest of the expanded cells were cryo-preserved after passage 2 in medium containing 30% FBS and 10% dimethylsulfoxide (DMSO, Sigma) in aliquots of 1 x 10^7 cells/ml until use.
On the day of surgery, aliquots of cryo-preserved cells were thawed on ice, washed with autologous serum and re-suspended in serum at a concentration of 1 x 10^6 cells/ml. The cell viability was determined by trypan blue exclusion. The BMSCs were transported to the operating room on ice in aliquots of 5.5 ml. During surgery, plasma was obtained by centrifuging 10 ml of venous blood at 1200 G in a plastic tube. The BMSCs aliquots were centrifuged at 300 G, the medium decanted and the cells were re-suspended in autologous plasma. Plasma with no cells or with BMSCs (0.5 x 10^6 cells/scaffold) was combined with the pre-wetted scaffolds and allowed to clot before implantation.

Surgical procedure

Each goat received six implants in the thoracolumbar area according to a randomized scheme (Table 2). Prior to surgery, the goats were sedated by an intravenous injection of detomidine and general inhalation anesthesia was provided by a halothane gas mixture. Six subcutaneous pockets were created in the dorsal thoracolumbar area by blunt dissection and filled with one of the implants according to a randomized scheme. To increase the statistical power to determine an effect of BMSCs, groups 5 and 6 and groups 7 and 8 (Table 1 and 2) were implanted pair-wise. The pockets were closed with a non-resorbable suture to indicate their location post-mortem. In addition to the subcutaneous implantations, in the course of separate studies, the goats also received ceramic implants intramuscularly and in osteoconduction chambers on the transverse processes of L3 and L5.[16,17] Postoperative pain relief was achieved by buprenorphin. To monitor the dynamics of calcification, the fluorochrome markers calcein green (10 mg/kg intravenously, Sigma-Aldrich), oxytetracyclin (32 mg/kg intramuscularly according to the manufacturer's instructions, Mycofarm, The Netherlands) and xylenol orange (80 mg/kg, intravenously, Sigma-Aldrich) were administered after 3, 5 and 7 weeks, respectively. At 9 weeks post-implantation, euthanasia was performed by an overdose of pentobarbital (Organon, The Netherlands).

Histology and histomorphometry

After explantation, the implants were fixed in a 4% phosphate buffered formaldehyde solution (pH = 7.4). The implants were dehydrated in graded series of alcohol and embedded in methylmethacrylate. After polymerization, sections were cut using a sawing microtome (Leica SP1600, Leica Microsystems, Nussloch, Germany) and stained with methylene blue/basic fuchsin or with hematoxylin/eosin for routine histology and his-

Table 2
Implantation scheme and location of the experimental groups

	Pocket contents						Pocket location		
Goat	1	2	3	4	5	6	Cranial		
1	M^{em} + C	M^{em}	B^{lo} + C	B^{lo}	B^{hi} + C	B^{hi}	1	Spine	4
2	B^{im} + C	Bl	M^{em} + C	M^{em}	B^{lo} + C	B^{lo}	2		5
3	B^{hi} + C	B^{hi}	B^{im} + C	Bl	M^{em} + C	M^{em}	3		6
4	B^{lo} + C	B^{lo}	B^{hi} + C	B^{hi}	B^{im} + C	M^{em}	Caudal		
5	M^{em}	M^{em} + C	B^{lo}	B^{lo} + C	B^{hi}	B^{hi} + C			
6	Bl	B^{im} + C	M^{em}	M^{em} + C	B^{lo}	B^{lo} + C			
7	B^{hi} + C	B^{hi}	M^{em}	B^{im} + C	Bl	M^{em} + C			
8	B^{lo} + C	B^{lo}	B^{hi} + C	B^{hi}	M^{em}	B^{im} + C			
9	M^{em} + C	B^{im} + C	B^{lo}+ C	B^{lo}	B^{hi} + C	B^{hi}			
10	B^{hi}	B^{hi} + C	M^{em}+ C	B^{im} + C	B^{lo} + C	B^{lo}			

B^{im} = $BMP^{impregnated}$; M^{em} = Mps^{empty}; M^{lo} = Mps-BMP^{low}; M^{hi} = Mps-BMP^{high}; Bl = blank;
C = autologous bone marrow stromal cells

tomorphometry. An additional unstained section was sawn for fluorescence microscopy. Using light and fluorescence microscopy, the general tissue response, bone formation and fluorochrome labels were evaluated. For histomorphometry, high resolution (300 dpi), low magnification (40 x) digital micrographs covering the complete implant were made of blinded sections. The areas of interest were pseudocolored and the colorized pixels were measured to calculate the percentage of scaffold porosity and bone area relative to the available pore space.

Statistical analysis

Both *in vitro* (n = 4) and *in vivo* (n = 4 or 8) results are reported as means ± standard deviations. Analysis of variance (ANOVA) with Bonferroni-corrected post-hoc tests were used to analyze differences in porosity between the experimental groups. A two-tailed paired Student's t-test was used to determine the effect of cells on the amount of newly formed bone in the Mps-BMP^{high} scaffolds (groups 7 and 8). All tests were performed by SPSS (version 13.0, SPSS Inc., Chicago, IL) and the level of significance was set at p = 0.05.

Results

Scaffold characterization

The entrapment efficiency of BMP-2 in the microspheres loaded at 8.0 µg/mg PLGA was 82 (± 3.6) % (n = 4), which resulted in a scaffold loading of approximately 39 µg BMP-2 per Mps-BMP^{high} implant. Despite the use of the strong desorption buffer and repetition of the extraction procedure, it was difficult to estimate the entrapment efficiency of the 0.08 µg/mg loaded microspheres. The entrapment efficiency of these microspheres varied between 8.1 and 78 % (n = 9). Based on these encapsulation yields, the amount of BMP-2 in the Mps-BMP^{low} scaffolds was estimated between 0.04 and 0.38 µg BMP-2 per implant. Since the BMP-2 loss during the impregnation process of the blank scaffolds was limited, the $BMP^{impregnated}$ scaffolds were loaded with 50 µg of BMP-2. This was also

approximately the starting amount for the fabrication of the Mps-BMP^{high} scaffolds.
The BMP-2 release profiles from the microsphere/scaffold composites and scaffolds impregnated with a BMP-2 solution are shown in figure 1. The BMP^{impregnated} scaffolds showed a considerable initial burst release of 34 (± 2.9) µg in the first day, followed by a rapid decline of the released amounts. The Mps-BMP^{high} scaffolds showed a much lower burst of 0.49 (± 0.07) µg in the first day, followed by a prolonged sustained release. The Mps-BMP^{low} scaffolds showed no measurable *in vitro* BMP-2 release during the first 2 days with a low sustained release for the rest of the experiment.

BMSC characterization

The bone marrow aspirates contained 5.6 (± 1.5) x 10^6 nucleated cells/ml which showed a colony forming efficiency of 1.9 (± 0.6) colonies per 1.0 x 10^5 cells. The doubling time of the proliferating BMSCs was 1.2 (± 0.6) days, resulting in cryopreservation of 60 to 100 million cells within 3 weeks after obtaining the aspirates. Trypan blue exclusion indicated 95% cell viability after thawing.

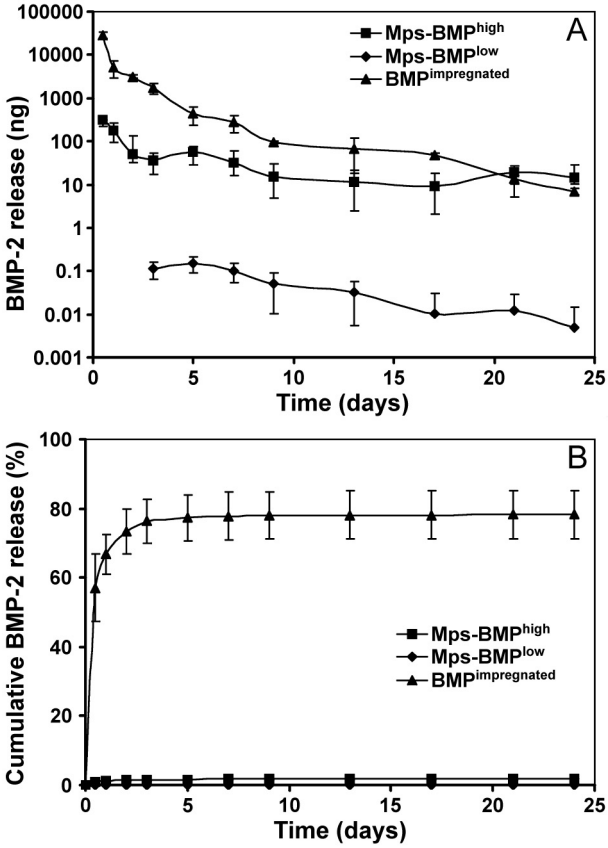

Figure 1: BMP-2 release profiles expressed as (A) Amount of released protein (in ng) and (B) normalized release (as % of initial loading) from different composites in PBS at 37℃.

Animals

During the experiments, all goats remained in good health and did not show any complications. After 9 weeks of implantation, all implants were easily identified and retrieved.

Histology

Microscopic evaluation of transverse sections showed that all composites maintained their original shape. All scaffolds were surrounded by fibrous tissue from which well vascularized connective tissue grew into the pores of the scaffold (figures 2A & 2B). Microfragmentation of PLGA was seen in the intact PPF network, indicating degradation of the microspheres (figure 2B). No signs of PPF degradation could be observed. The tissue response to the PLGA-PPF materials was relatively uniform. There was a mild foreign body reaction to the implanted materials as indicated by some inflammatory cells inside the pores of the scaffolds including macrophages and giant cells at the polymer-tissue interface.
Bone formation was observed in the pores of 11/16 of the Mps-BMP^{high} scaffolds and 1/8 of the BMP^{impregnated} scaffolds. No bone was formed in the blank, Mps^{empty} or Mps-BMP^{low} scaffolds. The newly formed bone was found throughout the implants, mainly clustered in the center of the pores with little contact between the bone and scaffold (Figs 2C & 2D). The bone had a woven or lamellar appearance, with osteocytes inside the matrix and osteoblasts lining the bone surfaces (Figs 2D & 2E). One of the BMP^{impregnated} scaffolds loaded with BMSCs showed trabecular bone in the fibrous capsule of the implant. Unfortunately, the excision margin of the other BMPimpregnated scaffolds was not large enough to investigate the bone formation outside the scaffold borders. Despite little auto-fluorescence of the tissue, no fluorochromes could be detected in the bone that had formed in the polymer scaffolds (figure 2F). Fluorescence microscopy did show all fluorochomes in scaffolds implanted in the same animals in the course of another study. This indicates the onset of bone mineralization was between 7 and 9 weeks, after the administration of the final fluorochrome.

Histomorphometry

Table 3 summarizes the measurements of scaffold porosity and bone formation for the different implant conditions. Bone formation was observed inside the pores of 1/8 of the BMP^{impregnated} scaffolds, 5/8 of the Mps-BMP^{high} scaffolds without cells and 6/8 of the Mps-BMP^{high} scaffolds with BMSCs. The porosity of the Blank/BMP^{impregnated} and Mps-BMP^{high} scaffolds was significantly higher compared to the Mps^{empty} and Mps-BMP^{low} scaffolds ($p < 0.05$). The bone formation in the Mps-BMP^{high} implants was 2.9 ± 3.0 % (varying from 0 to 7.2 %, n=8) and 2.7 ± 2.4 % (varying from 0 to 5.6 % n=8) of the available pore space for the scaffolds without cells and with BMSCs, respectively. BMSC seeding had no effect on bone formation. In the one PPF implant impregnated with BMP solution 0.2 % of the pore space was filled by newly formed bone.

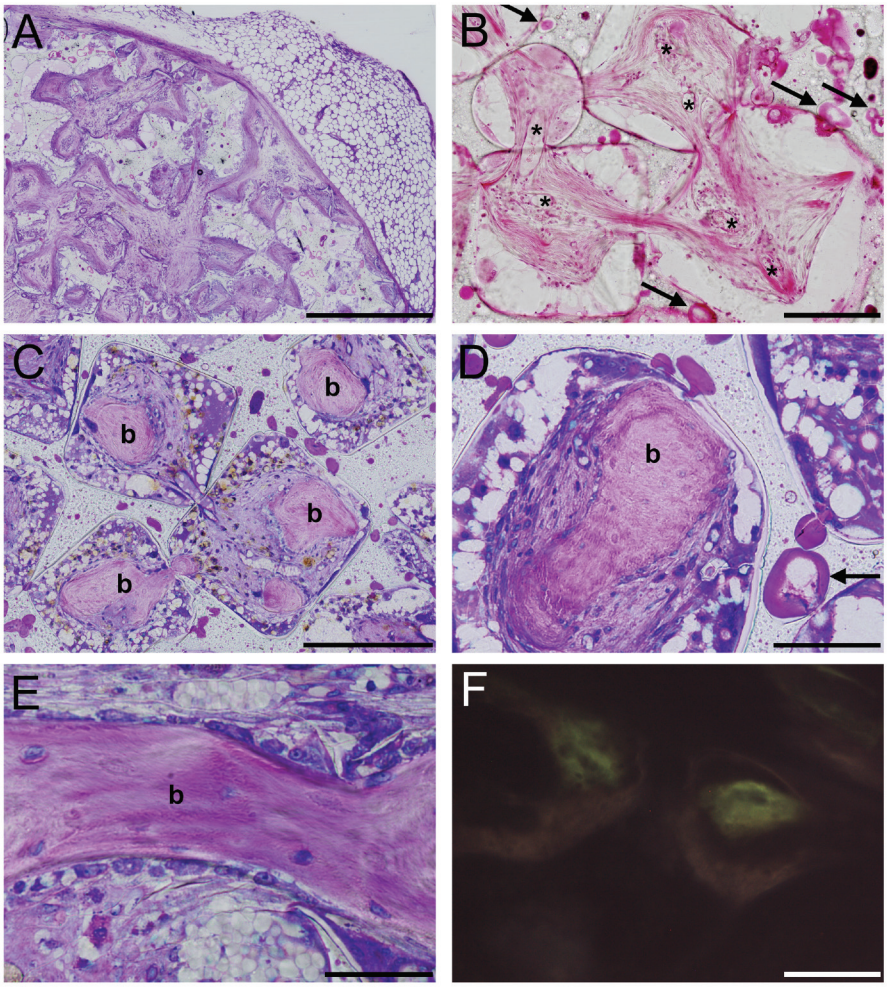

Figure 2: Methylene blue-basic fuchsine (A,C,D & E) and hematoxylin-eosin (B) stained or unstained (F) histological sections of (A,B) Mps-BMPlow and (C-F) Mps-BMPhigh composites after 9 weeks of subcutaneous implantation in goats. (A) Overview and (B) detailed view of an Mps-BMPlow implant showing ingrowth of well-vascularized fibrous tissue into the pores of the composite (vessels indicated by asterisks) and micro-fragmentation of PLGA in the intact PPF network (indicated by the central excavation and uneven staining of the microspheres at arrows). (C) Bone formation (indicated by letter b) was seen in the center of the pores of the Mps-BMPhigh implants. The bone had a woven (D) or lamellar (E) appearance, with osteocytes inside the matrix and osteoblasts on the surface. (F) Despite the little auto-fluorescence of the tissue, no fluorochromes could be detected in the newly formed bone. The scalebars represent 1 mm (A), 300 µm (C), 200 µm (B,F), 100 µm (D) and 50 µm (E).

Table 3
Histomorphometry results of the implants

	Scaffold	Cells	Porosity (%)	Bone (with bone/total)	Bone (% of pore space)
1	Blank	No cells	77.4 ± 4.5*	0/4	0
2	$BMP^{impregnated}$	BMSCs		1/8	0.0 ± 0.1
3	Mps^{empty}	No cells	71.7 ± 1.7	0/8	0
4	Mps^{empty}	BMSCs		0/8	0
5	Mps-BMP^{low}	No cells	73.1 ± 2.4	0/8	0
6	Mps-BMP^{low}	BMSCs		0/8	0
7	Mps-BMP^{high}	No cells	75.3 ± 2.2*	5/8	2.9 ± 3.0
8	Mps-BMP^{high}	BMSCs		6/8	2.7 ± 2.4

*Significantly higher than Mps^{empty} and Mps-BMP^{low} ($p<0.05$, ANOVA)
Mps = microparticles, BMP = bone morphogenetic protein-2, BMSCs = bone marrow stromal cells.

Discussion

This study demonstrates that PPF scaffolds can be rendered osteoinductive by incorporation of BMP-2 loaded PLGA microspheres. Compared to BMP-2 impregnated scaffolds, microsphere incorporation resulted in a lower burst and a more sustained *in vitro* release over a prolonged period of time. In contrast to the high burst release of the BMP-2 impregnated scaffolds, the sustained BMP-2 release from the PLGA microspheres resulted in a higher amount of ectopic bone in the scaffold pores after 9 weeks of implantation in goats. In the current experimental setup, the addition of autologous BMSCs before implantation had no significant effect on the osteoinductive capacity of the construct.

Previous *in vitro* studies have shown that PLGA microspheres are effective vehicles for sustained delivery of BMP-2.[15,18-20] The BMP-2 retention is based on physical entrapment as well as protein-polymer interactions as a result of ionic, hydrophobic and/or hydrogen-bonding.[18,19] During the fabrication process, the encapsulation and interactions lead to a reasonable encapsulation efficiency of the Mps-BMP^{high} microspheres. Probably due to the strong protein-polymer interactions, only a fraction of BMP-2 could be extracted from the Mps-BMP^{low} microspheres resulting in an underestimation of their entrapment efficiency. An alternative to the extraction/ELISA method for the entrapment efficiency measurements could be radioactive labeling of the BMP-2 prior to incorporation its into the microspheres. This method would obviate protein extraction and could also be used for the *in vitro* and *in vivo* release measurements.[21-27]

The PLGA microspheres were incorporated into the PPF scaffold in an attempt to better maintain local *in vivo* concentrations at osteoinductive levels for sufficient time. The impregnation of PPF scaffolds with a high BMP-2 dose is inherent to minimal retention and failed to consistently produce bone inside the scaffolds. In contrast, BMP-2 incorporation into PLGA microspheres resulted in a gradual *in vitro* release from the PPF composites. This gradual BMP-2 release was probably responsible for bone induction in the higher loaded microsphere/scaffold composites. Previous ectopic studies in rodents reported that BMP-2 induced bone formation was related to the dosage.[28-32] Apparently, the local BMP-2 concentrations in the composites with a lower loading were not sufficient to induce bone formation. Although the amounts released by the higher loaded scaffolds were sufficient to induce bone formation, both microsphere formulations released less than 2.5% of the incorporated BMP-2 in the first 24 days. Therefore, further optimization of the BMP-2 pharmacokinetics is required to obtain a release profile that coincides

better with the normal rate of bone formation.
Surprisingly, the peroperative seeding of autologous cryopreserved BMSCs on the composite formulations in this study did not enhance ectopic bone formation. Although the mechanism of bone induction in ceramics is completely different, the osteogenic potential of autologous BMSCs in goats was shown in ceramic scaffolds where they clearly enhanced ectopic bone formation.[16,33,34] Peroperative seeding of cryopreserved BMSCs resulted in similar amounts of newly formed bone in ceramic scaffolds as in pre-cultured constructs.[34] Therefore, this seeding method was also employed for this study to overcome complicated logistics for the preparation of preoperatively cultured constructs. Although the plasma polymerization during the preoperative seeding method resulted in a 100% cell loading efficiency and retention during implantation procedure, the behavior of the cells *in vivo* on the scaffolds applied in this study is unknown.
The absence of bone formation in the cell-seeded composites without BMP-2 was as expected, since these synthetic polymers do not possess osteoinductive characteristics in contrast to ceramics. Therefore, the initiation of the BMSC osteogenesis in the PPF scaffolds is likely to depend on BMP-2 signaling. However, the absence of an effect of autologous BMSCs on bone formation in BMP-2 loaded scaffolds is less clear. *In vitro* studies have shown that the osteogenic capacity of BMSCs in the presence of BMP-2 is dose-dependent.[35,36] Since the histological results show large amounts of non-resorbed PLGA in the PPF matrix after 9 weeks of follow up, the degradation of the PLGA microspheres and the subsequent release of the BMP-2 from the microspheres might have been too slow. This could have resulted in insufficient BMP-2 concentrations in the early days of implantation to induce differentiation of the seeded cells, since BMSC-derived osteogenesis normally starts within 3 weeks after implantation.[16] In the absence of such an osteoinductive stimulus, the undifferentiated BMSCs could have differentiated to the fibrous tissue in the microsphere/scaffold composite. The bone formation and late ossification by the BMP-2 released at a later time-point are probably derived from host cells that were locally recruited from for example the circulation.[37]
In conclusion, this study shows that sustained release of BMP-2 from microspheres contained in PPF scaffolds can induce ectopic bone formation in these scaffolds which are otherwise non-osteoinductive. In contrast to the enhanced ectopic bone formation on ceramic scaffolds by BMSCs, the addition of stem cells to the scaffolds in the current study did not further enhance bone formation, possibly due to a the slow rise of the local BMP concentration and a critical delay before the osteoinductive threshold dose is reached. Future studies should be aimed at improving the timing and rate of BMP-2 release to further stimulate the extent and rate of bone formation, either alone or in combination with mesenchymal stem cells.

References

1. Kempen, D.H.R., Kim, C.W., Lu, L., Dhert, W.J.A., Currier, B.L., and Yaszemski, M.J. Controlled release from poly(lactic-co-glycolic acid) microspheres embedded in an injectable, biodegradable scaffold for bone tissue engineering. Materials Science Forum, 3151, 2003.
2. Wang, S., Lu, L., and Yaszemski, M.J. Bone-tissue-engineering material poly(propylene fumarate): correlation between molecular weight, chain dimensions, and physical properties. Biomacromolecules 7, 1976, 2006.
3. Kempen, D.H.R., Kim, C.W., Lu, L., Dhert, W.J.A., Currier, B.L., and Yaszemski, M.J. Controlled release from poly(lactic-co-glycolic acid) microspheres embedded in an injectable, biodegradable scaffold

for bone tissue engineering. Material Science Forum 426-432, 3151, 2003.
4. Fisher, J.P., Vehof, J.W., Dean, D., van der Waerden, J.P., Holland, T.A., Mikos, A.G., and Jansen, J.A. Soft and hard tissue response to photocrosslinked poly(propylene fumarate) scaffolds in a rabbit model. J Biomed Mater Res 59, 547, 2002.
5. Hedberg, E.L., Kroese-Deutman, H.C., Shih, C.K., Crowther, R.S., Carney, D.H., Mikos, A.G., and Jansen, J.A. *In vivo* degradation of porous poly(propylene fumarate)/poly(DL-lactic-co-glycolic acid) composite scaffolds. Biomaterials 26, 4616, 2005.
6. Peter, S.J., Suggs, L.J., Yaszemski, M.J., Engel, P.S., and Mikos, A.G. Synthesis of poly(propylene fumarate) by acylation of propylene glycol in the presence of a proton scavenger. J Biomater Sci Polym Ed 10, 363, 1999.
7. Lee, K.W., Wang, S., Fox, B.C., Ritman, E.L., Yaszemski, M.J., and Lu, L. Poly(propylene fumarate) bone tissue engineering scaffold fabrication using stereolithography: effects of resin formulations and laser parameters. Biomacromolecules 8, 1077, 2007.
8. Lee, K.W., Wang, S., Lu, L., Jabbari, E., Currier, B.L., and Yaszemski, M.J. Fabrication and characterization of poly(propylene fumarate) scaffolds with controlled pore structures using 3-dimensional printing and injection molding. Tissue Eng 12, 2801, 2006.
9. Peter, S.J., Lu, L., Kim, D.J., and Mikos, A.G. Marrow stromal osteoblast function on a poly(propylene fumarate)/beta-tricalcium phosphate biodegradable orthopaedic composite. Biomaterials 21, 1207, 2000.
10. Peter, S.J., Lu, L., Kim, D.J., Stamatas, G.N., Miller, M.J., Yaszemski, M.J., and Mikos, A.G. Effects of transforming growth factor beta1 released from biodegradable polymer microparticles on marrow stromal osteoblasts cultured on poly(propylene fumarate) substrates. J Biomed Mater Res 50, 452, 2000.
11. Gerhart, T.N., Kirker-Head, C.A., Kriz, M.J., Holtrop, M.E., Hennig, G.E., Hipp, J., Schelling, S.H., and Wang, E. Healing segmental femoral defects in sheep using recombinant human bone morphogenetic protein. Clin Orthop Relat Res, 317, 1993.
12. Hollinger, J.O., Schmitt, J.M., Buck, D.C., Shannon, R., Joh, S.P., Zegzula, H.D., and Wozney, J. Recombinant human bone morphogenetic protein-2 and collagen for bone regeneration. J Biomed Mater Res 43, 356, 1998.
13. Vehof, J.W., Mahmood, J., Takita, H., van't Hof, M.A., Kuboki, Y., Spauwen, P.H., and Jansen, J.A. Ectopic bone formation in titanium mesh loaded with bone morphogenetic protein and coated with calcium phosphate. Plast Reconstr Surg 108, 434, 2001.
14. Weber, F.E., Eyrich, G., Gratz, K.W., Maly, F.E., and Sailer, H.F. Slow and continuous application of human recombinant bone morphogenetic protein via biodegradable poly(lactide-co-glycolide) foamspheres. Int J Oral Maxillofac Surg 31, 60, 2002.
15. Oldham, J.B., Lu, L., Zhu, X., Porter, B.D., Hefferan, T.E., Larson, D.R., Currier, B.L., Mikos, A.G., and Yaszemski, M.J. Biological activity of rhBMP-2 released from PLGA microspheres. J Biomech Eng 122, 289, 2000.
16. Kruyt, M.C., Dhert, W.J., Oner, F.C., van Blitterswijk, C.A., Verbout, A.J., and de Bruijn, J.D. Analysis of ectopic and orthotopic bone formation in cell-based tissue-engineered constructs in goats. Biomaterials 28, 1798, 2007.
17. Kruyt, M.C., Wilson, C.E., de Bruijn, J.D., van Blitterswijk, C.A., Oner, C.F., Verbout, A.J., and Dhert, W.J. The effect of cell-based bone tissue engineering in a goat transverse process model. Biomaterials 27, 5099, 2006.
18. Duggirala, S.S., Mehta, R.C., and DeLuca, P.P. Interaction of recombinant human bone morphogenetic protein-2 with poly(d,l lactide-co-glycolide) microspheres. Pharm Dev Technol 1, 11, 1996.
19. Schrier, J.A., and DeLuca, P.P. Recombinant human bone morphogenetic protein-2 binding and incorporation in PLGA microsphere delivery systems. Pharm Dev Technol 4, 611, 1999.
20. Schrier, J.A., Fink, B.F., Rodgers, J.B., Vasconez, H.C., and DeLuca, P.P. Effect of a freeze-dried CMC/PLGA microsphere matrix of rhBMP-2 on bone healing. AAPS PharmSciTech 2, E18, 2001.
21. Kempen, D.H., Lu, L., Classic, K.L., Hefferan, T.E., Creemers, L.B., Maran, A., Dhert, W.J., and Yaszemski, M.J. Non-invasive screening method for simultaneous evaluation of *in vivo* growth factor release profiles from multiple ectopic bone tissue engineering implants. J Control Release 130, 15, 2008.
22. Kempen, D.H., Lu, L., Hefferan, T.E., Creemers, L.B., Maran, A., Classic, K.L., Dhert, W.J., and Yaszemski, M.J. Retention of *in vitro* and *in vivo* BMP-2 bioactivities in sustained delivery vehicles for bone tissue engineering. Biomaterials 29, 3245, 2008.

23. Louis-Ugbo, J., Kim, H.S., Boden, S.D., Mayr, M.T., Li, R.C., Seeherman, H., D'Augusta, D., Blake, C., Jiao, A., and Peckham, S. Retention of 125I-labeled recombinant human bone morphogenetic protein-2 by biphasic calcium phosphate or a composite sponge in a rabbit posterolateral spine arthrodesis model. J Orthop Res 20, 1050, 2002.
24. Ruhe, P.Q., Boerman, O.C., Russel, F.G., Mikos, A.G., Spauwen, P.H., and Jansen, J.A. *In vivo* release of rhBMP-2 loaded porous calcium phosphate cement pretreated with albumin. J Mater Sci Mater Med 17, 919, 2006.
25. Uludag, H., D'Augusta, D., Palmer, R., Timony, G., and Wozney, J. Characterization of rhBMP-2 pharmacokinetics implanted with biomaterial carriers in the rat ectopic model. J Biomed Mater Res 46, 193, 1999.
26. Yamamoto, M., Takahashi, Y., and Tabata, Y. Controlled release by biodegradable hydrogels enhances the ectopic bone formation of bone morphogenetic protein. Biomaterials 24, 4375, 2003.
27. Yokota, S., Uchida, T., Kokubo, S., Aoyama, K., Fukushima, S., Nozaki, K., Takahashi, T., Fujimoto, R., Sonohara, R., Yoshida, M., Higuchi, S., Yokohama, S., and Sonobe, T. Release of recombinant human bone morphogenetic protein 2 from a newly developed carrier. Int J Pharm 251, 57, 2003.
28. Bessho, K., Carnes, D.L., Cavin, R., and Ong, J.L. Experimental studies on bone induction using low-molecular-weight poly (DL-lactide-co-glycolide) as a carrier for recombinant human bone morphogenetic protein-2. J Biomed Mater Res 61, 61, 2002.
29. Fujimura, K., Bessho, K., Kusumoto, K., Konishi, Y., Ogawa, Y., and Iizuka, T. Experimental osteoinduction by recombinant human bone morphogeneticprotein 2 in tissue with low blood flow: a study in rats. Br J Oral Maxillofac Surg 39, 294, 2001.
30. Matsushita, N., Terai, H., Okada, T., Nozaki, K., Inoue, H., Miyamoto, S., and Takaoka, K. A new bone-inducing biodegradable porous beta-tricalcium phosphate. J Biomed Mater Res A 70, 450, 2004.
31. Saito, N., Okada, T., Horiuchi, H., Murakami, N., Takahashi, J., Nawata, M., Ota, H., Nozaki, K., and Takaoka, K. A biodegradable polymer as a cytokine delivery system for inducing bone formation. Nat Biotechnol 19, 332, 2001.
32. Wang, E.A., Rosen, V., D'Alessandro, J.S., Bauduy, M., Cordes, P., Harada, T., Israel, D.I., Hewick, R.M., Kerns, K.M., LaPan, P., and et al. Recombinant human bone morphogenetic protein induces bone formation. Proc Natl Acad Sci U S A 87, 2220, 1990.
33. Kruyt, M.C., de Bruijn, J.D., Wilson, C.E., Oner, F.C., van Blitterswijk, C.A., Verbout, A.J., and Dhert, W.J. Viable osteogenic cells are obligatory for tissue-engineered ectopic bone formation in goats. Tissue Eng 9, 327, 2003.
34. Kruyt, M.C., de Bruijn, J.D., Yuan, H., van Blitterswijk, C.A., Verbout, A.J., Oner, F.C., and Dhert, W.J. Optimization of bone tissue engineering in goats: a peroperative seeding method using cryopreserved cells and localized bone formation in calcium phosphate scaffolds. Transplantation 77, 359, 2004.
35. Lecanda, F., Avioli, L.V., and Cheng, S.L. Regulation of bone matrix protein expression and induction of differentiation of human osteoblasts and human bone marrow stromal cells by bone morphogenetic protein-2. J Cell Biochem 67, 386, 1997.
36. Vehof, J.W., de Ruijter, A.E., Spauwen, P.H., and Jansen, J.A. Influence of rhBMP-2 on rat bone marrow stromal cells cultured on titanium fiber mesh. Tissue Eng 7, 373, 2001.
37. Otsuru, S., Tamai, K., Yamazaki, T., Yoshikawa, H., and Kaneda, Y. Bone marrow-derived osteoblast progenitor cells in circulating blood contribute to ectopic bone formation in mice. Biochem Biophys Res Commun 354, 453, 2007.

7

Non-invasive screening method for simultaneous evaluation of *in vivo* growth factor release profiles from multiple ectopic bone tissue engineering implants

Journal of Controlled Release 2008;130:15-21

D.H.R. Kempen
L. Lu
K.L. Classic
T.E. Hefferan
L.B. Creemers
A. Maran
W.J.A. Dhert
M.J. Yaszemski

Abstract

The purpose of this study was to develop and validate a screening method based on scintillation probes for the simultaneous evaluation of *in vivo* growth factor release profiles of multiple implants in the same animal. First, we characterized the scintillation probes in a series of *in vitro* experiments to optimize the accuracy of the measurement setup. The scintillation probes were found to have a strong geometric dependence and experience saturation effects at high activities. *In vitro* simulation of 4 subcutaneous limb implants in a rat showed minimal interference of surrounding implants on local measurements at close to parallel positioning of the probes. These characteristics were taken into consideration for the design of the probe setup and *in vivo* experiment. The measurement setup was then validated in a rat subcutaneous implantation model using 4 different sustained release carriers loaded with ^{125}I-BMP-2 per animal. The implants were removed after 42 or 84 days of implantation, for comparison of the non-invasive method to ex-vivo radioisotope counting. The non-invasive method demonstrated a good correlation with the ex-vivo counting method at both time-points of all 4 carriers. Overall, this study showed that scintillation probes could be successfully used for paired measurement of 4 release profiles with minimal interference of the surrounding implants, and may find use as non-invasive screening tools for various drug delivery applications.

Introduction

Over the past decades, the role of bioactive molecules in regenerative medicine has increased tremendously. As a result of modern genomic and proteomic technologies, increasing numbers of proteins are becoming available as potential candidates for the modulation of cellular behavior and tissue response. However, since most of these proteins have short *in vivo* half lives and exert their effect by acting locally on cells, they require a carrier system for localized and sustained delivery at the target site. Consequently, integration of drug delivery systems into biomaterial design has become a fundamental aspect of regenerative medicine.

Many biodegradable delivery systems have been developed for the controlled release of bioactive proteins. Since the biological responses to these proteins can be time- and concentration-dependent, the release profiles of these delivery systems are of crucial importance to their application. Most studies of newly developed carriers only characterized their *in vitro* protein release profiles. However, due to the differences between the *in vitro* and *in vivo* environment, the release profiles can change significantly upon implantation.[1-4] Therefore, new and reliable methods are needed to measure *in vivo* release profiles.

An effective method for determining *in vivo* pharmacokinetic profiles is provided by labeling proteins with radioactive tracers.[1,5-9] This allows quantification of protein release by correlating the remaining activity of the tracer in the implant to the amount of protein. The most accurate method for determining tracer activity is by conventional ex-vivo counting using the gamma counter. This *ex vivo* counting method is considered the gold standard because of the high spatial resolution and quantitative information, which allows the implantation of multiple implants per animal. Furthermore, the high sensitivity of the gamma counters allows the use of low isotope quantities.[10-12] However, ex-vivo quantification does not allow sequential measurements of the same implant or animal in time. Moreover, since the animals need to be sacrificed for the measurements, these pharmacokinetic studies often require large numbers of animals to obtain detailed release profiles.[10,13-16] Therefore, non-invasive methods that significantly reduce sample size and allow sequential measurements are being explored for determining release profiles.[3,4,17-21]

A feasible option for non-invasive determination of isotope content is the use of scintillation probes, which are commonly used devices to measure ionizing radiation. In nuclear medicine, they have been used for a long time to determine the iodine uptake of the thyroid to diagnose diseases of the thyroid gland. A recent validation study of the scintillation probe for non-invasive release measurement showed that it could also be reliably used as a screening tool for determining a single release profile of bioactive molecules.[17]

In this study, we validated this non-invasive screening method for the simultaneous evaluation of multiple *in vivo* release profiles by comparing it with the ex-vivo quantification method. The non-invasive method was validated in an ectopic implantation model in rats using four sustained release carriers delivering bone morphogenetic protein-2 (BMP-2). The *in vitro* and *in vivo* bioactivity of the released BMP-2 from these four carriers is reported in a separate manuscript.[22]

Materials and methods

Experimental design

First, the influence of the source-to-probe distance and counting rate linearity were characterized to optimize the accuracy of the measurement setup. Since the *in vivo* situation rarely allows perfect parallel positioning of the probes, we also determined the interference of multiple sources on the background signal at increasing deviations from parallel probe positioning (figure 1). The scintillation probe setup was then validated in an ectopic implantation model in 20 rats using four different local release carriers containing radioiodinated recombinant human bone morphogenetic protein-2 (BMP-2, Medtronic Sofamor Danek, MN). Release profiles as well as the excretion and blood profiles were determined over a period of 84 days. The implants were removed after 42 and 84 days of implantation for the comparison of the non-invasive method to the ex-vivo counting method. Post-mortem, several organs and the tissue surrounding the implant were evaluated for radioactivity to rule out local and systemic ^{125}I accumulation.

Detectors

The measurement setup consisted of four scintillation probes (Model 44-3 low energy gamma scintillator, Ludlum Measurements Inc., TX). The active portion of these probes contained a cylindrical sodium iodide (Tl) scintillator with a diameter of 2.5 cm and a thickness of 1 mm. The four probes were fixed in a frame and connected to a digital scaler with an adjustable timer (Model 1000 scaler, Ludlum Measurements Inc.). The probe was collimated with a hollow tube with a diameter of 2.6 cm and both the tube and active portion of the detector were wrapped in leaded tape. The high voltage of the detectors was adjusted to 0.8 (± 0.1) kV resulting in 2.9 x 10^5 (± 0.08 x 10^5) cpm for a 5.3 µCi ^{125}I point-source at a distance of 3 cm and a counting efficiency of 2.5 (± 0.1) %.
The *ex vivo* measurements were done using a gamma counter (Minaxi Auto Gamma 5000 series gamma counter, Packard Instruments, Downers Grove, IL) and radioisotope dose calibrator (CRC-5, Capintech. Montvale, NJ). The gamma counter and dose calibrator were calibrated using ^{125}I standards provided by the National Institute of Standards and Technology (NIST).

In vitro calibration of experimental setup

The influence of source-to-probe distance, counting rate linearity, and interference of surrounding sources were characterized using ^{125}I sources with different activities (figure 1). The sources were created by pipetting 1 to 50 µl of a Na^{125}I solution on absorbing wipes. The wipes were air-dried for 48 hrs before use and their activity was determined using the gamma counter and/or the dose calibrator. The influence of the implant-to-probe distance was determined with 0.4 and 4.0 µCi sources at increasing distances. The geometric efficiency was calculated by normalizing the counts to the estimated number of photons emitted by the source. For the other experiments we used a consistent distance of 3 cm.
The counting rate linearity of each detector was evaluated by measuring the counts of 20 sources with activities varying from 0.3 to 18 µCi. The interference of surrounding radioisotope sources on a local measurement was determined with the probes placed

at the corners of a 4.5 by 9 cm rectangle. This rectangle was based on measurements on cadaver rats which showed an estimated minimal distance of 4.5 cm between the left and right leg and a distance of 9 cm between front and hind leg. The background of each detector was measured in the presence and in the absence of a single 6.3 µCi radioactive source at one of the corners of the rectangle. The measurements were repeated with the source in each of the 4 corners and at angles of 0, 9, 18, 27 and 34 degrees of deviation from parallel placement of the probes. The background counts were normalized to the detector counts of the 6.3 µCi source at each position and expressed as percentage.

BMP-2 iodination

Recombinant human BMP-2 was radioiodinated with ^{125}I using Iodo-Gen® precoated test tubes according to the manufacturer's instructions (Pierce, Rockford, IL). Briefly, 100 µl of a 1.43 mg/ml BMP-2 solution, 20 µl of a 0.1 M NaOH solution and 2 mCi Na^{125}I were added to a 1,3,4,6-tetrachloro-3α,6α-diphenyl glycouril-coated glass test tube. The mixture was incubated for 15 minutes at room temperature with gentle shaking. To separate radiolabeled protein from free radioactive iodine, the solution was dialyzed (cutoff 10 kDa) for 24 hrs with 3 times media change against a buffer containing 5 mM glutamic acid, 2.5 wt% glycine, 0.5% sucrose and 0.01% Tween 80 (pH 4.5). The dialysis fractions of 3 radioiodination procedures were pooled and concentrated to a final concentration of 9.8 µCi/µl with a Vivaspin device (cutoff 10 kDa). Trichloroacetic acid (TCA) precipitation of the final ^{125}I-BMP-2 solution indicated 99% precipitable counts.

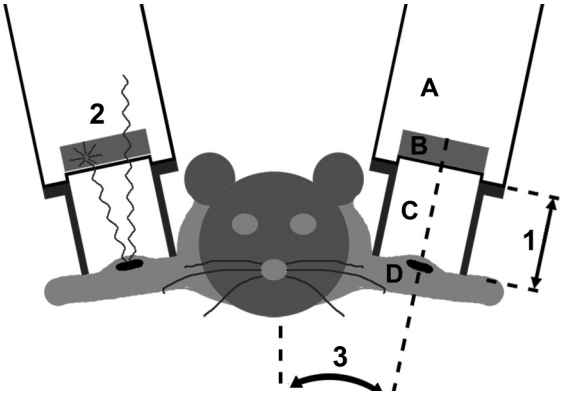

Figure 1: Schematic diagram of the non-invasive measurement method in the rat. The active portion of the measurement setup consisted of scintillation probes (A) containing a sodium iodide scintillator (B) were collimated with a hollow tube (C) and wrapped in leaded tape to determine the activity of subcutaneous implanted release vehicles (D) over time. The implant-to-probe distance (1), the detector linearity (2) and interference of multiple sources at different probe angles (3) were characterized prior to the *in vivo* experiment.

Implants

The selection of the local delivery vehicles used in this study, gelatin, poly(lactic-co-glycolic acid) and poly(propylene fumarate), was based on previous work demonstrating their capability of binding BMP-2 or extending protein release.[4,23-30] The materials were combined into composite formulations in order to further extend BMP-2 release over a prolonged period of time. Four local release carriers were used for the *in vivo* validation of the measurement setup, consisting of: A) a gelatin hydrogel, B) poly(lactic-co-glycolic acid) (PLGA) microspheres in a gelatin hydrogel, C) PLGA microspheres in a poly(propylene fumarate) (PPF) scaffold and D) PLGA microspheres in a PPF scaffold surrounded by a gelatin hydrogel. The implants were loaded with the ^{125}I-BMP2/BMP-2 mixture with a hot:cold ratio of 1:8. The equations 1 and 2 were used to determine the initial ^{125}I-BMP-2 activity of the implants:

$$\text{Equation 1:}\quad \text{Detectable counts (cpm)} = \frac{(\text{background (cpm)} \times 4)/e^{-(\ln 2/t_{1/2})xt}}{100 - \%\ \text{skin shielding}} \times 100$$

$$\text{Equation 2:}\quad \text{Implant activity (mCi)} = \frac{[\text{detectable counts (cpm)} / \text{detector efficiency (\%)}] \times 100}{2.22 \times 10^6\ \text{dpm/mCi}}$$

In these equations, the values for background activity and detector efficiency were obtained from the ex-vivo experiments. The skin shielding was determined on fresh cadaver rats using a dummy implant. The ^{125}I half-life (T½ = 60.1 days) was obtained from literature.

The gelatin hydrogels were prepared by chemically cross-linking a 10% filter-sterilized gelatin solution with 0.2% glutaraldehyde according to a previously described method.[15,16] The hydrogels were cross-linked for 6 hrs at 4ºC, which was followed by a 1 hr blocking period of the residual aldehyde groups in a 100 mM glycine solution. The resulting hydrogels were impregnated with 5 µl of the concentrated BMP-2 solution the day before implantation. The microspheres/hydrogel composite (implant B) or the microsphere/PPF/hydrogel composite (implant D) were created by combining PLGA microspheres or a microsphere/PPF composite with the gelatin hydrogel just before cross-linking.

The PLGA (50/50 DL, Mw 23000, Medisorb, Alkemers, Cincinnati, OH) microspheres loaded with BMP-2 were fabricated using a double emulsion-solvent extraction technique as previously described.[27] The final product consisted of spherical particles with a smooth surface. Based on the ^{125}I counts before and after the microsphere fabrication procedure, the entrapment efficiency of BMP-2 was 84 % or 1.4 µg/mg PLGA microspheres.

Poly(propylene fumarate) (Mn = 2900) was synthesized using a two-step procedure as previously described.[31] PPF (1g) was crosslinked using N-vinyl pyrrolidinone (0.5 ml, NVP, Acros, Pittsburgh, PA) as cross-linker and bis(2,4,6-trimethylbenzoyl) phenylphosphine oxide (5 mg, BAPO, Ciba Specialty Chemicals, Tarrytown, NY) as photo-initiator. The PPF/NVP/BAPO paste was combined with 55 wt% microspheres, forced into a glass cylindrical mold (Ø 1.6 mm) and placed under UV-light for 30 minutes for photo-crosslinking. The cross-linked cylinders were sectioned into 6 mm long rods and sterilized by ethanol evaporation. The implants were stored in sterile microcentrifuge tubes at –20 ℃ until use. For the ex-vivo counting method, the activity of the microcentrifuge tubes was measured before and after the surgical procedure to determine the implanted activity.

Subcutaneous implantation and *in vivo* release measurement

A total of twenty male 12-week-old Harlan Sprague Dawley rats (weight 317 (± 8) g) were used for the experiment, according to a protocol approved by the local animal care committee. The rats were allowed to acclimatize for 1 week before the start of the experiment. Anesthesia was provided with an intramuscular injection of a ketamine/xylazine mixture (45/10 mg/kg). Prior to surgery, the rats received an antibiotic prophylaxis of sulfonamide (40 mg/kg) and surgical sites were shaved and disinfected. Each rat received one ^{125}I-BMP-2 loaded implant in a subcutaneous pocket in each of the 4 legs and 2 non-radioactive implants (negative controls for reference 22) in a subcutaneous pocket in the lumbar area. The subcutaneous pockets were created on the dorsal site of the limb distal to the elbow and knee by blunt dissection through a 0.5 cm skin incision and filled with one implant according to a randomized scheme. The pockets were closed using non-resorbable nylon sutures.

Directly after closure of the wounds, the local activity of the implants was measured using the probe setup. The four probes were placed on top of the skin at the implantation sites and the signal was measured of two consecutive 1-minute periods. The rat was horizontally rotated 180º under the frame and the measurements were repeated with different detectors. The measurements were repeated weekly under ketamine/xylazine sedation (20/5 mg/kg). To determine the retention profile, the measurements were corrected for radioactive decay and background activity and expressed as percentage of the implanted dose. At the end of the 12 week follow up period, the linearity of each detector was re-evaluated to assure a stabile calibration curve.

During the follow up period, ten animals were placed in metabolic cages for a period of 24 hours before the release measurements to collect urine and feces samples. At the time of the release measurements, approximately 400 µl of blood was collected from the tail vein of 5 rats which were housed in the metabolic cages. The radioactivity of the urine, feces and blood samples was determined using the gamma counter and the total volumes of the urine and blood collection were recorded to determine the ^{125}I urine clearance using the equation 3:

$$\text{Equation 3: } {}^{125}\text{I clearance (ml/min)} = \frac{{}^{125}\text{I in 24 hr urine collection (cpm)}}{{}^{125}\text{I blood concentration (cpm)} \times 1440 \text{ (min/day)}}$$

Post mortem sample acquisition and *ex vivo* counting

After 6 and 12 weeks, the implants were excised and fixed in phosphate buffered saline (137 mM NaCl, 10 mM phosphate, 2.7 mM KCl) containing 1.5% glutaraldehyde. The fibrous capsule and part of the overlying skin was not removed because they were integrated with the degrading implant. The thyroid, stomach, kidneys, liver, spleen, and left femur were excised to evaluate the ^{125}I tissue distribution. The tissue surrounding the implant at the left hind limb was also harvested to determine the local ^{125}I accumulation. The implants and tissues were counted *ex vivo* using the gamma counter.

Statistical analysis

The *in vitro* data are expressed as average ± standard deviation (SD) of 3 consecutive 1-minute measurements of 4 detectors without subtraction of the background. The *in vivo* data are reported as means ± SD for n = 5 (blood measurements) and n = 10 (all other *in vivo* and ex-vivo measurements). Analysis of variance (ANOVA) was used to determine the effect of probe-to-source distance on the geometric efficiency per activity and the comparison of the interference of multiple sources and the comparison of the implant types. Bonferroni-corrected post-hoc tests were performed to analyze the differences between the groups. Linear regression analysis was applied to determine the relation between the source activity and the scintillation probe counts. A t-test was performed to detect differences between implant retentions measured by the non-invasive and ex-vivo method. All tests were performed using SPSS (version 13.0, SPSS Inc., Chicago, IL) and the level of significance was set at $p = 0.05$.

Results

Ex vivo calibration of experimental setup

The source-to-probe distance, counting rate linearity and interference of surrounding sources were characterized prior to the *in vivo* experiments to optimize the accuracy of the probe setup. As shown in figure 2A, the source-to-probe distance significantly affected the geometric efficiency ($p<0.001$). The source activity and the scintillation probe counts showed excellent linear relations in the range from 0 to 7.8 µCi with a squared correlation coefficient (R^2) between 0.991 and 0.999 and a regression coefficient β between 0.995 and 0.999 (figure 2B). Further increase in activity resulted in a decrease of the linear relation. Analysis of the linear relation at the end of the *in vivo* experiment showed that the calibration curve remained stable over the 12 week follow up period. The average background of the detectors was 250 ± 50 cpm in the absence of radioactive sources. The background significantly increased 1.5 fold in the presence of a 6.3 µCi source, which resulted in a normalized background of 0.17 ± 0.02 % of the source (figure 2C). An angular deviation from parallel probe positioning had no significant effect on the backgrounds of the opposing front/hind limbs. The background of the contra-lateral limb significantly increased at detector angles higher than 9 degrees pointing towards each other.

Implants

The counting threshold was set at 4 times the background signal to minimize the interference of surrounding implants with measurement of the release profiles. Based on a background activity of ± 300 cpm, a detector efficiency of 2.7 %, a skin shielding of 5.8 ± 1.7% and equations 1 and 2 proposed in the Materials and Methods, the implants required an activity of approximately 5.6 µCi to be able to detect 1.0 % ^{125}I-BMP-2 retention after 12 weeks of radioactive decay with an activity above the set threshold. The actual activity of implants after fabrication was 6.0 (± 0.5), 3.7 (± 0.6), 5.6 (± 0.5) and 5.8 (± 0.4) µCi for implants A, B, C and D, respectively. The corresponding variation coefficients for the ex-vivo measurements before implantation were 10.3, 16.3, 9.3 and 6.4 %. During the implantation procedure, 3.5 (± 5.2), 0.24 (± 0.42), 0.021 (± 0.038) and 0.10 (± 0.13) % of

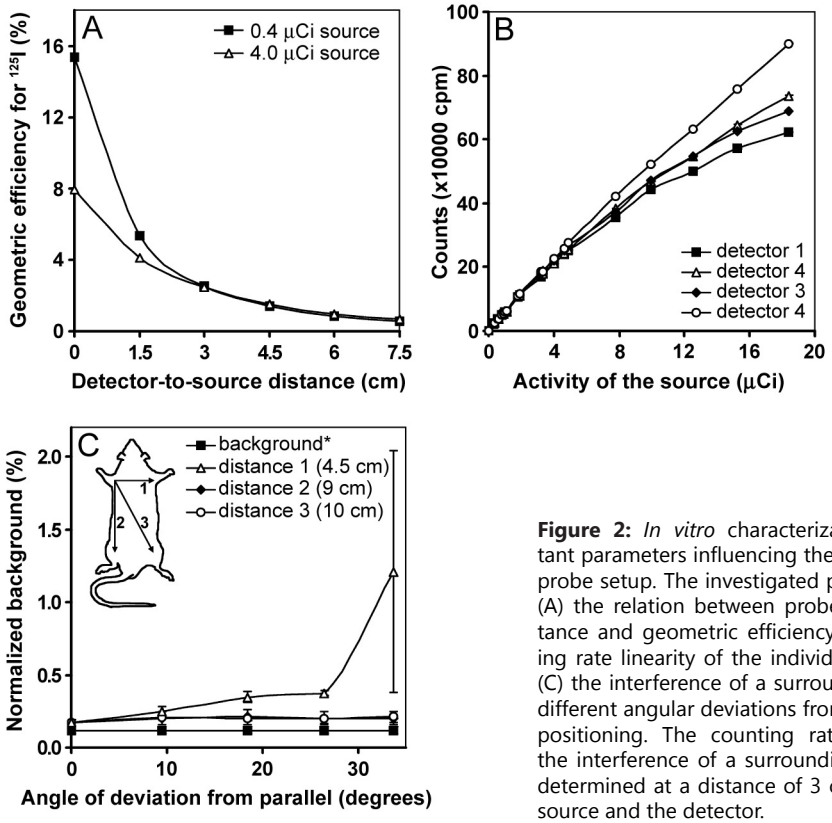

Figure 2: *In vitro* characterization of important parameters influencing the accuracy of the probe setup. The investigated parameters were (A) the relation between probe-to-source distance and geometric efficiency, (B) the counting rate linearity of the individual probes, and (C) the interference of a surrounding source at different angular deviations from parallel probe positioning. The counting rate linearity and the interference of a surrounding source were determined at a distance of 3 cm between the source and the detector.

the activity was lost. The variation coefficient of the non-invasive measurements just after implantation were 27.4, 19.6, 9.6 and 8.1 %.

In vivo validation

During follow-up, one rat was lost on day 56 during sedation for the release measurement, most likely due to an overdose of anesthetics. One implant was lost in another rat since it was removed by the animal from a subcutaneous pocket in the hind limb at the end of the first week of follow-up. All the other animals remained healthy during the experiment without any signs of complications during wound healing. A total of 4 implants, all placed in the front limbs of the first 3 operated rats, was excluded from the analysis. These implants were placed too proximal in the limbs, which resulted in incorrect day 0 measurements due to difficult probe placements. This problem was recognized immediately and did not occur in subsequent animals.

No other problems were encountered during the release measurements. The retention ^{125}I-BMP-2 profiles that were obtained with the scintillation probes are shown in figure 3. Implant A showed a burst release of 92.2 (± 4.4) % of the BMP-2 within the first 14 days of implantation. After 63 days of release, the activity of implant A dropped below the

threshold of 1.0% retention. The other scaffolds showed no initial burst release but a more sustained release over time.
The scintillation probe setup was validated by comparing the non-invasive measurements to the *ex vivo* measurements at 6 and 12 weeks of release (figure 4A). The implants were excised from the surrounding tissue for *ex vivo* counting; however the fibrous capsule was not removed because it was well integrated with the degrading implant. The retention of implant A at 12 weeks (0.1 ± 0.2 % by the *ex vivo* method and 0.2 ± 0.2 % by the non-invasive methods) was excluded from this validation, because these values were below the threshold. Comparison of both methods showed a slightly, not statistically significant increased data dispersion of the non-invasive method which resulted in an overestimation of 0.7 (± 1.2) % and 0.05 (± 0.29) % after 6 and 12 weeks of release, respectively. The measurements obtained by both methods showed an R^2 of 0.982 and an excellent intra-

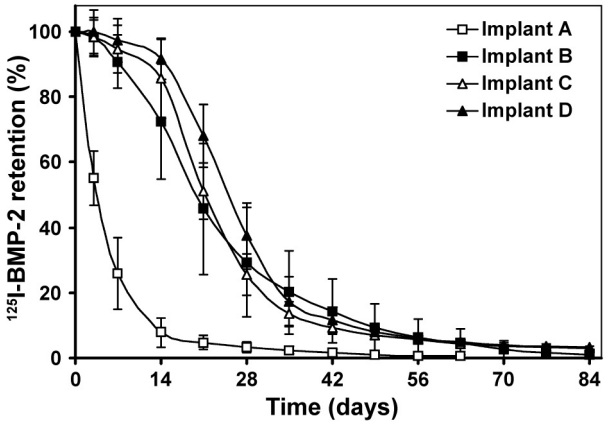

Figure 3: ^{125}I-BMP-2 release profiles from four different implants obtained by the non-invasive measurement method. The implants consisted of (A) BMP-2 loaded gelatin hydrogels, (B) BMP-2 loaded microspheres in a gelatin hydrogel, (C) BMP-2 loaded microspheres in a PPF scaffold and (D) BMP-2 loaded microspheres in a PPF scaffold surrounded by a gelatin hydrogel.

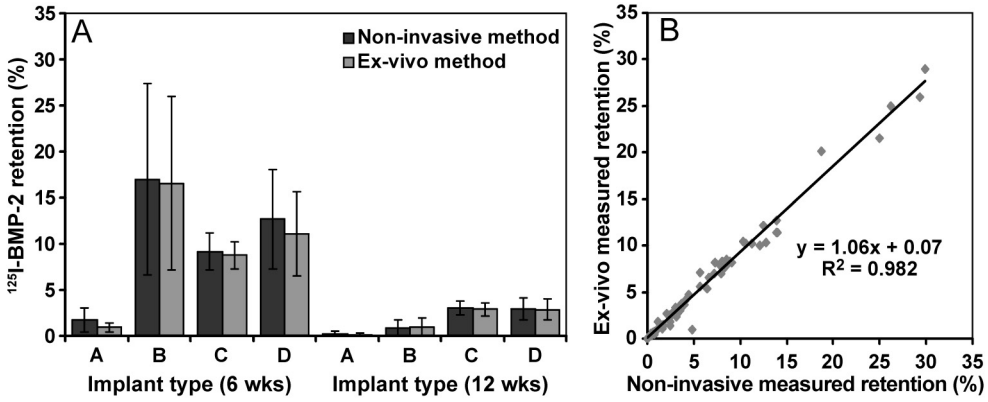

Figure 4: Average ^{125}I-BMP-2 retention in the 4 implants after 6 and 12 weeks of implantation measured using the non-invasive and ex-vivo method (A) and the correlation between the two methods (B). The implants consisted of (A) BMP-2 loaded gelatin hydrogels, (B) BMP-2 loaded microspheres in a gelatin hydrogel, (C) BMP-2 loaded microspheres in a PPF scaffold and (D) BMP-2 loaded microspheres in a PPF scaffold surrounded by a gelatin hydrogel.

class correlation coefficient of 0.993 (figure 4B).
Both the blood and excretion profiles correlated well with the ^{125}I-BMP-2 release profile from the implants and showed two peaks at 3 and 21 days that corresponded with the major releases of implant A and implants B, C & D, respectively (figure 5). The ^{125}I urine clearance over the 84 day period was 0.16 (± 0.8) ml/min. The tissue distribution after 6 and 12 weeks of implantation is shown in Table 1.

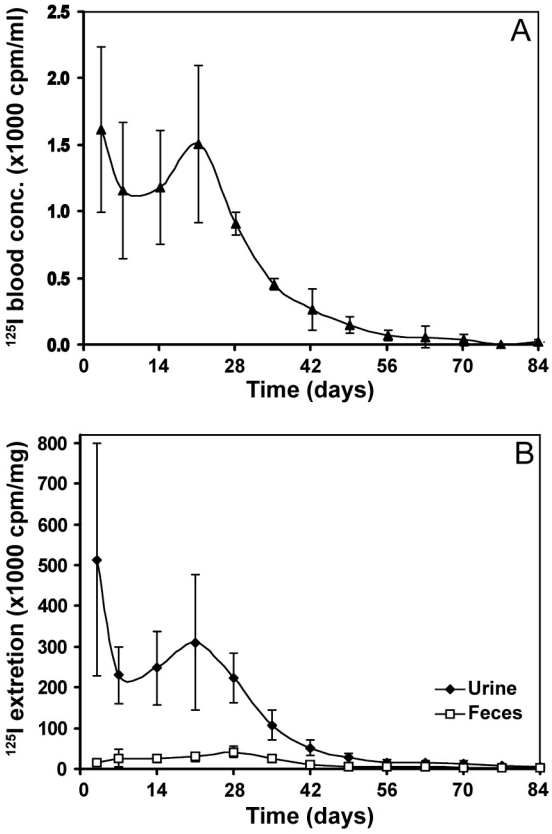

Figure 5: ^{125}I counts in the blood (A) and in 24 hour urine and feces excretions (B) after 125I-BMP-2 release from the 4 subcutaneously placed implants.

Table 1
Percent ^{125}I distribution of the initial implanted activity upon sacrifice at days 42 and 84

Implants/Tissue	*Day 42*	*Day 84*
Implants	8.7 ± 2.5	0.97 ± 0.43
Thyroid	0.75 ± 0.14	0.29 ± 0.15
Stomach	0.042 ± 0.021	< 0.005
Kidney	0.023 ± 0.003	< 0.005
Liver	0.017 ± 0.005	< 0.005
Muscle*	< 0.005	< 0.005
Spleen	< 0.005	< 0.005
Femur	< 0.005	< 0.005

* Muscle and fibrous tissue surrounding the implant

Discussion

In this study, a scintillation probe setup for simultaneous screening of multiple *in vivo* protein release profiles was validated. During the design of the experimental set-up, the implant-to-probe distance was identified as the most important factor influencing the accuracy of the measurement setup (figure 2A). Theoretically, the correlation between the implant-to-probe distance and the geometric efficiency obeys the inverse square law.[32] Therefore, small distance changes with a short collimator will have a larger effect on the acquired counts compared to a longer collimator. To balance the number of acquired counts and minimize the influence of small distance deviations, a 3-cm collimator was chosen for the experimental setup. The larger distance between the probe and the radioactive source potentially decreased data dispersion. However, it also required a higher amount of radioactivity to compensate for the loss of counting efficiency with the increased distance.

Another important parameter that affects the accuracy of the probe setup is the linear correlation between the activity and the number of acquired counts. This linear correlation is mainly determined by the intrinsic properties of the scintillation probes and must be without interference of dead-time effects.[32] The dead-time effects appear as the probe reaches its saturation level, resulting in missing counts at close range (figure 2A) and a non-linear activity-count relation of high activity sources (figure 2B). The linear range of the probes, which remained stable, was used for the *in vivo* experiment. Although adjustment of the high voltage of the detectors resulted in approximately similar counts at the same activity, the acquired counts still varied 2.7 % at 5.3 µCi. Therefore two probes were used for the *in vivo* measurements in case one of the detectors would fail to show a stable linear relation over the follow up period. Although not included in this study, additional probe controls, repetitions of probe positioning and probe measurements can be investigated depending on the sedation time of the animals.

Although implantation of multiple isotropic radiating sources induces the risk of cross-detection of surrounding implants, the interference in our ex-vivo measurements was minimal at near parallel positioning of the detectors (figure 2C). In the *in vivo* set up, maximizing the distance between the implants by creating the pockets as distal as possible allowed almost parallel positioning of the probes and resulted in minimal interference of the surrounding implants.

Until recently, few studies have characterized *in vivo* sustained release profiles from local protein carriers and even fewer publications are dealing with non-invasive detection methods. Recent studies investigating the use of a single-head gamma camera for simultaneous evaluation of implant release profiles suggest that the interference of surrounding implants can result in a 12 to 16% overestimation of a non-invasive method.[3,19] Compared to a gamma camera setup, collimated scintillation probes used in the present study allow good shielding of individual implants. The facilitated shielding helped decrease the overestimation of the scintillation probe method to 0.7 (± 1.2) % after 6 weeks of implantation.

During the validation by Delgado of a scintillation probe setup with a single injectable implant in a rat femur model, higher variation coefficients were seen just after implantation for the non invasive method compared to the ex-vivo counting method.[17] This was attributed to an inconsistent geometry during the measurements which was inherent to the implant injection method employed in that study. In our study, the difference between the variation coefficients at implantation varied between the implants. At the subcutane-

ous implantation site, the non-hydrated microsphere/PPF implants showed a minimal difference between the variation coefficients of the measurements with the two different methods. However, the 90% aqueous gelatin implants had a much larger difference between the variation coefficients. This is likely the result of a higher loss of implant activity during implantation and a rapid initial burst release after implantation. Consequently, non-invasive methods might be less suitable for measuring implant release profiles of implants with a significant protein loss during implantation and rapid burst release after implantation.

One of the limitations of non-invasive measurement techniques is the possibility of interference of systemic accumulation (e.g. ^{125}I thyroid accumulation interfering with the front limb measurements) or local accumulations (^{125}I connective tissue accumulation around the implant) with the measurement of the radioactive isotope in the delivery vehicle. Unlike other non-invasive measurement methods such as gamma cameras or SPECT scanners, scintillation detectors do not provide images that can show systemic isotope accumulations. Therefore we monitored the isotope clearance and studied the organ/tissue distribution upon sacrifice. The isotope excretion, blood and tissue distribution profiles indicated a rapid urine clearance and minimal organ accumulation. Previous studies have investigated the local accumulation of the isotope and showed a minimal accumulation of the growth factor in the fibrous capsule surrounding the implant.[3,19,21] Furthermore, after subcutaneous injection of a carrier-free ^{125}I-BMP-2 solution, the growth factor was rapidly cleared from the injection site with a T½ of 0.3 day.[3] Therefore, the interference of local isotope accumulation on the measurements of the BMP-2 release profiles is likely to be minimal.

During *in vivo* validation of the measurement setup, implants with a high binding capacity for BMP-2 were used in order to extend its release over a prolonged period of time. The different material and implant characteristics resulted in different losses of implant activity upon implantation and different release profiles. During the 12 week follow up period, all ^{125}I-BMP-2 loaded implants showed bone formation.[22] Due to the small amount of newly formed bone and the large animal variability of the release profile, the effect of bone formation on the release profile is expected to be limited in this study.

Overall, this study shows that scintillation probes can be successfully used as non-invasive screenings tool for simultaneous evaluation of *in vivo* protein release profiles of multiple implants in the same animal. By applying basic principles of physics (collimation, shielding and maximizing the inter-implant distance), the scintillation probe can be reliably used for paired measurement of four release profiles with minimal interference of the surrounding implants. This new method is available to every research laboratory that has access to facilities working with radioactive isotopes. Furthermore, the paired evaluation of release profiles in the same animal requires fewer animals and results in less radioactive waste. The screening method can be easily applied to determine the local release profiles of other growth factors or drugs; however ^{125}I-drug injection studies (without the carrier), clearance monitoring and organ accumulation monitoring need to be considered to provide additional information on the local or systemic accumulation of the radioactive tracer.

References

1. Hori, K., Sotozono, C., Hamuro, J., Yamasaki, K., Kimura, Y., Ozeki, M., Tabata, Y., and Kinoshita, S. Controlled-release of epidermal growth factor from cationized gelatin hydrogel enhances corneal epithelial wound healing. J Control Release, 2006.
2. Li, R.H., Bouxsein, M.L., Blake, C.A., D'Augusta, D., Kim, H., Li, X.J., Wozney, J.M., and Seeherman, H.J. rhBMP-2 injected in a calcium phosphate paste (alpha-BSM) accelerates healing in the rabbit ulnar osteotomy model. J Orthop Res 21, 997, 2003.
3. Ruhe, P.Q., Boerman, O.C., Russel, F.G., Mikos, A.G., Spauwen, P.H., and Jansen, J.A. *In vivo* release of rhBMP-2 loaded porous calcium phosphate cement pretreated with albumin. J Mater Sci Mater Med 17, 919, 2006.
4. Woo, B.H., Fink, B.F., Page, R., Schrier, J.A., Jo, Y.W., Jiang, G., DeLuca, M., Vasconez, H.C., and DeLuca, P.P. Enhancement of bone growth by sustained delivery of recombinant human bone morphogenetic protein-2 in a polymeric matrix. Pharm Res 18, 1747, 2001.
5. Abdiu, A., Walz, T.M., and Wasteson, A. Uptake of 125I-PDGF-AB to the blood after extravascular administration in mice. Life Sci 62, 1911, 1998.
6. Friess, W., Uludag, H., Foskett, S., Biron, R., and Sargeant, C. Characterization of absorbable collagen sponges as rhBMP-2 carriers. Int J Pharm 187, 91, 1999.
7. Gao, T., and Uludag, H. Effect of molecular weight of thermoreversible polymer on *in vivo* retention of rhBMP-2. J Biomed Mater Res 57, 92, 2001.
8. Hosseinkhani, H., Hosseinkhani, M., Khademhosseini, A., and Kobayashi, H. Bone regeneration through controlled release of bone morphogenetic protein-2 from 3-D tissue engineered nano-scaffold. J Control Release 117, 380, 2007.
9. Uludag, H., Gao, T., Wohl, G.R., Kantoci, D., and Zernicke, R.F. Bone affinity of a bisphosphonate-conjugated protein *in vivo*. Biotechnol Prog 16, 1115, 2000.
10. Uludag, H., D'Augusta, D., Golden, J., Li, J., Timony, G., Riedel, R., and Wozney, J.M. Implantation of recombinant human bone morphogenetic proteins with biomaterial carriers: A correlation between protein pharmacokinetics and osteoinduction in the rat ectopic model. J Biomed Mater Res 50, 227, 2000.
11. Uludag, H., Friess, W., Williams, D., Porter, T., Timony, G., D'Augusta, D., Blake, C., Palmer, R., Biron, B., and Wozney, J. rhBMP-collagen sponges as osteoinductive devices: effects of *in vitro* sponge characteristics and protein pI on *in vivo* rhBMP pharmacokinetics. Ann N Y Acad Sci 875, 369, 1999.
12. Uludag, H., Gao, T., Porter, T.J., Friess, W., and Wozney, J.M. Delivery systems for BMPs: factors contributing to protein retention at an application site. J Bone Joint Surg Am 83-A Suppl 1, S128, 2001.
13. Takahashi, Y., Yamamoto, M., and Tabata, Y. Enhanced osteoinduction by controlled release of bone morphogenetic protein-2 from biodegradable sponge composed of gelatin and beta-tricalcium phosphate. Biomaterials 26, 4856, 2005.
14. Uludag, H., D'Augusta, D., Palmer, R., Timony, G., and Wozney, J. Characterization of rhBMP-2 pharmacokinetics implanted with biomaterial carriers in the rat ectopic model. J Biomed Mater Res 46, 193, 1999.
15. Yamamoto, M., Tabata, Y., Hong, L., Miyamoto, S., Hashimoto, N., and Ikada, Y. Bone regeneration by transforming growth factor beta1 released from a biodegradable hydrogel. J Control Release 64, 133, 2000.
16. Yamamoto, M., Takahashi, Y., and Tabata, Y. Controlled release by biodegradable hydrogels enhances the ectopic bone formation of bone morphogenetic protein. Biomaterials 24, 4375, 2003.
17. Delgado, J.J., Evora, C., Sanchez, E., Baro, M., and Delgado, A. Validation of a method for non-invasive *in vivo* measurement of growth factor release from a local delivery system in bone. J Control Release 114, 223, 2006.
18. Louis-Ugbo, J., Kim, H.S., Boden, S.D., Mayr, M.T., Li, R.C., Seeherman, H., D'Augusta, D., Blake, C., Jiao, A., and Peckham, S. Retention of 125I-labeled recombinant human bone morphogenetic protein-2 by biphasic calcium phosphate or a composite sponge in a rabbit posterolateral spine arthrodesis model. J Orthop Res 20, 1050, 2002.
19. Ruhe, P.Q., Boerman, O.C., Russel, F.G., Spauwen, P.H., Mikos, A.G., and Jansen, J.A. Controlled release of rhBMP-2 loaded poly(dl-lactic-co-glycolic acid)/calcium phosphate cement composites *in vivo*. J Control Release 106, 162, 2005.
20. Seeherman, H., Li, R., and Wozney, J. A review of preclinical program development for evaluating injectable carriers for osteogenic factors. J Bone Joint Surg Am 85-A Suppl 3, 96, 2003.

21. Yokota, S., Uchida, T., Kokubo, S., Aoyama, K., Fukushima, S., Nozaki, K., Takahashi, T., Fujimoto, R., Sonohara, R., Yoshida, M., Higuchi, S., Yokohama, S., and Sonobe, T. Release of recombinant human bone morphogenetic protein 2 from a newly developed carrier. Int J Pharm 251, 57, 2003.
22. Kempen, D.H., Lu, L., Hefferan, T.E., Creemers, L.B., Maran, A., Classic, K.L., Dhert, W.J., and Yaszemski, M.J. Retention of *in vitro* and *in vivo* BMP-2 bioactivities in sustained delivery vehicles for bone tissue engineering. Biomaterials 29, 3245, 2008.
23. Boyan, B.D., Lohmann, C.H., Somers, A., Niederauer, G.G., Wozney, J.M., Dean, D.D., Carnes, D.L., Jr., and Schwartz, Z. Potential of porous poly-D,L-lactide-co-glycolide particles as a carrier for recombinant human bone morphogenetic protein-2 during osteoinduction *in vivo*. J Biomed Mater Res 46, 51, 1999.
24. Duggirala, S.S., Mehta, R.C., and DeLuca, P.P. Interaction of recombinant human bone morphogenetic protein-2 with poly(d,l lactide-co-glycolide) microspheres. Pharm Dev Technol 1, 11, 1996.
25. Kempen, D.H., Lu, L., Kim, C., Zhu, X., Dhert, W.J., Currier, B.L., and Yaszemski, M.J. Controlled drug release from a novel injectable biodegradable microsphere/scaffold composite based on poly(propylene fumarate). J Biomed Mater Res A 77, 103, 2006.
26. Kempen, D.H.R., Kim, C.W., Lu, L., Dhert, W.J.A., Currier, B.L., and Yaszemski, M.J. Controlled release from poly(lactic-co-glycolic acid) microspheres embedded in an injectable, biodegradable scaffold for bone tissue engineering. Materials Science Forum, 3151, 2003.
27. Oldham, J.B., Lu, L., Zhu, X., Porter, B.D., Hefferan, T.E., Larson, D.R., Currier, B.L., Mikos, A.G., and Yaszemski, M.J. Biological activity of rhBMP-2 released from PLGA microspheres. J Biomech Eng 122, 289, 2000.
28. Rai, B., Teoh, S.H., Hutmacher, D.W., Cao, T., and Ho, K.H. Novel PCL-based honeycomb scaffolds as drug delivery systems for rhBMP-2. Biomaterials 26, 3739, 2005.
29. Schrier, J.A., and DeLuca, P.P. Recombinant human bone morphogenetic protein-2 binding and incorporation in PLGA microsphere delivery systems. Pharm Dev Technol 4, 611, 1999.
30. Yamamoto, M., Ikada, Y., and Tabata, Y. Controlled release of growth factors based on biodegradation of gelatin hydrogel. J Biomater Sci Polym Ed 12, 77, 2001.
31. Wang, S., Lu, L., and Yaszemski, M.J. Bone-tissue-engineering material poly(propylene fumarate): correlation between molecular weight, chain dimensions, and physical properties. Biomacromolecules 7, 1976, 2006.
32. Ranger, N.T. Radiation detectors in nuclear medicine. Radiographics 19, 481, 1999.

8

Non-invasive monitoring of BMP-2 retention and bone formation in composites for bone tissue engineering using SPECT/CT and scintillation probes

Journal of Controlled Release 2009;134:169-176

D.H.R. Kempen
M.J. Yaszemski
A. Heijink
T.E. Hefferan
L.B. Creemers
J. Britson
A. Maran
K.L. Classic
W.J.A. Dhert
L. Lu

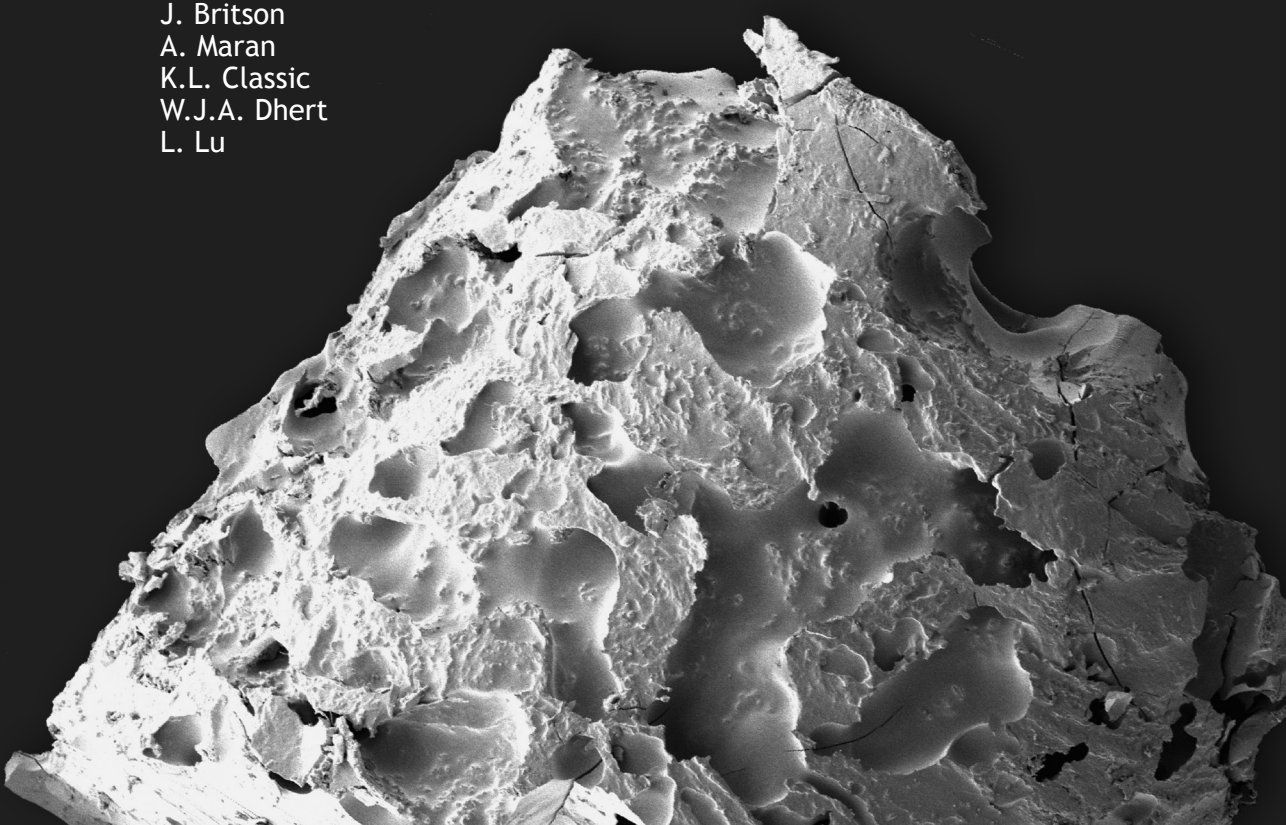

Abstract

Non-invasive imaging can provide essential information for the optimization of new drug delivery-based bone regeneration strategies to repair damaged or impaired bone tissue. This study investigates the applicability of nuclear medicine and radiological techniques to monitor growth factor retention profiles and subsequent effects on bone formation. Recombinant human bone morphogenetic protein-2 (BMP-2, 6.5 µg/scaffold) was incorporated into a sustained release vehicle consisting of poly(lactic-co-glycolic acid) microspheres embedded in a poly(propylene fumarate) scaffold surrounded by a gelatin hydrogel and implanted subcutaneously and in 5-mm segmental femoral defects in 9 rats for a period of 56 days. To determine the pharmacokinetic profile, BMP-2 was radiolabeled with ^{125}I and the local retention of ^{125}I-BMP-2 was measured by single photon emission computed tomography (SPECT), scintillation probes and *ex vivo* scintillation analysis. Bone formation was monitored by micro-computed tomography (µCT). The scaffolds released BMP-2 in a sustained fashion over the 56-day implantation period. A good correlation between the SPECT and scintillation probe measurements was found and there were no significant differences between the non-invasive and ex-vivo counting method after 8 weeks of follow up. SPECT analysis of the total body and thyroid counts showed a limited accumulation of ^{125}I within the body. Ectopic bone formation was induced in the scaffolds and the femur defects healed completely. *In vivo* µCT imaging detected the first signs of bone formation at days 14 and 28 for the orthotopic and ectopic implants, respectively, and provided a detailed profile of the bone formation rate. Overall, this study clearly demonstrates the benefit of applying non-invasive techniques in drug delivery-based bone regeneration strategies by providing detailed and reliable profiles of the growth factor retention and bone formation at different implantation sites in a limited number of animals.

Introduction

During the past decades, the accuracy and resolution of non-invasive monitoring techniques in medicine have greatly improved due to tremendous advances in knowledge, techniques and equipment. Due to the low morbidity of these procedures, they allow repeated evaluation of normal biological processes and diseases over time with limited risks of complications. As a result of the technological advances, many of these non-invasive techniques have also become available for research in small animals.[1-3]

One of the research fields that can especially benefit from non-invasive monitoring techniques is bone tissue engineering. This field strives to create living, functional bone tissue to repair large bone defects due to disease, damage, or congenital defects that would fail to heal by themselves.[4] Controlled release of growth factors involved in the natural process of bone healing has become of great importance for the local modulation of bone formation at the defect site.[5] Although many of these growth factor delivery vehicles appear promising in animal experimental settings, optimization of the vehicle properties, release profiles and site-specific pharmacological actions remains challenging.

While *in vivo* bone formation is relatively easy to quantify by non-invasively radiographic techniques, studying the local release kinetics of the growth factors from the delivery vehicle *in vivo* is more complicated. One of the moderately successful ways to monitor *in vivo* release profiles consists of tracing a radiolabeled protein. This technique has been applied in an invasive way by ex-vivo measuring of the radioactive protein retention after surgical removal of the implants.[6-11] Although this *ex vivo* method is considered the golden standard because of the high spatial resolution and quantitative information, it has several disadvantages. Ex-vivo counting does not allow sequential release measurements of the same implant and requires large numbers of animals.[12-16] Furthermore, simultaneous measurement of both growth factor release and bone formation is complicated, since the first event usually precedes the latter. Therefore, non-invasive nuclear medicine techniques are being explored for determining release profiles.[17-22]

Combining non-invasive nuclear medicine and radiological technologies holds great potential for the optimization of growth factor delivery vehicles, since they allow sequential measurements of both growth factor release and its biological effect (i.e. bone formation). The aim of this study was to investigate the feasibility of using non-invasive techniques to simultaneously monitor both growth factor release and bone formation. Single photon emission computed tomography (SPECT) and a previously described scintillation probe setup were used to determine local retention profiles and micro-computed tomography (μCT) was used for monitoring bone induction.[17,18] Both events were monitored at an ectopic and orthotopic implantation site in rats using a local delivery vehicle containing radioiodinated recombinant human bone morphogenetic protein-2 (BMP-2).

Materials and methods

Experimental design

A total of 18 rats were used for the experiment according to the approved protocol by the Institutional Animal Care and Use Committee. Growth factor release profiles and bone forming capacity were studied over a period of 8 weeks in an ectopic (subcutaneous) and orthotopic (critical sized femoral defect) implantation site in 9 rats. Release profiles

were determined non-invasively by SPECT/CT and scintillation probes. Bone formation was studied using µCT. The implants were removed after 8 weeks of implantation for the comparison of non-invasive and ex-vivo measurements. Additional femoral defects without an implant were used as controls for the autologous bone formation. The bone formation in these controls was only determined using the ex-vivo µCT.

BMP-2 radioiodination

Recombinant human BMP-2 (purchased as part of an Infuse® research kit, Medtronic Sofamor Danek, Minneapolis, MN) dissolved in a BMP-2 buffer (5 mM glutamic acid, 2.5% glycine, 0.5% sucrose, 0.01% Tween80 and pH 4.5) was radiolabeled with ^{125}I using Iodo-Gen® precoated test tubes according to the manufacturer's instructions (Pierce, Rockford, IL). Briefly, 100 µl of a 1.43 mg/ml BMP-2 solution, 20 µl of a 0.1 M NaOH solution and 2 mCi Na^{125}I were added to an Iodo-Gen® coated test tube and incubated for 30 minutes at room temperature. The radiolabeled protein was then separated from free ^{125}I by 24 hr dialysis (10 kDa molecular weight cutoff (MWCO) Slide-A-Lyzer®, Pierce) against the BMP-2 buffer and subsequently concentrated in a Vivaspin device (10 kDa MWCO, Sartorius AG, Germany). The final ^{125}I-BMP-2 solution had an estimated concentration of 1.5 µg/µl, an activity of 4.0 µCi/µg and a trichloroacetic acid (TCA) precipitability of 99.8% precipitable counts.

BMP-2 delivery vehicle

The sustained delivery vehicle consisted of BMP-2-containing poly(lactic-co-glycolic acid) (PLGA) microspheres embedded into a poly(propylene fumarate) (PPF) rod which was surrounded by a cylindrical gelatin hydrogel. The materials and scaffold design were based on previous work on BMP-2 binding and extended protein release.[23] The PLGA (acid end-capped, 50:50 L:G ratio, Mw 23 kDa, Medisorb®, Lakeshore Biomaterials, AL) microspheres were fabricated using a double-emulsion-solvent-extraction technique as previously described.[23,24] The starting amount for the microsphere fabrication was 7.4 mg BMP-2/g PLGA with a 1:4 hot:cold ratio of ^{125}I-BMP-2/BMP-2. Based on the ^{125}I counts before and after the fabrication procedure, the microsphere entrapment efficiency was estimated at 85 % or 1.1 µg BMP-2 per mg PLGA.

The microsphere/PPF composites were fabricated by photocrosslinking PPF with a Mw of 5,800 Da and a polydispersity index (PI) of 2.0 with N-vinylpyrrolidinone (NVP, Acros, Pittsburgh, PA) using the photoinitiator bis(2,4,6-trimethylbenzoyl) phenylphosphine oxide (BAPO, Ciba Specialty Chemicals, Tarrytown, NY) as previously described.[23,25-27] This resulted in cylindrical microsphere/PPF rods with a diameter of 1.6 mm, a length of 6 mm, an average activity of 5.3 ± 0.3 µCi and an estimated BMP-2 loading of 6.5 ± 0.4 µg. The rods were sterilized by ethanol evaporation and frozen down at –20 ℃ until use.

The microsphere/PPF composites were combined with a cylindrical shell composed of a gelatin (type A, 300 bloom, derived from acid-cured tissue, Sigma-Aldrich) hydrogel just before implantation. The gelatin hydrogels had an outer diameter of 3.5 mm and an inner diameter of 1.6 mm and were sterilized in 70% alcohol. Prior to implantation, the BMP-2 loaded microsphere/PPF composite were inserted into the gelatin cylinders.

Surgical procedure

A total of 18 male 12-week-old Sprague Dawley rats (weight 323 ± 9 g) were obtained from a professional stockbreeder (Harlan Sprague Dawley, Inc., Indianapolis, In) at least 1 week prior to the start of the experiment. Anesthesia was provided by an intramuscular injection of a ketamine/xylazine mixture (45/10 mg/kg) and the surgical sites were shaved and disinfected. For the orthotopic implant, a 2 cm skin incision was made along the lateral site of the right limb. By blunt dissection between the biceps femoris and the vastus lateralis muscle, the femur was exposed and circumferentially freed from muscles. A pre-drilled polyethylene plate (l x h x w, 22 x 3 x 4 mm) was fixed to the femur with 1mm Kirchner-wires (Zimmer, Warsaw, IN). Subsequently, a 5-mm segmental defect was created using a surgical drill, which was filled with the microsphere/PPF/gelatin implant. No additional fixation was required to keep the slightly oversized implant (6mm) with a PPF/microsphere rod diameter equal to the intra-medullary canal (1.6mm) in place in the 5mm femoral defect between inner 2 K-wires (7 mm apart). In the controls, the femoral defects were left empty. In addition to the orthotopic implant, the rats receive two ectopic implants in subcutaneous pockets in the lower left limb and the thoracolumbar area in the back. The limb pocket was filled with a ^{125}I-BMP-2 implant and the pocket in the back with a non-radioactive implant.

SPECT/CT imaging and image analysis

Animal imaging was performed with a SPECT/CT system (X-SPECT, Gamma Medica-Ideas, Inc., Northridge, CA, USA) equipped with a single X-ray tube-detector unit and two identical high-resolution gamma cameras. The gamma cameras were collimated by low-energy, high-resolution, parallel-hole collimators with a 12.5 cm x 12.5 cm field of view. Fixed system settings and imaging geometries were used throughout the course of the study. The maximum resolution of the SPECT and CT system are 1-2 mm and 50 µm, respectively. The counting rate linearity of the SPECT system was determined by scanning micro-centrifuge tubes containing 20 µl of ^{125}I-BMP-2 solutions with activities varying from 0.041 to 12 µCi. The activity of the tube and the number of acquired counts showed a linear correlation with an R^2 of 1.000.

The animals were imaged under ketamine/xylazine sedation (20/5 mg/kg) postoperatively and at days 3, 7, 14, 21, 28, 35, 42, 49 and 56. During imaging, the rats remained stationary on a platform in the center of the system, while the X-ray unit and gamma cameras rotated around the platform. Due to the limited field of view, the areas cranial and caudal to the diaphragm were imaged by two separate scans. For each area, a total of 64 projections at 10 seconds per projection were acquired over a 13 minute period for the SPECT image. The CT image acquisition (256 projections) was performed in 1 minute using 0.25 mA and 80 kVp. To allow co-registration of the 3D images, both the SPECT and CT projections were reconstructed in a 7.97 cm (diameter) by 7.97 cm (length) image with a voxel size of 0.311 mm using a modified Feldkamp reconstruction algorithm and a Filtered Backprojection algorithm, respectively.

Analysis of the ^{125}I-BMP-2 release in co-registered SPECT/CT reconstructions was performed using PMOD Biomedical Image Quantification and Kinematic Modeling Software (PMOD Technologies, Switserland). In the postoperative scans, a volume of interest (VOI) was drawn around the full implantation site. These VOIs were loaded into the SPECT images of the consecutive scans and re-positioned over the implants. The counts within

each VOI were recorded, corrected for background activity and radioactive decay, and normalized to the activity at day 0 to obtain the release profiles.
Both the cranial and caudal SPECT scans were used to study the total body accumulation and thyroid uptake of ^{125}I. The total body accumulation was determined by outlining the rat in the CT scans. The counts within the total body VOI were corrected for background activity and compared to the sum of the ectopic and orthotopic implant VOIs. The thyroid gland was outlined with a wide margin on the CT scan and the thyroid activity was expressed as percentage of the total administered ^{125}I-BMP-2 dose.
Analysis of bone formation in the consecutive µCT images was performed using the Analyze software package (Biomedical Imaging Resource, Mayo Clinic, Rochester, MN). The ectopic and orthotopic bone volumes in each scan were extracted and quantified by adjusting the threshold till the soft tissue was completely masked. Any visual scattering of the K-wires outside the cortical area of the femur was removed manually.

Scintillation probe measurements

The ^{125}I-BMP-2 release profiles of the implants were also determined by a scintillation probe setup as previously described.[18] The scintillation probe setup consisted of two scintillation detectors (Model 44-3 low energy gamma scintillator, Ludlum measurements Inc., Tx, USA) connected to digital scalers (Model 1000 scaler, Ludllum measurements Inc.) which were collimated by a 3-cm hollow tube wrapped in lead tape. Postoperatively and at the other time points, the administered dose was determined by measuring the implant activity over four 1-minute periods using both detectors (2 measurements per detector) while the animal was still sedated. To determine the retention profile, the measurements were corrected for background activity and radioactive decay and expressed as percentage of the implanted dose.

Ex vivo counting

After 8 weeks of implantation, the rats were euthanized by an overdose of pentobarbital and the scaffolds were excised and fixed in 1.5% glutaraldehyde in phosphate buffered saline. The thyroid, stomach, kidneys, liver and spleen were also excised to evaluate the ^{125}I tissue distribution. The ^{125}I activity of the implants and tissues was determined using the gamma counter. The acquired implant counts were corrected for radioactive decay and normalized to activity before implantation.

Ex vivo µCT imaging

The two Kirchner-wires in the femur closest to the orthotopic implant were removed prior to *ex vivo* µCT imaging. The implants were scanned *ex vivo* at 0.49° angular increments using a µCT-system at 18 keV.[28] Individual projections were digitized and reconstructed to a 3-dimentional image consisting of 20 µm cubic voxels in a 16-bit grayscale using a modified Feldkamp cone beam tomographic reconstruction algorithm. Image analysis was also performed using the Analyze software package. The µCT scans were used to make 3D reconstructions of the calcified tissue and to quantify the volume of the newly formed bone. The same threshold for extracting the bone volume at the orthotopic site

was used to extract the ectopic bone volume. All *ex vivo* reconstructions and volume quantifications were obtained using standardized threshold.

Histology

To visualize bone formation over time during the histological analysis, the rats received the fluorochrome markers alizarin red (10 mg/kg, IP) and calcein green (10mg/kg, IP,) after 4 and 6 weeks of scaffold implantation, respectively. After µCT analysis, the implants were dehydrated in graded series of alcohol and embedded in methylmethacrylate for histological analysis. Sections were stained by Goldner's trichrome, methylene blue/basic fuchsin and hematoxilin/eosin for routine histology. Unstained sections were used for the evaluation of the fluorochromes by fluorescence microscopy.

Statistical analysis

All data are reported as means ± standard deviations (SD) for n = 8. The local and systemic ^{125}I-BMP-2 distribution, the implant retention profiles and the ectopic bone formation were analyzed using a general linear model with repeated measurements. The intra-class correlation coefficient was determined between the non-invasive release measurements obtained by SPECT imaging and the scintillation probe setup. Comparison between the methods for determination BMP-2 retention in the implants was performed by two-way analysis of variance (ANOVA). Bonferroni corrected post-hoc tests were done to analyze the differences between the groups. A paired t-test was performed for the analysis of orthotopic bone formation. All tests were performed by SPSS (version 13.0, SPSS Inc., Chicago, IL) at a significance level of $p < 0.05$.

Results

Animals

All rats, except two, remained healthy during the experiment. One animal showed a femur fracture at the distal K-wire during imaging at day 3. Despite the fracture, the rat remained in good health and the release measurements were included in the analysis. Since healing of the fracture resulted in an abnormal shape of the femur and femoral defect, the rat was excluded for bone volume analysis. Another rat developed a deep infection of the surgical wound after 4 weeks of follow up and was therefore excluded from the analysis.

SPECT/CT imaging

Although the intensity of the radioactive signal decreased, the ^{125}I-BMP-2 loaded implants remained visible over the full 56 day implantation period (figure 1). The background signal of the scans remained negligible over time and no specific uptake of the ^{125}I tracer was seen in any other organs except the thyroid gland. The corresponding CT images showed regeneration of the femoral defect over time.

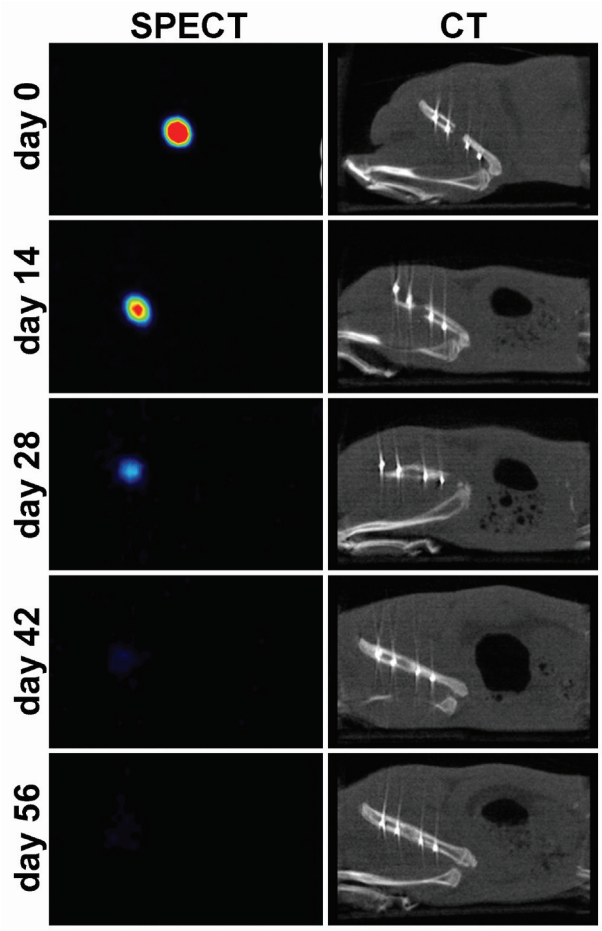

Figure 1: Consecutive SPECT (left) and CT (right) images of femoral implant of the same animal at different time points. The ^{125}I-BMP-2 release from the implant is illustrated by the decreased activity over time. The regeneration of the femoral defect is shown in the CT images.

^{125}I-BMP-2 retention

The amount of ^{125}I-BMP-2 within the implants slowly decreased over the 56 day period (figure 2). The retention of the ^{125}I-BMP-2 in the ectopic implants was significantly higher compared to the orthotopic implants ($p=0.01$). Although the measurements with SPECT resulted in lower retention percentages at all time points compared to the measurements with the scintillation probes, these differences were not significant ($p=0.07$). The measurements obtained by SPECT and the scintillation probes showed an excellent intra-class correlation coefficient of 0.977 (figure 3A). Comparison of the measurements obtained by the non-invasive methods and the ex-vivo counting method showed a significant overestimation of orthotopic BMP-2 retention by scintillation probes ($p=0.01$, figure 3B). Ectopic BMP-2 retention was measured without significant differences between the different methods ($p>0.30$).

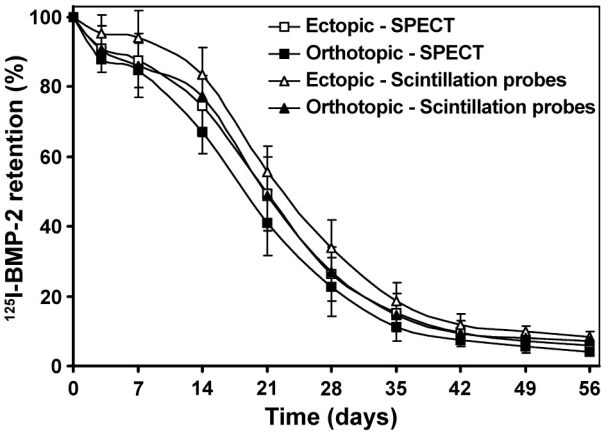

Figure 2: Normalized ^{125}I-BMP-2 retention profiles of the ectopic and orthotopic implants measured by the SPECT and scintillation probe setup as a function of time. Data represent means ± SD for n = 8.

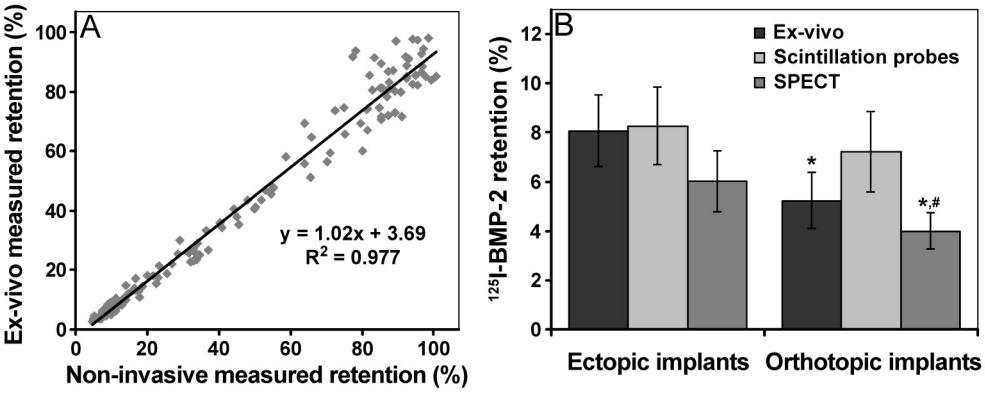

Figure 3: Comparison of the different methods to determine *in vivo* growth factor retention. (A) The correlation between the measurements acquired by the SPECT and scintillation probe setup. (B) Comparison of the ^{125}I-BMP-2 implant retention after 56 days determined by the two non-invasive methods and the *ex vivo* counting methods. Data in (B) represent means ± SD for n = 8. * and # designate significant difference relative to the ectopic retention of the implant measured with the same method and the orthotopic implant measured with the scintillation probe setup, respectively.

Total body accumulation and thyroid uptake of ^{125}I

To obtain more insight into the organ accumulation and excretion of ^{125}I-BMP-2 or its degradation products after their release from the implant, the total body and thyroid counts were measured using both cranial and caudal SPECT images. Comparison of total body counts and total implant counts showed identical profiles over time with no significant differences in count numbers (p=0.54, data not shown). To indicate the relation between the ^{125}I uptake in the thyroid gland and the implanted ^{125}I-BMP-2 activity, the normalized thyroid activity is shown in figure 4. The highest uptake of 0.58 ± 0.28 % was measured after 35 days of implantation, which corresponded to a ^{125}I dose of 40 ± 18 nCi.

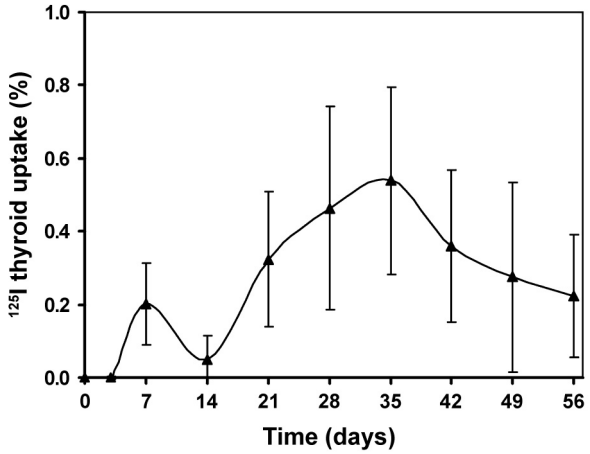

Figure 4: Thyroid ^{125}I uptake profile after implantation of radiolabeled BMP-2 containing ectopic and orthotopic implants as a function of time. Data represent means ± SD for n = 8.

µCT analysis of bone formation

In vivo mineralization could be observed as early as 14 days in the femoral defect and 28 days in the subcutaneous ^{125}I-BMP-2 loaded implants (images not shown). Quantification of bone volumes showed the orthotopic bone volumes increased significantly after 21 days of implantation compared to the 0 and 3 day time points (figure 5). Apart from the sequential *in vivo* imaging, high-resolution *ex vivo* µCT scans were made of the explants after sacrifice (figure 6). Although some bone formation was seen on the defect edges, none of the control implants showed bone bridging of the femoral defect. *In vivo* and *ex vivo* µCT measurements did not yield statistically significant differences in ectopic bone volume values, nor were differences found between ^{125}I-labeled and non-labeled BMP-2 implants (Table 1). For orthotopic bone volume, the values generated by *ex vivo* measurement were significantly higher compared to those provided by *in vivo* scanning (p=0.02). The ex-vivo bone volume analysis showed a significantly higher bone volume in the ^{125}I-BMP-2 implants compared to the empty controls.

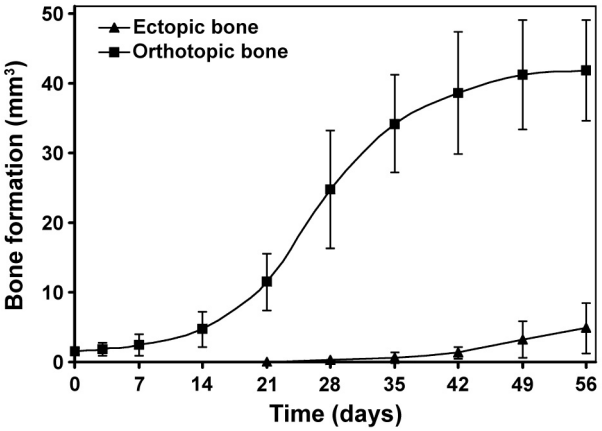

Figure 5: Bone formation at the ectopic and orthotopic sites over the 56 day implantation period determined by consecutive *in vivo* (CT scanning and image analysis. Data represent means ± SD for n = 8.

Table 1
Bone volume after 56 days of implantation

Measurement method	*^{125}I-BMP-2 ectopic implant (mm^3)*	*non-labeled BMP-2 ectopic implant (mm^3)*	*^{125}I-BMP-2 filled femoral defect (mm^3)*	*Empty femoral defect*
Non-invasive	4.9 ± 3.6	6.0 ± 2.2	43.1 ± 7.3*	Not determined
Ex-vivo	4.5 ± 1.7	4.4 ± 1.5	35.0 ± 4.8$^{*,+}$	15.1 ± 6.6

(*p=0.02 and $^{+}$ p<0.01)

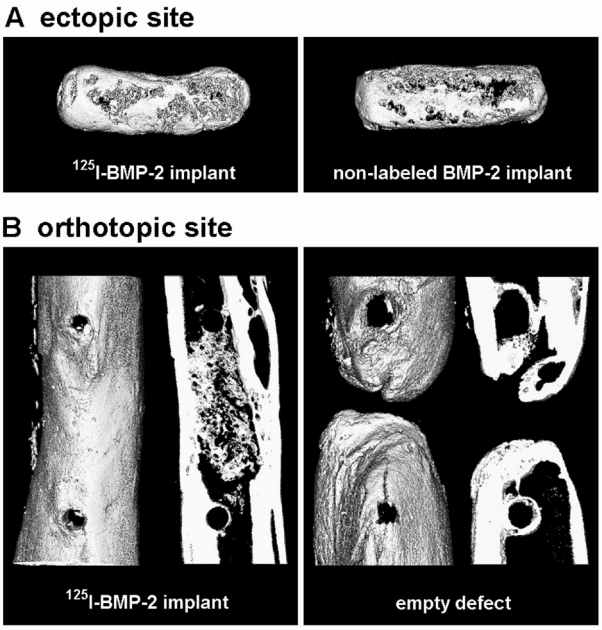

Figure 6: 3D *ex vivo* µCT renderings of ectopic bone formation in the ^{125}I-BMP-2 and non-labeled BMP-2 loaded scaffolds (A) and 3D rentering and 400 µm mid-coronal slice of an empty femoral defect or defect containing a ^{125}I-BMP-2 loaded implant (B) 8 weeks postoperatively.

Histology

Bone formation as evaluated by histology (figure 7) was in line with the data obtained by µCT. The gelatin shell around the solid microsphere/PPF rod was completely resorbed after 56 days of implantation. Homogeneous degradation of the microspheres inside the PPF resulted in an interconnected, porous network that was filled with connective, adipous and bone tissue. The ectopic bone had a woven and trabecular appearance with osteoid depositions along the bone surface. No microscopic difference could be observed between the tissues formed in the ^{125}I-BMP-2 loaded and non-labeled BMP-2 loaded ectopic implants. The appearance of bone formed inside the pores of the orthotopic ^{125}I-BMP-2 loaded scaffolds was similar to bone formed in the ectopic implants. The osseous bridge between the proximal and distal part of the femur consisted of cortical and trabecular bone. In the empty defects, the newly formed bone that extended from the defects edges was not sufficient to bridge the defect. The rest of the empty defect was filled with well-vascularized connective tissue. Fluorescence microscopy showed the

presence of both fluorochromes in all samples. Calcein green was found throughout the complete cortical bridge in the femoral defects (figure 7D) confirming the extensive mineralization in the µCT scans of the femoral defects before 4 weeks of implantation. In the ectopic implants the dye was found in small circles along the surface of the implants, indicating that ossification had started simultaneously at multiple sites in the ectopic sites (data not shown).

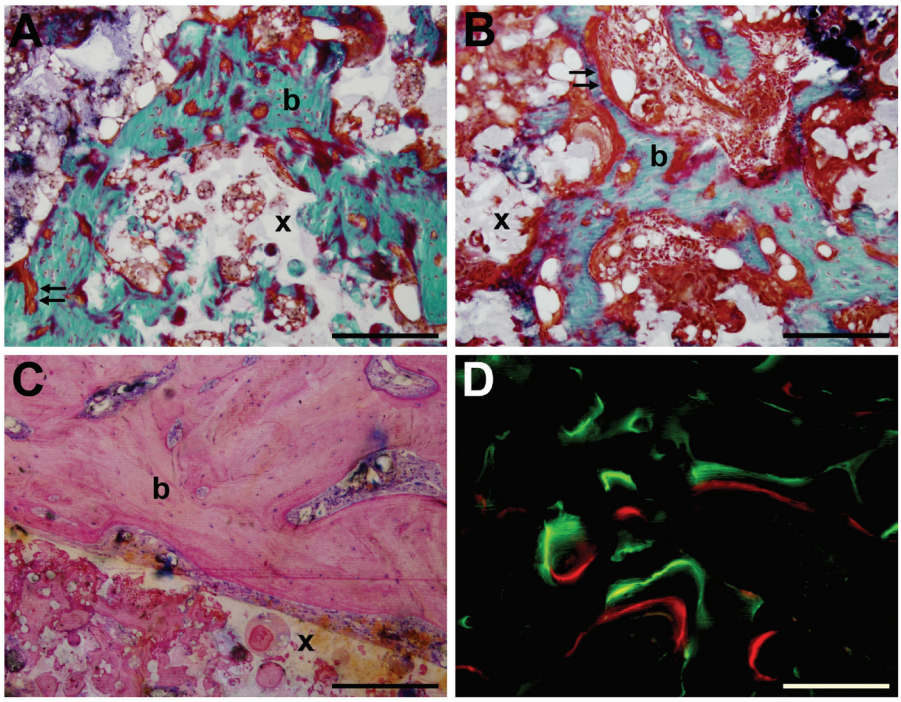

Figure 7: Histological sections of ^{125}I-BMP-2 loaded (A, C, D) and BMP-2 loaded (B) implants after 8 weeks of ectopic (A,B) and orthotopic (C,D) implantation in rats. Degradation of the microspheres resulted in an interconnected porous PPF network (x). Goldner-stained sections showed bone formation (b) and osteoid deposition (arrows) on the surface and inside the pores of the microsphere/PPF scaffold (x). Fluorochrome analysis showed calceine green and alizarin red deposition in newly formed bone (D).

Discussion

This study clearly shows the benefit of using non-invasive techniques to monitor the growth factor retention and bone formation in local delivery vehicles during bone regeneration. The sequential measurements provided detailed profiles of both events in a small number of animals which results in less radioactive waste compared to ex-vivo measurement methods. The nuclear medicine and radiological techniques were able to detect ^{125}I-BMP-2 retention and bone induction in both a superficial ectopic and a deep

orthotopic implantation site. Comparison of the ^{125}I detection methods showed a good correlation between the SPECT and scintillation probe measurements and no significant differences between the non-invasive and *ex vivo* analysis after 8 weeks of follow up.
Two non-invasive nuclear medicine techniques with a tremendous difference in spatial resolution were used to determine the local ^{125}I-BMP-2 retention profiles. The SPECT system uses 2 collimated gamma cameras equipped with multiple small NaI detectors to obtain multiple projections which can be reconstructed into high-resolution 3D images. The single NaI detector of the scintillation probe cannot even localize the implant in a 2D plane and therefore has no spatial resolution at all. Despite the difference in spatial resolution, the local ^{125}I-BMP-2 retention profiles had similar shapes with an excellent correlation between the non-invasive methods. This indicates that spatial resolution is less of an issue during local ^{125}I-BMP-2 retention measurements.
The limited influence of spatial resolution is mainly the result of the ^{125}I-BMP-2 administration method and pharmacokinetic characteristics. In contrast to immunodetection studies of cancer or non-oncological diseases, ^{125}I-BMP-2 is not injected systemically but loaded into a local delivery vehicle and implanted at a known location.[3,29] The fixed position of the delivery vehicle after implantation facilitates consistent probe positioning. Furthermore, the favorable pharmacokinetic characteristics of BMP-2 help minimize the interference of non-implant related gamma-radiation. Previous ^{125}I-BMP-2 injection and sustained release studies have shown a fast ^{125}I clearance from the injection site or tissue surrounding the implant.[18,19,22,30] Apart from these local favorable conditions, the SPECT images and total body counts from this study also show a rapid systemic clearance and minimal organ accumulation of ^{125}I-BMP-2 or its degradation products. The current study is line with the low blood concentrations and high urine excretion of the ^{125}I-label from previous studies.[18,22] The fixed implant position and the minimal interference of non-implant related gamma irradiation allowed the accurate and reliable measurement of the ^{125}I-BMP-2 retention profile using the scintillation probe setup.[17,18]
The advantage of both the SPECT and the scintillation probe setup is their high sensitivity for the detection of ^{125}I. This isotope was favorable for the measurement of sustained release profiles due to its 60 day half-life and low energy gamma rays. Its relatively long half life allows a lower radioactive starting dose for the long term release measurements, whereas its low energy gamma radiation is unlikely to cause extensive biological damage.[31]
Not surprisingly, comparison of bone volumes in the ^{125}I-BMP-2 and non-labeled BMP-2 implants showed no significant effect of ^{125}I-radiation on local ectopic bone formation. However, although the energy deposition of the ^{125}I gamma rays is limited, the highly localized ionizations from Auger and conversion electrons can result in considerable biological consequences at the implantation site.[31] Since ^{125}I-BMP-2 and its degradation products are rapidly cleared upon their release from the implant, we expect that most of the ^{125}I label is located in the extracellular fluids where these electrons are potentially less toxic. The final choice of detection technology will depend on the intended application and research aims. The SPECT method has the advantage that it can be easily applied to new drugs or growth factors, since its high spatial resolution also provides insight in the pharmacokinetics, bio-distribution and ^{125}I-labeling stability of the bioactive molecule. For growth factors with well studied, favorable pharmacokinetic profiles, the scintillation probe setup can be a simple and cheap non-invasive method to obtain detailed release profiles.
Although tracing of radioactively labeled proteins is an effective method to determine their *in vivo* pharmacokinetic profile, one of its general limitations is the possibility of

detachment of the radioactive tracer from the protein. Since free ^{125}I has a high affinity for the thyroid gland and to some extent for the stomach, monitoring of the radioisotope uptake in these organs can be used as an indicator for de-iodination. In this study, measurements of the thyroid and stomach by respectively SPECT and *ex vivo* counting indicated a limited accumulation of free ^{125}I over the 8 week follow up period. This indicated that the ^{125}I-BMP-2 is sufficiently stable towards *in vivo* de-iodination. Furthermore, it is unlikely that the exposure of the thyroid gland to these low ^{125}I dosages will impair its function.[32]

From a bone regeneration perspective, μCT imaging can assist in determining the onset and extent of bone induction over time. Since BMP-2 release preceded bone formation, monitoring of both events in the same animal over a prolonged period of time may be useful for optimizing the drug delivery vehicles. In the ectopic implantation site, the *in vivo* and *ex vivo* mCT systems were equally effective in determining bone volumes. The difference between the *in vivo* and *ex vivo* determined orthotopic bone volumes is likely the result of X-ray scattering of metal K-wires. However, this problem can be simply overcome in future studies by using different orthotopic models or alternative non-metal fixation methods.

All techniques allowed the simultaneous evaluation of the bone tissue engineering construct in both an ectopic and orthotopic site without interference between implantation sites. Whereas the femoral defect represents a clinically applicable site, the ectopic site showed the osteoinductive potential of the construct without interference of osteoconduction or periosteal bone formation as disturbing mechanisms in the BMP-2 induced bone formation. As shown by the femoral defect controls, the critical size defect did not heal spontaneously. Evaluation of the bone regeneration rate of the polymer construct with or without BMP-2 showed that the carrier alone was not able to promote healing of the defect.

The significant differences in protein release and bone formation between the ectopic and orthotopic implantation sites were not surprising. The differences between the surgical sites (e.g. location, wound bed dimensions and haematoma size) likely influenced the local physiologic environment around the delivery vehicle, which could have affected local BMP-2 release as well as the local response to this growth factor. Furthermore, the normal auto-inductive capacity of bone can be expected to enhance BMP-2 induced bone regeneration at the orthotopic implantation.

In conclusion, this study shows that non-invasive monitoring techniques can be used to obtain detailed profiles of growth factor retention and bone formation simultaneously in a limited number of animals. Our study has utilized 2 different methods to measure the growth factor retention from 2 different (ecotopic and orthotopic) implantation sites and examined its biological effects. Comparison of the SPECT and scintillation probe setup showed that both methods were equally effective for the measurement of the ^{125}I-BMP-2 retention profile. By combining these nuclear medicine techniques with radiological imaging techniques, detailed profiles of both release and bone formation were obtained, which can assist in the optimization of the drug delivery vehicles and site-specific pharmacological actions in bone regeneration.

References

1. Beckmann, N., Kneuer, R., Gremlich, H.U., Karmouty-Quintana, H., Ble, F.X., and Muller, M. *In vivo* mouse imaging and spectroscopy in drug discovery. NMR Biomed 20, 154, 2007.
2. Gross, S., and Piwnica-Worms, D. Molecular imaging strategies for drug discovery and development. Curr Opin Chem Biol 10, 334, 2006.
3. Peremans, K., Cornelissen, B., Van Den Bossche, B., Audenaert, K., and Van de Wiele, C. A review of small animal imaging planar and pinhole spect Gamma camera imaging. Vet Radiol Ultrasound 46, 162, 2005.
4. Langer, R., and Vacanti, J.P. Tissue engineering. Science 260, 920, 1993.
5. Rose, F.R., Hou, Q., and Oreffo, R.O. Delivery systems for bone growth factors - the new players in skeletal regeneration. J Pharm Pharmacol 56, 415, 2004.
6. Abdiu, A., Walz, T.M., and Wasteson, A. Uptake of 125I-PDGF-AB to the blood after extravascular administration in mice. Life Sci 62, 1911, 1998.
7. Friess, W., Uludag, H., Foskett, S., Biron, R., and Sargeant, C. Characterization of absorbable collagen sponges as rhBMP-2 carriers. Int J Pharm 187, 91, 1999.
8. Gao, T., and Uludag, H. Effect of molecular weight of thermoreversible polymer on *in vivo* retention of rhBMP-2. J Biomed Mater Res 57, 92, 2001.
9. Hori, K., Sotozono, C., Hamuro, J., Yamasaki, K., Kimura, Y., Ozeki, M., Tabata, Y., and Kinoshita, S. Controlled-release of epidermal growth factor from cationized gelatin hydrogel enhances corneal epithelial wound healing. J Control Release, 2006.
10. Hosseinkhani, H., Hosseinkhani, M., Khademhosseini, A., and Kobayashi, H. Bone regeneration through controlled release of bone morphogenetic protein-2 from 3-D tissue engineered nano-scaffold. J Control Release 117, 380, 2007.
11. Uludag, H., Gao, T., Wohl, G.R., Kantoci, D., and Zernicke, R.F. Bone affinity of a bisphosphonate-conjugated protein *in vivo*. Biotechnol Prog 16, 1115, 2000.
12. Takahashi, Y., Yamamoto, M., and Tabata, Y. Enhanced osteoinduction by controlled release of bone morphogenetic protein-2 from biodegradable sponge composed of gelatin and beta-tricalcium phosphate. Biomaterials 26, 4856, 2005.
13. Uludag, H., D'Augusta, D., Golden, J., Li, J., Timony, G., Riedel, R., and Wozney, J.M. Implantation of recombinant human bone morphogenetic proteins with biomaterial carriers: A correlation between protein pharmacokinetics and osteoinduction in the rat ectopic model. J Biomed Mater Res 50, 227, 2000.
14. Uludag, H., D'Augusta, D., Palmer, R., Timony, G., and Wozney, J. Characterization of rhBMP-2 pharmacokinetics implanted with biomaterial carriers in the rat ectopic model. J Biomed Mater Res 46, 193, 1999.
15. Yamamoto, M., Tabata, Y., Hong, L., Miyamoto, S., Hashimoto, N., and Ikada, Y. Bone regeneration by transforming growth factor beta1 released from a biodegradable hydrogel. J Control Release 64, 133, 2000.
16. Yamamoto, M., Takahashi, Y., and Tabata, Y. Controlled release by biodegradable hydrogels enhances the ectopic bone formation of bone morphogenetic protein. Biomaterials 24, 4375, 2003.
17. Delgado, J.J., Evora, C., Sanchez, E., Baro, M., and Delgado, A. Validation of a method for non-invasive *in vivo* measurement of growth factor release from a local delivery system in bone. J Control Release 114, 223, 2006.
18. Kempen, D.H., Lu, L., Classic, K.L., Hefferan, T.E., Creemers, L.B., Maran, A., Dhert, W.J., and Yaszemski, M.J. Non-invasive screening method for simultaneous evaluation of *in vivo* growth factor release profiles from multiple ectopic bone tissue engineering implants. J Control Release 130, 15, 2008.
19. Louis-Ugbo, J., Kim, H.S., Boden, S.D., Mayr, M.T., Li, R.C., Seeherman, H., D'Augusta, D., Blake, C., Jiao, A., and Peckham, S. Retention of 125I-labeled recombinant human bone morphogenetic protein-2 by biphasic calcium phosphate or a composite sponge in a rabbit posterolateral spine arthrodesis model. J Orthop Res 20, 1050, 2002.
20. Ruhe, P.Q., Boerman, O.C., Russel, F.G., Spauwen, P.H., Mikos, A.G., and Jansen, J.A. Controlled release of rhBMP-2 loaded poly(dl-lactic-co-glycolic acid)/calcium phosphate cement composites *in vivo*. J Control Release 106, 162, 2005.
21. Woo, B.H., Fink, B.F., Page, R., Schrier, J.A., Jo, Y.W., Jiang, G., DeLuca, M., Vasconez, H.C., and DeLuca, P.P. Enhancement of bone growth by sustained delivery of recombinant human bone morphogenetic protein-2 in a polymeric matrix. Pharm Res 18, 1747, 2001.

22. Yokota, S., Uchida, T., Kokubo, S., Aoyama, K., Fukushima, S., Nozaki, K., Takahashi, T., Fujimoto, R., Sonohara, R., Yoshida, M., Higuchi, S., Yokohama, S., and Sonobe, T. Release of recombinant human bone morphogenetic protein 2 from a newly developed carrier. Int J Pharm 251, 57, 2003.
23. Kempen, D.H., Lu, L., Hefferan, T.E., Creemers, L.B., Maran, A., Classic, K.L., Dhert, W.J., and Yaszemski, M.J. Retention of *in vitro* and *in vivo* BMP-2 bioactivities in sustained delivery vehicles for bone tissue engineering. Biomaterials 29, 3245, 2008.
24. Oldham, J.B., Lu, L., Zhu, X., Porter, B.D., Hefferan, T.E., Larson, D.R., Currier, B.L., Mikos, A.G., and Yaszemski, M.J. Biological activity of rhBMP-2 released from PLGA microspheres. J Biomech Eng 122, 289, 2000.
25. Wang, S., Lu, L., and Yaszemski, M.J. Bone-tissue-engineering material poly(propylene fumarate): correlation between molecular weight, chain dimensions, and physical properties. Biomacromolecules 7, 1976, 2006.
26. Kempen, D.H.R., Lu, L., Hefferan, T.E., Creemers, L.B., Maran, A., Classic, K.L., Dhert, W.J.A., and Yaszemski, M.J. Retention of *in vitro* and *in vivo* BMP-2 bioactivity in sustained delivery vehicles for bone tissue engineering. Biomaterials 29, 3245, 2008.
27. Kempen, D.H.R., Lu, L., Heijink, A., Hefferan, T.E., Creemers, L.B., Maran, A., Yaszemski, M.J., and Dhert, W.J.A. The effect of local sequential VEGF and BMP-2 delivery on ectopic and orthotopic bone regeneration. Submitted to the Journal of Bone and Mineral Research.
28. Jorgensen, S.M., Demirkaya, O., and Ritman, E.L. Three-dimensional imaging of vasculature and parenchyma in intact rodent organs with X-ray micro-CT. Am J Physiol 275, H1103, 1998.
29. Goldenberg, D.M., and Larson, S.M. Radioimmunodetection in cancer identification. J Nucl Med 33, 803, 1992.
30. Ruhe, P.Q., Boerman, O.C., Russel, F.G., Mikos, A.G., Spauwen, P.H., and Jansen, J.A. *In vivo* release of rhBMP-2 loaded porous calcium phosphate cement pretreated with albumin. J Mater Sci Mater Med 17, 919, 2006.
31. Bloomer, W.D., and Adelstein, S.J. Iodine-125 cytotoxicity: implications for therapy and estimation of radiation risk. Int J Nucl Med Biol 8, 171, 1981.
32. Doniach, I., and Shale, D.J. Biological effects of 131I and 125I isotopes of iodine in the rat. J Endocrinol 71, 109, 1976.

9

Retention of *in vitro* and *in vivo* BMP-2 bioactivities in sustained delivery vehicles for bone tissue engineering

Biomaterials 2008;29:3245-3252

D.H.R. Kempen
L. Lu
T.E. Hefferan
L.B. Creemers
A. Maran
K.L. Classic
W.J.A. Dhert
M.J. Yaszemski

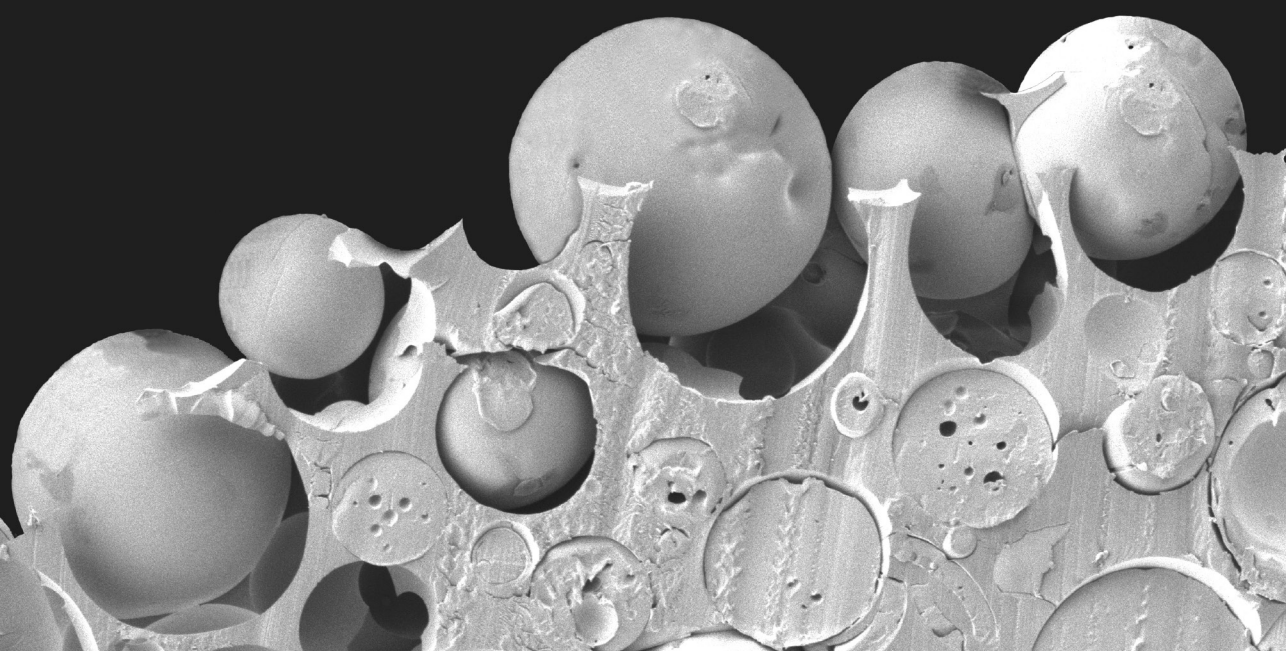

Abstract

In this study, we investigated the *in vitro* and *in vivo* biological activities of bone morphogenetic protein 2 (BMP-2) released from four sustained delivery vehicles for bone regeneration. BMP-2 was incorporated into 1) a gelatin hydrogel, 2) poly(lactic-co-glycolic acid) (PLGA) microspheres embedded in a gelatin hydrogel, 3) microspheres embedded in a poly(propylene fumarate) (PPF) scaffold and 4) microspheres embedded in a PPF scaffold surrounded by a gelatin hydrogel. A fraction of the incorporated BMP-2 was radiolabeled with ^{125}I to determine its *in vitro* and *in vivo* release profiles. The release and bioactivity of BMP-2 were tested weekly over a period of 12 weeks in preosteoblast W20-17 cell line culture and in a rat subcutaneous implantation model. Outcome parameters for *in vitro* and *in vivo* bioactivities of the released BMP-2 were alkaline phosphatase (AP) induction and bone formation, respectively. The four implant types showed different *in vitro* release profiles over the 12-week period, which changed significantly upon implantation. The AP induction by BMP-2 released from gelatin implants showed a loss in bioactivity after 6 weeks in culture, while the BMP-2 released from the other implants continued to show bioactivity over the full 12-week period. Micro-CT and histological analysis of the delivery vehicles after 6 weeks of implantation showed significantly more bone in the microsphere/PPF scaffold composites (implant 3, $p < 0.02$). After 12 weeks, the amount of newly formed bone in the microsphere/PPF scaffolds remained significantly higher than that in the gelatin and microsphere/gelatin hydrogels ($p < 0.001$), however there was no statistical difference compared to the microsphere/PPF/gelatin composite. Overall, the results from this study show that BMP-2 could be incorporated into various bone tissue engineering composites for sustained release over a prolonged period of time with retention of bioactivity.

Introduction

In orthopaedic surgery, the increasing number of grafting procedures and the disadvantages of current autograft treatments (e.g. limited graft quantity and donor site morbidity) drive the quest for alternative methods to reconstruct large bone defects. In 1965, the observation of ectopic bone regeneration from its own devitalized, demineralized matrix launched the promising strategy of bone tissue regeneration using bioactive proteins.[1] Since then, many growth factors with important roles in skeletal repair have been isolated and the advances in recombinant DNA technology have enabled their large scale production for research and therapeutic purposes. Most trials have focused on members of the bone morphogenetic protein (BMP) family, due to their osteogenic capacity.[2-6] So far, these studies have resulted in two commercially available BMP-based products (BMP-2 and BMP-7) for specific orthopedic indications.[7-10]

Although BMPs can be potent osteoinductive growth factors, their administration during orthopedic applications is complicated by their short biological half-lives, localized actions and rapid local clearance.[11] To overcome these problems, effective BMP treatments of bone defects require their incorporation into a biomaterial for its local sustained delivery at the target site. The delivery vehicle should maintain a local BMP concentration within the therapeutic window for a sufficient period of time to allow osteoprogenitor cells to migrate to the target site and differentiate into osteoblasts.[5,12] Furthermore, the biomaterial should act as a biologically and biomechanically compatible framework that enhances cell migration, bone formation and mechanical stability. Although current clinical BMP delivery vehicles show promising results, optimization of the biomaterial design and site-specific pharmacological actions remain challenging. Animal studies demonstrated that the collagen powder or sponges currently used have a large initial burst release and a retention of less than 5% after 14 days of implantation.[13,14] In contrast to this rapid release, during normal bone repair the *in situ* expression profiles of BMPs known to be ectopically osteoinductive (BMP-2, BMP-4, BMP-6 and BMP-7) show an up-regulation for a longer period of time that peaks at/after 21 days.[15-17] Therefore, it is postulated that the site-specific pharmacological actions of BMPs could be improved by a more prolonged growth factor release profile that coincides with the normal rate of BMP expression and bone formation.

Sustained growth factor delivery can be established through different non-covalent retention mechanisms including physical entrapment, absorption and complexation.[18] Based upon these mechanisms, the current study employs three different polymers to design biomaterials for the sustained delivery of BMP-2. The natural polymer gelatin is a type of denatured collagen, which can be used to create hydrogels for the absorption and complexation of BMP.[19] The synthetic polymer poly(lactic-co-glycolic acid) (PLGA) is a well-characterized biodegradable material which can be used for the fabrication of microspheres for BMP encapsulation and complexation.[20-25] Poly(propylene fumarate) (PPF) is a crosslinkable linear polyester with suitable mechanical properties for bone replacement that can be used to encapsulate PLGA microspheres in order to extend their release.[26,27] By combining these three polymers into composite biomaterials, the release of BMP-2 could be extended for a prolonged period of time in an ectopic implantation model.[28]

Although the osteoinductive capacity of BMP-2 loaded carriers composed of these materials has been tested *in vivo*, little is known about the effect of prolonged growth factor retention on the stability of the protein. Therefore, the aim of this study was to assess both the *in vitro* and *in vivo* stabilities of released BMP-2 from the sustained delivery

vehicles over time. Since the pharmacological effects of the growth factor closely depend on its structural integrity, the *in vitro* and *in vivo* biological effects of BMP-2 were used as indicator for protein stability.

Materials and methods

Experimental design

The selection of gelatin, poly(lactic-co-glycolic acid) and poly(propylene fumarate) for the fabrication of BMP-2 delivery vehicles was based on previous work demonstrating their capability of binding BMP-2 or extending protein release.[19-22,24-27,29] The materials were combined into composite formulations in order to further extend BMP-2 release over a prolonged period of time. Four different implants were tested consisting of 1) BMP–2 absorbed in a gelatin hydrogel and BMP-2 loaded microspheres embedded in a 2) gelatin hydrogel, 3) PPF scaffold or 4) PPF scaffold surrounded by a gelatin hydrogel. Implants loaded with the buffer solution were used as controls. The *in vitro* and *in vivo* release profiles from the composites were determined by radiolabeling a fraction of the incorporated growth factor with ^{125}I and correlating the measured radioactive signal to the amount of BMP-2. The *in vitro* biological activity of the released BMP-2 was investigated over a period of 12 weeks in consecutive 7-day cell cultures. The *in vivo* BMP-2 bioactivity was determined by testing its bone forming capacity after 6 and 12 weeks of subcutaneous implantation in rats. A subcutaneous implantation site was chosen to rule out osteoconduction or periosteal bone formation as disturbing mechanisms in the BMP-2 induced bone formation.

BMP-2 radioiodination

To determine the *in vitro* and *in vivo* release profiles, a fraction of the incorporated BMP-2 (Medtronic Sofamor Danek, MN) was radiolabeled with ^{125}I using Iodo-Gen® precoated test tubes (Pierce, Rockford, IL) according to the manufacturer's instructions. Briefly, 100 ml of a 1.43 mg/ml BMP-2 solution, 20 µl of a 0.1 M NaOH solution and 2 mCi Na^{125}I were added to a 1,3,4,6-tetrachloro-3α, 6α-diphenyl glycouril-coated glass test tube. The mixture was incubated for 15 min. at room temperature with gentle shaking. To separate the radiolabeled protein from free radioactive iodine, the solution was dialyzed (10 kDa molecular weight cutoff (MWCO) Slide-A-Lyzer®, Pierce) for 24 hrs with 3 times media change against an aqueous BMP-2 buffer (pH 4.5) containing 5 mM glutamic acid, 2.5 wt% glycine, 0.5 wt% sucrose and 0.01 wt% Tween 80 (all from Sigma-Aldrich, St. Louis, MO). The dialysis fractions of 3 radioiodination procedures were pooled and concentrated to a final concentration of 2.6 µg/µl with a Vivaspin device (10 kDa MWCO, Sartorius AG, Germany). Trichloroacetic acid (TCA) precipitation of the final ^{125}I-BMP-2 solution indicated 99% precipitable counts. The ^{125}I-BMP-2 was mixed with non-labeled BMP-2 to obtain a solution with a concentration of 9.0 mg/ml and a hot:cold ratio of 1:8.

Microsphere fabrication

Poly(lactic-co-glycolic acid) (PLGA; Medisorb®, Lakeshore Biomaterials, AL) with a lactic to glycolic acid ratio of 50:50, a weight-average molecular weight (Mw) of 23,000 Dalton,

and an acid number of 0.34 was used for the microsphere preparation. The microspheres were fabricated using a previously described water-in-oil-in water (W1-O-W2) double-emulsion-solvent-extraction technique.[22] The fabrication process was performed under semi-sterile conditions and all liquids were sterilized using a 0.22 µm filter. Briefly, 118 µl of the 9.0 mg/ml ^{125}I-BMP-2/BMP-2 solution was emulsified in a solution of 500 mg of PLGA in 1.25 ml of dichloromethane using a vortex at 3050 rpm. The mixture was re-emulsified for 30 sec. in 2 ml of 1% w/v aqueous poly(vinyl alcohol) (PVA, 87-89% mole hydrolyzed, Mw=13,000-23,000, Sigma-Aldrich) solution to create the double emulsion. The content was then added to 100 ml of a 0.3 % w/v aqueous PVA solution and 100 ml of a 2% w/v aqueous isopropanol solution with stirring for 1 hr. The extraction of the dichloromethane to the external alcoholic phase resulted in precipitation of the dissolved polymers and subsequently the formation of microspheres. The microspheres were collected by centrifugation, washed twice with distilled deionized water (ddH_2O), and finally vacuum-dried to a free flowing powder. Microspheres loaded with the BMP-2 buffer were used as negative controls.

Fabrication of microsphere/PPF composites

PPF with a number-average molecular weight (Mn) of 5,800 and a polydispersity index of 2.0 was synthesized via a two-step reaction process as previously described.[30] Diethyl fumarate and excess amount of 1,2-propylene glycol were polymerized together with hydroquinone (cross-linking inhibitor) and zinc chloride (catalyst) first at 100 °C for 1 h and then at 150 °C for 7 h to obtain the intermediate dimer. The intermediate dimer was polymerized to PPF via condensation under vacuum at 130 °C for another 4 h. The microsphere/PPF composites (Implant 3) were fabricated by photocrosslinking PPF with N-vinylpyrrolidinone (NVP, Acros, Pittsburgh, PA) using bis(2,4,6-trimethylbenzoyl) phenylphosphine oxide (BAPO, Ciba Specialty Chemicals, Tarrytown, NY).[27,31] Briefly, 1.0 g of PPF and 50 µl of a 100 mg/ml BAPO/dichloromethane solution were dissolved in 0.5 ml of NVP. The PPF/NVP/BAPO paste (45 wt%) was mixed with PLGA microspheres (55 wt%) and mixed using a spatula. The mixture was transferred to a 3.0 ml syringe, forced into a glass cylindrical mold of 1.5 mm in diameter and allowed to polymerize at room temperature under UV light for 30 min. The crosslinked cylinders were removed from the glass mold, lyophilized, sectioned into 6 mm long rods, sterilized by ethanol evaporation and frozen at –20℃ until use.

Fabrication of gelatin hydrogels and composites

Gelatin (type A, 300 bloom, derived from acid-cured tissue, Sigma-Aldrich) hydrogels were fabricated as described previously.[32] The hydrogels were prepared under sterile conditions and all solutions were sterilized using a 0.22 µm filter. Briefly, 1 ml of a 40℃ pre-heated 10 wt% aqueous solution of gelatin was mixed with 40 µl of a 10 wt% aqueous glutaraldehyde solution for 15 seconds using a vortex at 3050 rpm. The resulting solution was cast into cylindrical glass molds with a length of 8 mm and a diameter of 3.5 mm. The gelatin was allowed to crosslink for 6 hrs at 4℃ and crosslinked gelatin hydrogels were placed in a 100 mM aqueous glycine solution for 1 hr to block the residual aldehyde groups of glutaraldehyde. Finally, the hydrogels were washed with ddH_2O, frozen at -20 ℃, removed from the glass mold and stored at -20℃ until use. One day before implanta-

tion, the gelatin hydrogels were loaded with 5 µL of a diluted ^{125}I-BMP-2/BMP-2 solution. PLGA microspheres were embedded into the gelatin hydrogel by combining 72 mg microspheres per ml gelatin solution prior to the crosslinking (Implant 2). Microsphere/PPF composites were embedded in a gelatin hydrogel by placing 1 composite scaffold per mold before hydrogel crosslinking (Implant 4).

In vitro BMP-2 release and bioactivity

The *in vitro* biological activity of released BMP-2 was investigated over a period of 12 weeks by determining its ability to induce an increase in alkaline phosphatase activity in a cell culture model. W20-17 cells (kindly donated by Wyeth, Madison, NJ) were cultured in the presence of BMP-2 containing microspheres or composites. The W20 clone 17 cell line is a mouse bone marrow stromal line known to respond to BMP-2 with an increase in AP activity.[33] Over the 12-week period, the composites were transferred weekly to new cell cultures in order to determine the alkaline phosphatase response over consecutive 7-day periods.

Before the start of the experiment, the W20-17 cells had been expanded, pooled to create a homogeneous mixture, and cryopreserved in multiple aliquots. The cells were cultured in Dulbecco's Modified Eagle's Medium (DMEM) containing 4.5% glucose, 10% fetal bovine serum and penicillin/streptomycin. For each consecutive time point, an aliquot was thawed, expanded for 3 days and re-plated in 24-well plates at 20,000 cells/cm^2 (passage 26 upon use). One day post-plating, the medium was changed and cells were exposed for a period of 3.5 or 7 days to transwells containing the BMP-2-loaded microspheres or composites. Additional cultures containing empty transwells (negative control) were used to determine the basal AP activity of W20-17 cells. To test the dose responsiveness of the stimulated alkaline phosphatase activity, cell cultures were treated with culture media containing 0.0, 0.01, 0.1, 1.0 and 5.0 µg BMP-2/ml (positive controls). For each time point, the transwells were transferred to a new cell culture and the exposed cultures were used to determine the alkaline phosphatase activity, total protein content of the cells, and the BMP-2 release in the medium. For the first two time points, the transwells were already transferred to new cell cultures after 3.5 days. For the rest of the time points, the medium was changed after 3.5 days and the cell culture replacements were done weekly. AP activity was measured using an AP assay kit (Sigma Diagnostics, St. Louis, MO) which immediately lysed the cells. The AP activities were normalized to protein contents of the cell lysate as measured by the bicinchoninic acid assay (BCA Protein Assay Kit, Pierce). To determine the BMP-2 release over the 12-week period, all media changes and cell lysates were assayed for ^{125}I counts on a gamma counter. After 84 days, the implants were collected to determine the remaining activity. All ^{125}I counts were corrected for decay and normalized to the starting amount. The *in vitro* release profiles and BMP-2 culture concentrations were determined by correlating the gamma-irradiation in counts/minute to the amount of incorporated growth factor in microspheres or composites.

Animals and surgical procedure

Twenty male 12-week-old Harlan Sprague Dawley rats (weight 310-335 g) were used for the experiment, according to an approved protocol by local animal care and use committee. Prior to surgery, the rats received an antibiotic prophylaxis of Tribrissen (sul-

fonamide, 40 mg/kg, SC) and were anesthetized with ketamine/xylazine (45/10 mg/kg, IM). After shaving and disinfecting, small skin incisions were made in the proximal part of each limb and in the lumbar area. At each site, a subcutaneous pocket was created and filled with one implant according to a randomized scheme. The four limb pockets were filled with ^{125}I-BMP-2 containing implants and the two lumbar pockets with negative controls (implants containing buffer solution). The rats received the fluorochrome markers calcein green (10mg/kg, paravenously) and tetracycline (10mg/kg, paravenously) at 3 and 9 weeks postoperatively, respectively. Ten animals were sacrificed after 6 and 12 weeks to evaluate bone formation using micro-computed tomography (μCT) and histology.

In vivo release measurements

The *in vivo* BMP-2 release from the different carriers was measured by using four scintillation probes connected to digital scalers as previously described.[28] At different time points, the rats were sedated with ketamine/xylazine (15/3 mg/kg, IM) for measurements of the remaining radioactivity at the implant site over three 1-min. periods with 2 different detectors. The ^{125}I counts were corrected for decay and normalized to the postoperative measurement at day 0.

μCT and histological analysis

After 6 and 12 weeks postoperatively, 10 rats were euthanized and the implants were excised and fixed in a 1.5% phosphate buffered glutaraldehyde solution. The implants were scanned using a μCT-system at 0.49° angular increments, which provided 721 views around 360°.[34] Images were recorded, digitized, and transferred to a controlling computer for reconstruction using a modified Feldkamp cone beam tomographic reconstruction algorithm. The 3-D images consisted of 20 μm cubic voxels and the radiopacity of each voxel was represented by a 16-bit grayscale value. Image analysis was performed using the Analyze software package. (Biomedical Imaging Resource, Mayo Clinic, Rochester, MN) The volume of the subcutaneously formed bone was quantified in μCT reconstructions of the calcified tissue. The threshold for the 3D-reconstructions of the calcified tissue was determined prior to the volume quantification. All reconstructions and volume quantifications were obtained using the same standardized threshold.
After μCT analysis, the implants were dehydrated in a graded series of alcohol and embedded in methylmethacrylate for histological analysis. Sections were stained with hematoxylin/eosin, methylene blue and trichrome Goldner for evaluation of the general tissue response and bone formation. Unstained sections were used for fluorescence microscopy.

Statistical analysis

All data are given as means ± standard deviations (SD) for n = 4 (*in vitro* experiments) and n = 10 (*in vivo* experiments). Single factor analysis of variance (ANOVA) with Bonferroni's *post hoc* tests for multiple comparisons was used to identify differences in mean BMP-2 implant loading and BMP-2 release at each time point. The BMP-2-induced AP activity per time-point was statistically compared to the negative and positive controls using single factor ANOVA with Dunnett's *post hoc* tests and additional Bonferroni's correction for the number of tests. The general linear model with Bonferroni-corrected *post hoc*

tests (for composite effect) and unpaired t-tests (for time effect) were used to assess the statistical significance of the subcutaneous bone volumes. The data analyses were performed with SPSS software (version 13.0, SPSS Inc., Chicago, IL) and differences were considered significant at $p<0.05$.

Results

BMP-2 labeling and incorporation

The radiolabeling procedure of the protein resulted in an activity of 3.8 µCi/µg BMP-2. The addition of ^{125}I-BMP-2 to a preosteoblast W20-17 cell line culture indicated that the growth factor remained bioactive after the iodination reaction (data not shown). Based on the ^{125}I counts before and after the microsphere fabrication procedure, the entrapment efficiency of BMP-2 was 84% or 1.4 µg per mg microspheres. The BMP-2 content of the different composite formulations is summarized in Table 1. Due to the manufacturing process, the composites consisting of PLGA microspheres in a gelatin hydrogel had a significantly lower BMP-2 loading compared to the other scaffolds.

Table 1
Experimental groups and implant characteristics

Name	*Implant composition*	*Initial activity (µCi)*	*BMP-2/implant (µg)*
Gelatin	Gelatin hydrogel	6.0 ± 0.5	9.8 ± 0.8
Mps/Gelatin	Mps in a gelatin hydrogel	3.7 ± 0.6*	6.0 ± 1.0*
Mps/PPF	Mps in a solid PPF cylinder	5.6 ± 0.5	9.1 ± 0.8
Mps/PPF/Gelatin	Mps in a PPF cylinder surounded by a gelatin hydrogel	5.8 ± 0.4	9.5 ± 0.6

Mps = poly(lactic-co-glycolic acid) microparticles loaded with BMP-2
* significantly lower loading relative to other implants

In vitro BMP-2 release and bioactivity

The *in vitro* BMP-2 retention profiles of the PLGA microspheres and the 4 different implants were studied in a cell culture model that allowed simultaneous release and bioactivity measurements. During the first week, water absorption and implant swelling were seen in all composites. The microspheres showed a typical initial burst release which was followed by a sustained S-shaped release profile for the rest of the *in vitro* study (figure 1). The released BMP-2 retained its bioactivity during the course of the study as indicated by the increased AP response over basal levels of the cells (figure 1). The AP increase induced by the BMP-2 released from the microspheres was equal (3/11 time-points) or significantly higher (8/11 timepoints, $p \leq 0.001$) compared to comparable BMP-2 concentrations of the dose-response curve that had been directly added to the culture medium of the cells.

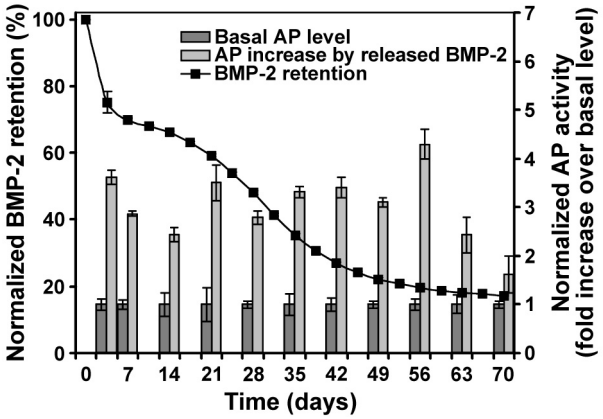

Figure 1: ^{125}I-BMP-2 release kinetics from PLGA microspheres and biological activity of the released BMP-2 obtained from the same cell culture model. The left axis and sqaires (▪) show the normalized retention profile in the microspheres at 37℃ in culture media. The right axis and bars show the alkaline phosphatase activity of consecutive 3 or 7-day W20-17 cell cultures in the presence of BMP-2 contraining microspheres or empty transwells (control culture). The alkaline phosphatase activity at each time point was normalized to the control cultures without BMP-2.

The gelatin hydrogel-only implants showed an initial burst release of the incorporated BMP-2 of 33 (± 8) % during the first 3.5 days, which leveled off over 2 weeks to assume an almost linear sustained release (R^2=0.983) for the rest of the time frame (figure 2). The release profile of the other 3 composites showed an initial burst between 4.9 (± 0.3) % and 6.8 (± 0.2) %, which was followed by an S-shaped release profile for the microsphere/gelatin and microsphere/PPF/gelatin scaffolds. The microsphere/PPF scaffolds exhibited a linear release for the first 56 days (R^2=0.998) which leveled off towards the end of the experiment (figure 2A).

The bioactivity of BMP-2 released from the microspheres and composites was studied by determining the ability to induce an AP activity increase over basal W20-17 cell levels (negative controls) in consecutive 7-day cell cultures, and by comparing the cell response to a BMP-2 dose response curve directly added to the culture medium (positive control). The AP activity response and BMP-2 culture concentrations were analyzed in several ways to distinguish between time- and dose-related effects (figure 2B). Overall, the BMP-2 released from all implants was able to induce a significantly increased AP activity over basal levels during the first 42 days ($p<0.001$, figure 2B). After 42 days, the alkaline phosphatase activity of cultures containing the BMP-2 releasing gelatin hydrogels did not show significantly increased AP levels above basal levels, whereas the cultures containing the microspheres or other implants continued to show significantly higher alkaline phosphatase activities for the rest of time ($p<0.001$). Although no AP induction over basal levels was seen after 42 days for the BMP-2 released from the gelatin hydrogels, comparable concentrations of BMP-2 containing medium in the dose response curve were still able to significantly increase the AP activity (figure 2C). The increase in AP activity for the rest of the implants was equal or significantly higher compared to comparable BMP-2 concentrations of the dose-response curve that had been directly added to the culture medium of the cells ($p<0.05$)

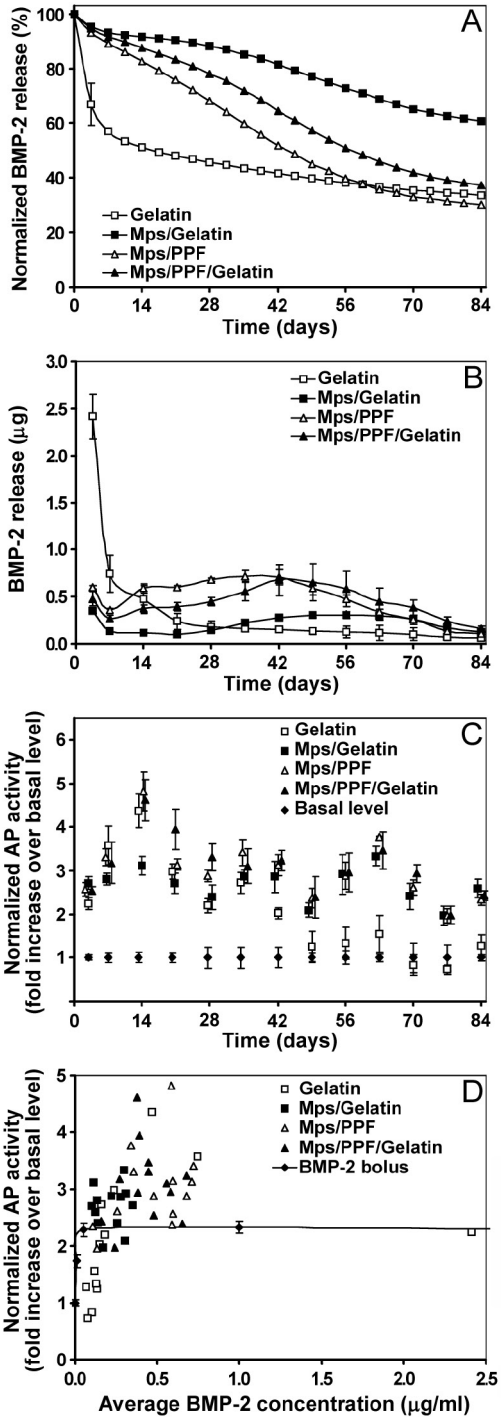

Figure 2: ^{125}I-BMP-2 release kinetics from the implants and its bioactivity on consecutive W20-17 cell cultures. The *in vitro* 125I-BMP-2 release profiles are expressed as (A) normalized release (% of the initial loading) and (B) amount of released protein (in μg) from the 4 different implants at 37 ℃ in the culture media. (C) AP activity of consecutive new W20-17 cell cultures exposed to empty transwells (basal level) or transwells containing the BMP-2 implants. The alkaline phosphatase activity was normalized to the cell protein contents and expressed as an increase over the basal levels for each time point. (D) Relationship between the BMP-2 concentration in the culture medium (obtained from B) and the normalized alkaline phosphatase activity (obtained from B). The line (•) shows the dose-response curve of cell cultures treated with media containing 0.0, 0.01, 0.1, 1.0 and 5.0 μg BMP-2/ml.

Animals

One rat died during the release measurements as a result of an overdose of anesthetics. Another rat removed the Mps/PPF/gelatin implant from its subcutaneous pocket of the hind limb at the end of the first week. After the paravenous administration of tetracycline at the tail base, some of the rats developed a small necrotic area of the skin at the injection site. The rest of the animals showed no complications in wound healing and remained healthy during the 12 week follow up.

In vivo BMP-2 release

Compared to the *in vitro* profiles, the ^{125}I-BMP-2 release of the implants was significantly different upon implantation (figure 3). The gelatin scaffolds showed a prolonged and enlarged burst release of 92.2 (± 4.4) % within the first 14 days, which was followed by an almost linear release for the remaining amount of growth factor. The other three scaffolds also exhibited a much faster BMP-2 release upon implantation. They showed no significant burst release during the first 3 days and an S-shaped sustained release profile spanning the entire period of the 84 days.

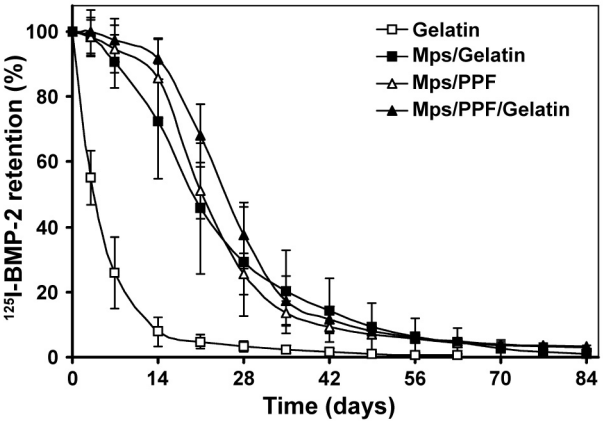

Figure 3: Normalized *in vivo* release profile of ^{125}I-BMP-2 from the 4 different implants in a rat subcutaneous implantation model. Adapted from reference 28.

µCT analysis

After 6 and 12 weeks of implantation, all implants were easily identified and retrieved for analysis by µCT and histology. The µCT reconstructions showed calcifications in all BMP-2-loaded implants which varied in size from $5.5x10^{-4}$ to 24 mm^3. The bone was formed as a solid shell on part of the surface and as a trabecular structure inside the cylindrical implants (figure 4). No bone formation was observed in the control composites containing microspheres without BMP-2.

Quantification of the bone volume after 6 weeks of implantation showed significantly more bone in the Mps/PPF implants compared to all other implants ($p \leq 0.012$, figure 5). The gelatin and Mps/PPF/gelatin scaffolds also contained significantly more bone compared to the Mps/gelatin composites ($p \leq 0.036$). At 12 weeks, the Mps/PPF scaffolds

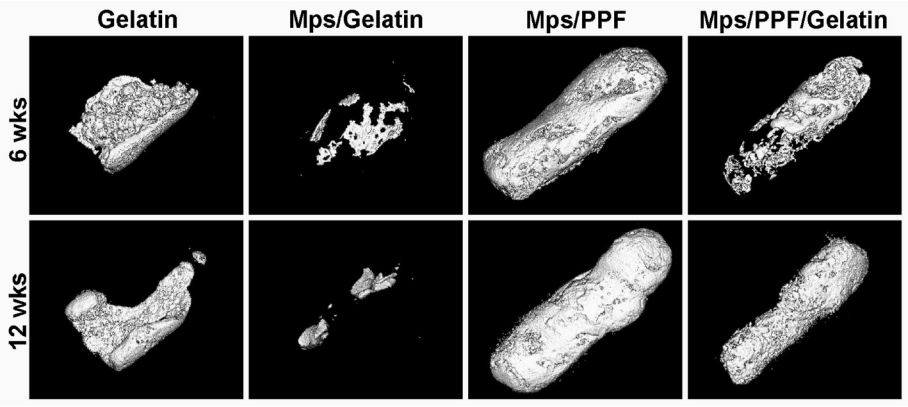

Figure 4: New bone formation after 6 and 12 weeks of implantation in a rat subcutaneous model. Image reconstruction was derived from µCT scans using standardized thresholds.

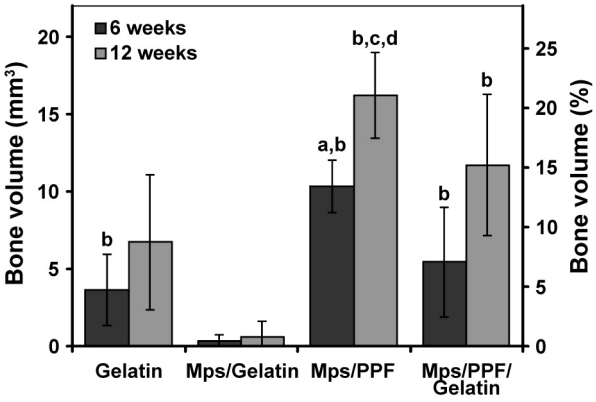

Figure 5: Average volumes of newly formed bone in the 4 different scaffolds after 6 and 12 weeks of subcutaneous implantation in rats (left axis), and normalized to an 8 mm long, 3.5 mm diameter cylindrical scaffold (right axis). Significant difference relative to (a) all other implants, (b) Mps/gelatin implant and (c) gelatin implant at the same time-point. (d) Significant increase in bone formation relative to the previous time-point.

still contained more bone than the gelatin and Mps/gelatin scaffold implants ($p<0.001$), however no statistical difference was found between the Mps/PPF and Mps/PPF/gelatin scaffolds. The bone formation in the Mps/PPF/gelatin composites remained significantly higher than that of the Mps/gelatin scaffold implants ($p<0.001$). Only the Mps/PPF scaffold showed a significant increase in bone formation over time ($p<0.001$).

Histology

Histological evaluation confirmed the subcutaneous bone formation that was seen in the µCT scans (figure 6). The hydrogel-containing implants showed resorption of gelatin at the surface with poor cell infiltration into the intact gelatin network (figure 6A, 6B & 6D). As a result, the bone was mainly formed as a shell around the resorbed hydrogel. The

microsphere/PPF cylinders showed a more homogeneous degradation that resulted in an interconnected porous network (figure 6C & 6D). This network was filled with osteoid, bone and well vascularized connective tissue. Overall, the newly formed bone was found along the degrading implants and had a woven or trabecular appearance with osteoid depositions at its surface (figure 6E). Fluorochrome analysis indicated that bone mineralization was present as early as 3 weeks after implantation (figure 6F). The calcein green injected at 3 weeks was visible in 1/19 Mps/gelatin implants, 11/18 Mps/PPF/gelatin implants, 16/19 gelatin implants and 19/19 Mps/PPF implants. The label was mainly seen as small circles along the implant surface indicating that ossification started simultaneously at multiple sites. The 9-week label tetracycline could not be found in any of the implants. Given the µCT-measured increase in bone formation between 6 and 12 weeks and the superficial necrotic skin reactions to tetracycline injection, it was suspected that the absence of label was due to unsuccessful systemic administration.

Discussion

This study clearly shows that biologically active BMP-2 can be released over a prolonged period of time from sustained delivery vehicles. The delivery vehicles, based on the three different polymers gelatin, PLGA, and PPF, exhibited an *in vitro* release of biologically active BMP-2 for at least 42 to 84 days. Compared to the *in vitro* retention profiles, the delivery vehicles exhibited a significantly faster *in vivo* BMP-2 release. Although all scaffolds showed bone induction after 42 and 84 days of subcutaneous implantation, the amount of newly formed bone varied significantly between the delivery vehicles. The carriers based on the gelatin hydrogel showed less bone formation compared to those based on PPF.

Until recently, few studies have focused on the prolonged retention of BMP-2 in delivery vehicles and its subsequent effect on the biological activity of the released protein. So far, studies performing separate pharmacokinetic and bioactivity assays of BMP-2 showed bioactivity retention of the released or retained protein up to 48 days.[29,35] In this study, both pharmacokinetic and bioactivity assays have been combined in one experimental model to determine the dose- and time-related effects on the bioactivity. However, the W20-17 cells treated with various concentrations of BMP-2 directly added to the culture medium already reached a maximum AP response at 50 ng/ml in our experimental model, in contrast to the AP increase found previously for these cells at concentrations up to 800 ng/ml.[33] As a result, any difference in bioactivity for the released protein at concentrations over 50 ng/ml was impossible to detect. The percentage of bioactive BMP-2 in the total amount of released protein could only be reliably determined under this threshold. For values above this threshold, the bioactivity per amount of released protein could not be expressed as a percentage of the released protein.

Consecutive cell cultures in the presence of various composites showed that protein incorporation in the polymeric delivery vehicles resulted in the release of bioactive BMP-2 for at least 42, >70 and >84 days from the gelatin, PLGA microspheres only, and other implants, respectively. Since the biological activity of the protein closely depends on its structural integrity, its pharmacological effect is an indicator for the stability of the released protein. The decreased bioactivity of the gelatin hydrogels at later time points compared to the other vehicles is likely due to the difference in material properties and may indicate that gelatin is less effective in stabilizing BMP-2 in a physiologic environ-

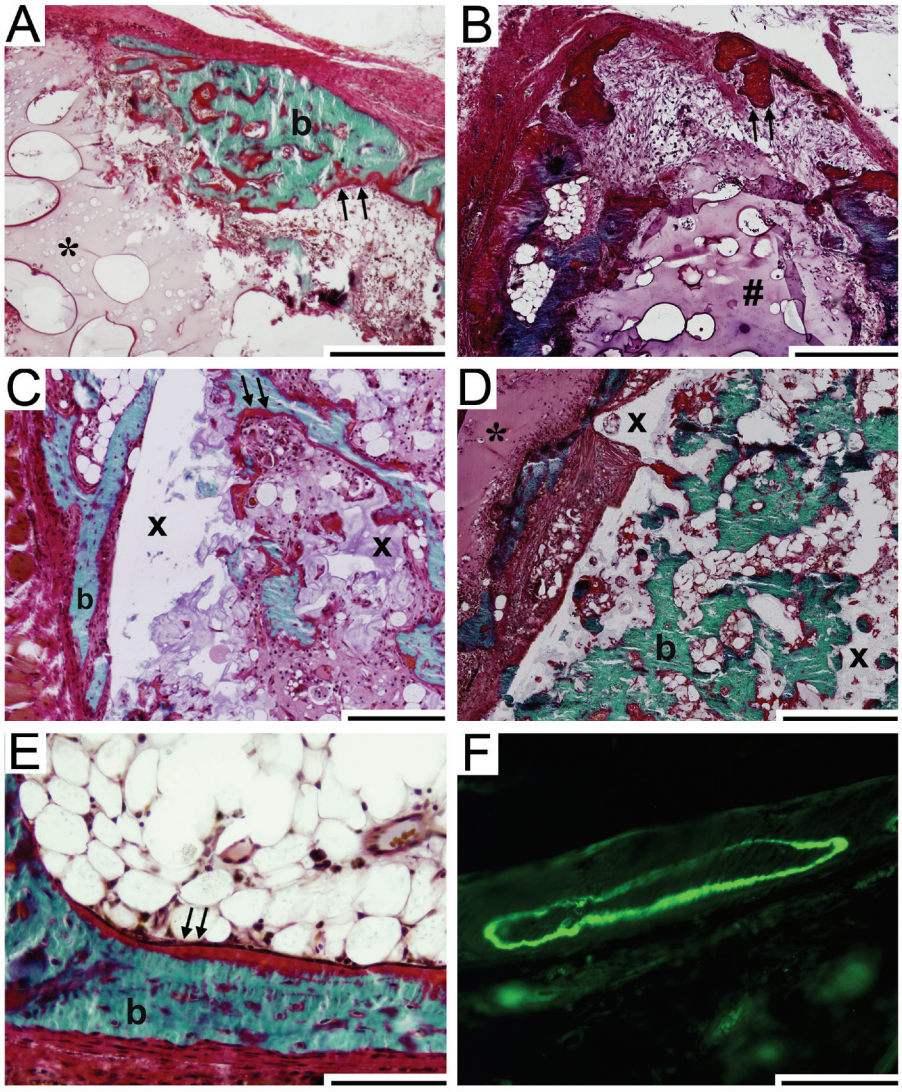

Figure 6: Goldner stained and unstained histological sections of gelatin (A & E), Mps/gelatin (B), Mps/PPF (C & F), Mps/PPF/gelatin (D) implants after 6 (A, C, E & F) and 12 (B & D) weeks of subcutaneous implantation in rats. (A, B & D) Surface resorption and minimal cell infiltration were seen in the gelatin and microsphere/gelatin hydrogels. (A, B, C, D & E) Bone formation (b) and osteoid deposition (arrows) were seen on the surface and inside the gelatin (*), microsphere/gelatin (#) and microsphere/PPF (x) scaffold components. (C & D) Degradation of the Mps/PPF scaffold resulted in an interconnected porous network for tissue ingrowth and bone formation inside the solid Mps/PPF cylinders. (F) Fluorochrome analysis showed calcein green deposition in newly formed bone. The scalebars represent 500 µm (A), 400 µm (B), 200 µm (C,D), 100 µm (F) and 50 µm (E).

ment at 37℃ compared to materials containing PLGA microspheres.
Surprisingly, the bioactivity of the BMP-2 released by composites frequently was higher than similar concentrations of BMP-2 added directly to the control cultures. During the initial characterization of W20-17 cells, loss of growth factor bioactivity was seen at low dosages when fresh cultures were treated with BMP-2 containing media that was previously added to W20-17 cells for 24 hrs.[33] These findings could indicate that BMP-2 is susceptible to degradation or inactivation in the culture medium by molecules such as serum proteins. Therefore, the higher AP activities in the cultures exposed to the sustained delivery vehicles could be the result of the different BMP-2 administration mechanisms. The BMP-2 dose in the control cultures was immediately exposed to the culture conditions from the start of the experiment, whereas the implants had gradually released the same dose over the full 7-day culture period.
In terms of protein release, all *in vitro* profiles underestimated the *in vivo* release rate of the sustained delivery vehicles. These findings are similar to previous studies involving BMP-2 release studies with different solutions (phosphate buffered saline, fetal calf serum and/or DMEM).[11,36] One difference between the two environments with a profound effect on the release of the entrapped and bound protein is the mechanism of implant degradation. Apart from *in vitro* and *in vivo* hydrolysis of the polymer matrix in an aqueous environment, cellular enzymatic actions accelerate implant degradation upon implantation. Furthermore, proteins such as those found in serum enhance the desorption of bound growth factors.[11,37,38] The accelerated degradation and faster protein desorption in the more protein-rich *in vivo* environment may have contributed to the underestimation of the *in vitro* release profiles.
The role of the sustained delivery vehicle materials during *in vivo* bone formation is diverse. In addition to maintaining local BMP concentrations at sufficient levels over time, implants should also provide a mechanically stable and biodegradable framework that enhances cell migration, attachment and differentiation. Although it is difficult to distinguish between release-related effects and scaffold-related effects, this study shows remarkable differences in bone formation in the various composites. Histology and μCT showed that the addition of gelatin to the scaffold construct had a negative effect on cell infiltration and efficacy of bone formation. This indicates that the biodegradable, non-porous structure of the gelatin hydrogel is a less favorable substrate for cell infiltration and bone formation compared to the biodegradable, non-porous PLGA/PPF constructs.
Another remarkable difference in bone formation was seen between the gelatin and the microsphere/gelatin hydrogels. Although part of the difference in bone formation is caused by the significant lower dose of the microsphere/gelatin hydrogels, this difference in dosage does not fully explain the decreased bone formation. Previous BMP-2 dose-response studies in a similar dose range in collagen or PLGA carriers showed a decrease of approximately 50% or less of the calcium content at a 0.2-fold lower dose in a similar range.[39,40] In this study, a smaller difference in BMP-2 dosage (0.6 fold) resulted in a larger decrease (90%) in bone formation. Most likely, the prolongation of the retention of BMP-2 in the microsphere/gelatin hydrogel is partially responsible for the decreased osteoinductive capacity. This could indicate that BMP-2 bound to the 90% aqueous gelatin hydrogel is more susceptible to spontaneous and/or enzymatic degradation before its release compared to the protein entrapped in the dense PLGA/PPF polymer network.
In conclusion, this study demonstrates that BMP-2 can be incorporated into polymeric composites for its sustained release over a prolonged period of time. The entrapment, absorption and complexation of BMP-2 into the composites resulted in the release of

biologically active protein for at least 42 days *in vitro*. However, the composite release profiles were significantly different upon *in vivo* implantation. The ectopic osteoinductive capacity of the released BMP-2 varied among the different composites. Overall, the incorporation of BMP-2 loaded PLGA microspheres in the hydrophobic, solid PPF matrix enhanced bone formation, and therefore may find use as carriers for prolonged release of bioactive proteins for bone tissue engineering.

References

1. Urist, M.R. Bone: formation by autoinduction. Science 150, 893, 1965.
2. Reddi, A.H., and Cunningham, N.S. Initiation and promotion of bone differentiation by bone morphogenetic proteins. J Bone Miner Res 8 Suppl 2, S499, 1993.
3. Sampath, T.K., Maliakal, J.C., Hauschka, P.V., Jones, W.K., Sasak, H., Tucker, R.F., White, K.H., Coughlin, J.E., Tucker, M.M., Pang, R.H., and et al. Recombinant human osteogenic protein-1 (hOP-1) induces new bone formation *in vivo* with a specific activity comparable with natural bovine osteogenic protein and stimulates osteoblast proliferation and differentiation *in vitro*. J Biol Chem 267, 20352, 1992.
4. Wang, E.A., Rosen, V., D'Alessandro, J.S., Bauduy, M., Cordes, P., Harada, T., Israel, D.I., Hewick, R.M., Kerns, K.M., LaPan, P., and et al. Recombinant human bone morphogenetic protein induces bone formation. Proc Natl Acad Sci U S A 87, 2220, 1990.
5. Wozney, J.M. Overview of bone morphogenetic proteins. Spine 27, S2, 2002.
6. Wozney, J.M., Rosen, V., Celeste, A.J., Mitsock, L.M., Whitters, M.J., Kriz, R.W., Hewick, R.M., and Wang, E.A. Novel regulators of bone formation: molecular clones and activities. Science 242, 1528, 1988.
7. Burkus, J.K., Transfeldt, E.E., Kitchel, S.H., Watkins, R.G., and Balderston, R.A. Clinical and radiographic outcomes of anterior lumbar interbody fusion using recombinant human bone morphogenetic protein-2. Spine 27, 2396, 2002.
8. Friedlaender, G.E., Perry, C.R., Cole, J.D., Cook, S.D., Cierny, G., Muschler, G.F., Zych, G.A., Calhoun, J.H., LaForte, A.J., and Yin, S. Osteogenic protein-1 (bone morphogenetic protein-7) in the treatment of tibial nonunions. J Bone Joint Surg Am 83-A Suppl 1, S151, 2001.
9. Govender, S., Csimma, C., Genant, H.K., Valentin-Opran, A., Amit, Y., Arbel, R., Aro, H., Atar, D., Bishay, M., Borner, M.G., Chiron, P., Choong, P., Cinats, J., Courtenay, B., Feibel, R., Geulette, B., Gravel, C., Haas, N., Raschke, M., Hammacher, E., van der Velde, D., Hardy, P., Holt, M., Josten, C., Ketterl, R.L., Lindeque, B., Lob, G., Mathevon, H., McCoy, G., Marsh, D., Miller, R., Munting, E., Oevre, S., Nordsletten, L., Patel, A., Pohl, A., Rennie, W., Reynders, P., Rommens, P.M., Rondia, J., Rossouw, W.C., Daneel, P.J., Ruff, S., Ruter, A., Santavirta, S., Schildhauer, T.A., Gekle, C., Schnettler, R., Segal, D., Seiler, H., Snowdowne, R.B., Stapert, J., Taglang, G., Verdonk, R., Vogels, L., Weckbach, A., Wentzensen, A., and Wisniewski, T. Recombinant human bone morphogenetic protein-2 for treatment of open tibial fractures: a prospective, controlled, randomized study of four hundred and fifty patients. J Bone Joint Surg Am 84-A, 2123, 2002.
10. Vaccaro, A.R., Anderson, D.G., Patel, T., Fischgrund, J., Truumees, E., Herkowitz, H.N., Phillips, F., Hilibrand, A., Albert, T.J., Wetzel, T., and McCulloch, J.A. Comparison of OP-1 Putty (rhBMP-7) to iliac crest autograft for posterolateral lumbar arthrodesis: a minimum 2-year follow-up pilot study. Spine 30, 2709, 2005.
11. Ruhe, P.Q., Boerman, O.C., Russel, F.G., Mikos, A.G., Spauwen, P.H., and Jansen, J.A. *In vivo* release of rhBMP-2 loaded porous calcium phosphate cement pretreated with albumin. J Mater Sci Mater Med 17, 919, 2006.
12. Seeherman, H., Wozney, J., and Li, R. Bone morphogenetic protein delivery systems. Spine 27, S16, 2002.
13. Committee for Medicinal Products for Human Use, E.M.A. scienfitic discussion for the approval of Osigraft. http://www.emea.europa.eu/humandocs/PDFs/EPAR/osigraft/039301en6.pdf, 2004.
14. Uludag, H., D'Augusta, D., Palmer, R., Timony, G., and Wozney, J. Characterization of rhBMP-2 pharmacokinetics implanted with biomaterial carriers in the rat ectopic model. J Biomed Mater Res 46, 193, 1999.

15. Cho, T.J., Gerstenfeld, L.C., and Einhorn, T.A. Differential temporal expression of members of the transforming growth factor beta superfamily during murine fracture healing. J Bone Miner Res 17, 513, 2002.
16. Groeneveld, E.H., and Burger, E.H. Bone morphogenetic proteins in human bone regeneration. Eur J Endocrinol 142, 9, 2000.
17. Niikura, T., Hak, D.J., and Reddi, A.H. Global gene profiling reveals a downregulation of BMP gene expression in experimental atrophic nonunions compared to standard healing fractures. J Orthop Res 24, 1463, 2006.
18. Luginbuehl, V., Meinel, L., Merkle, H.P., and Gander, B. Localized delivery of growth factors for bone repair. Eur J Pharm Biopharm 58, 197, 2004.
19. Yamamoto, M., Ikada, Y., and Tabata, Y. Controlled release of growth factors based on biodegradation of gelatin hydrogel. J Biomater Sci Polym Ed 12, 77, 2001.
20. Boyan, B.D., Lohmann, C.H., Somers, A., Niederauer, G.G., Wozney, J.M., Dean, D.D., Carnes, D.L., Jr., and Schwartz, Z. Potential of porous poly-D,L-lactide-co-glycolide particles as a carrier for recombinant human bone morphogenetic protein-2 during osteoinduction *in vivo*. J Biomed Mater Res 46, 51, 1999.
21. Duggirala, S.S., Mehta, R.C., and DeLuca, P.P. Interaction of recombinant human bone morphogenetic protein-2 with poly(d,l lactide-co-glycolide) microspheres. Pharm Dev Technol 1, 11, 1996.
22. Oldham, J.B., Lu, L., Zhu, X., Porter, B.D., Hefferan, T.E., Larson, D.R., Currier, B.L., Mikos, A.G., and Yaszemski, M.J. Biological activity of rhBMP-2 released from PLGA microspheres. J Biomech Eng 122, 289, 2000.
23. Ruhe, P.Q., Boerman, O.C., Russel, F.G., Spauwen, P.H., Mikos, A.G., and Jansen, J.A. Controlled release of rhBMP-2 loaded poly(dl-lactic-co-glycolic acid)/calcium phosphate cement composites *in vivo*. J Control Release 106, 162, 2005.
24. Schrier, J.A., and DeLuca, P.P. Recombinant human bone morphogenetic protein-2 binding and incorporation in PLGA microsphere delivery systems. Pharm Dev Technol 4, 611, 1999.
25. Woo, B.H., Fink, B.F., Page, R., Schrier, J.A., Jo, Y.W., Jiang, G., DeLuca, M., Vasconez, H.C., and DeLuca, P.P. Enhancement of bone growth by sustained delivery of recombinant human bone morphogenetic protein-2 in a polymeric matrix. Pharm Res 18, 1747, 2001.
26. Kempen, D.H., Lu, L., Kim, C., Zhu, X., Dhert, W.J., Currier, B.L., and Yaszemski, M.J. Controlled drug release from a novel injectable biodegradable microsphere/scaffold composite based on poly(propylene fumarate). J Biomed Mater Res A 77, 103, 2006.
27. Kempen, D.H.R., Kim, C.W., Lu, L., Dhert, W.J.A., Currier, B.L., and Yaszemski, M.J. Controlled release from poly(lactic-co-glycolic acid) microspheres embedded in an injectable, biodegradable scaffold for bone tissue engineering. Materials Science Forum, 3151, 2003.
28. Kempen, D.H., Lu, L., Classic, K.L., Hefferan, T.E., Creemers, L.B., Maran, A., Dhert, W.J., and Yaszemski, M.J. Non-invasive screening method for simultaneous evaluation of *in vivo* growth factor release profiles from multiple ectopic bone tissue engineering implants. J Control Release 130, 15, 2008.
29. Rai, B., Teoh, S.H., Hutmacher, D.W., Cao, T., and Ho, K.H. Novel PCL-based honeycomb scaffolds as drug delivery systems for rhBMP-2. Biomaterials 26, 3739, 2005.
30. Wang, S., Lu, L., and Yaszemski, M.J. Bone-tissue-engineering material poly(propylene fumarate): correlation between molecular weight, chain dimensions, and physical properties. Biomacromolecules 7, 1976, 2006.
31. Kempen, D.H., Kruyt, M.C., Lu, L., Wilson, C.E., Florschutz, A.V., Creemers, L.B., Yaszemski, M.J., and Dhert, W.J. Effect of autologous bone marrow stromal cell seeding and bone morphogenetic protein-2 delivery on ectopic bone formation in a microsphere/poly(propylene fumarate) composite. Tissue Eng Part A 15, 587, 2009.
32. Yamamoto, M., Takahashi, Y., and Tabata, Y. Controlled release by biodegradable hydrogels enhances the ectopic bone formation of bone morphogenetic protein. Biomaterials 24, 4375, 2003.
33. Thies, R.S., Bauduy, M., Ashton, B.A., Kurtzberg, L., Wozney, J.M., and Rosen, V. Recombinant human bone morphogenetic protein-2 induces osteoblastic differentiation in W-20-17 stromal cells. Endocrinology 130, 1318, 1992.
34. Jorgensen, S.M., Demirkaya, O., and Ritman, E.L. Three-dimensional imaging of vasculature and parenchyma in intact rodent organs with X-ray micro-CT. Am J Physiol 275, H1103, 1998.
35. Kim, H.D., and Valentini, R.F. Retention and activity of BMP-2 in hyaluronic acid-based scaffolds *in vitro*. J Biomed Mater Res 59, 573, 2002.

36. Li, R.H., Bouxsein, M.L., Blake, C.A., D'Augusta, D., Kim, H., Li, X.J., Wozney, J.M., and Seeherman, H.J. rhBMP-2 injected in a calcium phosphate paste (alpha-BSM) accelerates healing in the rabbit ulnar osteotomy model. J Orthop Res 21, 997, 2003.
37. Laffargue, P., Fialdes, P., Frayssinet, P., Rtaimate, M., Hildebrand, H.F., and Marchandise, X. Adsorption and release of insulin-like growth factor-I on porous tricalcium phosphate implant. J Biomed Mater Res 49, 415, 2000.
38. Lind, M., Overgaard, S., Soballe, K., Nguyen, T., Ongpipattanakul, B., and Bunger, C. Transforming growth factor-beta 1 enhances bone healing to unloaded tricalcium phosphate coated implants: an experimental study in dogs. J Orthop Res 14, 343, 1996.
39. Bessho, K., Carnes, D.L., Cavin, R., and Ong, J.L. Experimental studies on bone induction using low-molecular-weight poly (DL-lactide-co-glycolide) as a carrier for recombinant human bone morphogenetic protein-2. J Biomed Mater Res 61, 61, 2002.
40. Fujimura, K., Bessho, K., Kusumoto, K., Konishi, Y., Ogawa, Y., and Iizuka, T. Experimental osteoinduction by recombinant human bone morphogeneticprotein 2 in tissue with low blood flow: a study in rats. Br J Oral Maxillofac Surg 39, 294, 2001.

10

Growth factor interactions in bone regeneration

Tissue Engineering part B 2010;16:551-566

D.H.R. Kempen
L.B. Creemers
J. Alblas
L. Lu
A.J. Verbout
M.J. Yaszemski
W.J.A. Dhert

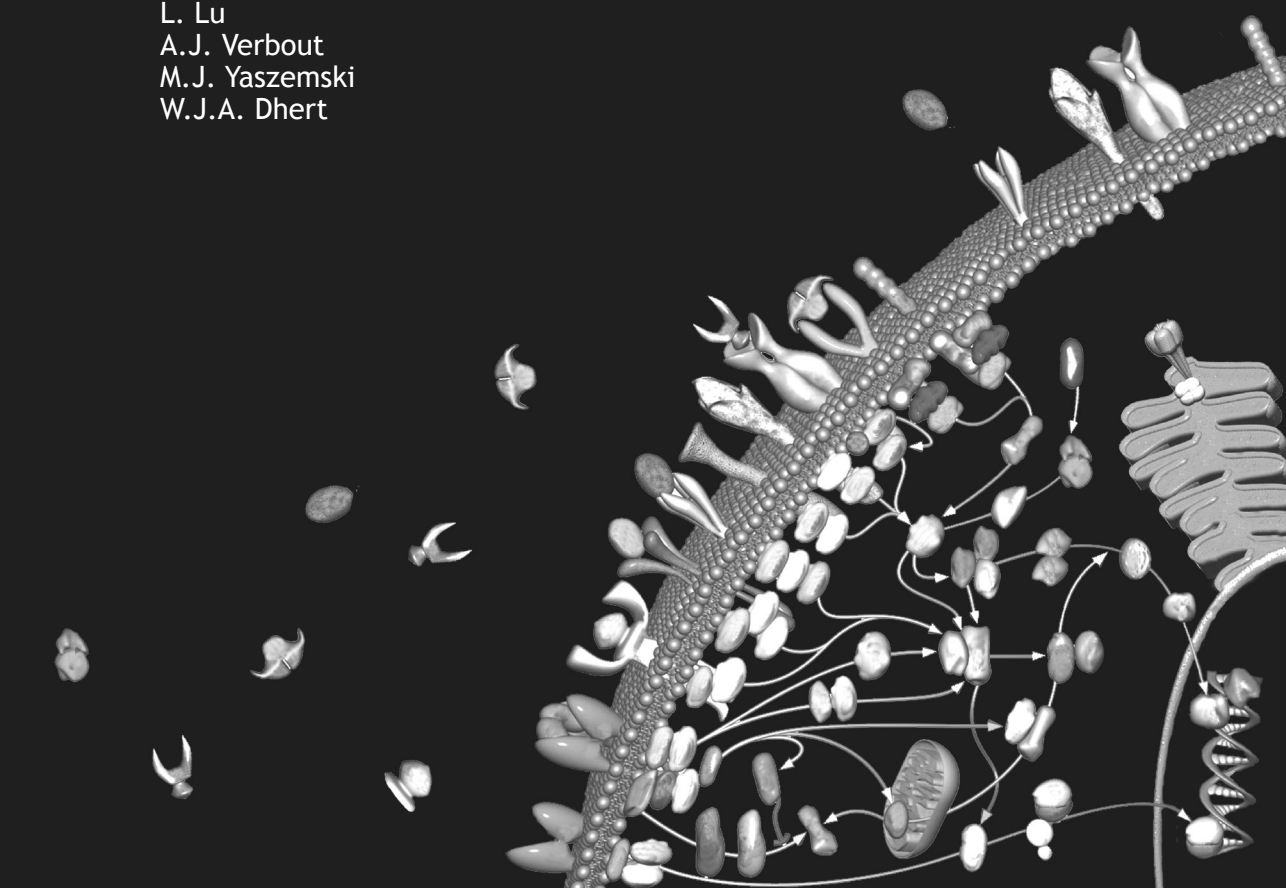

Abstract

Bone regeneration is a complex process regulated by a large number of bioactive molecules. Many growth factors and cytokines involved in the natural process of bone healing have been identified and tested as potential therapeutic candidates to enhance the regeneration process. Although many of these studies show an enhancement of the bone regeneration process by a single drug therapy, *in vivo* bone regeneration is the result of a complex interplay between the applied growth factor and various endogenous produced growth factors. To investigate these growth factor interactions, various studies have investigated the effect of growth factor combinations on bone regeneration. This review provides an overview of the growth factor and cytokine combinations tested in translational bone regeneration studies and shows that their interaction may result in an enhancement or inhibition of bone formation.

Introduction

Bone is, after blood, the most commonly transplanted tissue. Worldwide, an estimated 2.2 million grafting procedures are performed annually in order to repair bone defects in orthopedics, neurosurgery and dentistry.[1] Given the demographic challenges of a growing and aging population, this number is expected to increase. The increasing number of grafting procedures and the disadvantages of current autograft treatments (e.g. limited graft quantity and donor site morbidity) and allograft treatments (e.g. reduced rate of graft incorporation and risk of disease transmission) drive the quest for alternative methods to treat large bone defects.[2-6]

The ability of devitalized, demineralized bone to induce ectopic bone formation and the recognition that proteins were responsible for this bone induction launched the promising strategy of bone tissue engineering based on bioactive molecules.[7,8] Since then, various proteins with an important role in this auto-inductive process were isolated and investigated for their therapeutic potential in bone regeneration including bone morphogenetic proteins (BMPs), transforming growth factor-beta (TGF-β), fibroblast growth factor (FGF), insulin-like growth factor (IGF), vascular endothelial growth factor (VEGF), platelet derived growth factor (PDGF), epidermal growth factor (EGF), parathyroid hormone (related protein) (PTH/PTHrP) and interleukins (IL). Although many studies show an enhancement of the regeneration process by applying one of these proteins, the exact molecular coordination of the bone regeneration process has not been fully defined. Moreover, as various growth factors and cytokines are involved simultaneously in natural bone healing, the combined addition of several factors in specific temporal fashion is likely to be more effective in exogenous stimulation of healing.

Normal bone regeneration (e.g. during fracture healing) is a complex process that involves a large number of growth factors and cytokines for its regulation. No matter how influential one factor may appear in the process, its action in isolation may have little effect without interaction with endogenously produced growth factors and cytokines. Therefore, determination of growth factor interactions is essential to understand and/or control the process of bone regeneration. This review provides an overview of the combinations of growth factors that have been investigated in translational bone regeneration studies. Since most research focuses on combinations with BMPs due to their potent osteoinductive capacity, these growth factors will play a central role in this review.

Bone morphogenetic proteins and their combinations

Over 20 members of the BMP family have been identified and at least 7 of them have documented osteoinductive capacities.[9] The biologically active form of BMPs consist of 30-38 kDa proteins composed of two disulfide-linked polypeptide subunits. Based on their amino acid sequence homology, the osteoinductive BMPs have been divided into separate subgroups, which include the BMP-2/-4 group and the osteogenic protein-1 or OP-1 group (BMP-5 to -8).[10-12] Most research in the field of bone regeneration focuses on the commercially available BMP homodimers. However, BMP members can also form heterodimers consisting of for example one BMP-2 and one BMP-7 subunit and displaying much higher affinities for BMP receptors than homodimers.[13] Given the number of BMP genes, the possible number of combinations is large. So far, native BMP-heterodimers have not been identified *in vivo* and their separation from homodimers in experimental

studies remains difficult because of the biochemical similarity between BMPs.[11,14]
Although BMPs are involved in numerous developmental and pathophysiological processes, their effects on bone formation have been studied most extensively. In bone, they are synthesized by skeletal cells such as osteoblasts and sequestered in the extracellular bone matrix.[7,15,16] *In vitro*, BMPs can differentiate mesenchymal stem cells into the osteoblastic phenotype.[17,18] When implanted ectopically, the osteoinductive BMPs can initiate the complete cascade of bone formation, including the migration of mesenchymal stem cells and their differentiation into osteoblasts.[11] This bone induction occurs through endochondral as well as intramembranous ossification and results in the formation of normal woven and/or lamellar bone.[11,19]
In contrast to the numerous studies in which the effect of separate BMP homodimers was investigated, few studies focussed on the combined administration of BMP family members (Table 1).[20-25] So far, none of the studies using BMP homodimers has been able to show an enhanced effect of the combinations.[23-25] Neither the *in vitro* capacity to induce osteogenic cell differentiation nor the *in vivo* capacity to induce ectopic bone showed an effect of administration of homodimer mixtures compared to an equal dose of one of the BMP homodimers separately. In contrast to the homodimer mixtures, several recombinant BMP heterodimers (particularly BMP2/6, BMP2/7 and BMP4/7) were more potent *in vitro* and *in vivo* compared to a corresponding amount of their homodimers.[24,25] This increase in osteoinductive activity was even 20 fold in case of BMP2/7. Also transduction studies using non-viral or adenoviral osteoinductive BMP vectors showed more efficient induction of osteoblast differentiation and spinal fusion.[18,21,26-28]
A possible explanation for the different effects between homodimers and heterodimers may be found in the BMP signalling pathway (summarized in refs. [29-31]). The BMP signalling pathway converges at the receptor and intracellular signalling level. BMPs bind to two different types of serine/threonine kinase receptors, known as type I and type II receptors (Figure 1). The type I receptors are subdivided into three different activin receptor-like kinases (ALK), known as ALK2, ALK3 and ALK6. Of these type I receptors, ALK3 and ALK6 have a high affinity for BMP-2/-4 group and a low affinity for the OP-1 group, whereas

Table 1
Combinations of BMPs

Growth factors	*Form (dose)*	*Setting*	*Outcome parameters*	*Effect*	*Ref.*
BMP-2/BMP-7	Homodimers (100 μg/100 μg)	Tooth extraction defect in primates	Bone area	n.s.[a]	23
BMP-4/BMP-7	Hetero- & homodimers	Critical sized femoral defect in rats	Bone volume Mechanical strength	homodimers n.s.[a] heterodimers synergistic[b]	25
Various BMP combinations	Hetero- & homodimers	Intramuscular implants in mice/rats	Bone volume	homodimers n.s.[a] heterodimers synergistic[b]	24
BMP-2/BMP-7	Gene therapy	Critical sized calvarial defect in mice	Bone volume	Additive effect[c]	26
BMP-2/BMP-7	Gene therapy	Subcutaneous implants in mice	Alk. Phos. Activity Calcium content Phosphate content	Synergistic[c]	27
BMP-2/BMP-7	Gene therapy	Posterolateral spinal fusion model in rats	Bone volume Alk. Phos. Activity Osteocalcin	Synergistic[c]	21

a: combination of homodimers compared each homodimer alone
b: heterodimers compared to homodimers
c: adenovirus vectors encoding BMP2 (AdBMP-2) and BMP-7 (AdBMP-7) compared to each vector alone
BMP, bone morphogenetic protein; n.s., not significant; Alk. Phos., Alkaline phosphatase

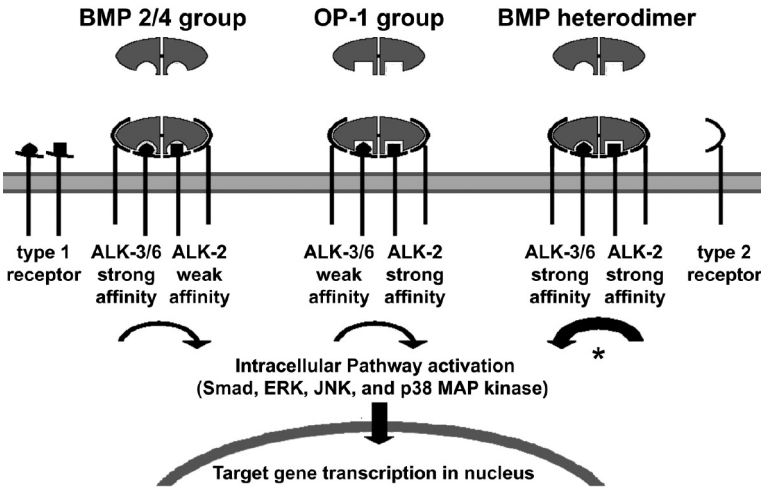

Figure 1: Signal transduction via BMP receptors. Upon BMP binding, the receptors most likely form tetramers consisting of two pairs of type I and type II receptors which subsequently activate the intracellular signalling pathways. Since the 3 type I receptors (ALK2, ALK3 and ALK6) have different affinity for the various BMP molecules, the potency of the intracellular signalling activation varies between the different BMP-receptor complexes. The combination of ALK3 or ALK6 with ALK2 type I receptor signalling was shown to be more potent in inducing transcriptional activation than signalling by either receptor alone (*). ALK, activin receptor-like kinases; BMP, bone morphogenetic protein

ALK2 preferentially binds the OP-1 group.[32-35] In contrast to the type I receptors, the three type II receptors (BMPR-II, ActR-IIA and ActR-IIB) appear to bind most BMPs. Upon BMP binding, the receptors form multimers, most likely a tetramer consisting of two pairs of type I and type II receptors.[36] This allows the activation of the type I receptor and subsequent intracellular signalling. The combination of ALK3 or ALK6 with ALK2 type I receptor signalling was shown to be more potent in inducing transcriptional activation than signalling by either receptor alone.[12] Binding of heterodimers may be more likely to induce such a combined receptor activation than homodimers. Another explanation for the enhanced activity of heterodimers may lie in differential Noggin antagonism of BMP action, which was shown to be decreased for heterodimers compared to homodimer signalling.[37]

Transforming growth factor-beta

TGF-βs are multifunctional growth factors with a broad range of biological activities in various cell types in many different tissues. Three isoforms of TGF-β have been found in humans (TGF-β1 through 3), which all consist of 25 kDa homodimers sharing 60 to 80% similarity in their amino acid sequence. TGF-β is synthesized by many different cell types and is stored as an inactive complex with latency-associated peptide in the extracellular bone matrix.[38] Another major source of this factor are platelets in the blood clot formed after a fracture. Release of the protein from the complex and subsequent induction of its bioactivity is tightly regulated and can occur through different mechanisms.[39] In general, TGF-β stimulates migration of osteoprogenitor cells and is a potent regulator of cell pro-

liferation, cell differentiation and extracellular matrix synthesis.[40,41] Its use for bone regeneration has been evaluated in various experimental settings which show both stimulatory and inhibitory effects on bone formation. Overall, stimulatory effects on bone healing and bone formation predominate.[40] Although no osteoinductive capacity is reported in rodent studies, intramuscular bone induction was found in a TGF-β-loaded collagenous matrix in primates.[42,43]

In several studies attempts were made to enhance bone regeneration by combining TGF-β and BMPs (Table 2).[42-50] In order to investigate a possible interaction between TGF-β and BMP during bone induction, the combination was always compared to similar dosages of each of the individual growth factor. Despite the differences in experimental settings, isoforms used and delivery vehicles, most studies showed an additive or synergistic effect of the combination. Ectopic implantation studies in primates showed that TGF-β enhanced BMP-7-induced bone formation in a dose-responsive manner.[42,43] The largest synergistic effect was seen after co-administration of low TGF and BMP dosages combined with culture-expanded bone marrow stromal cells in RGD-modified alginate hydrogels.[49]

Although the exact molecular actions of the growth factor combinations are not fully understood, several effects have been proposed by which the different isoforms of TGF-β synergize with BMPs. In the early phase after implantation, both growth factors can directly increase the local pool of osteoprogenitor cells by stimulating their migration.[40] Since the circulation is one of the sources of osteoprogenitor cells during ectopic BMP–induced bone regeneration[51], cell recruitment may also be indirectly enhanced by their combined effect on angiogenesis. It has been suggested that TGF-β1 and BMP–7 synergistically interact to enhance angiogenesis and vascular invasion since their co-administration increased vessel formation in a chick chorioallantoic membrane assay and type IV collagen expression in ectopic ossicles in primates.[42,52] The mitogenic effect of TGF-β may further

Table 2
Combinations with TGF-β

Growth factor dose	*Setting*	*Outcome parameters*	*Effect* [a]	*Ref.*
15 ng TGF-β[b] 2 mg BMP-2	Intramuscular implants in mice	Bone area	Synergistic	48
0.5-15 μg TGF-β1 20-100 μg BMP-7	Intramuscular implants in primates	Bone area Alk Phos Activity	Synergistic	43
0.5-100 μg TGF-β1 20-100 μg BMP-7	Intramuscular and calvarial defect implants in primates	Bone area Alk Phos activity Collagen expression	Synergistic	42
10 ng TGF-β1 15 mg bBMP[c]	3-mm segmental radial defect in dogs	Bone area	Additive	46
140 ng TGF-β2 & 25-400 ng bBMP[c] per mg implant	Subcutaneous implants in rats	Bone (semi-quant.) Alk Phos Activity	Synergistic	44,45
12 μg TGF-β2 25 μg BMP-2	Titanium implant model in dogs	Implant fixation (if) Bone area (ba)	Additive (if) Non-significant (ba)	50
20 ng TGF-β3 200 ng BMP-2	Subcutaneous implants in mice	Bone area	Synergistic	49
0.2 μg TGF-β3 2 μg BMP-2	Critical sized femoral defect in rats	Bone volume Mechanical strength	Non-significant	47

a: Effect of combination of growth factors compared to TGF-β and BMP alone
b: TGF-β extracted from platelets by acid/ethanol procedure and chromatography
c: BMP extracted and purified from bovine bone
TGF-β, Transforing growth factor-beta

increase the osteoprogenitor cell pool by stimulating cell proliferation. *In vitro*, this mitogenic effect did not modify the osteoinductive responsiveness of the cells to BMP.[53]
Apart from their combined effects on angiogenesis, cell recruitment and proliferation, TGF-β and BMPs also interact during osteoblast differentiation (extensively reviewed by Janssens et al[40]). Despite the conflicting results of numerous *in vitro* experiments, it seems TGF-β1 may have stimulatory effects on osteoblast differentiation during the early stage and an inhibitory effect on differentiation and mineralization at later stages. This altered biological effect would seem to be the result of cross-talk between the intracellular signaling pathways of BMP-2 and TGF-β1. Although TGF-β1 seems to inhibit matrix mineralization at later stages, the *in vivo* consequences of these inhibitory effects might be limited since the expression of TGF-β receptors is down-regulated when cell differentiation progresses. This results in a decreased responsiveness to TGF-β1 at later differentiation stages.

Fibroblast growth factor

FGFs are considered potent regulators of cell growth and wound healing. The FGF family consists of 25 members, which vary in size from 17 to 34 kDa, share a 16 to 65% similarity in amino acid sequence and fall into different subgroups.[54] In bone, they are produced by various cells including osteoblasts, macrophages and endothelial cells and are stored in their active form in the extracellular bone matrix. When released or secreted, FGFs act in an autocrine and paracrine way as a mitogen on many cell types. In addition to their mitogenic effects, FGFs are involved in a number of other cellular processes, including angiogenesis, wound healing and cell differentiation. During fracture healing, distinct groups of FGFs are differentially expressed suggesting an active stage-specific role for FGF signaling during the repair process.[55] In the early phase, FGF 1, 2 and 5 genes are expressed, which is associated with a rapid increase in local cell population.[55,56] At later stages, the expression of other FGFs is up-regulated suggesting that these growth factors are involved in the regulation of chondrogenesis and osteogenesis.[55] The best studied family member on bone regeneration is fibroblast growth factor-2 (FGF-2; also known as bFGF). Although FGF-2 alone is not capable of inducing ectopic bone formation, it plays an important role in the regulation of normal bone healing.[57] Exogenous FGF-2 enhances callus formation and stimulates bone healing in various orthopedic applications.[58-64]
In various studies FGF-2 or FGF-4 was combined with BMPs in an attempt to enhance bone regeneration and it was shown that the effects of FGF were time and dose-dependent (Table 3). Using a local BMP-2 delivery vehicle in combination with subcutaneous FGF-4 injections for 3 consecutive days, FGF administration at an early stage after implantation (days 2-4) increased the amount of newly formed bone, whereas its administration at later time points (days 6-8 or 9-11) had no effect.[65] When implanted in a delivery vehicle, low FGF dosages in combination with a single BMP dose synergistically enhanced BMP-induced bone formation, however, bone formation was inhibited by co-administration of high FGF dosages.[66-69] The shift from an enhanced to an inhibitory effect occurred between approximately 16 to 2000 ng FGF per delivery vehicle.
So far, little is known about the mechanism underlying the dose- and time-dependent FGF effects. The time-dependent effect may suggest that FGF plays an important role in cell recruitment and expansion during the early phase of bone regeneration. This is also suggested *in vitro*, where successive exposure of mesenchymal stem cells to FGF followed

Table 3
Combinations with FGF

Growth factor dose	*Setting*	*Outcome parameters*	*Effect* [a]	*Ref.*
10 ng FGF-2 1µg BMP-2	Onlay of implants on rabbit cranium	Bone area	Additive at 3 wks Synergistic at 6 & 9 wks	166
0.8 µg FGF-2 0.1 µg BMP-2	Subcutaneous implants in rats	Alk Phos Activity (AP) Calcium content (Ca) Collagen content (Col)	Synergistic on AP & Ca, inhibitory on Col at 2 wks, non-significant at later times	167
Cells exposed to 2.5/50 ng/ml FGF-2/ BMP-2 for 6 days	Implants with seeded cells subcutaneous in rats	Semiquantitative histologic score	Synergistic	70
0.1 µg FGF-2 0.6 µg BMP-2	Bone chamber model in rabbits	Bone area Bone ingrowth	Inhibitory	168
0.016–50 µg FGF-2 2 µg BMP-2	Intramuscular implants in rats	Bone area Alk Phos Activity	Synergistic at a dose ≤ 400 ng inhibitory at a dose ≥ 2 µg	66
0.001–5 µg FGF-2 5 µg BMP-2	Intramuscular implants in mice	BMD Bone area	Synergistic at a dose ≤ 10 ng inhibitory at a dose ≥ 100 ng	68
0.016 – 5 µg FGF-2 2 µg BMP-2	Intramuscular implants in rats	BMD, BMC Bone area Alk Phos activity	Synergistic at a dose ≤ 16 ng inhibitory at a dose ≥ 80 ng	67
0.2 mg FGF-2 1 mg BMP-2	Femoral osteotomy in rabbits	Bone area	Additive compared to BMP-2 alone[b]	84
12.5 µg FGF-2 5 µg BMP-2	Implants seeded with cells and cultured for 1 wk placed in rabbit spinal fusion model	Fusion determined by radiograps & palpation	Additive	169
0.1 mg FGF-2/kg/day for 3 days [BMP] unknown	Subcutaneous BMP implants in rats and 3 FGF injections	Bone density	Synergistic with FGF administration at days 2,3,4	65

a: Effect of combination of growth factors compared to FGF and BMP alone
b: Control group FGF alone was missing
FGF, Fibroblast growth factor; BMD, bone mineral density; BMC, bone mineral content

by BMP was equally successful in inducing calcium deposition compared to combined growth factor exposure during the same period.[70,71] *In vivo*, the combined angiogenic and migration effects of FGF could indirectly or directly enhance the recruitment of mesenchymal stem cells to the implantation site.[52] Furthermore, the mitogenic effect of FGF likely stimulates the proliferation of the local osteoprogenitor cells. BMPs can subsequently commit the enlarged osteoprogenitor cell pool towards the osteoblastic lineage, which ultimately results in the enhanced local bone formation.

Interestingly, *in vitro*, FGF-2/-9 were shown to stimulate mesenchymal stem cell proliferation and reversibly inhibit their differentiation in a dose-dependent manner.[71-73] An inhibitory effect on the production of differentiation markers like alkaline phosphatase activity and induction of mineralization were also seen in cultures containing FGF-2/-9 in combination with BMP-2 in a 1:5 ratio or with osteogenic medium.[71,73,74] However, in cultures containing FGF-2 and BMP-2 at a ratio of 1:10 or higher, the combination had a stimulatory effect on the bone differentiation markers compared to BMP alone.[70] These studies suggest a ratio dependent FGF/BMP effect in which the mitogenic FGF stimulus overrules the BMP-induced osteogenic differentiation at high FGF concentrations. *In vivo*, the excessive amount of FGF at the time of BMP release might have inhibited bone induction.

In an attempt to further elucidate the mechanism behind the dose-related FGF effect, the expression of genes associated with BMP signaling was studied in cells surrounding ectopically implanted FGF-2/BMP-2 delivery vehicles.[68] Whereas BMP-2 alone induced an

upregulation of ALK-3 and BMPR-II receptors, exposure to BMP-2 with FGF-2 resulted in an additional up-regulation of ALK-6 receptor expression.[68] *In vitro*, this FGF-enhanced ALK-6 expression augments BMP-induced Smad signaling and expression of alkaline phosphatase activity.[75] Furthermore, FGF-2 stimulated the expression of Smad 6 (an inhibitory Smad) in a dose-dependent manner, which may explain the inhibition of BMP-2-mediated differentiation at higher FGF concentrations. Although it is not known whether these changes in gene expression profiles are responsible for the *in vivo* physiological response, they clearly show a dose-dependent cross-talk between the FGF and BMP signaling pathways.

Insulin-like growth factor

IGF-I and IGF-II are small single-chain polypeptides of approximately 7.5 kDa which play an important role in bone metabolism and are essential to skeletal growth and maintenance of bone mass. They are synthesized by multiple tissues and elicit their effects in an endocrine, paracrine and autocrine way. The majority of IGFs exist in complexes, bound to one of the IGF-binding proteins which modulate their biological actions in a cell-specific manner.[76] IGFs are the most abundant growth factors produced by bone cells and are stored at the highest concentration of all growth factors in the bone matrix. Although there is still debate about its exact role in bone cell proliferation and differentiation, IGF has an anti-apoptotic effect on (pre)osteoblasts and enhances bone matrix synthesis.[77] *In vivo*, systemic IGF infusion showed an increase in bone formation, bone volume and/or bone turnover in animal models and clinical trials for osteoporosis.[78] However, major drawbacks of systemic free IGF administration are its side effects such as hypoglycemia, intracranial hypertension, headache, fatigue and dyspnea.[79] Consequently, localized IGF delivery was explored and showed to enhance bone formation without increasing circulating IGF-I levels.[80,81] Although insulin can bind to the IGF receptor as well, higher concentrations will be required due to its lower affinity. Since this may cause hypoglycaemia, insulin will probably never be considered as a therapeutic agent for bone regeneration.

A limited number of studies have investigated the effect of combined IGF-I and BMP addition on *in vitro* and *in vivo* osteogenesis. *In vitro*, sequential exposure to BMP-2 followed by IGF-I led to synergistically enhanced mesenchymal cell proliferation and alkaline phosphatase activity.[82] Similar effects were seen after exogenous BMP-7 and IGF-I administration or co-transfection of both genes in fetal calvarial cell cultures.[83] Both studies suggest that IGF-I enhances the mitogenic action as well as the differentiation activity of BMPs. In an *in vivo* bone-implant integration model, combined delivery of IGF-I and BMP-2 from coated titanium screws significantly improved bone formation compared to BMP-2 alone (Table 4).[84] Thus, the IGF/BMP combination seems to enhance both *in vitro* and *in vivo* osteogenesis.

The combination of IGF and TGF-β has been studied more extensively. Unfortunately, few studies compared the growth factor combination versus single IGF and TGF-β controls and their experimental set up varied greatly, in particular with respect to dose and delivery vehicle (Table 4).[85-88] Compared to TGF-β alone, nanogram dosages of the IGF/TGF-β combination in solution or released from gelatin hydrogels did not result in significantly enhanced mechanical properties or bone formation in rat marginal cortical defects, tibial defects and mandibular defects, but the release of micrograms of the growth factor combination from a coated titanium implant enhanced the mechanical properties and callus

Table 4
Combinations with IGF

Growth factors	*Setting*	*Outcome parameters*	*Effect* [a]	*Ref.*
0.25 mg IGF-I 1 mg BMP-2	Femoral osteotomy in rabbits	Bone area	Additive compared to BMP-2 alone[b]	84
10 ng IGF-I 25 ng TGF-β	Solution with growth factors in a marginal femoral defect in rats	Biomechanical test	Non-significant	85
50 μg IGF-I 10 μg TGF-β1	Coated titanium implants in a midshaft tibia fracture in rats	Biomechanical test Callus formation	Aditive/synergistic	88
25 ng IGF-I 0.1 μg TGF-β1	Gelatin hydrogel in a segmental tibia defect in rats	Bone formation (X-ray)	Non-significant	86
25 ng IGF-I 0.1 μg TGF-β1	Gelatin hydrogel in a marginal mandibular defect in rats	Bone formation (X-ray)	Non-significant	87

a: Effect of combination of growth factors compared to IGF and BMP alone
b: Control group IGF alone was missing
IGF, Insulin-like growth factor

formation in a rat tibial fracture model (Table 4).
Although only the latter *in vivo* study showed enhanced effects of the IGF/TGF-β combination over TGF-β alone, *in vitro* studies clearly suggest an interaction of both growth factors in regulation of bone formation. Synthesis of IGFs and IGF binding proteins by osteoblasts is regulated by various growth factors including TGF-β.[89,90] Furthermore, exogenously administered combinations of IGF-I and TGF-β synergistically enhanced cell proliferation and matrix synthesis in osteoblast cultures.[91-94] A similar synergistic effect of IGF-I and FGF was seen on cell proliferation and matrix synthesis in osteoblast cultures.[91,92] Unfortunately, no studies have been performed to investigate the effect of an IGF/FGF combination on *in vivo* bone regeneration.

Vascular endothelial growth factor

Vascular endothelial growth factor (VEGF) is considered one of the key regulators of angiogenesis during bone formation.[95] The biologically active form of VEGF, also referred to as VEGF-A, is a dimeric protein which may consist of different splice variants (121 to 206 amino-acids) of a single gene. Most cell types produce several VEGF forms simultaneously and their expression can be enhanced by hypoxia or other cytokines. *In vivo*, VEGF induces angiogenesis as well as permeabilization of capillaries.[96,97] During bone repair, these newly formed vessels and vascular changes are crucial for nutrient supply, transport of macromolecules and invading cells. The important role of VEGF during bone regeneration has been shown in various experimental models, demonstrating stimulation or disruption of the normal bone regeneration process in response to VEGF administration or inhibition respectively.[98-101]
Several *in vitro* studies suggest a BMP/VEGF-regulated coupling between osteogenesis and angiogenesis through reciprocal signaling. Co-cultures demonstrated that osteoblast-like cells stimulated the proliferation of endothelial cells by production of VEGF, whereas endothelial cells stimulated the differentiation of osteoprogenitor cells by production of BMP-2.[102,103] Furthermore, BMP-induced differentiation of preosteoblast-like cells enhanced endogenous production of VEGF.[104-106] These studies show the importance of angiogenesis during osteogenesis and emphasize the possible benefits of combining

VEGF and BMPs for bone regeneration.
So far, VEGF has only been combined with BMPs in an attempt to enhance bone regeneration (Table 5). The combined implantation of VEGF expressing cells with BMP-2 or BMP-4 expressing cells synergistically enhanced bone formation at an ectopic implantation site.[101,107,108] This effect on bone regeneration was dependent on the amount of cells applied and the ratio of VEGF/BMP expressing cells. Interestingly, co-implantation of cells expressing the VEGF-antagonist soluble Flt1 had an inhibitory effect on bone induction by BMP-2 or BMP-4 expressing cells.[101,107] The enhancement of BMP-induced osteogenesis by VEGF was further investigated using local delivery vehicles releasing recombinant VEGF in combination with a BMP-4 plasmid or recombinant BMP-2.[109-111] Although these studies showed enhancement of BMP-induced bone formation by VEGF, the effects with recombinant growth factor(s) were less pronounced compared to the studies using *ex vivo* transduced cells.
Several mechanisms could be responsible for the enhanced BMP-2-induced bone formation by VEGF. In addition to BMP, VEGF may stimulate the recruitment of mesenchymal stem cells.[112,113] Furthermore, VEGF-induced vascular changes (e.g. increased vascular support network and vascular permeability) could enhance this cell recruitment. In combination with BMP-transduced cells, the VEGF-induced angiogenesis could also have resulted in an increased survival of BMP expressing cells. Such a larger pool of BMP expressing cells could have resulted in higher local dose of the osteoinductive factor and a subsequent larger amount of bone as a result of the dose-response relation between BMP and bone formation.

Table 5
Combinations with VEGF

Growth factor dose	*Setting*	*Outcome parameters*	*Effect* [a]	*Ref.*
cells expressing VEGF or BMP-2	Intramuscular implants (im) and calcarial defect (cd) in mice	Bone area	Synergistic (im) Additive (cd)	101
cells expressing VEGF or BMP-2	Intramuscular implants in mice	Bone area	Synergistic at 4 wks Non-significant at 8 wks	108
2 μg VEGF 6.6 μg BMP-2	Subcutaneous (sc) and critical sized femoral defect (fd) in rats	Bone volume	Additive (sc) Non-significant (fd)	110
12 μg VEGF 2 μg BMP-2	Cranial defect in rats	Bone volume	Synergistic at 4 wks Non-significant at 12 wks	111
cells expressing VEGF or BMP-4	Intramuscular implants (im) and calvarial defect (cd) in mice	Bone area	Synergistic (im) Additive (cd)	107
3 μg VEGF BMP-4 plasmid	Subcutaneous implants in mice	Bone area Bone mineral density Bone mineral content	Additive	109

a: Effect of combination of growth factors compared to VEGF and BMP alone
VEGF, vascular endothelial growth factor

Platelet derived growth factor

PDGF is considered one of the key regulators of general tissue repair.[114] Its family consists of dimeric proteins of approximately 30 kDa composed of disulfide-linked polypeptides encoded by 4 different genes (PDGF-A, B, C and D) which form homodimers (PDGF-AA, -BB, -CC and –DD) and heterodimers (PDGF-AB). During the early phase of wound healing, platelets are the major source of PDGF. Following injury and haemorrhage, platelets aggregate and release cytokine-loaded granules containing various amounts of PDGFs. Upon release, PDGFs stimulate the recruitment of neutrophils, macrophages and mesenchymal cells, which then serve as an ongoing source of PDGFs during the healing process. PDGF also enhances proliferation of various bone cell types and enhances angiogenesis by its induction of sprouting from adjacent blood vessels and expression of VEGF. Although both PDGF and VEGF stimulate angiogenesis, PDGF stimulates the migration of a population of mesenchymal cells which appears to be different from those stimulated by VEGF.[115,116] Apart from its positive effect on soft tissue healing, the therapeutic potential of PDGF was also demonstrated in various animal models for skeletal reconstruction.[114]

The effect of various dosages of PDGF-BB was studied in combination with BMPs in a collagen matrix in a craniotomy defect (Table 6).[117] Whereas BMPs caused a dose-dependent increase in radiopacity and bone area in the defect, BMP-induced bone formation was inhibited by PDGF-BB dosages between 20 and 200 µg. Also in combination with demineralised bone matrix (DBM), which contains various growth factors including BMPs, PDGF showed a similar inhibitory effect.[118] This inhibitory effect of PDGF on BMP- or DBM-induced bone formation could be the result of its inhibitory effect on osteoprogenitor differentiation as indicated by its *in vivo* inhibitory effect on the bone matrix apposition rate and *in vitro* inhibition of the osteoblast phenotypic markers osteocalcin and alkaline phosphatase.[119-122] As PDGF stimulates active bone resorption, the inhibitory effect could also be attributed to a reduction of available surface for bone formation as the surface is eroded by the increased number of osteoclasts.[120]

The effect of the PDGF/IGF combination has been studied in a partial thickness tibial defects in pigs.[123] Comparison of growth factor-treated defects and empty intra-animal control defects showed that the combination of PDGF/IGF-I increased callus area and

Table 6
Combinations with PDGF

Growth factors	*Setting*	*Outcome parameters*	*Effect* [a]	*Ref.*
20-100 µg PDGF-BB 30-150 µg BMP	Cranial defect in rats	Radioopacity and bone area	Inhibitory	117
50 µL PRP[b] 200 ng BMP-2	Cranial defect in rats	Bone mineral density Bone mineral content	Synergistic	134
100 µL PRP[b] 15 µg BMP-2	Cranial defect in rabbits	Bone area	Non significant	135
10 µg PDGF-BB 10 µg IGF-I	Periodontal defect in primates	Bone area New tooth attachments	Non-significant	129
6 µg PDGF-BB 6 µg IGF-I	Partial thickness tibial defect in pigs	Callus formation	Synergistic[c]	123

a: Effect of combination compared to PDGF or PRP and BMP alone
b: Platelet rich plasma (platelet concentrate containing various growth factors including PDGF, TGF-β, IGF-I and VEGF)
c: Compared to intra-animal controls, however absolute IGF-I values were higher or equal compared to combination group
PDGF, platelet-derived growth factor.

thickness, whereas neither of the growth factors alone enhanced regeneration. However, interpretation of these data remains difficult since the absolute callus area and thickness of implants containing IGF-I alone were equal or higher compared to the PDGF/IGF-I combination. In contrast to this ambiguous *in vivo* effect, *in vitro* studies did show enhanced effects of the PDGF/IGF combination. *In vitro*, increased proliferation of several bone cell types, deposition of collagen and formation of bone matrix was found, compared to the same amount of either of the growth factors individually.[91,94] Further studies are required to characterize the interaction of these growth factors in bone regeneration. The combination of PDGF and IGF has been studied more extensively in periodontal regeneration. Several *in vivo* studies showed the formation of substantial amounts of new bone, cementum, and periodontal ligament by a combination of PDGF-BB and IGF-I.[124-127] In a clinical trial, the local application of a high dose (150 µg/ml) of rhPDGF/rhIGF-I significantly increased alveolar bone formation compared to controls without growth factor.[128] However, in only one study the PDGF/IGF-I combination was compared to individual growth factor controls.[129] In this primate model, the tested dose of IGF-I alone had no significant effect on bone formation and the formation of new attachments between the tooth and periodontal bone. Although the PDGF/IGF-I combination significantly enhanced bone and new attachment formation compared to the delivery vehicle alone, no significant differences were seen compared to PDGF alone.

A substance that typically contains PDGF in addition to several other growth factors is platelet rich plasma (PRP) or platelet gel. The platelets in PRP contain several growth factors including PDGF, TGF-β, IGF-I and VEGF which are released upon their activation. Since this event also occurs after normal bone injury, the concept to enhance bone regeneration with autologous PRP is obvious. So far, the effects of PRP in various clinical and animal models of bone regeneration are ambiguous, with both enhancement of bone regeneration and lack of additional effects reported.[130-133] In combination with BMP-2, human PRP improved angiogenesis and resulted in enhanced bone healing compared to BMP-2 alone in a rat cranial defect.[134] However, no statistically significant differences of platelet growth factor release was seen after combined implantation of rabbit PRP/BMP-2 gels compared to fibrin/BMP-2 gels in rabbit cranial defects.[135] Moreover, in a clinical trial, the combination of PRP and BMP has shown to be even less effective compared to BMPs alone.[136] In addition to the variation in experimental setups between these studies, growth factor concentrations in PRP are known to be variable between species and individuals[137], all adding to the confusion around effectivity of PRP and combinations with BMPs.

Cytokines

The term cytokine encompasses a large and diverse family of proteins which historically refers to the immunomodulating agents (interleukins, interferons, tumor necrosis factors, etc.). However, as more was learned about them, it appeared these molecules play an essential role in the complex crosstalk between the immune and skeletal system. Although the mechanisms are still poorly understood, it has become apparent that many cytokines are involved in bone metabolism and are able to stimulate or inhibit the formation and function of osteoblasts, osteoclasts or their precursor cells.[138-141]

Despite the large number of available cytokines, only interleukin-11 (IL-11) has been studied in combination with BMP-2 in bone regeneration models (Table 7). IL-11 is pro-

Table 7
Combinations with cytokines

Growth factors	*Setting*	*Outcome parameters*	*Effect* [a]	*Ref.*
20-200 μg IL-11 6 μg BMP-2	Subcutaneous implants in rats	Calcium content	Synergistic	147
200 μg IL-11 1 mg BMP-2	Segmental bone defect in rabbits	Bone volume (bv) Mechenical strength (ms)	Synergistic (bv) Non significant (ms)	148

a: Effect of combination compared to IL-11 and BMP alone
IL, interleukin

duced by various cells and has several biological activities including roles in hematopoiesis, immune responses and bone metabolism.[142,143] *In vitro*, IL-11 enhances osteoclast formation and bone resorption, but also stimulates the expression of osteoblastic markers in mesenchymal progenitor cells.[144-146] During osteogenesis, IL-11 synergizes with BMP-2 in a dose-dependent fashion to enhance the *in vitro* osteoblastic differentiation of progenitor cells.[146] Although the mechanical properties of the formed bone were not significantly different compared to BMP-2 alone, a similar synergistic increase in bone formation rate was seen after combined implantation of IL-11 and BMP-2 in a rat ectopic and rabbit segmental bone defect model.[147,148] Overall, these results show that IL-11 actions predominantly enhance BMP-2 induced bone formation.

Systemic regulators

In contrast to the local application of the previously mentioned growth factors and cytokines, some systemically administered hormones also enhance bone formation. Of particular interest is PTH, a major systemic regulator of bone metabolism. It is secreted from the parathyroid glands and travels through the bloodstream to act upon bone. Whereas continuous PTH infusion causes the bone disease osteitis fibrosa, its intermittent subcutaneous administration enhances bone formation.[149,150] The anabolic effect of intermittent PTH on bone has made it an effective treatment for osteoporosis in humans, where it was shown to increase bone mass and reduce fracture rate.[151] So far, the mechanism behind this dual effect is still not completely understood. It has been suggested that PTH-induced stimulation of bone formation is due to an increase in osteoblast number. This increase in osteoblast number is not dependent on osteoblastogenesis, rather is the result of activation of existing bone-lining cells which undergo hypertrophy and resume matrix synthesis.[149,152-155] Another proposed method for its effect is the inhibition of osteoblast apoptosis.[149,153]
Since PTH acts upon cells committed to the osteoblastic lineage, it has been combined with osteoinductive BMPs (Table 8). Ectopically, systemic PTH treatment increased the local BMP-2-induced bone formation and reversed the age-related decrease in osteoinductive potential of BMP-2.[156-158] Although systemic PTH treatment enhanced healing of a partial thickness tibial defect, no significant effect of BMP-7 and no synergistic effect of the PTH/BMP-7 combination were seen.[159] In a critical sized femoral defect, the effects of BMP-2 and PTH alone were opposite and their combination synergistically enhanced bone formation.[158] The discrepancy between these studies may be due to the different orthotopic models. In the partial thickness defect, endogenous production of BMPs was

Table 8
Combinations with systemically administered hormones

Growth factor dose	*Setting*	*Outcome parameters*	*Effect* [a]	*Ref.*
20 & 40 μg/kg/day PTH 5 μg BMP-2	Subcutaneous BMP-2 implants in rats	Alk phos activity Calcium content	Synergistic	156
10 μg/kg/day PTH 5 μg BMP-2	Subcutaneous BMP-2 implants in mice	Bone mineral density Calcium content	Synergistic	157
10 μg/kg/day PTH 6.5 μg BMP-2	BMP-2 implants in subcutaneous (sc) and femoral defects (fd) in rats	Bone mineral density Bone volume	Synergistic (sc) Additive (fd)	158
10 μg/kg/day PTH 200 μg BMP-7	BMP-7 implants in a partial thickness tibial defect in rabbits	Bone mineral content Bone volume Mechanical strength	Non-significant	159
0.2 & 0.4 μg/kg/day PGE_2 5 μg BMP-2	Subcutaneous BMP-2 implants in rats	Alk Phos Activity Calcium content	Synergistic	156
50 & 100 ng/kg/day $VitD_3$ 5 μg BMP-2	Subcutaneous BMP-2 implants in rats	Alk Phos Activity Calcium content	Synergistic	156

a: Effect of combination compared to the hormone and BMP alone
PTH, parathyroid hormone; $VitD_3$, 1-alpha,25-dihydroxyvitamin D_3

sufficient to heal the defect. Consequently, PTH enhanced this endogenously induced bone formation and addition of BMP-7 had no significant effect.[159] The interference of this local autoinduction was less in the critical sized defects where no spontaneous healing was seen in empty defects and bone formation was significantly enhanced by BMP–2.[158] Apart from the PTH/BMP-2 combination, BMP-2 has also been combined with systemic administration of prostaglandin E_2 and [1,25-dihydroxy]vitamin D_3.[156] In bone, the anabolic actions of systemically administered prostaglandin E_2 increases bone formation and bone mass.[160,161] In combination with BMP-2, a low dose of prostaglandin E_2 significantly increased alkaline phosphatase activity and calcium content of ectopic implants in rats.
In addition to PTH, vitamin D is an important regulator of bone mineral homeostasis. It plays an important role in osteoblast/osteoclast communication by stimulating the production of receptor activator of nuclear factor-κB ligand (RANKL) by osteoblasts, which enhances the recruitment and activation of osteoclasts.[162] In addition to the stimulation of osteoblastic activity, it also inhibits osteoblast apoptosis. Despite its complex actions on both osteoblast and osteoclast activity, vitamin D treatment of osteoporotic patients resulted in a modest enhancement of bone mineral density.[163-165] Systemic administration of vitamin D_3 significantly increased alkaline phosphatase activity and calcium content of ectopic BMP-2 loaded implants.[156] So far, the mechanism behind this effect is not known and further studies are required to characterize this vitamin D_3/BMP-2 interaction.

Summary and future directions

Ever since the discovery of the auto-inductive capacity of bone by bioactive peptides, researchers have attempted to enhance bone regeneration by modulating the cellular behavior using growth factors, cytokines and hormones. Although their exact role during the regeneration process has not been fully defined, many of these molecules are able to enhance bone formation with varying potency and efficacy. As shown by the studies summarized in this review, many of these growth factors interact during bone formation. Depending on the combination of growth factors their routes of delivery, the dosage

used and the animal model, this interaction could result in an enhancement or inhibition of bone formation compared to the individual growth factors. Synergistic effects on bone formation are seen for most combinations, which in the case of fabricated BMP heterodimers even resulted in a 20 fold increase in bone formation compared to homodimers. Since these translational studies are performed to develop new therapies for bone regeneration, growth factor combinations with *in vitro* inhibitory effects are unlikely studied in translational bone regeneration studies. This may be the reason that only few studies with non-significant or inhibitory effects of combination therapies could be found.

To date, the fragmentary results on combinations of usually two growth factors with a limited number of growth factor concentrations and timing suggest that this is a rather understudied area of investigation in bone regeneration, despite its tremendous potential and virtually endless possible combinations. It is recommended that future studies address these challenges by systematically analyzing the many possibilities and that new, high throughput screening techniques will be required to achieve this. Overall, this review shows we are only beginning to understand the possibilities of applying multiple growth factors and cytokines *in vivo*, the signaling pathways involved and their convergence points.

Bone regeneration based on the delivery of bioactive molecules is a promising strategy that could revolutionize the way bone grafting procedures are performed in orthopedics, neurosurgery and dentistry. Despite the success of current single-drug treatments, our knowledge of the bone regeneration process and growth factor interactions is still limited. Therefore, further molecular, cellular and translational studies are required to obtain a better understanding of the actions and interactions of the different regulators of the regeneration process. In addition, the challenge in translational research will be to improve local delivery vehicles and their pharmacokinetic profiles. So far, many of the growth factor combinations have been released from relatively simple delivery vehicles with unknown pharmacokinetic profiles. New delivery vehicles with adjustable release profiles would help identify the optimal amounts, ratio, timing and release sequence of these regulators to optimize the bone regeneration process and ensure consistent success in clinical applications.

References

1. Giannoudis, P.V., Dinopoulos, H., and Tsiridis, E. Bone substitutes: an update. Injury 36 Suppl 3, S20, 2005.
2. Buck, B.E., Malinin, T.I., and Brown, M.D. Bone transplantation and human immunodeficiency virus. An estimate of risk of acquired immunodeficiency syndrome (AIDS). Clin Orthop Relat Res, 129, 1989.
3. Younger, E.M., and Chapman, M.W. Morbidity at bone graft donor sites. J Orthop Trauma 3, 192, 1989.
4. Arrington, E.D., Smith, W.J., Chambers, H.G., Bucknell, A.L., and Davino, N.A. Complications of iliac crest bone graft harvesting. Clin Orthop Relat Res, 300, 1996.
5. Norman-Taylor, F.H., and Villar, R.N. Bone allograft: a cause for concern? J Bone Joint Surg Br 79, 178, 1997.
6. Silber, J.S., Anderson, D.G., Daffner, S.D., Brislin, B.T., Leland, J.M., Hilibrand, A.S., Vaccaro, A.R., and Albert, T.J. Donor site morbidity after anterior iliac crest bone harvest for single-level anterior cervical discectomy and fusion. Spine 28, 134, 2003.
7. Urist, M.R. Bone: formation by autoinduction. Science 150, 893, 1965.
8. Urist, M.R., Iwata, H., Ceccotti, P.L., Dorfman, R.L., Boyd, S.D., McDowell, R.M., and Chien, C. Bone morphogenesis in implants of insoluble bone gelatin. Proc Natl Acad Sci U S A 70, 3511, 1973.

9. Riley, E.H., Lane, J.M., Urist, M.R., Lyons, K.M., and Lieberman, J.R. Bone morphogenetic protein-2: biology and applications. Clin Orthop Relat Res, 39, 1996.
10. Rengachary, S.S. Bone morphogenetic proteins: basic concepts. Neurosurg Focus 13, e2, 2002.
11. Wozney, J.M. Overview of bone morphogenetic proteins. Spine 27, S2, 2002.
12. Aoki, H., Fujii, M., Imamura, T., Yagi, K., Takehara, K., Kato, M., and Miyazono, K. Synergistic effects of different bone morphogenetic protein type I receptors on alkaline phosphatase induction. J Cell Sci 114, 1483, 2001.
13. Hazama, M., Aono, A., Ueno, N., and Fujisawa, Y. Efficient expression of a heterodimer of bone morphogenetic protein subunits using a baculovirus expression system. Biochem Biophys Res Commun 209, 859, 1995.
14. Sampath, T.K., Coughlin, J.E., Whetstone, R.M., Banach, D., Corbett, C., Ridge, R.J., Ozkaynak, E., Oppermann, H., and Rueger, D.C. Bovine osteogenic protein is composed of dimers of OP-1 and BMP-2A, two members of the transforming growth factor-beta superfamily. J Biol Chem 265, 13198, 1990.
15. Canalis, E., Economides, A.N., and Gazzerro, E. Bone morphogenetic proteins, their antagonists, and the skeleton. Endocr Rev 24, 218, 2003.
16. Wang, E.A., Rosen, V., Cordes, P., Hewick, R.M., Kriz, M.J., Luxenberg, D.P., Sibley, B.S., and Wozney, J.M. Purification and characterization of other distinct bone-inducing factors. Proc Natl Acad Sci U S A 85, 9484, 1988.
17. Cheng, H., Jiang, W., Phillips, F.M., Haydon, R.C., Peng, Y., Zhou, L., Luu, H.H., An, N., Breyer, B., Vanichakarn, P., Szatkowski, J.P., Park, J.Y., and He, T.C. Osteogenic activity of the fourteen types of human bone morphogenetic proteins (BMPs). J Bone Joint Surg Am 85-A, 1544, 2003.
18. Luu, H.H., Song, W.X., Luo, X., Manning, D., Luo, J., Deng, Z.L., Sharff, K.A., Montag, A.G., Haydon, R.C., and He, T.C. Distinct roles of bone morphogenetic proteins in osteogenic differentiation of mesenchymal stem cells. J Orthop Res 25, 665, 2007.
19. Wang, E.A., Rosen, V., D'Alessandro, J.S., Bauduy, M., Cordes, P., Harada, T., Israel, D.I., Hewick, R.M., Kerns, K.M., LaPan, P., and et al. Recombinant human bone morphogenetic protein induces bone formation. Proc Natl Acad Sci U S A 87, 2220, 1990.
20. Niikura, T., Hak, D.J., and Reddi, A.H. Global gene profiling reveals a downregulation of BMP gene expression in experimental atrophic nonunions compared to standard healing fractures. J Orthop Res 24, 1463, 2006.
21. Zhu, W., Rawlins, B.A., Boachie-Adjei, O., Myers, E.R., Arimizu, J., Choi, E., Lieberman, J.R., Crystal, R.G., and Hidaka, C. Combined bone morphogenetic protein-2 and -7 gene transfer enhances osteoblastic differentiation and spine fusion in a rodent model. J Bone Miner Res 19, 2021, 2004.
22. Cho, T.J., Gerstenfeld, L.C., and Einhorn, T.A. Differential temporal expression of members of the transforming growth factor beta superfamily during murine fracture healing. J Bone Miner Res 17, 513, 2002.
23. Ripamonti, U., Crooks, J., Petit, J.C., and Rueger, D.C. Periodontal tissue regeneration by combined applications of recombinant human osteogenic protein-1 and bone morphogenetic protein-2. A pilot study in Chacma baboons (Papio ursinus). Eur J Oral Sci 109, 241, 2001.
24. Israel, D.I., Nove, J., Kerns, K.M., Kaufman, R.J., Rosen, V., Cox, K.A., and Wozney, J.M. Heterodimeric bone morphogenetic proteins show enhanced activity *in vitro* and *in vivo*. Growth Factors 13, 291, 1996.
25. Aono, A., Hazama, M., Notoya, K., Taketomi, S., Yamasaki, H., Tsukuda, R., Sasaki, S., and Fujisawa, Y. Potent ectopic bone-inducing activity of bone morphogenetic protein-4/7 heterodimer. Biochem Biophys Res Commun 210, 670, 1995.
26. Koh, J.T., Zhao, Z., Wang, Z., Lewis, I.S., Krebsbach, P.H., and Franceschi, R.T. Combinatorial gene therapy with BMP2/7 enhances cranial bone regeneration. J Dent Res 87, 845, 2008.
27. Zhao, M., Zhao, Z., Koh, J.T., Jin, T., and Franceschi, R.T. Combinatorial gene therapy for bone regeneration: cooperative interactions between adenovirus vectors expressing bone morphogenetic proteins 2, 4, and 7. J Cell Biochem 95, 1, 2005.
28. Kawai, M., Bessho, K., Maruyama, H., Miyazaki, J., and Yamamoto, T. Simultaneous gene transfer of bone morphogenetic protein (BMP) -2 and BMP-7 by *in vivo* electroporation induces rapid bone formation and BMP-4 expression. BMC Musculoskelet Disord 7, 62, 2006.
29. Miyazono, K., Maeda, S., and Imamura, T. BMP receptor signaling: transcriptional targets, regulation of signals, and signaling cross-talk. Cytokine Growth Factor Rev 16, 251, 2005.
30. Yanagita, M. BMP antagonists: Their roles in development and involvement in pathophysiology. Cytokine Growth Factor Rev 16, 309, 2005.

31. Wrana, J.L., and Attisano, L. The Smad pathway. Cytokine Growth Factor Rev 11, 5, 2000.
32. Rosen, V., Thies, R.S., and Lyons, K. Signaling pathways in skeletal formation: a role for BMP receptors. Ann N Y Acad Sci 785, 59, 1996.
33. ten Dijke, P., Yamashita, H., Sampath, T.K., Reddi, A.H., Estevez, M., Riddle, D.L., Ichijo, H., Heldin, C.H., and Miyazono, K. Identification of type I receptors for osteogenic protein-1 and bone morphogenetic protein-4. J Biol Chem 269, 16985, 1994.
34. Ebisawa, T., Tada, K., Kitajima, I., Tojo, K., Sampath, T.K., Kawabata, M., Miyazono, K., and Imamura, T. Characterization of bone morphogenetic protein-6 signaling pathways in osteoblast differentiation. J Cell Sci 112 (Pt 20), 3519, 1999.
35. Macias-Silva, M., Hoodless, P.A., Tang, S.J., Buchwald, M., and Wrana, J.L. Specific activation of Smad1 signaling pathways by the BMP7 type I receptor, ALK2. J Biol Chem 273, 25628, 1998.
36. Tsumaki, N., and Yoshikawa, H. The role of bone morphogenetic proteins in endochondral bone formation. Cytokine Growth Factor Rev 16, 279, 2005.
37. Zhu, W., Kim, J., Cheng, C., Rawlins, B.A., Boachie-Adjei, O., Crystal, R.G., and Hidaka, C. Noggin regulation of bone morphogenetic protein (BMP) 2/7 heterodimer activity *in vitro*. Bone 39, 61, 2006.
38. Lawrence, D.A. Latent-TGF-beta: an overview. Mol Cell Biochem 219, 163, 2001.
39. Annes, J.P., Munger, J.S., and Rifkin, D.B. Making sense of latent TGFbeta activation. J Cell Sci 116, 217, 2003.
40. Janssens, K., ten Dijke, P., Janssens, S., and Van Hul, W. Transforming growth factor-beta1 to the bone. Endocr Rev 26, 743, 2005.
41. Bostrom, M.P., and Asnis, P. Transforming growth factor beta in fracture repair. Clin Orthop Relat Res, S124, 1998.
42. Duneas, N., Crooks, J., and Ripamonti, U. Transforming growth factor-beta 1: induction of bone morphogenetic protein genes expression during endochondral bone formation in the baboon, and synergistic interaction with osteogenic protein-1 (BMP-7). Growth Factors 15, 259, 1998.
43. Ripamonti, U., Duneas, N., Van Den Heever, B., Bosch, C., and Crooks, J. Recombinant transforming growth factor-beta1 induces endochondral bone in the baboon and synergizes with recombinant osteogenic protein-1 (bone morphogenetic protein-7) to initiate rapid bone formation. J Bone Miner Res 12, 1584, 1997.
44. Bentz, H., Nathan, R.M., Rosen, D.M., Armstrong, R.M., Thompson, A.Y., Segarini, P.R., Mathews, M.C., Dasch, J.R., Piez, K.A., and Seyedin, S.M. Purification and characterization of a unique osteoinductive factor from bovine bone. J Biol Chem 264, 20805, 1989.
45. Bentz, H., Thompson, A.Y., Armstrong, R., Chang, R.J., Piez, K.A., and Rosen, D.M. Transforming growth factor-beta 2 enhances the osteoinductive activity of a bovine bone-derived fraction containing bone morphogenetic protein-2 and 3. Matrix 11, 269, 1991.
46. Heckman, J.D., Ehler, W., Brooks, B.P., Aufdemorte, T.B., Lohmann, C.H., Morgan, T., and Boyan, B.D. Bone morphogenetic protein but not transforming growth factor-beta enhances bone formation in canine diaphyseal nonunions implanted with a biodegradable composite polymer. J Bone Joint Surg Am 81, 1717, 1999.
47. Oest, M.E., Dupont, K.M., Kong, H.-J., Mooney, D.J., and Guldberg, R.E. Delivery of BMP-2 & TGF-beta3 additively enhance functional repair of segmental defects. Proceedings of the 53rd Meeting of the Orthopedic Research Society, San Diego, CA, February 10-14, 2007, 2007.
48. Si, X., Jin, Y., and Yang, L. Induction of new bone by ceramic bovine bone with recombinant human bone morphogenetic protein 2 and transforming growth factor beta. Int J Oral Maxillofac Surg 27, 310, 1998.
49. Simmons, C.A., Alsberg, E., Hsiong, S., Kim, W.J., and Mooney, D.J. Dual growth factor delivery and controlled scaffold degradation enhance *in vivo* bone formation by transplanted bone marrow stromal cells. Bone 35, 562, 2004.
50. Sumner, D.R., Turner, T.M., Urban, R.M., Virdi, A.S., and Inoue, N. Additive enhancement of implant fixation following combined treatment with rhTGF-beta2 and rhBMP-2 in a canine model. J Bone Joint Surg Am 88, 806, 2006.
51. Otsuru, S., Tamai, K., Yamazaki, T., Yoshikawa, H., and Kaneda, Y. Bone marrow-derived osteoblast progenitor cells in circulating blood contribute to ectopic bone formation in mice. Biochem Biophys Res Commun 354, 453, 2007.
52. Ramoshebi, L.N., and Ripamonti, U. Osteogenic protein-1, a bone morphogenetic protein, induces angiogenesis in the chick chorioallantoic membrane and synergizes with basic fibroblast growth factor and transforming growth factor-beta1. Anat Rec 259, 97, 2000.

53. Fromigue, O., Marie, P.J., and Lomri, A. Bone morphogenetic protein-2 and transforming growth factor-beta2 interact to modulate human bone marrow stromal cell proliferation and differentiation. J Cell Biochem 68, 411, 1998.
54. Eswarakumar, V.P., Lax, I., and Schlessinger, J. Cellular signaling by fibroblast growth factor receptors. Cytokine Growth Factor Rev 16, 139, 2005.
55. Schmid, G.J., Kobayashi, C., Sandell, L.J., and Ornitz, D.M. Fibroblast growth factor expression during skeletal fracture healing in mice. Dev Dyn 238, 766, 2009.
56. Bourque, W.T., Gross, M., and Hall, B.K. Expression of four growth factors during fracture repair. Int J Dev Biol 37, 573, 1993.
57. Marie, P.J. Fibroblast growth factor signaling controlling osteoblast differentiation. Gene 316, 23, 2003.
58. Kato, T., Kawaguchi, H., Hanada, K., Aoyama, I., Hiyama, Y., Nakamura, T., Kuzutani, K., Tamura, M., Kurokawa, T., and Nakamura, K. Single local injection of recombinant fibroblast growth factor-2 stimulates healing of segmental bone defects in rabbits. J Orthop Res 16, 654, 1998.
59. Kawaguchi, H., Kurokawa, T., Hanada, K., Hiyama, Y., Tamura, M., Ogata, E., and Matsumoto, T. Stimulation of fracture repair by recombinant human basic fibroblast growth factor in normal and streptozotocin-diabetic rats. Endocrinology 135, 774, 1994.
60. Nakamura, T., Hara, Y., Tagawa, M., Tamura, M., Yuge, T., Fukuda, H., and Nigi, H. Recombinant human basic fibroblast growth factor accelerates fracture healing by enhancing callus remodeling in experimental dog tibial fracture. J Bone Miner Res 13, 942, 1998.
61. Okazaki, H., Kurokawa, T., Nakamura, K., Matsushita, T., Mamada, K., and Kawaguchi, H. Stimulation of bone formation by recombinant fibroblast growth factor-2 in callotasis bone lengthening of rabbits. Calcif Tissue Int 64, 542, 1999.
62. Radomsky, M.L., Aufdemorte, T.B., Swain, L.D., Fox, W.C., Spiro, R.C., and Poser, J.W. Novel formulation of fibroblast growth factor-2 in a hyaluronan gel accelerates fracture healing in nonhuman primates. J Orthop Res 17, 607, 1999.
63. Radomsky, M.L., Thompson, A.Y., Spiro, R.C., and Poser, J.W. Potential role of fibroblast growth factor in enhancement of fracture healing. Clin Orthop Relat Res, S283, 1998.
64. Nakajima, F., Ogasawara, A., Goto, K., Moriya, H., Ninomiya, Y., Einhorn, T.A., and Yamazaki, M. Spatial and temporal gene expression in chondrogenesis during fracture healing and the effects of basic fibroblast growth factor. J Orthop Res 19, 935, 2001.
65. Kubota, K., Iseki, S., Kuroda, S., Oida, S., Iimura, T., Duarte, W.R., Ohya, K., Ishikawa, I., and Kasugai, S. Synergistic effect of fibroblast growth factor-4 in ectopic bone formation induced by bone morphogenetic protein-2. Bone 31, 465, 2002.
66. Fujimura, K., Bessho, K., Okubo, Y., Kusumoto, K., Segami, N., and Iizuka, T. The effect of fibroblast growth factor-2 on the osteoinductive activity of recombinant human bone morphogenetic protein-2 in rat muscle. Arch Oral Biol 47, 577, 2002.
67. Kakudo, N., Kusumoto, K., Kuro, A., and Ogawa, Y. Effect of recombinant human fibroblast growth factor-2 on intramuscular ectopic osteoinduction by recombinant human bone morphogenetic protein-2 in rats. Wound Repair Regen 14, 336, 2006.
68. Nakamura, Y., Tensho, K., Nakaya, H., Nawata, M., Okabe, T., and Wakitani, S. Low dose fibroblast growth factor-2 (FGF-2) enhances bone morphogenetic protein-2 (BMP-2)-induced ectopic bone formation in mice. Bone 36, 399, 2005.
69. Tanaka, E., Ishino, Y., Sasaki, A., Hasegawa, T., Watanabe, M., Dalla-Bona, D.A., Yamano, E., van Eijden, T.M., and Tanne, K. Fibroblast growth factor-2 augments recombinant human bone morphogenetic protein-2-induced osteoinductive activity. Ann Biomed Eng 34, 717, 2006.
70. Hanada, K., Dennis, J.E., and Caplan, A.I. Stimulatory effects of basic fibroblast growth factor and bone morphogenetic protein-2 on osteogenic differentiation of rat bone marrow-derived mesenchymal stem cells. J Bone Miner Res 12, 1606, 1997.
71. Fakhry, A., Ratisoontorn, C., Vedhachalam, C., Salhab, I., Koyama, E., Leboy, P., Pacifici, M., Kirschner, R.E., and Nah, H.D. Effects of FGF-2/-9 in calvarial bone cell cultures: differentiation stage-dependent mitogenic effect, inverse regulation of BMP-2 and noggin, and enhancement of osteogenic potential. Bone 36, 254, 2005.
72. Martin, I., Muraglia, A., Campanile, G., Cancedda, R., and Quarto, R. Fibroblast growth factor-2 supports *ex vivo* expansion and maintenance of osteogenic precursors from human bone marrow. Endocrinology 138, 4456, 1997.

73. Quarto, N., and Longaker, M.T. FGF-2 inhibits osteogenesis in mouse adipose tissue-derived stromal cells and sustains their proliferative and osteogenic potential state. Tissue Eng 12, 1405, 2006.
74. Varkey, M., Kucharski, C., Haque, T., Sebald, W., and Uludag, H. *In vitro* osteogenic response of rat bone marrow cells to bFGF and BMP-2 treatments. Clin Orthop Relat Res 443, 113, 2006.
75. Singhatanadgit, W., Salih, V., and Olsen, I. Up-regulation of bone morphogenetic protein receptor IB by growth factors enhances BMP-2-induced human bone cell functions. J Cell Physiol 209, 912, 2006.
76. Conover, C.A. Insulin-like growth factor-binding proteins and bone metabolism. Am J Physiol Endocrinol Metab 294, E10, 2008.
77. Niu, T., and Rosen, C.J. The insulin-like growth factor-I gene and osteoporosis: a critical appraisal. Gene 361, 38, 2005.
78. Rosen, C.J. Insulin-like growth factor I and bone mineral density: experience from animal models and human observational studies. Best Pract Res Clin Endocrinol Metab 18, 423, 2004.
79. Geusens, P.P., and Boonen, S. Osteoporosis and the growth hormone-insulin-like growth factor axis. Horm Res 58 Suppl 3, 49, 2002.
80. Fowlkes, J.L., Thrailkill, K.M., Liu, L., Wahl, E.C., Bunn, R.C., Cockrell, G.E., Perrien, D.S., Aronson, J., and Lumpkin, C.K., Jr. Effects of systemic and local administration of recombinant human IGF-I (rhIGF-I) on de novo bone formation in an aged mouse model. J Bone Miner Res 21, 1359, 2006.
81. Meinel, L., Zoidis, E., Zapf, J., Hassa, P., Hottiger, M.O., Auer, J.A., Schneider, R., Gander, B., Luginbuehl, V., Bettschart-Wolfisberger, R., Illi, O.E., Merkle, H.P., and von Rechenberg, B. Localized insulin-like growth factor I delivery to enhance new bone formation. Bone 33, 660, 2003.
82. Raiche, A.T., and Puleo, D.A. *In vitro* effects of combined and sequential delivery of two bone growth factors. Biomaterials 25, 677, 2004.
83. Yeh, L.C., Adamo, M.L., Olson, M.S., and Lee, J.C. Osteogenic protein-1 and insulin-like growth factor I synergistically stimulate rat osteoblastic cell differentiation and proliferation. Endocrinology 138, 4181, 1997.
84. Lan, J., Wang, Z., Wang, Y., Wang, J., and Cheng, X. The effect of combination of recombinant human bone morphogenetic protein-2 and basic fibroblast growth factor or insulin-like growth factor-I on dental implant osseointegration by confocal laser scanning microscopy. J Periodontol 77, 357, 2006.
85. Blumenfeld, I., Srouji, S., Lanir, Y., Laufer, D., and Livne, E. Enhancement of bone defect healing in old rats by TGF-beta and IGF-1. Exp Gerontol 37, 553, 2002.
86. Srouji, S., Blumenfeld, I., Rachmiel, A., and Livne, E. Bone defect repair in rat tibia by TGF-beta1 and IGF-1 released from hydrogel scaffold. Cell Tissue Bank 5, 223, 2004.
87. Srouji, S., Rachmiel, A., Blumenfeld, I., and Livne, E. Mandibular defect repair by TGF-beta and IGF-1 released from a biodegradable osteoconductive hydrogel. J Craniomaxillofac Surg 33, 79, 2005.
88. Schmidmaier, G., Wildemann, B., Gabelein, T., Heeger, J., Kandziora, F., Haas, N.P., and Raschke, M. Synergistic effect of IGF-I and TGF-beta1 on fracture healing in rats: single versus combined application of IGF-I and TGF-beta1. Acta Orthop Scand 74, 604, 2003.
89. Kveiborg, M., Flyvbjerg, A., Eriksen, E.F., and Kassem, M. Transforming growth factor-beta1 stimulates the production of insulin-like growth factor-I and insulin-like growth factor-binding protein-3 in human bone marrow stromal osteoblast progenitors. J Endocrinol 169, 549, 2001.
90. Okazaki, R., Durham, S.K., Riggs, B.L., and Conover, C.A. Transforming growth factor-beta and forskolin increase all classes of insulin-like growth factor-I transcripts in normal human osteoblast-like cells. Biochem Biophys Res Commun 207, 963, 1995.
91. Giannobile, W.V., Whitson, S.W., and Lynch, S.E. Non-coordinate control of bone formation displayed by growth factor combinations with IGF-I. J Dent Res 76, 1569, 1997.
92. Kasperk, C.H., Wergedal, J.E., Mohan, S., Long, D.L., Lau, K.H., and Baylink, D.J. Interactions of growth factors present in bone matrix with bone cells: effects on DNA synthesis and alkaline phosphatase. Growth Factors 3, 147, 1990.
93. Mott, D.A., Mailhot, J., Cuenin, M.F., Sharawy, M., and Borke, J. Enhancement of osteoblast proliferation *in vitro* by selective enrichment of demineralized freeze-dried bone allograft with specific growth factors. J Oral Implantol 28, 57, 2002.
94. Pfeilschifter, J., Oechsner, M., Naumann, A., Gronwald, R.G., Minne, H.W., and Ziegler, R. Stimulation of bone matrix apposition *in vitro* by local growth factors: a comparison between insulin-like growth factor I, platelet-derived growth factor, and transforming growth factor beta. Endocrinology 127, 69, 1990.

95. Gerstenfeld, L.C., Cullinane, D.M., Barnes, G.L., Graves, D.T., and Einhorn, T.A. Fracture healing as a post-natal developmental process: molecular, spatial, and temporal aspects of its regulation. J Cell Biochem 88, 873, 2003.
96. Hansen-Algenstaedt, N., Joscheck, C., Wolfram, L., Schaefer, C., Muller, I., Bottcher, A., Deuretzbacher, G., Wiesner, L., Leunig, M., Algenstaedt, P., and Ruther, W. Sequential changes in vessel formation and micro-vascular function during bone repair. Acta Orthop 77, 429, 2006.
97. Neufeld, G., Cohen, T., Gengrinovitch, S., and Poltorak, Z. Vascular endothelial growth factor (VEGF) and its receptors. Faseb J 13, 9, 1999.
98. Street, J., Bao, M., deGuzman, L., Bunting, S., Peale, F.V., Jr., Ferrara, N., Steinmetz, H., Hoeffel, J., Cleland, J.L., Daugherty, A., van Bruggen, N., Redmond, H.P., Carano, R.A., and Filvaroff, E.H. Vascular endothelial growth factor stimulates bone repair by promoting angiogenesis and bone turnover. Proc Natl Acad Sci U S A 99, 9656, 2002.
99. Eckardt, H., Ding, M., Lind, M., Hansen, E.S., Christensen, K.S., and Hvid, I. Recombinant human vascular endothelial growth factor enhances bone healing in an experimental nonunion model. J Bone Joint Surg Br 87, 1434, 2005.
100. Kaigler, D., Wang, Z., Horger, K., Mooney, D.J., and Krebsbach, P.H. VEGF scaffolds enhance angiogenesis and bone regeneration in irradiated osseous defects. J Bone Miner Res 21, 735, 2006.
101. Peng, H., Usas, A., Olshanski, A., Ho, A.M., Gearhart, B., Cooper, G.M., and Huard, J. VEGF improves, whereas sFlt1 inhibits, BMP2-induced bone formation and bone healing through modulation of angiogenesis. J Bone Miner Res 20, 2017, 2005.
102. Kaigler, D., Krebsbach, P.H., West, E.R., Horger, K., Huang, Y.C., and Mooney, D.J. Endothelial cell modulation of bone marrow stromal cell osteogenic potential. Faseb J 19, 665, 2005.
103. Wang, D.S., Miura, M., Demura, H., and Sato, K. Anabolic effects of 1,25-dihydroxyvitamin D3 on osteoblasts are enhanced by vascular endothelial growth factor produced by osteoblasts and by growth factors produced by endothelial cells. Endocrinology 138, 2953, 1997.
104. Deckers, M.M., van Bezooijen, R.L., van der Horst, G., Hoogendam, J., van Der Bent, C., Papapoulos, S.E., and Lowik, C.W. Bone morphogenetic proteins stimulate angiogenesis through osteoblast-derived vascular endothelial growth factor A. Endocrinology 143, 1545, 2002.
105. Kozawa, O., Matsuno, H., and Uematsu, T. Involvement of p70 S6 kinase in bone morphogenetic protein signaling: vascular endothelial growth factor synthesis by bone morphogenetic protein-4 in osteoblasts. J Cell Biochem 81, 430, 2001.
106. Yeh, L.C., and Lee, J.C. Osteogenic protein-1 increases gene expression of vascular endothelial growth factor in primary cultures of fetal rat calvaria cells. Mol Cell Endocrinol 153, 113, 1999.
107. Peng, H., Wright, V., Usas, A., Gearhart, B., Shen, H.C., Cummins, J., and Huard, J. Synergistic enhancement of bone formation and healing by stem cell-expressed VEGF and bone morphogenetic protein-4. J Clin Invest 110, 751, 2002.
108. Samee, M., Kasugai, S., Kondo, H., Ohya, K., Shimokawa, H., and Kuroda, S. Bone morphogenetic protein-2 (BMP-2) and vascular endothelial growth factor (VEGF) transfection to human periosteal cells enhances osteoblast differentiation and bone formation. J Pharmacol Sci 108, 18, 2008.
109. Huang, Y.C., Kaigler, D., Rice, K.G., Krebsbach, P.H., and Mooney, D.J. Combined angiogenic and osteogenic factor delivery enhances bone marrow stromal cell-driven bone regeneration. J Bone Miner Res 20, 848, 2005.
110. Kempen, D.H., Lu, L., Heijink, A., Hefferan, T.E., Creemers, L.B., Maran, A., Yaszemski, M.J., and Dhert, W.J. Effect of local sequential VEGF and BMP-2 delivery on ectopic and orthotopic bone regeneration. Biomaterials 30, 2816, 2009.
111. Patel, Z.S., Young, S., Tabata, Y., Jansen, J.A., Wong, M.E., and Mikos, A.G. Dual delivery of an angiogenic and an osteogenic growth factor for bone regeneration in a critical size defect model. Bone, 2008.
112. Fiedler, J., Leucht, F., Waltenberger, J., Dehio, C., and Brenner, R.E. VEGF-A and PlGF-1 stimulate chemotactic migration of human mesenchymal progenitor cells. Biochem Biophys Res Commun 334, 561, 2005.
113. Fiedler, J., Roderer, G., Gunther, K.P., and Brenner, R.E. BMP-2, BMP-4, and PDGF-bb stimulate chemotactic migration of primary human mesenchymal progenitor cells. J Cell Biochem 87, 305, 2002.
114. Hollinger, J.O., Hart, C.E., Hirsch, S.N., Lynch, S., and Friedlaender, G.E. Recombinant human platelet-derived growth factor: biology and clinical applications. J Bone Joint Surg Am 90 Suppl 1, 48, 2008.

115. Greenberg, J.I., Shields, D.J., Barillas, S.G., Acevedo, L.M., Murphy, E., Huang, J., Scheppke, L., Stockmann, C., Johnson, R.S., Angle, N., and Cheresh, D.A. A role for VEGF as a negative regulator of pericyte function and vessel maturation. Nature 456, 809, 2008.
116. Zhang, F., Tang, Z., Hou, X., Lennartsson, J., Li, Y., Koch, A.W., Scotney, P., Lee, C., Arjunan, P., Dong, L., Kumar, A., Rissanen, T.T., Wang, B., Nagai, N., Fons, P., Fariss, R., Zhang, Y., Wawrousek, E., Tansey, G., Raber, J., Fong, G.H., Ding, H., Greenberg, D.A., Becker, K.G., Herbert, J.M., Nash, A., Yla-Herttuala, S., Cao, Y., Watts, R.J., and Li, X. VEGF-B is dispensable for blood vessel growth but critical for their survival, and VEGF-B targeting inhibits pathological angiogenesis. Proc Natl Acad Sci U S A 106, 6152, 2009.
117. Marden, L.J., Fan, R.S., Pierce, G.F., Reddi, A.H., and Hollinger, J.O. Platelet-derived growth factor inhibits bone regeneration induced by osteogenin, a bone morphogenetic protein, in rat craniotomy defects. J Clin Invest 92, 2897, 1993.
118. Ranly, D.M., McMillan, J., Keller, T., Lohmann, C.H., Meunch, T., Cochran, D.L., Schwartz, Z., and Boyan, B.D. Platelet-derived growth factor inhibits demineralized bone matrix-induced intramuscular cartilage and bone formation. A study of immunocompromised mice. J Bone Joint Surg Am 87, 2052, 2005.
119. Kubota, K., Sakikawa, C., Katsumata, M., Nakamura, T., and Wakabayashi, K. Platelet-derived growth factor BB secreted from osteoclasts acts as an osteoblastogenesis inhibitory factor. J Bone Miner Res 17, 257, 2002.
120. Hock, J.M., and Canalis, E. Platelet-derived growth factor enhances bone cell replication, but not differentiated function of osteoblasts. Endocrinology 134, 1423, 1994.
121. Canalis, E., McCarthy, T.L., and Centrella, M. Effects of platelet-derived growth factor on bone formation *in vitro*. J Cell Physiol 140, 530, 1989.
122. Cochran, D.L., Rouse, C.A., Lynch, S.E., and Graves, D.T. Effects of platelet-derived growth factor isoforms on calcium release from neonatal mouse calvariae. Bone 14, 53, 1993.
123. Lynch, S.E., Trippel, S.B., Finkelman, R.D., Hernandez, R.A., Kiritsy, C.P., and Antoniades, H.N. The combination of platelet-derived growth factor-BB and insulin-like growth factor-I stimulates bone repair in adult Yucatan miniature pigs. Wound Repair Regen 2, 182, 1994.
124. Giannobile, W.V., Finkelman, R.D., and Lynch, S.E. Comparison of canine and non-human primate animal models for periodontal regenerative therapy: results following a single administration of PDGF/IGF-I. J Periodontol 65, 1158, 1994.
125. Lynch, S.E., Buser, D., Hernandez, R.A., Weber, H.P., Stich, H., Fox, C.H., and Williams, R.C. Effects of the platelet-derived growth factor/insulin-like growth factor-I combination on bone regeneration around titanium dental implants. Results of a pilot study in beagle dogs. J Periodontol 62, 710, 1991.
126. Lynch, S.E., de Castilla, G.R., Williams, R.C., Kiritsy, C.P., Howell, T.H., Reddy, M.S., and Antoniades, H.N. The effects of short-term application of a combination of platelet-derived and insulin-like growth factors on periodontal wound healing. J Periodontol 62, 458, 1991.
127. Lynch, S.E., Williams, R.C., Polson, A.M., Howell, T.H., Reddy, M.S., Zappa, U.E., and Antoniades, H.N. A combination of platelet-derived and insulin-like growth factors enhances periodontal regeneration. J Clin Periodontol 16, 545, 1989.
128. Howell, T.H., Fiorellini, J.P., Paquette, D.W., Offenbacher, S., Giannobile, W.V., and Lynch, S.E. A phase I/II clinical trial to evaluate a combination of recombinant human platelet-derived growth factor-BB and recombinant human insulin-like growth factor-I in patients with periodontal disease. J Periodontol 68, 1186, 1997.
129. Giannobile, W.V., Hernandez, R.A., Finkelman, R.D., Ryan, S., Kiritsy, C.P., D'Andrea, M., and Lynch, S.E. Comparative effects of platelet-derived growth factor-BB and insulin-like growth factor-I, individually and in combination, on periodontal regeneration in Macaca fascicularis. J Periodontal Res 31, 301, 1996.
130. Boyapati, L., and Wang, H.L. The role of platelet-rich plasma in sinus augmentation: a critical review. Implant Dent 15, 160, 2006.
131. Kitoh, H., Kitakoji, T., Tsuchiya, H., Mitsuyama, H., Nakamura, H., Katoh, M., and Ishiguro, N. Transplantation of marrow-derived mesenchymal stem cells and platelet-rich plasma during distraction osteogenesis--a preliminary result of three cases. Bone 35, 892, 2004.
132. Savarino, L., Cenni, E., Tarabusi, C., Dallari, D., Stagni, C., Cenacchi, A., Fornasari, P.M., Giunti, A., and Baldini, N. Evaluation of bone healing enhancement by lyophilized bone grafts supplemented with platelet gel: a standardized methodology in patients with tibial osteotomy for genu varus. J Biomed Mater Res B Appl Biomater 76, 364, 2006.

133. Simman, R., Hoffmann, A., Bohinc, R.J., Peterson, W.C., and Russ, A.J. Role of platelet-rich plasma in acceleration of bone fracture healing. Ann Plast Surg 61, 337, 2008.
134. Park, E.J., Kim, E.S., Weber, H.P., Wright, R.F., and Mooney, D.J. Improved bone healing by angiogenic factor-enriched platelet-rich plasma and its synergistic enhancement by bone morphogenetic protein-2. Int J Oral Maxillofac Implants 23, 818, 2008.
135. Jung, R.E., Schmoekel, H.G., Zwahlen, R., Kokovic, V., Hammerle, C.H., and Weber, F.E. Platelet-rich plasma and fibrin as delivery systems for recombinant human bone morphogenetic protein-2. Clin Oral Implants Res 16, 676, 2005.
136. Calori, G.M., D'Avino, M., Tagliabue, L., Albisetti, W., d'Imporzano, M., and Peretti, G. An ongoing research for evaluation of treatment with BMPs or AGFs in long bone non-union: protocol description and preliminary results. Injury 37 Suppl 3, S43, 2006.
137. van den Dolder, J., Mooren, R., Vloon, A.P., Stoelinga, P.J., and Jansen, J.A. Platelet-rich plasma: quantification of growth factor levels and the effect on growth and differentiation of rat bone marrow cells. Tissue Eng 12, 3067, 2006.
138. Lorenzo, J., Horowitz, M., and Choi, Y. Osteoimmunology: interactions of the bone and immune system. Endocr Rev 29, 403, 2008.
139. Nakashima, T., and Takayanagi, H. The dynamic interplay between osteoclasts and the immune system. Arch Biochem Biophys 473, 166, 2008.
140. Takayanagi, H. Osteoimmunology: shared mechanisms and crosstalk between the immune and bone systems. Nat Rev Immunol 7, 292, 2007.
141. Weitzmann, M.N., and Pacifici, R. The role of T lymphocytes in bone metabolism. Immunol Rev 208, 154, 2005.
142. Du, X., and Williams, D.A. Interleukin-11: review of molecular, cell biology, and clinical use. Blood 89, 3897, 1997.
143. Du, X.X., and Williams, D.A. Interleukin-11: a multifunctional growth factor derived from the hematopoietic microenvironment. Blood 83, 2023, 1994.
144. Girasole, G., Passeri, G., Jilka, R.L., and Manolagas, S.C. Interleukin-11: a new cytokine critical for osteoclast development. J Clin Invest 93, 1516, 1994.
145. Hill, P.A., Tumber, A., Papaioannou, S., and Meikle, M.C. The cellular actions of interleukin-11 on bone resorption *in vitro*. Endocrinology 139, 1564, 1998.
146. Suga, K., Saitoh, M., Fukushima, S., Takahashi, K., Nara, H., Yasuda, S., and Miyata, K. Interleukin-11 induces osteoblast differentiation and acts synergistically with bone morphogenetic protein-2 in C3H10T1/2 cells. J Interferon Cytokine Res 21, 695, 2001.
147. Suga, K., Saitoh, M., Kokubo, S., Fukushima, S., Kaku, S., Yasuda, S., and Miyata, K. Interleukin-11 acts synergistically with bone morphogenetic protein-2 to accelerate bone formation in a rat ectopic model. J Interferon Cytokine Res 23, 203, 2003.
148. Suga, K., Saitoh, M., Kokubo, S., Nozaki, K., Fukushima, S., Yasuda, S., Sasamata, M., and Miyata, K. Synergism between interleukin-11 and bone morphogenetic protein-2 in the healing of segmental bone defects in a rabbit model. J Interferon Cytokine Res 24, 343, 2004.
149. Lotinun, S., Sibonga, J.D., and Turner, R.T. Differential effects of intermittent and continuous administration of parathyroid hormone on bone histomorphometry and gene expression. Endocrine 17, 29, 2002.
150. Qin, L., Raggatt, L.J., and Partridge, N.C. Parathyroid hormone: a double-edged sword for bone metabolism. Trends Endocrinol Metab 15, 60, 2004.
151. Neer, R.M., Arnaud, C.D., Zanchetta, J.R., Prince, R., Gaich, G.A., Reginster, J.Y., Hodsman, A.B., Eriksen, E.F., Ish-Shalom, S., Genant, H.K., Wang, O., and Mitlak, B.H. Effect of parathyroid hormone (1-34) on fractures and bone mineral density in postmenopausal women with osteoporosis. N Engl J Med 344, 1434, 2001.
152. Dobnig, H., and Turner, R.T. Evidence that intermittent treatment with parathyroid hormone increases bone formation in adult rats by activation of bone lining cells. Endocrinology 136, 3632, 1995.
153. Jilka, R.L., Weinstein, R.S., Bellido, T., Roberson, P., Parfitt, A.M., and Manolagas, S.C. Increased bone formation by prevention of osteoblast apoptosis with parathyroid hormone. J Clin Invest 104, 439, 1999.
154. Leaffer, D., Sweeney, M., Kellerman, L.A., Avnur, Z., Krstenansky, J.L., Vickery, B.H., and Caulfield, J.P. Modulation of osteogenic cell ultrastructure by RS-23581, an analog of human parathyroid hormone (PTH)-related peptide-(1-34), and bovine PTH-(1-34). Endocrinology 136, 3624, 1995.

155. Onyia, J.E., Bidwell, J., Herring, J., Hulman, J., and Hock, J.M. *In vivo*, human parathyroid hormone fragment (hPTH 1-34) transiently stimulates immediate early response gene expression, but not proliferation, in trabecular bone cells of young rats. Bone 17, 479, 1995.
156. Kabasawa, Y., Asahina, I., Gunji, A., and Omura, K. Administration of parathyroid hormone, prostaglandin E2, or 1-alpha,25-dihydroxyvitamin D3 restores the bone inductive activity of rhBMP-2 in aged rats. DNA Cell Biol 22, 541, 2003.
157. Horiuchi, H., Saito, N., Kinoshita, T., Wakabayashi, S., Tsutsumimoto, T., Otsuru, S., and Takaoka, K. Enhancement of recombinant human bone morphogenetic protein-2 (rhBMP-2)-induced new bone formation by concurrent treatment with parathyroid hormone and a phosphodiesterase inhibitor, pentoxifylline. J Bone Miner Metab 22, 329, 2004.
158. Kempen, D.H.R., Lu, L., Hefferan, T.E., Creemers, L.B., Heijink, A., Maran, A., Dhert, W.J.A., and Yaszemski, M.J. Enhanced BMP-2 induced ectopic and orthotopic bone formation by intermittent PTH(1-34) administration. Submitted to Tissue Engineering part A.
159. Morgan, E.F., Mason, Z.D., Bishop, G., Davis, A.D., Wigner, N.A., Gerstenfeld, L.C., and Einhorn, T.A. Combined effects of recombinant human BMP-7 (rhBMP-7) and parathyroid hormone (1-34) in metaphyseal bone healing. Bone 43, 1031, 2008.
160. Cui, L., Ma, Y.F., Yao, W., Zhou, H., Setterberg, R.B., Liang, T.C., and Jee, W.S. Cancellous bone of aged rats maintains its capacity to respond vigorously to the anabolic effects of prostaglandin E2 by modeling-dependent bone gain. J Bone Miner Metab 19, 29, 2001.
161. Zhou, H., Ma, Y.F., Yao, W., Cui, L., Setterberg, R., Liang, C.T., and Jee, W.S. Lumbar vertebral cancellous bone is capable of responding to PGE2 treatment by stimulating both modeling and remodeling-dependent bone gain in aged male rats. Calcif Tissue Int 68, 179, 2001.
162. Montero-Odasso, M., and Duque, G. Vitamin D in the aging musculoskeletal system: an authentic strength preserving hormone. Mol Aspects Med 26, 203, 2005.
163. Dawson-Hughes, B., Harris, S.S., Krall, E.A., and Dallal, G.E. Effect of calcium and vitamin D supplementation on bone density in men and women 65 years of age or older. N Engl J Med 337, 670, 1997.
164. Ooms, M.E., Roos, J.C., Bezemer, P.D., van der Vijgh, W.J., Bouter, L.M., and Lips, P. Prevention of bone loss by vitamin D supplementation in elderly women: a randomized double-blind trial. J Clin Endocrinol Metab 80, 1052, 1995.
165. Shevde, N.K., Plum, L.A., Clagett-Dame, M., Yamamoto, H., Pike, J.W., and DeLuca, H.F. A potent analog of 1alpha,25-dihydroxyvitamin D3 selectively induces bone formation. Proc Natl Acad Sci U S A 99, 13487, 2002.
166. Ono, I., Tateshita, T., Takita, H., and Kuboki, Y. Promotion of the osteogenetic activity of recombinant human bone morphogenetic protein by basic fibroblast growth factor. J Craniofac Surg 7, 418, 1996.
167. Takita, H., Tsuruga, E., Ono, I., and Kuboki, Y. Enhancement by bFGF of osteogenesis induced by rh-BMP-2 in rats. Eur J Oral Sci 105, 588, 1997.
168. Vonau, R.L., Bostrom, M.P., Aspenberg, P., and Sams, A.E. Combination of growth factors inhibits bone ingrowth in the bone harvest chamber. Clin Orthop Relat Res, 243, 2001.
169. Minamide, A., Yoshida, M., Kawakami, M., Okada, M., Enyo, Y., Hashizume, H., and Boden, S.D. The effects of bone morphogenetic protein and basic fibroblast growth factor on cultured mesenchymal stem cells for spine fusion. Spine 32, 1067, 2007.

11

Effect of local sequential VEGF and BMP-2 delivery on ectopic and orthotopic bone regeneration

Biomaterials 2009;30:2816-2825

D.H.R. Kempen
L. Lu
A. Heijink
T.E. Hefferan
L.B. Creemers
A. Maran
M.J. Yaszemski
W.J.A. Dhert

Abstract

Bone regeneration is a coordinated cascade of events regulated by several cytokines and growth factors. Angiogenic growth factors are predominantly expressed during the early phases for re-establisment of the vascularity, whereas osteogenic growth factors are continuously expressed during bone formation and remodeling. Since vascular endothelial growth factor (VEGF) and bone morphogenetic proteins (BMPs) are key regulators of angiogenesis and osteogenesis during bone regeneration, the aim of this study was to investigate if their sequential release could enhance BMP-2 induced bone formation. A composite consisting of poly(lactic-co-glycolic acid) microspheres loaded with BMP-2 embedded in a poly(propylene) scaffold surrounded by a gelatin hydrogel loaded with VEGF was used for the sequential release of the growth factors. Empty composites or composites loaded with VEGF and/or BMP-2 were implanted ectopically and orthotopically in Sprague Dawley rats (n=9). Following implantation, the local release profiles were determined by measuring the activity of ^{125}I-labeled growth factors using scintillation probes. After 8 weeks blood vessel and bone formation were analyzed using microangiography, μCT and histology. The scaffolds exhibited a large initial burst release of VEGF within the first 3 days and a sustained release of BMP-2 over the full 56 day implantation period. Although VEGF did not induce bone formation, it did increase the formation of the supportive vascular network ($p = 0.03$) in ectopic implants. In combination with local sustained BMP-2 release, VEGF significantly enhanced ectopic bone formation compared to BMP-2 alone ($p = 0.008$). In the orthotopic defects, no effect of VEGF on vascularisation was found, nor was bone formation higher by the combination of growth factors, compared to BMP-2 alone. This study demonstrates that a sequential angiogenic and osteogenic growth factor release may be beneficial for the enhancement of bone regeneration.

Introduction

During fracture healing or grafting procedures, a specialized form of wound healing occurs in which bone regenerates itself by auto-induction. This auto-inductive capacity of bone is the basis of the numerous successful grafting procedures performed in orthopedic surgery. However, the increasing number of grafting procedures and the disadvantages associated with graft harvesting (e.g. limited graft quantity and donor site morbidity) drive the quest for alternative methods to regenerate bone tissue.[1-3] A strategy that may obviate the need for bone grafts and holds great promise in bone regeneration is the local delivery of bioactive molecules that are instrumental in the initiation of auto-induction by bone.

Bone regeneration may be accomplished by using various bioactive molecules with varying potency and efficacy. Bone morphogenetic proteins (BMPs) are an important class of bioactive molecules which play a central role in most bone regeneration strategies. Extensive data have shown that members of the BMP family can initiate the complete cascade of bone formation, including the migration of mesenchymal stem cells and their differentiation into osteoblasts.[4] The high osteoinductive potential of some BMPs is illustrated by their ability to induce bone formation in ectopic locations.[5-9]

Apart from osteoinduction, angiogenesis is considered essential for proper bone regeneration. The process of angiogenesis involves new vessel formation from pre-existing vascular network. These newly formed vessels are crucial for sufficient nutrient supply, transport of macromolecules, invasion of cells and maintenance of the appropriate metabolic microenvironment during bone repair. Vascular endothelial growth factor (VEGF) is considered one of the key regulators of angiogenesis during bone formation.[10] The important role of VEGF during bone regeneration has been demonstrated in various experimental bone formation models, which show stimulation or disruption of normal fracture healing or *in vivo* bone formation in response to respectively VEGF administration or inhibition.[11-14]

In vitro studies have suggested that VEGF and BMPs play an important role in the cellular communication during angiogenesis and osteogenesis. Co-culture experiments demonstrated that osteoblast-like cells stimulated the proliferation of endothelial cells by production of VEGF, whereas endothelial cells stimulated the differentiation of osteoprogenitor cells by production of BMP-2.[12,15] Furthermore, BMP-induced differentiation of preosteoblast-like cells enhanced the production of VEGF by the resulting osteoblasts.[16,17] These *in vitro* studies suggest a BMP/VEGF regulated coupling between osteogenesis and angiogenesis. This BMP/VEGF interaction has also been demonstrated in bone regeneration studies where enhanced bone formation was shown when both growth factors were released or expressed simultaneously.[13,18-20]

During normal bone healing, VEGF expression was shown to peak during the early days while BMP expression peaked at a later time point.[21-26] Since establishment of the vascular bed is an early event that precedes the formation of bone, a similar temporal release profile concordant with their natural expression might be beneficial for bone regenerations. To address such an issue, new advanced biomaterials capable of releasing VEGF and BMP in a sequential fashion are required. Apart from its delivery purpose, such a biomaterial should also act as a biologically and biomechanically compatible framework that enhances angiogenesis, osteogenesis, and mechanical stability.

A previously designed sustained delivery vehicle capable of supporting BMP-2 induced bone formation was modified to create a biomaterial with a sequential VEGF/BMP release

profile.[27,28] In this study, we investigated the VEGF and BMP-2 release profiles from the composite and their effect on ectopic and orthotopic bone formation *in vivo*.

Materials and methods

Experimental design

A total of 63 rats were used for the experiment according to the approved protocol by the Institutional Animal Care and Use Committee. The growth factor release profiles and bone forming capacity were studied in both ectopic (subcutaneous) and orthotopic (critical sized femoral defect) implantation models. Each of the animals received one of the seven treatments for both sites as stated in table 1. The first two groups received ^{125}I–labeled VEGF- or BMP-2- loaded composites to study the growth factor release profile. The release profile was determined by measuring the radioactivity of the implant using scintillation probes. The other four groups were used to study the bone and vessel forming capacity of different growth factor treatments, consisting of 1) empty composites, 2) VEGF-loaded composites, 3) BMP-2 loaded composites and 4) VEGF & BMP-2 loaded composites. Femoral defects without implants served as controls for scaffold-mediated bone regeneration at the orthotopic site. Fluorochrome labels were administered after 4 and 6 weeks and post-mortem micro-angiography was performed after 8 weeks of implantation. All composites and empty defects were characterized for vessel formation and bone formation by micro-computed tomography (μCT) and histology.

Table 1
Experimental groups

	Scaffold	*Dosage/scaffold*	*Analysis*	n
1	^{125}I-VEGF	2.0 μg	Release	9
2	^{125}I-BMP-2	6.5 μg	Release	9
3	No implant[a]	None	μCT & histology	9
4	Non-loaded	None	μCT & histology	9
5	VEGF	2.0 μg	μCT & histology	9
6	BMP-2	6.6 μg	μCT & histology	9
7	VEGF/BMP-2	2.0 μg/6.6 μg	μCT & histology	9

a: This group was only studied in the orthotopic site to show the femoral defect was critical

Composite design and fabrication

The composite consisted of poly(lactic-co-glycolic acid) (PLGA) microspheres incorporated into a solid poly(propylene fumarate) (PPF) rod which was surrounded by a cylindrical gelatin hydrogel (figure 1). The rapid degrading hydrogel served as a delivery vehicle for VEGF (R&D Systems, Minneapolis, MN) whereas the solid PLGA/PPF rod served as a sustained release vehicle for BMP-2 (Medtronic Sofamor Danek, MN).
The BMP-2-loaded PLGA (Medisorb®, Lakeshore Biomaterials, AL) microspheres were fabricated using a previously described water-in-oil-in water (W1-O-W2) double-emul-

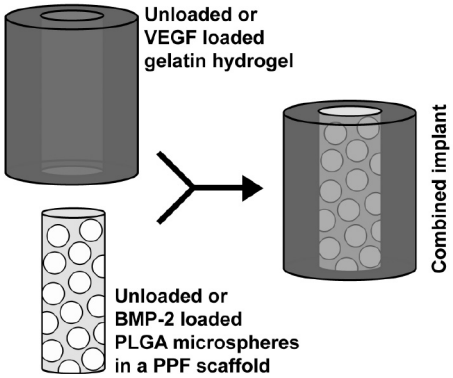

Figure 1: Schematic drawing of the composite scaffolds for the sequential release of VEGF and BMP-2. The PPF rod and the gelatin shell were prepared separately and combined just before implantation.

sion-solvent-extraction technique.[28,29] Briefly, 100 µl of a 10 mg/ml BMP-2 solution was emulsified in a solution of 500 mg of PLGA (50:50 L:G ratio, Mw 23 kDa) in 1.25 ml of dichloromethane. The mixture was re-emulsified for 30 seconds in 2 ml of 1% w/v aqueous poly(vinyl alcohol) (PVA, 87-89% mole hydrolyzed, Mw=13,000-23,000, Sigma-Aldrich, MO) solution to create the double emulsion. The content was then added to 100 ml of a 0.3 % w/v aqueous PVA solution and 100 ml of a 2% w/v aqueous isopropanol solution and stirred for one hour. The microspheres were collected by centrifugation, washed twice with ddH_2O and vacuum-dried (Savant Speedvac systems, NY) into a free flowing powder.

The microsphere/PPF composites were fabricated by photocrosslinking PPF (Mw 5,800 Da, PI 2.0), fabricated by a two-step reaction process as previously described[30] with N-vinylpyrrolidinone (NVP, Acros, Pittsburgh, PA) using the photoinitiator bis(2,4,6-trimethylbenzoyl) phenylphosphine oxide (BAPO, Ciba Specialty Chemicals, NY). Briefly, 1.0 g of PPF and 50 µl of a 100 mg/ml BAPO/dichloromethane solution were dissolved in 0.5 ml of NVP. The PPF/NVP/BAPO paste (45 wt%) was mixed with the microspheres. The resulting PPF/microsphere mixture was transferred to a 3.0 cc syringe, forced into a glass cylindrical mold of 1.6 mm in diameter and allowed to polymerize at room temperature under UV light. The crosslinked cylinders were removed from the glass mold, lyophilized, sectioned into 6 mm long rods, sterilized by ethanol evaporation and frozen down at –20 ℃ until use.

The hydrogels were fabricated from gelatin (300 Bloom number, derived from porcine skin, Sigma-Aldrich) derived from acid-cured collagen. The hydrogel was fabricated separately under semi-sterile conditions by chemically crosslinking 1 ml of a 40℃ pre-heated 10 wt% aqueous gelatin solution with 40 µL of a 10 wt % aqueous glutaraldehyde solution. The resulting solution was casted into hollow tubular molds with an outer diameter of 3.5 mm and an inner diameter of 1.6 mm. This solution was then allowed to crosslink for 1 hr at 4℃, which was followed by a blocking period of 1 hr in a 100 mM aqueous glycine solution to block the residual aldehyde groups. Finally, the gelatin hydrogel was sectioned in 6 mm tubes, sterilized in 70% alcohol, rinsed in phosphate buffered saline, impregnated with 5 µl of a 0.4 mg/ml VEGF solution and stored at -20℃ until use.

Based on the ^{125}I-BMP-2 counts before and after the fabrication procedure, the microsphere entrapment efficiency was estimated at 85 % or 1.1 µg BMP-2 per mg PLGA. The ^{125}I-BMP-2 (1.2 µCi/µg BMP-2) loaded microsphere/PPF rods had an average activity of

5.3 ± 0.3 µCi and an estimated BMP-2 loading of 6.5 ± 0.4 µg/scaffold. The average weight of the unlabeled BMP 2 rods was 10.5 ± 0.8 mg/scaffold, which results in an estimated BMP-2 loading of 6.6 ± 0.5 µg/scaffold. Previous studies have shown that the BMP-2 remained bioactive after this incorporation process and the dose was above the osteoinductive threshold.[28,31] Based on previous VEGF studies, the tubular hydrogels were impregnated with a dose of 2.0 µg VEGF per scaffold.[32] The tubular hydrogels were impregnated with 2.0 µg VEGF per scaffold. The BMP-2 loaded microsphere/PPF composite was inserted into the VEGF loaded gelatin cylinders just before implantation.

Surgical procedure

The growth factor release profiles and bone forming capacity of the scaffolds were studied in a subcutaneous and femoral defect implantation site using 12-week-old Harlan Sprague Dawley rats (weight 329 ± 13 g). The rats were anesthetized with an intramuscular injection of a ketamine/xylazine mixture (45/10 mg/kg i.m.) and the surgical sites were shaved and disinfected with a 30% betadine solution. The right femur was exposed through a lateral approach and was circumferentially stripped from soft tissue and periosteum. A polyethylene plate (22 x 3 x 4 mm) was fixed along the antero-lateral side of the femur using two distal and two proximal threaded Kirschner wires (diameter 1 mm, Zimmer, IN). A 5 mm segmental defect was made in the middle of the femoral shaft using a surgical bur and was irrigated with saline to remove bone debris and bone marrow. The implant was inserted into the defect, and the wound was closed using resorbable sutures (Vicryl 1/0, Ethicon Inc., NJ) and non-resorbable nylon skin sutures. In addition to the orthotopic implant, the rats receive two ectopic implants in subcutaneous pockets in the lower left limb and the thoracolumbar area in the back. The pockets were created by blunt dissection through a 0.5 cm skin incision and each was filled with one implant. Post-operative analgesia was provided by intramuscular injections of buprenorphine (0.02–0.1 mg/kg) for 72 hrs and acetaminophen (160 mg in 5 ml added to a pint water bottle) for the duration of one week. The fluorochrome labels calcein green (10 mg/kg, Sigma-Aldrich) and alizarin red (20 mg/kg, Sigma-Aldrich) were administered paravenously after respectively 4 and 6 weeks to obtain more information on the rate of bone formation and femoral defect healing.

In vitro and *in vivo* growth factor release

To study the release profiles of VEGF and BMP-2, a fraction of the incorporated growth factors was radiolabeled with ^{125}I using Iodo-Gen® precoated test tubes according to the manufacturer's instructions (Pierce, IL). Briefly, 100 µl of a 1.3 mg/ml BMP-2 solution and 20 µl of a 0.1 M NaOH solution or 25 µl of a 2.0 mg/ml VEGF solution were combined with a 2 mCi Na^{125}I solution in an Iodo-Gen® coated test tube and incubated for 30 min. at room temperature. The radiolabeled protein was then separated from the free ^{125}I by 24 hr dialysis (10 kDa molecular weight cut-off (MWCO) Slide-A-Lyzer®, Pierce) against the growth factor buffer solution and concentrated in a Vivaspin device (10 kDa MWCO, Sartorius AG, Germany). The final ^{125}I-BMP-2 and ^{125}I-VEGF solutions contained respectively 99.8 and 96.7 % TCA-precipitable counts, which indicated the percentage of covalently bound ^{125}I to the protein. The ^{125}I-labeled growth factor solutions were mixed with non-labeled BMP-2 and VEGF (1:5 hot:cold ratio) and incorporated into the composite

according to the method described in "composite design and fabrication".
For the *in vitro* release profiles, scaffolds loaded with VEGF or BMP-2 were placed in microcentrifuge tubes containing 1.0 ml of pH 7.4 phosphate buffered saline with 10% fetal bovine serum and maintained at 37℃ on an orbital shaker to ensure continuous mixing. Twice a week, the supernatant was collected, assayed for ^{125}I counts and replaced with fresh medium. The release profiles were obtained by correcting the ^{125}I counts for decay and normalizing them to the starting amount.
To determine the *in vivo* release profiles, the radioactive composites were implanted subcutaneously and in the femoral defect and the release profile was determined by a scintillation probe setup as previously described in chapter 7.[27] The scintillation probe setup consisted of two scintillation detectors (Model 44-3 low energy gamma scintillator, Ludlum measurements Inc., TX, USA) connected to digital scalers (Model 1000 scaler, Ludllum measurements Inc.) which were collimated by a 3 cm hollow tube wrapped in lead tape. Postoperatively, the implant activity was measured over four 1-minute periods using both detectors (2 measurements per detector). The measurements were repeated weekly while the rats were under ketamine/xylazine sedation (20/5 mg/kg). To determine the release profiles, the measurements were corrected for background activity and radioactive decay and normalized to the post-operative measurement.

Microangiography

After 8 weeks, the animals were sacrificed by an overdose of pentobarbital and microangiography was performed using Microfil® (Flow Tech, MA). Following a midline laparotomy, the aorta and vena cava were exposed and canulated with 22-gauge angiocatheters. To clear the vessels of blood, the lower extremities were perfused with 50 ml of heparinized saline. The blue collared, liquid, radioopaque, low viscosity polymer Microfil® was subsequently infused at a flow rate of 2 ml/min until the toes were clearly collared blue. After polymerization of the compound in approximately 2 hours, the implants were removed and fixed in a 1.5% glutaraldehyde solution for further evaluation.

Micro-computed tomography

The fixed samples were imaged with µCT to determine blood vessel and bone volume. The implants were scanned at 0.49° angular increments (providing 721 views around 360°) using a custom-built µCT-system.[33] The images were recorded, digitized, and transferred to a computer for reconstruction using a modified Feldkamp cone beam tomographic reconstruction algorithm. The 3-D images consisted of 20 µm cubic voxels with a radiopacity represented by a 16-bit grayscale value. Reconstructions of the vessels and bone were made with standardized thresholds using the Analyze software package (Biomedical Imaging Resource, Mayo Clinic, MN). The µCT scans of ectopic implants were used to quantify the volume of the vascular support network and newly formed bone. The vessels in the ectopic implants were reconstructed by extracting all voxels with a minimum of 26 connections with gray values between 750 and 1300. Any residual bone was manually removed from the reconstructions. The bone volume in the ectopic and orthotopic scans was reconstructed by extracting the voxels with gray values between 1300 and 10000. The femoral defects were analyzed for a connection between the proximal and distal part of the femur and total volume of newly formed bone. Due to the difficulty to distinguish

the newly formed bone from the original femur, a 6 mm section between the middle two K-wires was used for the quantificantion of the orthotopic bone volume.

Histology

After µCT analysis, the subcutaneous implants and femurs were dehydrated in a graded series of alcohol and embedded in respectively glycol-methylmethacrylate and methylmethacrylate for histological analysis. The samples were longitudinally sectioned using a rotary microtome (subcutaneous samples; Reichert-Jung Supercut 2050 microtome, Leica Microsystems, Germany) or sawing microtome (femurs; Leica SP1600, Leica Microsystems) and stained with Goldner's trichrome, hematoxylin/eosin and/or methylene blue/basic fuchsin. The sections were evaluated for vessel formation and bone formation. Additional unstained sections were evaluated for the incorporation of fluorochrome labels using a fluorescence microscope (E600 Nikon, Japan) with a double filter block (dichroic mirror 505 nm and 590 nm).

Histomorphometry

Since the orthotopic vessel formation could not be determined in the µCT scans, histomorphometric analysis was used for its quantification. High resolution (300 dpi), low magnification (40x) digital micrographs covering the complete implant area were made for the analysis. In a standardized region of interest covering the complete defect, the blue Microfil was pseudocolored and the colorized pixels were measured to calculate the surface area of the vessels filled with Microfil.

Statistical analysis

All data are reported as means ± standard deviations (SD) for n = 9. The ^{125}I-VEGF and ^{125}I-BMP-2 release results were analyzed using repeated measurements analysis. Comparison of vessel volumes present in the ectopical implants was performed using two-way ANOVA. An independent two-sided t-test was performed to analyze the ectopic bone volume. Comparison of the orthotopic vessel and bone formation between the individual groups was performed by a one-way ANOVA with LSD corrected post-hoc tests. All tests were performed by SPSS and the level of significance was set at $p < 0.05$.

Results

Animals

Three animals (1 in the ^{125}I-BMP-2 group, 1 in the no-implant group and 1 in the non-loaded implant group) developed deep infections of their femoral defects during the study. Their release and volume measurements were excluded from further analysis. One rat from the ^{125}I-BMP-2 group had a femur fracture at the distal K-wire. Despite the fracture, the rat remained in good health and the release measurements were included in the analysis.

Growth factor release

In vitro, the implant showed an initial VEGF burst release of 58 ± 5 % during the first 3.5 days, which leveled off over 2 weeks to assume an almost linear sustained release for the rest of the time frame (figure 2). The *in vitro* release profile of BMP-2 showed a minimal burst of 3.3 ± 0.05 % which was followed by a linear release for the remaining time (R^2=0.994, figure 2).

The release profiles of VEGF and BMP-2 changed significantly upon implantation. The ^{125}I-VEGF loaded implants showed a large initial burst release of 89.9 ± 2.9 % and 83.7 ± 5.6 % at the ectopic and orthotopic site, respectively (figure 3). The remaining 0.20 µg (10.1%) and 0.33 µg (16.3%) of VEGF was released in a more sustained fashion over a period of 35 days. Overall, the VEGF release from the ectopic implants was significantly faster than the orthotopic implants ($p < 0.05$). ^{125}I-BMP-2 release was more sustained over the full 56 day implantation period (figure 3). These implants exhibited a minimal burst release of 4.8 ± 5.3 % (ectopically) and 9.5 ± 5.3 % (orthotopically). ^{125}I-BMP-2 release was most pronounced between day 14 and 35. The orthotopic implants showed a significantly faster BMP-2 release compared to the ectopic implants ($p = 0.04$).

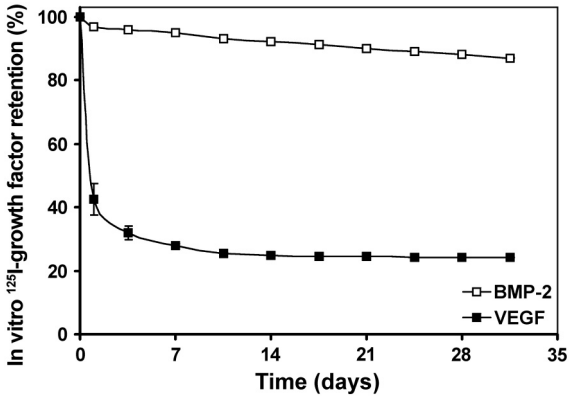

Figure 2: *In vitro* BMP-2 and VEGF release profiles from microphere/PPF/gelatin constructs in phosphate buffered saline with 10% fetal bovine serum at 37℃.

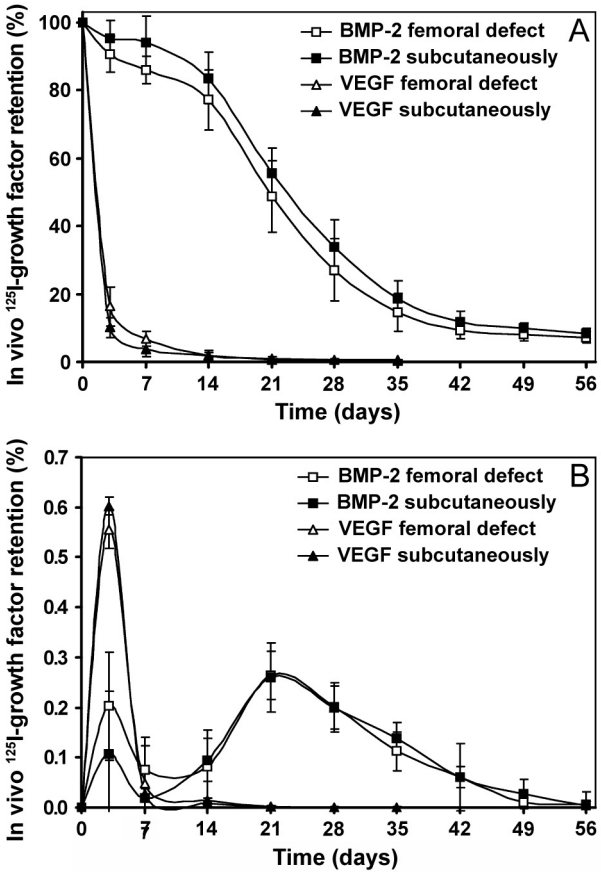

Figure 3: Pharmacokinetic profiles of VEGF and BMP-2 from the composite scaffolds over 8 weeks of implantation in rats. A fraction of the incorporated growth factors was radiolabeled with ^{125}I and their retention was determined by correlating the local gamma-irradiation to the amount of growth factor in the implant. The measurements were corrected for background activity and radioactive decay and normalized to the implanted dose. The growth factor release profiles are shown as (A) normalized growth factor retention and (B) amount of released growth factor per day.

µCT analysis

The effects of the local growth factor release on the ectopic vessel and bone formation after 8 weeks of implantation was studied by microangiography and µCT imaging at a 20 µm resolution. Three-dimensional µCT reconstructions revealed vessel formation directly around the implants (figure 4A). The vascular network appeared denser around the VEGF-containing scaffolds compared to the other scaffolds. Quantification of the vascular network revealed that the local VEGF release resulted in a significant increase of the total vessel volume inside the composites ($p = 0.003$, figure 4B). Vessel volume was not significantly increased in VEGF/BMP-releasing scaffolds compared to scaffolds containing only VEGF. Ectopic bone formation was only seen in the BMP-2 releasing implants (figure 4A). The bone had a trabecular appearance inside the cylindrical scaffold and a compact shell covered part of its surface. The amount of newly formed bone in the VEGF/BMP-2 releasing scaffold was significantly higher compared to scaffolds loaded with BMP-2 alone ($p = 0.008$, figure 4C).

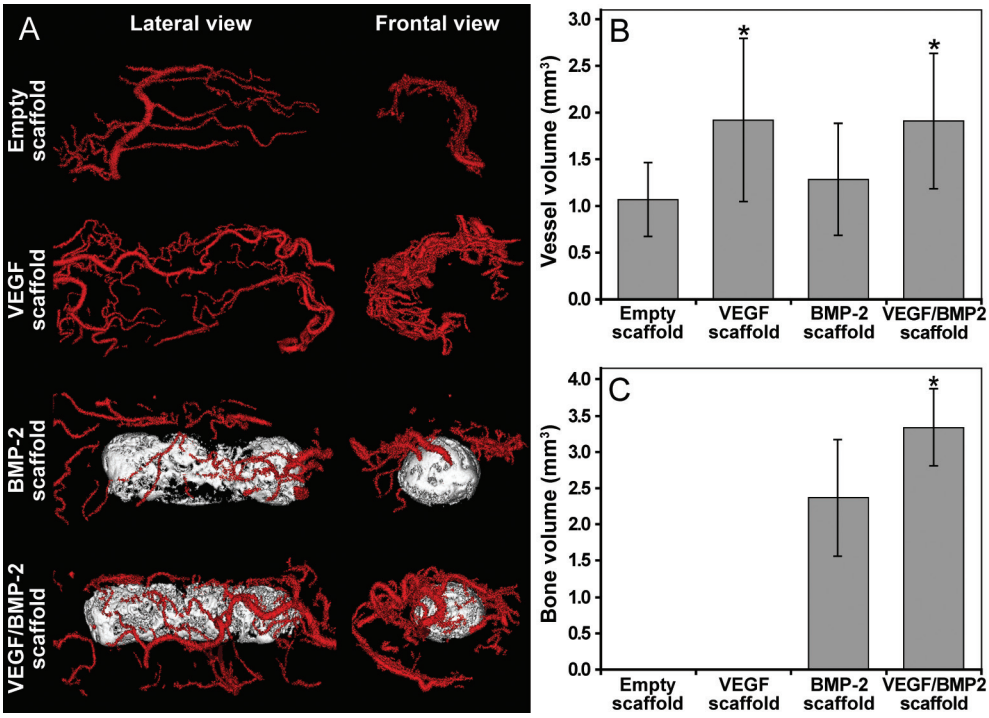

Figure 4: Analysis of the formation of the vascular network and bone after 8 weeks of implantation in a rat subcutaneous model. (A) 3-D volume rendered µCT images of blood vessels (red) and bone (white) were obtained by performing microangiography and µCT imaging at a 20 µm resolution. The renderings were used to quantify (B) the total volume of the vessels surrounding the implant and (C) the volume of newly formed bone. VEGF containing scaffolds had a significantly higher local vessel volume compared to the non-VEGF loaded implants ($p = 0.040$). The bone volume in the VEGF/BMP-2 containing implants was significantly higher compared to the BMP-2 only implants ($p = 0.009$).

Unfortunately, it was impossible to extract the vessels from the µCT scans of the orthotopic implants and hence no data were obtained for orthotopic vessel volume. Analysis of orthotopic bone formation showed that none of the unfilled defects had osseous connections between the proximal and distal part of the femur (figure 5A). Only 2/8 of the empty scaffolds and 2/9 of the VEGF-loaded scaffolds showed small areas of trabecular bridging of the femoral defect. In contrast, most of the defects filled with BMP-2 and VEGF/BMP-2 scaffolds showed circumferential cortical regeneration. Although no full circumferential bridging of the cortex was seen, multiple trabecular connections were seen in all BMP-2 scaffold-containing defects. Quantification of the newly formed bone showed no significant differences between unfilled defects or defects filled with empty or VEGF-only scaffolds (figure 5B). Implantation of BMP-2-loaded scaffolds resulted in significantly more bone in the femoral defect ($p < 0.001$). Although the combination of growth factors resulted in a slight increase in bone formation compared to BMP-2 alone, the difference between these implants was not significant ($p = 0.10$).

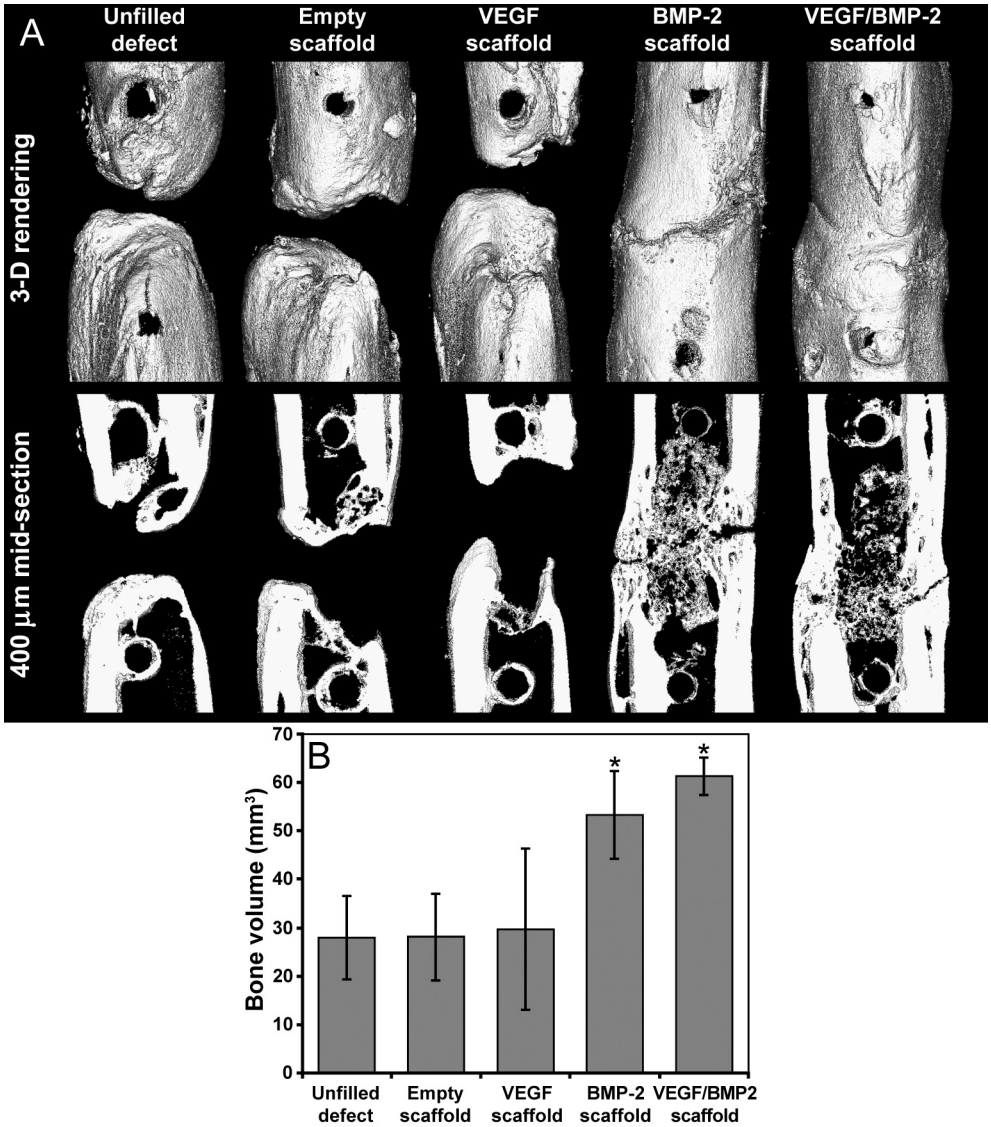

Figure 5: Analysis of the bone formation in the 5-mm critical size femoral defect model. (A) 3-D µCT reconstructions and 400 µm central slices of the composites in the bone defect. (B) Quantification of the bone volume in the 6-mm section between the two middle K-wires showed that local BMP-2 release resulted in significantly more bone formation in the femoral defect compared to the non-BMP-2 loaded implants ($p < 0.001$).

Histology

Microscopic evaluation of ectopic implant sections showed that the gelatin hydrogel was completely resorbed and replaced by a fibrous capsule surrounding the microsphere/PPF rod. The vascular network in the fibrous capsule could be easily identified by the blue Microfil® contrast agent and appeared denser around the VEGF-containing implants (figure 6A). From the fibrous capsule, connective tissue grew into the interconnected porous polymer network of the rod that resulted from PLGA degradation in the PPF matrix. Ectopic bone formation and osteoid depositions were seen around the microsphere/PPF rod and inside the pores of the BMP-2-containing implants (figure 6B & 6C). The bone had a woven and trabecular appearance. No osteoid depositions or bone formation were seen in the non-loaded and VEGF-loaded implants. Fluorochrome analysis showed the calcein green label along the surface of the implant and the alizarin red label at both the surface and center of the implant. This indicated that bone formation and mineralization had started at the periphery and progressed to the centers (figure 6D).
In the orthotopic site, the gelatin hydrogel was also completely resorbed and partial degradation of the PLGA resulted in an interconnected porous network within the microsphere/PPF rods. Histological analysis confirmed the bone formation that was observed in the μCT scans. Newly formed bone extending from the original defect edges partially bridged the empty defect and the defects filled with empty or VEGF-containing composites (figure 7A & 7B). The rest of these defects was filled with well-vascularized connective tissue. Although the majority of the empty and VEGF-loaded composites were filled with well-vascularized fibrous tissue, bone formation was seen inside the pores at the defect edges (figure 7A). In contrast to these defects, the BMP-2-loaded composites showed extensive woven and lamellar bone formation inside the porous microsphere/PPF rod and almost full bridging of the cortices with well vascularized bone (figure 7C & 7D). In most BMP-2 composite containing defects, a narrow non-osseous area could be observed that was filled with dense connective tissue containing chondrocyte-like cells and showed signs of endochondral ossification (figure 7E). Fluorescence microscopy showed the presence of both fluorochromes in all samples (figure 7F). Calcein green and alizarin red were found throughout the newly formed bone in the defect indicating that mineralization and bone formation started before 4 weeks and continued over the rest of the follow up period.

Histomorphometry

Only the vessels with the blue Microfil® contrast agent were identified and pseudocolored in the histological sections. Quantification of the vessels showed no differences in vessel surface area between the different implants ($p = 0.18$, figure 8)

Discussion

In the present study, we evaluated the effects of a local time-dependent VEGF and/or BMP-2 release on osteogenesis and vasculogenesis in Mps/PPF/gelatin composites for bone regeneration. Analysis of the pharmacokinetic profile of the growth factors from Mps/PPF/gelatin composites showed a rapid release of VEGF in the first 2 weeks and a more sustained release of BMP-2 over the full 8 week period. In the ectopic implantation

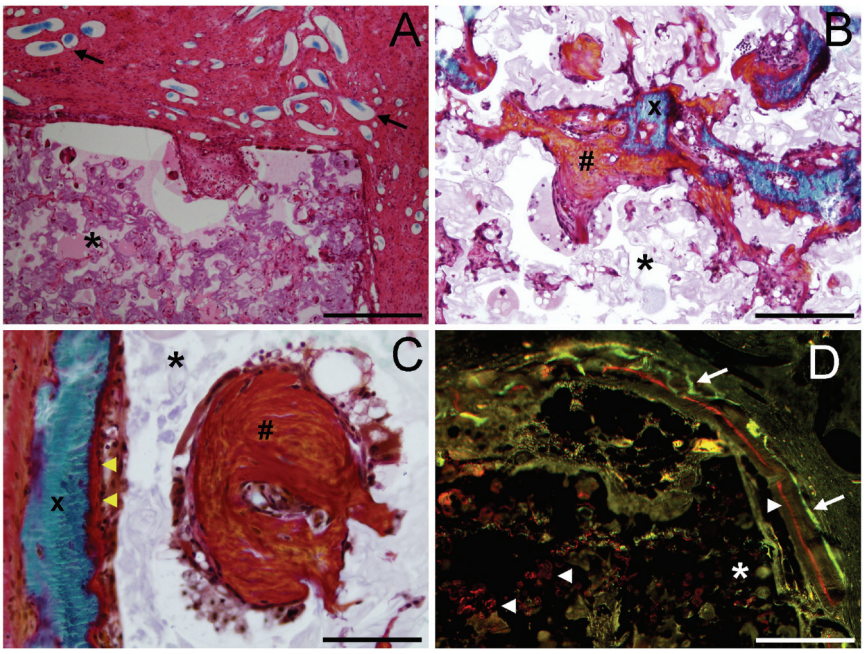

Figure 6: Histological sections of the implants after 56 days of ectopic implantation in rats. The sections represent VEGF loaded (A), BMP-2 loaded (C) and BMP-2/VEGF (B, D) loaded implants. They were hematoxillin/eosin (A) and Goldner (B, C) stained for routine histology or left unstained (D) for analysis of the fluorochromes by fluorescent microscopy. (A) Section showing the dense vascular network (filled with the blue contrast agent, indicated by the arrows) in the fibrous capsule around an ectopic VEGF loaded implant. (B,C) Newly formed bone (x) and osteoid (# and black arrow heads) were seen along the surface and within the pores of the microsphere/PPF rod (*) of the BMP-2/VEGF (B) and BMP-2 (C) loaded implants. Woven and lamellar bone formation was seen as osteoid was deposited within the pores (#) or along the existing bone (black arrow heads). (D) Unstained sections showed deposition of calceine green along the surface (white arrows) and alizarin red along the surface and in the center of the scaffold (white arrow heads). The scalebars represent 500 µm (A, D), 200 µm (B) and 100 µm (C).

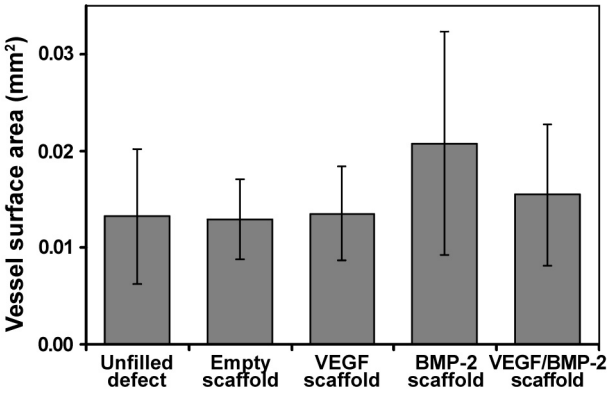

Figure 8: Analysis of the vessel formation in the 5-mm critical size femoral defect model. Quantification of the surface area of the vessels filled with the blue Microfil® contrast agent showed no significant difference between the different implants (p = 0.18).

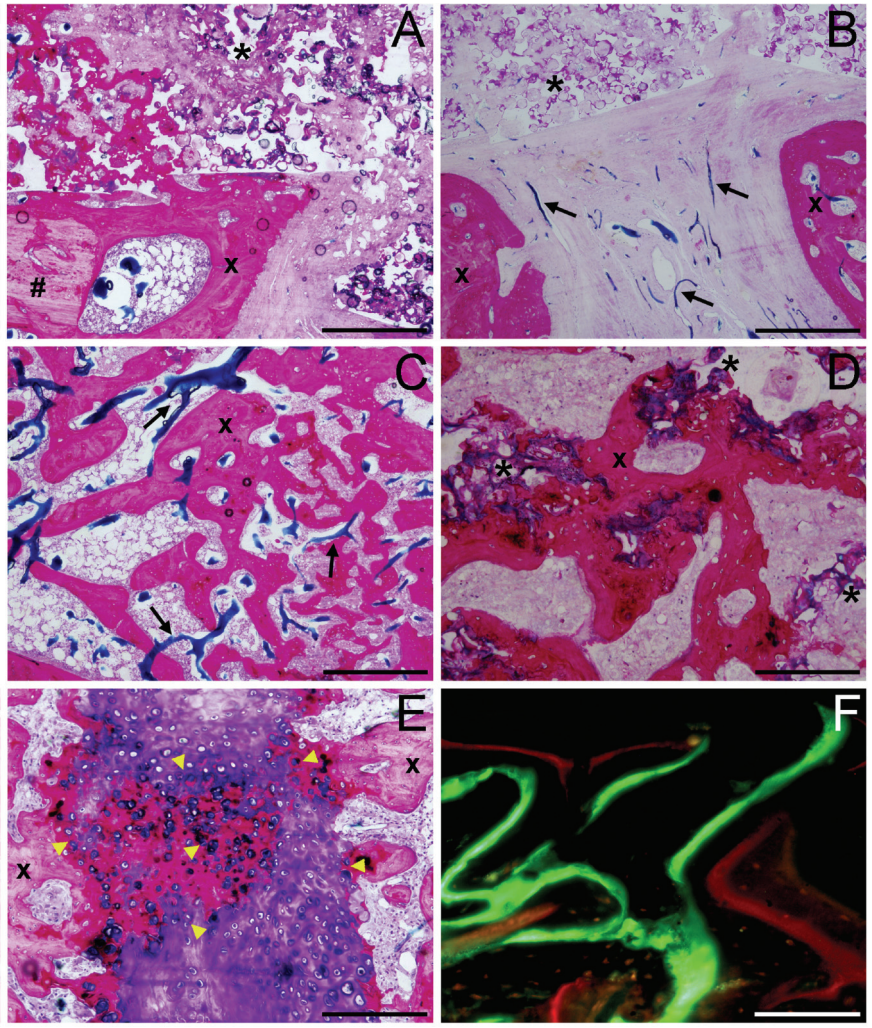

Figure 7: Histological sections of the implants after 56 days of orthotopic (A-F) implantation in rats. The sections represent non-loaded (A), VEGF loaded (B), BMP-2 loaded (D, E, F) and BMP-2/VEGF (C) loaded implants. They were methylene blue/basic fuchsin (A-E) stained for routine histology or left unstained (F) for analysis of the fluorochromes by fluorescent microscopy. Within the femoral defect, the vascular network in the bone and fibrous tissue is visualized by the blue contrast agent of the microangiography (indicated by black arrows). The sections of the orthotopic implants (A-E) showed bone formation (x) extending from the original femur edges (#) into the defect and the pores of the microsphere/PPF scaffold (*). (E) Signs of endochondral ossification were seen in the center of the defects of the BMP-2 containing implants (indicated by yellow arrow heads). Fluorochrome analysis of unstained sections (F) showed calceine green and alizarin red deposition in newly formed bone. The scalebars represent 500 µm (A, B, C), 200 µm (D, E) and 100 µm (F).

site, the local release of VEGF and BMP-2 was able to enhance angiogenesis and osteogenesis, respectively. Their combined delivery significantly increased bone formation compared to BMP-2 alone. Although the trend in orthotopic osteogenesis was similar as ectopically, the combination of growth factors was not able to significantly enhance bone formation compared to an equal dose of BMP-2 alone.

The optimization of biomaterial design and site-specific pharmacological actions of growth factors remain challenging in translational bone regeneration studies. The synthetic polymer PLGA is a well-characterized biodegradable material which has been used extensively as controlled delivery vehicle for BMPs.[29,34-38] It is capable of retaining BMP-2 with preservation of its bioactivity over a longer period of time compared to gelatin.[28] Since the *in vivo* expression of BMPs with documented ectopic osteoinductive capacities (BMP-2, BMP-4, BMP-6 and BMP-7) during spontaneous bone regeneration showed a slow increasing up-regulation with a peak at/after 21 days, PLGA was a better candidate for releasing BMP-2.[21,22,24] Although its release from the composite coincided well with its expression pattern during normal bone healing, the BMP-2 release found in the current study could be further adjusted by altering the molecular weight of PLGA.

So far, various strategies have been successfully applied to obtain dual release profiles including alterations in biomaterial design or characteristics and combinations of biomaterials. However, most of these newly developed carriers have only been characterized *in vitro*. Since the *in vitro* release profile changes significantly upon implantation, characterization of their *in vivo* pharmacokinetics is essential in bone regeneration.[28,38-41] Cross-linked gelatin has been explored as VEGF/BMP-2 delivery vehicle and showed a significantly slower *in vitro* release of VEGF compared to BMP-2.[42] However, their release profiles appeared similar upon implantation.[42] Therefore, the cross-linking density of gelatin was altered to tailor its release profile, which resulted in a successful *in vivo* dual release profile of both growth factors in a gelatin/PPF construct.[43,44]

In the current study, another strategy based on the altered growth factor binding/entrapment properties of two different materials was used to obtain a sequential release profile. Previous studies have shown that the incorporation of VEGF in gelatin with a low cross-linking density results in an early release of the growth factor. Therefore, gelatin was a good candidate for releasing VEGF, since normal VEGF expression is up-regulated within the first 10 days with a peak around day 5-10.[23,25,26] Although the composite released 98% of the VEGF within the first 14 days, the peak of its release occurred earlier compared to the normal expression pattern.

Despite this high burst release during the early days of implantation, VEGF was still able to significantly enhance vessel formation and increased BMP-2-induced bone formation at the ectopic site. Since the early VEGF release likely preceded the BMP-2-induced osteogenesis, direct effects of VEGF on osteoblasts are expected to contribute little to the enhanced bone formation. Most likely, VEGF enhanced bone formation indirectly by increasing the supportive vascular network and vascular permeability, as shown here, and supported by previous studies.[45,46] Since the circulation is a major source of osteoprogenitor cells during ectopic BMP-2 induced bone formation, these vascular changes could result in an increased local blood flow and thus enhanced accessibility of the implantation site for cells.[47] Furthermore, VEGF may serve as an early chemo-attractant for mesenchymal stem cells in addition to BMP-2.[48,49] These indirect effects of VEGF can enhance cell recruitment and result in more efficient bone regeneration at similar concentrations of the osteoinductive factor.

In contrast to previous studies, no significant effect of VEGF was seen on orthotopic vessel

and bone formation.[12,14,50] Given the lack of effect in the current study, the peak release may have indeed occurred too early for enhancement of orthoptopic bone regeneration. Further prolongation of release by increasing the cross-linking density of gelatin or by exploring other carriers materials may be a promising approach in future studies.[11,14,43,51] In addition to the differences in VEGF delivery vehicle, this difference may also have been due to the VEGF dosage or the local micro-environment. In the current study, increased local blood loss due to a larger surgical procedure may have resulted in a subsequent larger orthotopic haematoma compared to the ectopic site, which is a source for endogenous chemotactic, angiogenic and mitogenic growth factors. This may also explain the lack of additive effects of VEGF on BMP-2 induced bone formation at this location.[16,17]
A similar non-significant long term effect on bone formation was seen with a combination of 12 µg VEGF and 2 µg BMP-2 on a rat calvarial defect.[19] However, this reversed ratio significantly enhanced bone formation compared to the individual growth factors at an earlier time point (4 weeks). Overall, it appears the enhanced effect of the VEGF/BMP-2 combination is both time- and location-dependent. Apart from the larger local hematoma as a source for endogenous growth factors and the interfering auto-induction of bone at the opposing femur ends, the exposed marrow cavity and periosteum at the defect edges may serve as an abundant local source for mesenchymal stem cells.[52-54] This could decrease the influence of VEGF induced angiogenesis in the orthotopic defect and may have also contributed to the lack of a significant difference compared to the ectopic site. The interference of these mechanisms might be further studied in larger animal models since the distance between the bony ends of the defect increases and haemostasis is better controlled in larger defects.
Previous gene-therapy studies found an additive effect of angiogenic and osteogenic growth factors on bone regeneration for the combination of VEGF-expressing cells with BMP-2- or BMP-4-expressing cells and a combination of recombinant VEGF with BMP-4-encoding plasmid DNA.[13,18,20] Although the VEGF/BMP-2 combination resulted in an additive effect on bone formation in the current study, this was less pronounced compared to the application of combinations of growth factor expressing cells.[13,20] This difference could be the result of dose-related effects which can occur when using BMP expressing cells. In addition, VEGF-induced angiogenesis could have resulted in an enhanced survival of BMP-expressing cells, which can subsequently lead to even higher local dosages of the osteoinductive growth factors.
In conclusion, this study clearly shows the advantage of using a composite biomaterial to sequentially deliver a combination of angiogenic and osteogenic growth factors to enhance bone regeneration. Whereas the early release of VEGF alone did not affect bone formation, it significantly enhanced BMP-2 induced bone formation in an ectopic site. Although a similar trend was seen at the orthotopic site, the VEGF and BMP-2 delivery did not result in significant effects. Future studies are required to further optimize the amounts, ratio and timing of these growth factors for the augmentation of bone regeneration in challenging clinical settings.

References

1. Arrington, E.D., Smith, W.J., Chambers, H.G., Bucknell, A.L., and Davino, N.A. Complications of iliac crest bone graft harvesting. Clin Orthop Relat Res, 300, 1996.
2. Silber, J.S., Anderson, D.G., Daffner, S.D., Brislin, B.T., Leland, J.M., Hilibrand, A.S., Vaccaro, A.R., and Albert, T.J. Donor site morbidity after anterior iliac crest bone harvest for single-level anterior cervical

discectomy and fusion. Spine 28, 134, 2003.
3. Younger, E.M., and Chapman, M.W. Morbidity at bone graft donor sites. J Orthop Trauma 3, 192, 1989.
4. Wozney, J.M. Overview of bone morphogenetic proteins. Spine 27, S2, 2002.
5. Kang, Q., Sun, M.H., Cheng, H., Peng, Y., Montag, A.G., Deyrup, A.T., Jiang, W., Luu, H.H., Luo, J., Szatkowski, J.P., Vanichakarn, P., Park, J.Y., Li, Y., Haydon, R.C., and He, T.C. Characterization of the distinct orthotopic bone-forming activity of 14 BMPs using recombinant adenovirus-mediated gene delivery. Gene Ther 11, 1312, 2004.
6. Li, J.Z., Li, H., Sasaki, T., Holman, D., Beres, B., Dumont, R.J., Pittman, D.D., Hankins, G.R., and Helm, G.A. Osteogenic potential of five different recombinant human bone morphogenetic protein adenoviral vectors in the rat. Gene Ther 10, 1735, 2003.
7. Sampath, T.K., Maliakal, J.C., Hauschka, P.V., Jones, W.K., Sasak, H., Tucker, R.F., White, K.H., Coughlin, J.E., Tucker, M.M., Pang, R.H., and et al. Recombinant human osteogenic protein-1 (hOP-1) induces new bone formation *in vivo* with a specific activity comparable with natural bovine osteogenic protein and stimulates osteoblast proliferation and differentiation *in vitro*. J Biol Chem 267, 20352, 1992.
8. Wang, E.A., Rosen, V., D'Alessandro, J.S., Bauduy, M., Cordes, P., Harada, T., Israel, D.I., Hewick, R.M., Kerns, K.M., LaPan, P., and et al. Recombinant human bone morphogenetic protein induces bone formation. Proc Natl Acad Sci U S A 87, 2220, 1990.
9. Wozney, J.M., Rosen, V., Celeste, A.J., Mitsock, L.M., Whitters, M.J., Kriz, R.W., Hewick, R.M., and Wang, E.A. Novel regulators of bone formation: molecular clones and activities. Science 242, 1528, 1988.
10. Gerstenfeld, L.C., Cullinane, D.M., Barnes, G.L., Graves, D.T., and Einhorn, T.A. Fracture healing as a post-natal developmental process: molecular, spatial, and temporal aspects of its regulation. J Cell Biochem 88, 873, 2003.
11. Eckardt, H., Ding, M., Lind, M., Hansen, E.S., Christensen, K.S., and Hvid, I. Recombinant human vascular endothelial growth factor enhances bone healing in an experimental nonunion model. J Bone Joint Surg Br 87, 1434, 2005.
12. Kaigler, D., Wang, Z., Horger, K., Mooney, D.J., and Krebsbach, P.H. VEGF scaffolds enhance angiogenesis and bone regeneration in irradiated osseous defects. J Bone Miner Res 21, 735, 2006.
13. Peng, H., Usas, A., Olshanski, A., Ho, A.M., Gearhart, B., Cooper, G.M., and Huard, J. VEGF improves, whereas sFlt1 inhibits, BMP2-induced bone formation and bone healing through modulation of angiogenesis. J Bone Miner Res 20, 2017, 2005.
14. Street, J., Bao, M., deGuzman, L., Bunting, S., Peale, F.V., Jr., Ferrara, N., Steinmetz, H., Hoeffel, J., Cleland, J.L., Daugherty, A., van Bruggen, N., Redmond, H.P., Carano, R.A., and Filvaroff, E.H. Vascular endothelial growth factor stimulates bone repair by promoting angiogenesis and bone turnover. Proc Natl Acad Sci U S A 99, 9656, 2002.
15. Wang, D.S., Miura, M., Demura, H., and Sato, K. Anabolic effects of 1,25-dihydroxyvitamin D3 on osteoblasts are enhanced by vascular endothelial growth factor produced by osteoblasts and by growth factors produced by endothelial cells. Endocrinology 138, 2953, 1997.
16. Deckers, M.M., van Bezooijen, R.L., van der Horst, G., Hoogendam, J., van Der Bent, C., Papapoulos, S.E., and Lowik, C.W. Bone morphogenetic proteins stimulate angiogenesis through osteoblast-derived vascular endothelial growth factor A. Endocrinology 143, 1545, 2002.
17. Kozawa, O., Matsuno, H., and Uematsu, T. Involvement of p70 S6 kinase in bone morphogenetic protein signaling: vascular endothelial growth factor synthesis by bone morphogenetic protein-4 in osteoblasts. J Cell Biochem 81, 430, 2001.
18. Huang, Y.C., Kaigler, D., Rice, K.G., Krebsbach, P.H., and Mooney, D.J. Combined angiogenic and osteogenic factor delivery enhances bone marrow stromal cell-driven bone regeneration. J Bone Miner Res 20, 848, 2005.
19. Patel, Z.S., Young, S., Tabata, Y., Jansen, J.A., Wong, M.E., and Mikos, A.G. Dual delivery of an angiogenic and an osteogenic growth factor for bone regeneration in a critical size defect model. Bone, 2008.
20. Peng, H., Wright, V., Usas, A., Gearhart, B., Shen, H.C., Cummins, J., and Huard, J. Synergistic enhancement of bone formation and healing by stem cell-expressed VEGF and bone morphogenetic protein-4. J Clin Invest 110, 751, 2002.
21. Cho, T.J., Gerstenfeld, L.C., and Einhorn, T.A. Differential temporal expression of members of the transforming growth factor beta superfamily during murine fracture healing. J Bone Miner Res 17, 513, 2002.

22. Groeneveld, E.H., and Burger, E.H. Bone morphogenetic proteins in human bone regeneration. Eur J Endocrinol 142, 9, 2000.
23. Komatsu, D.E., and Hadjiargyrou, M. Activation of the transcription factor HIF-1 and its target genes, VEGF, HO-1, iNOS, during fracture repair. Bone 34, 680, 2004.
24. Niikura, T., Hak, D.J., and Reddi, A.H. Global gene profiling reveals a downregulation of BMP gene expression in experimental atrophic nonunions compared to standard healing fractures. J Orthop Res 24, 1463, 2006.
25. Pufe, T., Wildemann, B., Petersen, W., Mentlein, R., Raschke, M., and Schmidmaier, G. Quantitative measurement of the splice variants 120 and 164 of the angiogenic peptide vascular endothelial growth factor in the time flow of fracture healing: a study in the rat. Cell Tissue Res 309, 387, 2002.
26. Uchida, S., Sakai, A., Kudo, H., Otomo, H., Watanuki, M., Tanaka, M., Nagashima, M., and Nakamura, T. Vascular endothelial growth factor is expressed along with its receptors during the healing process of bone and bone marrow after drill-hole injury in rats. Bone 32, 491, 2003.
27. Kempen, D.H., Lu, L., Classic, K.L., Hefferan, T.E., Creemers, L.B., Maran, A., Dhert, W.J., and Yaszemski, M.J. Non-invasive screening method for simultaneous evaluation of *in vivo* growth factor release profiles from multiple ectopic bone tissue engineering implants. J Control Release 130, 15, 2008.
28. Kempen, D.H., Lu, L., Hefferan, T.E., Creemers, L.B., Maran, A., Classic, K.L., Dhert, W.J., and Yaszemski, M.J. Retention of *in vitro* and *in vivo* BMP-2 bioactivities in sustained delivery vehicles for bone tissue engineering. Biomaterials 29, 3245, 2008.
29. Oldham, J.B., Lu, L., Zhu, X., Porter, B.D., Hefferan, T.E., Larson, D.R., Currier, B.L., Mikos, A.G., and Yaszemski, M.J. Biological activity of rhBMP-2 released from PLGA microspheres. J Biomech Eng 122, 289, 2000.
30. Wang, S., Lu, L., and Yaszemski, M.J. Bone-tissue-engineering material poly(propylene fumarate): correlation between molecular weight, chain dimensions, and physical properties. Biomacromolecules 7, 1976, 2006.
31. Kempen, D.H., Yaszemski, M.J., Heijink, A., Hefferan, T.E., Creemers, L.B., Britson, J., Maran, A., Classic, K.L., Dhert, W.J., and Lu, L. Non-invasive monitoring of BMP-2 retention and bone formation in composites for bone tissue engineering using SPECT/CT and scintillation probes. J Control Release 134, 169, 2009.
32. Elcin, Y.M., Dixit, V., and Gitnick, G. Extensive *in vivo* angiogenesis following controlled release of human vascular endothelial cell growth factor: implications for tissue engineering and wound healing. Artif Organs 25, 558, 2001.
33. Jorgensen, S.M., Demirkaya, O., and Ritman, E.L. Three-dimensional imaging of vasculature and parenchyma in intact rodent organs with X-ray micro-CT. Am J Physiol 275, H1103, 1998.
34. Boyan, B.D., Lohmann, C.H., Somers, A., Niederauer, G.G., Wozney, J.M., Dean, D.D., Carnes, D.L., Jr., and Schwartz, Z. Potential of porous poly-D,L-lactide-co-glycolide particles as a carrier for recombinant human bone morphogenetic protein-2 during osteoinduction *in vivo*. J Biomed Mater Res 46, 51, 1999.
35. Duggirala, S.S., Mehta, R.C., and DeLuca, P.P. Interaction of recombinant human bone morphogenetic protein-2 with poly(d,l lactide-co-glycolide) microspheres. Pharm Dev Technol 1, 11, 1996.
36. Ruhe, P.Q., Boerman, O.C., Russel, F.G., Spauwen, P.H., Mikos, A.G., and Jansen, J.A. Controlled release of rhBMP-2 loaded poly(dl-lactic-co-glycolic acid)/calcium phosphate cement composites *in vivo*. J Control Release 106, 162, 2005.
37. Schrier, J.A., and DeLuca, P.P. Recombinant human bone morphogenetic protein-2 binding and incorporation in PLGA microsphere delivery systems. Pharm Dev Technol 4, 611, 1999.
38. Woo, B.H., Fink, B.F., Page, R., Schrier, J.A., Jo, Y.W., Jiang, G., DeLuca, M., Vasconez, H.C., and DeLuca, P.P. Enhancement of bone growth by sustained delivery of recombinant human bone morphogenetic protein-2 in a polymeric matrix. Pharm Res 18, 1747, 2001.
39. Hori, K., Sotozono, C., Hamuro, J., Yamasaki, K., Kimura, Y., Ozeki, M., Tabata, Y., and Kinoshita, S. Controlled-release of epidermal growth factor from cationized gelatin hydrogel enhances corneal epithelial wound healing. J Control Release, 2006.
40. Li, R.H., Bouxsein, M.L., Blake, C.A., D'Augusta, D., Kim, H., Li, X.J., Wozney, J.M., and Seeherman, H.J. rhBMP-2 injected in a calcium phosphate paste (alpha-BSM) accelerates healing in the rabbit ulnar osteotomy model. J Orthop Res 21, 997, 2003.
41. Ruhe, P.Q., Boerman, O.C., Russel, F.G., Mikos, A.G., Spauwen, P.H., and Jansen, J.A. *In vivo* release of rhBMP-2 loaded porous calcium phosphate cement pretreated with albumin. J Mater Sci Mater Med 17, 919, 2006.

42. Yamamoto, M., Ikada, Y., and Tabata, Y. Controlled release of growth factors based on biodegradation of gelatin hydrogel. J Biomater Sci Polym Ed 12, 77, 2001.
43. Patel, Z.S., Ueda, H., Yamamoto, M., Tabata, Y., and Mikos, A.G. *In vitro* and *in vivo* release of vascular endothelial growth factor from gelatin microparticles and biodegradable composite scaffolds. Pharm Res 25, 2370, 2008.
44. Patel, Z.S., Yamamoto, M., Ueda, H., Tabata, Y., and Mikos, A.G. Biodegradable gelatin microparticles as delivery systems for the controlled release of bone morphogenetic protein-2. Acta Biomater 4, 1126, 2008.
45. Hansen-Algenstaedt, N., Joscheck, C., Wolfram, L., Schaefer, C., Muller, I., Bottcher, A., Deuretzbacher, G., Wiesner, L., Leunig, M., Algenstaedt, P., and Ruther, W. Sequential changes in vessel formation and micro-vascular function during bone repair. Acta Orthop 77, 429, 2006.
46. Neufeld, G., Cohen, T., Gengrinovitch, S., and Poltorak, Z. Vascular endothelial growth factor (VEGF) and its receptors. Faseb J 13, 9, 1999.
47. Otsuru, S., Tamai, K., Yamazaki, T., Yoshikawa, H., and Kaneda, Y. Bone marrow-derived osteoblast progenitor cells in circulating blood contribute to ectopic bone formation in mice. Biochem Biophys Res Commun 354, 453, 2007.
48. Fiedler, J., Leucht, F., Waltenberger, J., Dehio, C., and Brenner, R.E. VEGF-A and PlGF-1 stimulate chemotactic migration of human mesenchymal progenitor cells. Biochem Biophys Res Commun 334, 561, 2005.
49. Fiedler, J., Roderer, G., Gunther, K.P., and Brenner, R.E. BMP-2, BMP-4, and PDGF-bb stimulate chemotactic migration of primary human mesenchymal progenitor cells. J Cell Biochem 87, 305, 2002.
50. Leach, J.K., Kaigler, D., Wang, Z., Krebsbach, P.H., and Mooney, D.J. Coating of VEGF-releasing scaffolds with bioactive glass for angiogenesis and bone regeneration. Biomaterials 27, 3249, 2006.
51. Tabata, Y., Miyao, M., Ozeki, M., and Ikada, Y. Controlled release of vascular endothelial growth factor by use of collagen hydrogels. J Biomater Sci Polym Ed 11, 915, 2000.
52. Anitua, E., Andia, I., Ardanza, B., Nurden, P., and Nurden, A.T. Autologous platelets as a source of proteins for healing and tissue regeneration. Thromb Haemost 91, 4, 2004.
53. Pintucci, G., Froum, S., Pinnell, J., Mignatti, P., Rafii, S., and Green, D. Trophic effects of platelets on cultured endothelial cells are mediated by platelet-associated fibroblast growth factor-2 (FGF-2) and vascular endothelial growth factor (VEGF). Thromb Haemost 88, 834, 2002.
54. Weltermann, A., Wolzt, M., Petersmann, K., Czerni, C., Graselli, U., Lechner, K., and Kyrle, P.A. Large amounts of vascular endothelial growth factor at the site of hemostatic plug formation *in vivo*. Arterioscler Thromb Vasc Biol 19, 1757, 1999.

12

Enhanced BMP-2 induced ectopic and orthotopic bone formation by intermittent PTH(1-34) administration

Tissue Engineering Part A 2010;16:3769-3777

D.H.R. Kempen
L. Lu
T.E. Hefferan
L.B. Creemers
A. Heijink
A. Maran
W.J.A. Dhert
M.J. Yaszemski

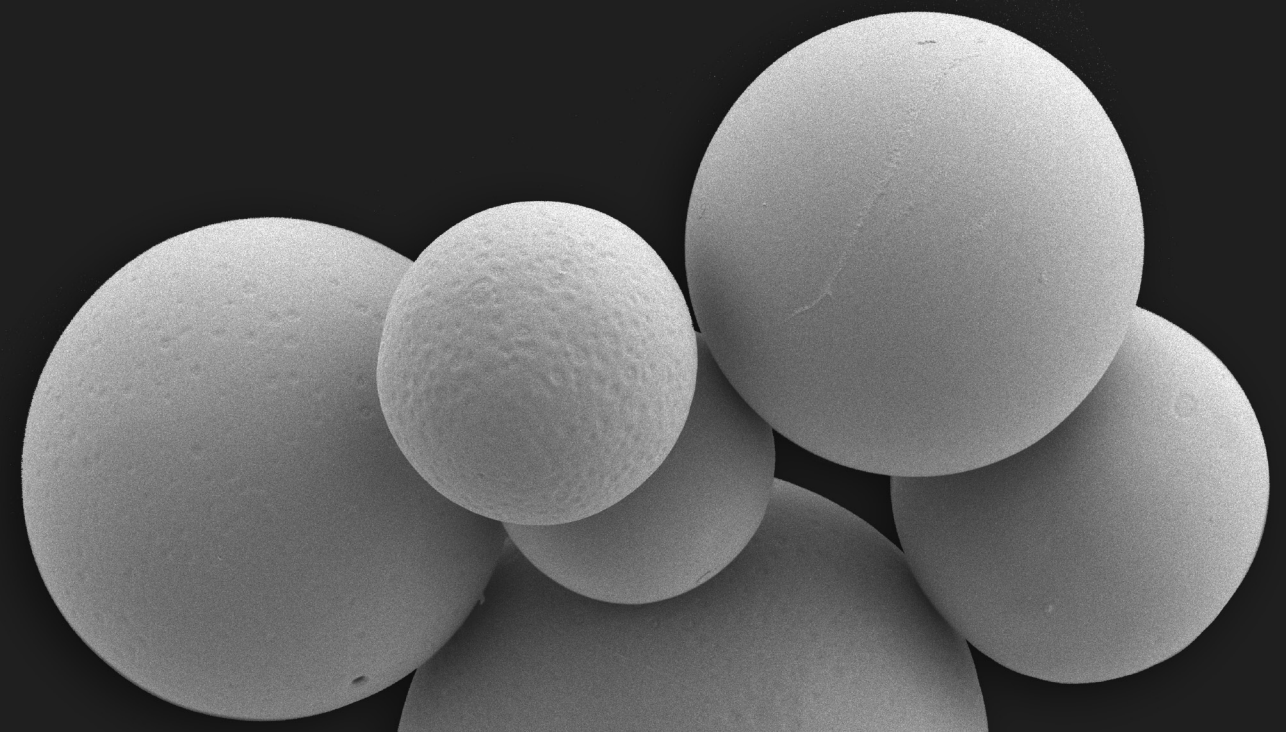

Abstract

Bone morphogenetic proteins (BMPs) play a central role in local bone regeneration strategies, whereas the anabolic features of parathyroid hormone (PTH) are particularly appealing for the systemic treatment of generalized bone loss. The aim of the current study is to investigate whether local BMP-2 induced bone regeneration could be enhanced by systemic administration of PTH(1-34). Empty or BMP-2 loaded poly(lactic-co glycolic acid)/poly(propylene fumarate)/gelatin composites were implanted subcutaneously and in femoral defects in rats (n=9). For the orthotopic site, empty defects were also tested. Each of the conditions was investigated in combination with daily administered subcutaneous PTH(1-34) injections in the neck. After 8 weeks of implantation, bone mineral density (BMD) and bone volume were analyzed using micro-computed tomography (μCT) and histology. Ectopic bone formation and almost complete healing of the femoral defect were only seen in rats that received BMP-2 loaded composites. Additional treatment of the rats with PTH(1-34) resulted in significantly ($p<0.05$) enhanced BMD and bone volume in the BMP-2 composites at both implantation sites. Despite its effect on BMD in the humerus and vertebra, PTH(1-34) treatment had no significant effect on BMD and bone volume in the empty femoral defects and the ectopically or orthotopically implanted empty composites. Histological analysis showed that the newly formed bone had a normal woven and trabecular appearance. Overall, this study suggests that intermittent administration of a low PTH dose alone has limited potential to enhance local bone regeneration in a critical sized defect in rats. However, when combined with local BMP-2 releasing scaffolds, PTH administration significantly enhanced osteogenesis in both ectopic and orthotopic sites.

Introduction

Bone tissue engineering has the potential to provide alternative therapies for the increasing number of grafting procedures in orthopedic surgery. It strives to create the appropriate *in vivo* environment to form autologous bone by inducing the regeneration potential of the patient's own tissue. A promising strategy to build up such a local environment is the use of a drug delivery vehicle for local release of bioactive molecules that are essential to the bone regeneration process.

Bone morphogenetic proteins (BMPs) play a central role in most bone regenerative strategies. Several members of the BMP family are capable of initiating the complete cascade of bone formation, including the recruitment of mesenchymal stem cells and their differentiation into osteoblasts.[1] These osteoinductive BMPs have generated significant interest as alternative therapy for the repair of local bone defect and spinal fusion. So far, this has resulted in the approval of two BMPs (BMP-2 and BMP-7) in collagen delivery vehicles for specific orthopedic applications in humans.[2-4]

In contrast to the localized actions of BMPs, parathyroid hormone (PTH) is one of the major systemic regulators of bone metabolism. It is secreted from the parathyroid glands and travels through the bloodstream to act upon bone. Interestingly, PTH is a double-edged sword for bone metabolism: whereas continuous PTH infusion causes the bone disease osteitis fibrosa, pulsed administration induces bone formation.[5,6] The anabolic features of intermittent PTH administration have made it particularly appealing for the treatment of patients with generalized bone loss in osteoporosis, in which it was shown to increase bone mass and reduce fracture rate.[7]

Given the enhanced bone formation by local application of BMPs or systemic application of PTH, combination therapies may be beneficial for bone tissue engineering. PTH has shown to restore the age-related reduction in osteoinductive capacity and increased bone mineral density of ectopic ossicles induced by BMP-2 loaded collagen delivery vehicles.[8,9] However, the effects of PTH or its combination with BMP-2 on orthotopic bone regeneration in bone tissue engineering remain relatively unexplored.

The aim of this study was to investigate the effect of PTH, BMP-2 and combination treatments on ectopic and orthotopic bone formation. Implants were based on poly(lactic-co glycolic acid)/poly(propylene fumarate)/gelatin (PLGA/PPF/gelatin) microsphere/scaffold composites. These composites are biodegradable and mechanically stable scaffolds previously shown to release BMP-2 over a period of time that coincides with normal expression of osteoinductive factors during bone healing.[10-12]

Materials and methods

Experimental design

A total of 54 rats were used for the experiment. The rats were divided into six groups of nine animals for each treatment (Table 1). The three different surgical treatments consisted of 1) no implant, 2) implantation of empty composite, and 3) implantation of BMP-2 loaded composite. Each of the surgical treatments was studied alone or in combination with PTH injections administered in the subcutis of the neck. The treatments were studied in both ectopic (subcutaneous) and orthotopic (critical sized femoral defect) sites. Whereas the ectopic site shows the osteoinductive potential of the construct without in-

Table 1
Experimental groups and group size

Scaffold (orthotopic/ectopic)	*No treatment*	*PTH(1-34) treatment*
Unfilled defect (control)*	n = 9	n = 9
Empty implant	n = 9	n = 9
BMP-2 loaded implant	n = 9	n = 9

* Only applicable for the orthotopic location

terference of osteoconduction or periosteal bone formation as disturbing mechanisms in the BMP-2 induced bone formation, the femoral defect represents a clinically applicable site. The empty defect with no implant was only studied orthotopically. The implants were removed after 8 weeks of implantation for evaluation of bone formation by micro-computed tomography (μCT), dual energy X-ray absorptiometry (DEXA) and histology.

Materials

Poly(lactic-co-glycolic acid) (PLGA) with a 50:50 lactic to glycolic acid ratio and a weight-average molecular weight (Mw) of 23 kDa was used for microsphere preparation. Poly(propylene fumarate) (PPF) with a Mw of 3,100 and a polydispersity index of 2.7 was synthesized by using a two-step reaction process as previously described.[13] Recombinant human BMP-2 (Medtronic Sofamor Danek, Minneapolis, MN) was concentrated by centrifuging at 5000 g in a Centricon-10 filter unit and reconstituted to the appropriate concentrations in an aqueous buffer consisting of 5 mM glutamate, 5 NaCl, 0.5% sucrose, 2.5% glycine and 0.01% polysorbate 80; pH 4.5. The receptor binding 34-amino acid N–terminal fragment of the PTH molecule (PTH(1-34), Bachem, Torrance, Ca) was diluted in an aqueous buffer for injection consisting of 0.9% NaCl, 2% heat inactivated serum (obtained from Sprague-Dawley rats) and 1 mM HCl. N-vinylpyrrolidinone (NVP, Acros, Pittsburgh, PA), bis(2,4,6-trimethylbenzoyl) phenylphosphine oxide (BAPO), gelatin (300 Bloom number, derived from acid-cured porcine skin), glutaraldehyde and glycine were used as received.

BMP-2 delivery vehicle

The implant consisted of PLGA microspheres incorporated into a solid PPF rod which was surrounded by a cylindrical gelatin hydrogel. The fabrication procedure of the PLGA microsphere/PPF/gelatin composites was described previously.[11,12] The BMP-2 loaded or unloaded PLGA microspheres were fabricated using a water-in-oil-in water double-emulsion-solvent-extraction technique.[14] Based on an starting amount of 1.3 μg BMP-2/mg PLGA and a previously achieved entrapment efficiency of 85%, the loading of the microspheres was estimated at 1.1 μg BMP-2/mg PLGA.[12]
The cylindrical microsphere/PPF scaffolds were then created by photocrosslinking PPF with NVP under UV-light using BAPO as a photoinitiator.[15] PLGA microspheres (55 wt%) were combined with a PPF/NVP paste (45 wt%) and injected into a glass mold to create a

solid cylindrical composite with a diameter of 1.6 mm and a length of 5.5 mm.[11,12] Based on an average weight of 10.3 ± 0.8 mg/cylinder, BMP-2 loading in the microsphere/PPF rods was estimated at 6.5 ± 0.5 µg/cylinder. The gelatin hydrogels were fabricated by chemically crosslinking a 10 wt% aqueous gelatin solution with 0.004 wt% glutaraldehyde in tubular molds (1.6 mm inner diameter and 3.5 mm outer diameter) for a period of 1 hour.[10,11,16,17] The crosslinked hydrogels were placed in a 100 mM glycine solution for 1 hour to block the residual aldehyde groups. The microsphere/PPF rods and gelatin hydrogels were sterilized separately in 70% alcohol, washed in PBS and stored at -20℃. The microsphere/PPF rods were inserted into the tubular gelatin hydrogels just before implantation.

Animals and procedures

The bone forming capacity of the scaffolds was tested in both ectopic and orthotopic models in 12-week-old Harlan Sprague Dawley rats (weight 324 ± 12 g). The experiments were performed according to established protocols approved by the Institutional Animal Care and Use Committee at the Mayo Clinic. The rats were anesthetized with an intramuscular injection of a ketamine/xylazine mixture (45/10 mg/kg) and the surgical sites were shaved and disinfected with a 30% Betadine solution. The right femur was exposed through a lateral approach and was circumferentially stripped from soft tissue and periosteum. A predrilled, high density polyethylene plate (23 x 4 x 4 mm, custom-made), was fixed along the anterior cortex of the femur using four threaded Kirschner wires (1 mm diameter). After plate fixation, a 5-mm mid-diaphyseal, full-thickness defect was created using a surgical burr and irrigated with physiologic saline to remove bone debris and bone marrow. After insertion of the implant in the defect, the wound was closed in layers using resorbable sutures (Vicryl 1/0) and non-resorbable nylon skin sutures. In addition to the orthotopic implant, each rat received an ectopic implant in a subcutaneous pocket at the lower left limb.

Post-operative analgesia was provided by intramuscular injections of buprenorphine (0.1 mg/kg) for the duration of 72 hours and acetaminophen (880mg/L added to the water bottle) for the duration of one week.

PTH(1-34) treatment was started on the third postoperative day. PTH injections were administered in the subcutis of the neck at a dosage of 10 µg/kg/day for 5 days a week till the end of the 8 week follow up period. In addition to PTH injections, the rats received fluorochrome markers calceine green (10mg/kg) and alizarin red (10mg/kg) after 4 and 6 weeks, respectively. After 8 weeks, the animals were sacrificed by an overdose of pentobarbital and the vessels were perfused with Microfil® to study vessel formation at the implantation site using previously described methods.[11] Following a midline laparatomy, the aorta and vena cava were canulated to clear the lower extremities from blood with heparinized saline. The vessels were subsequently infused until the toes were clearly colored blue by the Microfil® compound. Since there were no significant differences between the treatment groups, these data are not shown. After polymerization of the compound, the implants were removed and fixed in PBS containing 1.5% glutaraldehyde. The vertebral column and humerus were also harvested to analyze the effects of PTH treatment on overall bone density. Prior to µCT and DEXA scans, the two K-wires closest to the defect were removed from the femur.

Bone mineral density measurements

Bone mineral density (BMD) measurements were performed by DEXA using a PIXImus densitometer (software version 1.44.005, Lunar Corp., Madison, WI). Prior to the measurements, the PIXImus densitometer was calibrated using a hydroxyapatite phantom that was provided by the manufacturer. The excised implants, humerus and vertebral column were scanned by the machine and the regions of interest were identified for the analysis of the bone mineral density.

µCT analysis

The implants were scanned on a custom-build µCT system at 0.49° angular increments (providing 721 views around 360°) using 18 keV.[18] The projections were reconstructed using a modified Feldkamp cone beam tomographic reconstruction algorithm into a three-dimensional image consisting of 20 µm cubic voxels with a radiopacity represented by a 16-bit grayscale value. The bone formation in the implants was analyzed using the image analysis software Analyze 6.0. Due to the difficulty to distinguish the newly formed bone from the original femur, a 6-mm section of the femur was used for bone quantifications. The reconstructions and volume quantification of the ectopic and orthotopic bone were obtained using standardized thresholds.

Histology

After µCT and bone mineral density measurements, the subcutaneous implants and femurs were dehydrated in a graded series of alcohol and embedded in respectively glycol-methylmethacrylate and methylmethacrylate for histological evaluation as previously described in chapter 11.

Statistical analysis

All data are given as means ± standard deviations (SD) for n = 9. Independent t-tests were performed to analyze the BMD and bone volumes of the ectopic implants. The BMD and bone volumes of the orthotopic implants were statistically compared using one-way ANOVA with Bonferroni's *post hoc* tests. The effect of PTH treatment on overall BMD was analyzed using two-way ANOVA. All tests were performed by SPSS (version 13.0) and the level of significance was set at $p < 0.05$.

Results

Animal

Six animals (1 in empty defect group, 2 in empty defect/PTH group, 1 in empty composite group and 2 in the empty composite/PTH group) developed deep infections of their femoral defects during the study. Their BMD and bone volume measurements were excluded from further analysis. The other animals remained in good health and did not show any signs of complications.

Bone mineral density

After 8 weeks of implantation, all implants were easily identified and retrieved for further analysis. At the ectopic site, bone formation was only seen in BMP-2 loaded scaffolds. The ectopic BMP-2 implants in the PTH-treated animals had a significantly ($p<0.05$) higher BMD compared to the BMP-2 implants in the non-treated animals (figure 1). At the orthotopic site, the BMP-2 loaded scaffolds had a significantly higher BMD compared to the unfilled defects or defects filled with empty scaffolds ($p<0.02$). Furthermore, BMD of the BMP-2 containing scaffolds in these femoral defects was significantly higher in the animals treated with PTH injections ($p<0.04$). PTH administration had no effect on the BMD of empty defects or defects treated with empty scaffolds. The BMD of the right humerus and vertebra L1 of the PTH-treated rats was significantly higher compared to the non-treated rats ($p<0.05$).

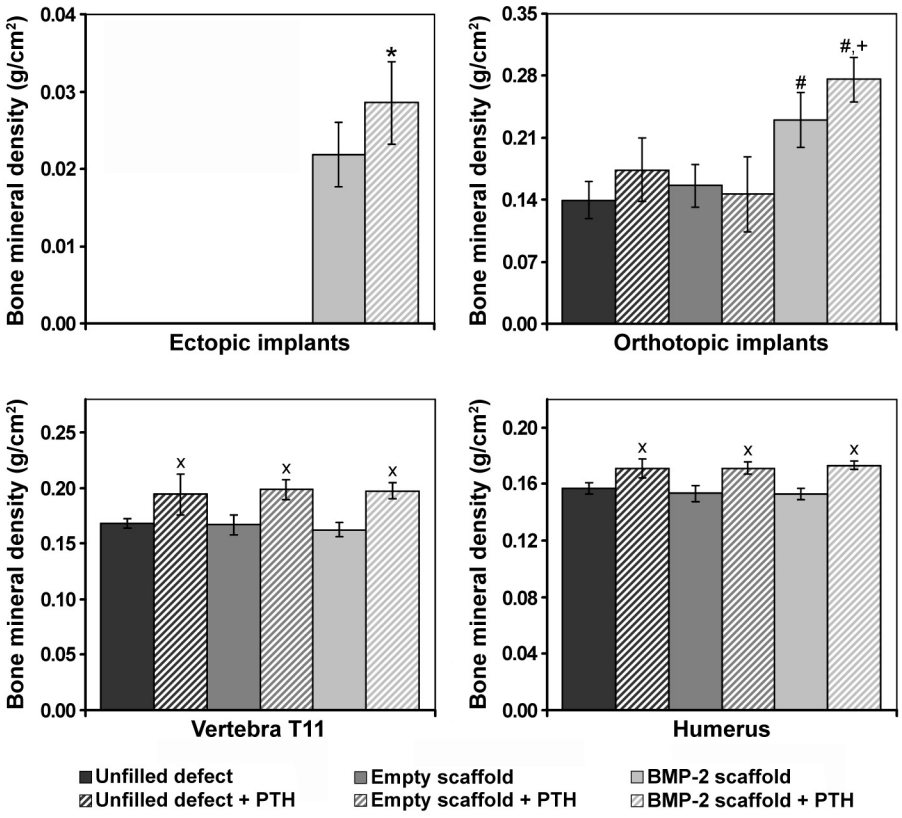

Figure 1: Bone mineral density of the ectopic implants, orthotopic implants, vertebra L1 and humerus after 8 weeks of follow up. The symbols indicate significant differences relative to (*) ectopic BMP-2 loaded implants, (#) unfilled and empty scaffold filled orthotopic defects, (+) all other groups or (x) non-treated vertebrae or humeri ($p<0.05$).

Bone volume

The effects of BMP-2 released from the scaffold and of PTH treatment on the ectopic and orthotopic volumes of the newly formed bone were studied by µCT imaging at 20 µm resolution. No radiological signs of bone formation were seen in the ectopically implanted empty scaffolds. Ectopic bone formation was seen in the µCT reconstructions of BMP-2 containing implants. Part of the ectopic implant surface was covered by a compact shell of bone and trabecular bone was seen inside the pores of the scaffold (figure 2A). Quantification of the bone volume showed that PTH had a significant effect on ectopic bone formation in these scaffolds (p=0.02, figure 2B).

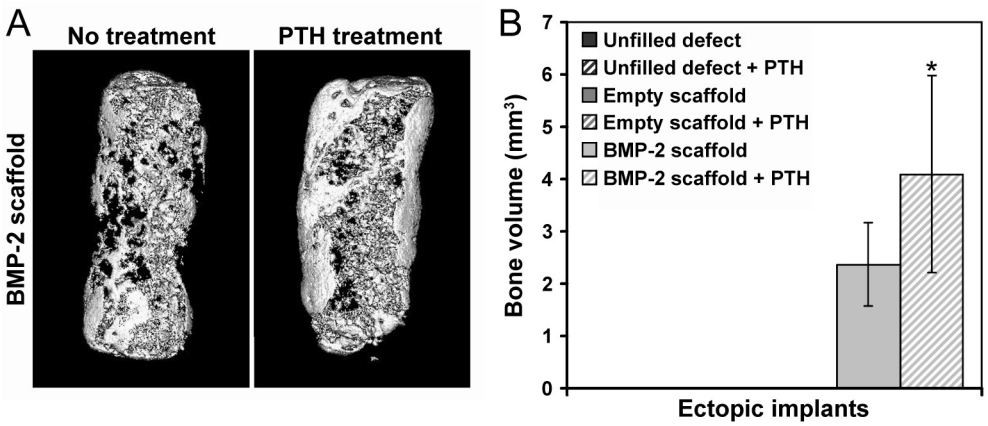

Figure 2: 3D µCT reconstructions (A) and bone volumes (B) of subcutaneously formed bone after 8 weeks of implantation in rats. The asterisk (*) indicates significant difference relative to BMP-2 loaded implants (p=0.02).

All orthotopic sites showed some newly formed bone around the defect edges (figure 3A). Analysis of connections between the proximal and distal part of the femur showed that none of the unfilled defects contained an osseous connection between the two femur parts. Trabecular connections between the two parts were observed in 2/8 and 2/7 of the untreated or PTH-treated defects filled with empty scaffolds, respectively, whereas almost full cortical regeneration was seen in all of the defects containing the BMP-2 loaded implants. The defects filled with BMP-2 loaded implants contained significantly more bone compared to the untreated unfilled defects and defects filled with empty scaffolds (p=0.04). The bone volume in the defects of animals treated with both BMP-2 scaffolds and PTH injections was significantly higher than all other groups (p=0.02). No significant differences were found between the untreated and PTH-treated unfilled defects or defects filled with empty scaffolds.

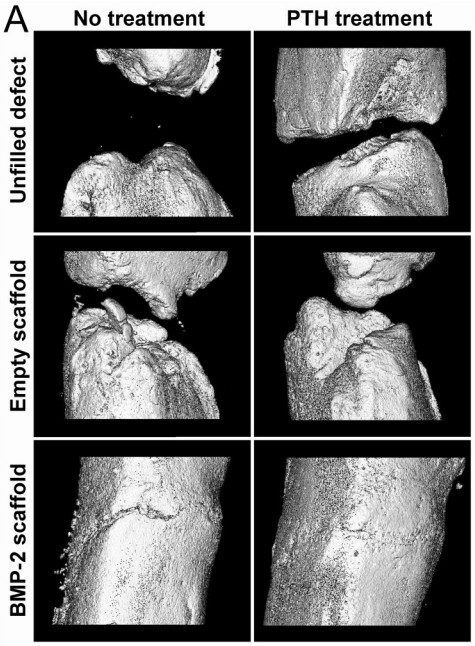

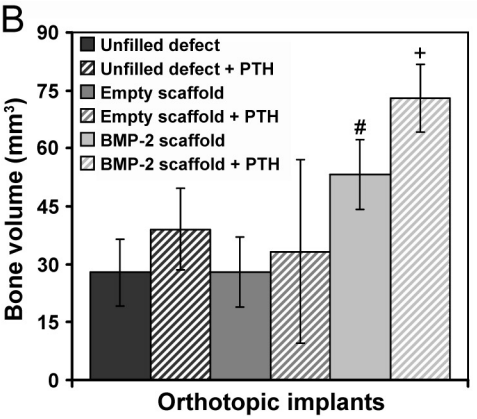

Figure 3: 3D µCT reconstructions (A) and bone volumes (B) of newly formed bone in the 5-mm femoral defects after 8 weeks of follow up. The symbols indicate significant differences relative to (#) unfilled defects, defects filled with empty scaffolds or defects filled with empty scaffolds treated with PTH injections and (+) all defects ($p<0.05$).

Histology

Microscopic evaluation of transverse sections showed that the gelatin hydrogel around the microsphere/scaffold composite was completely resorbed and the PLGA microspheres were degrading to create a porous PPF network. In the ectopic site, the gelatin hydrogel was replaced by a well vascularized fibrous capsule. There was a mild foreign body reaction to the microsphere/PPF rod as indicated by some inflammatory cells inside the pores of the scaffold. The interconnected pores of the ectopically implanted empty scaffolds were filled with connective tissue (figure 4A). Ectopic bone formation and osteoid depositions were seen on the surface and inside the pores of BMP-2 containing implants (figure 4B–4D). Bone formation was more extensive in the ectopic BMP-2 implants of rats treated with PTH compared to the non-treated animals. Fluorochrome analysis showed the presence of calcein green along the surface and alizarin red at both the surface and in the pores of the implant indicating that mineralization started at the periphery and progressed towards the center.

In the orthotopic implant, new bone formation extending from the femur edges was seen in all implants (figure 5). The empty defects were filled with inter-positioning muscles, fibrous tissue and a limited amount of bone (figure 5A). Implantation of empty scaffolds resulted in bone formation at the surface and in the scaffold pores at the defect edges, whereas the center was filled with connective tissue (figure 5B). In contrast to the empty defects and defects filled with empty scaffold, almost full cortical bridging was seen in the BMP-2 composite containing defects (figure 5C-5D). A narrow area with dense connective tissue containing chondrocyte-like cells showing signs of endochondral ossification

could be observed in the center of most of these defects (figure 5E). Overall, the rats treated with PTH showed broadening of the preexisting parts of the femur and newly formed cortices with a more compact structure of the bone (figure 5C-5D). The calcein green and alizarin red were found throughout the newly formed cortical bone indicating that mineralization was present in the entire cortical area before 4 weeks and continued over the rest of the follow up period (figure 5F).

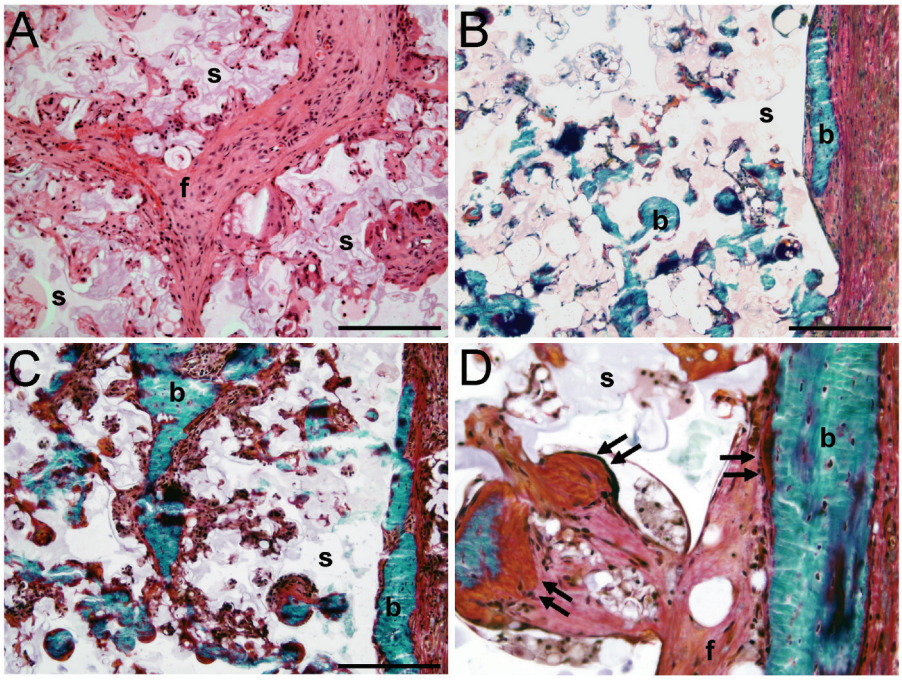

Figure 4: Histological sections of subcutaneously implanted empty (A) or BMP-2 (B-D) scaffolds in rats that were treated with (A, C, D) or without (B) PTH. Hematoxilin/eosin stained section (A) showing the interconnected porous polymer network and fibrous tissue (f) in the scaffold. Goldner stained sections (B-D) showing bone formation (b) and osteoid deposition (arrows) at the surface and in the pores of BMP-2 scaffolds (s). Scale bars represent 500 µm (A, D), 200 µm (B) and 50 µm (C).

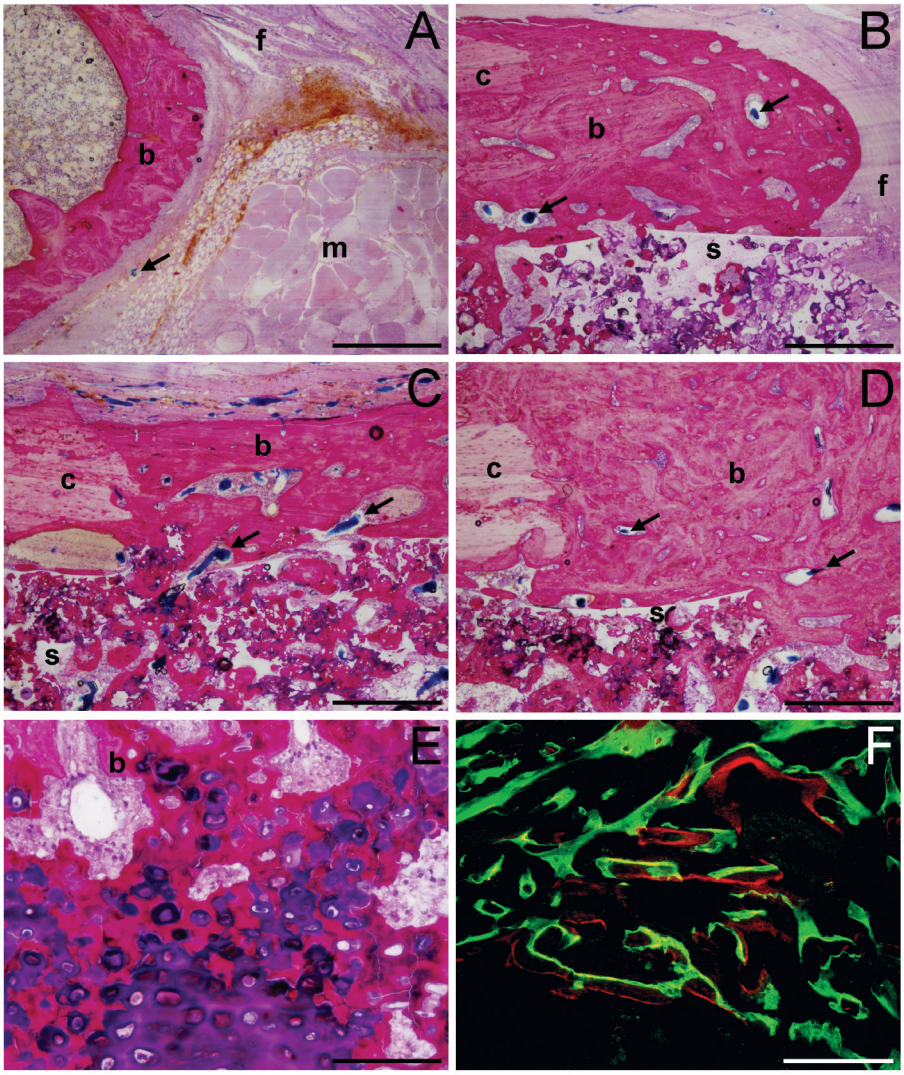

Figure 5: Histological sections of an empty femoral defect (A) and defects filled with empty (B) or BMP-2 scaffolds (C-F) in rats treated without (A,C) or with (B,D-F) PTH. Methylene blue/basic fuchsin stained sections (A-E) showing inter-positioning of muscles (m), fibrous tissue formation (f), bone formation (b) extending from the original femur cortices (c) into the defect and the pores of the scaffold (s). The vascular network in the bone and fibrous tissue is visualized by the blue Microfil® agent (arrows). Endochondral ossification was seen in the center of the defects of BMP-2 containing implants (E). Fluorochrome analysis of unstained sections (F) showed calceine green and alizarin red deposition in newly formed bone. Scale bars represent 500 µm (A-D), 50 µm (D-E), 500 µm (F).

Discussion

This study clearly shows the benefits of combined PTH and BMP-2 treatment on ectopic and orthotopic bone formation in a microsphere/scaffold composite for bone tissue engineering. Although an anabolic effect on the rest of the skeleton was seen, the 10 µg PTH/kg/day treatment had no significant effect on local bone regeneration in unfilled and empty scaffold filled defects. Implantation of BMP-2 loaded scaffolds resulted in a significant increase of bone mineral density and bone volume in both sites as opposed to the empty scaffolds. The combination of BMP-2 containing scaffolds with daily PTH injections resulted in a further increase of both ectopic and orthotopic bone volumes.

The exact cellular mechanism underlying the anabolic effect of PTH treatment is not fully understood. Histological observations have shown that intermittently administered PTH stimulates new bone formation on existing surfaces by increasing the osteoblast number.[5,19-21] Previous studies have suggested that this increase in osteoblast number is not dependent on the proliferation of osteoprogenitor cells and osteoblastogenesis, but the result of PTH effects on existing cells.[19,20,22] Likely target cells for short term PTH effects are bone-lining cells, which are thought to be inactive osteoblasts. These lining cells may undergo hypertrophy and resume matrix synthesis in response to PTH treatment.[5,19,21] Another proposed method for the continued effect of long-term PTH treatments is the inhibition of osteoblast apoptosis.[5,20]

The absence of bone formation in the ectopically implanted empty scaffolds was anticipated, as the synthetic polymers are not osteoinductive. Since PTH is expected to act upon cells committed to the osteoblastic lineage, it was not surprising that PTH was not able to affect ectopic bone formation in these empty scaffolds.[15] Although PTH cannot induce bone formation from uncommitted cells, it can enhance bone formation once it has been initiated. Previous bone fracture, distraction and conduction chamber models have shown a strong dose-related effect of intermittent PTH administration on local bone regeneration.[23-26] Despite bone induction at the edges of the unfilled or empty scaffold filled defects and the positive PTH effects on preexistent bone, no significant differences were found between these untreated and PTH-treated defects. The discrepancy between previous studies and these results may be due to the more challenging critical sized defect model and low PTH dose used in this study.

In contrast to PTH, BMP-2 plays an essential role in the commitment and differentiation of mesenchymal stem cells towards the osteoblastic lineage. Its high osteoinductive potential is clearly demonstrated by its ability to induce bone formation in an ectopic implantation site.[27,28] The BMP-induced bone formation occurs through endochondral (through a cartilage intermediate) and/or intramembranous (direct) ossification and results in woven bone which is later remodeled into normal bone.[27,28] In our study, after implantation of the microsphere/PPF/gelatin delivery vehicle, clear signs of endochondral and intramembranous ossification were also seen at the ectopic or orthotopic location.

Despite the non-significant effect of PTH alone, PTH significantly enhanced the BMP-2 induced bone formation at both ectopic and orthotopic locations. This clearly shows that the different mechanisms of action of BMP-2 and PTH enhance each other when used as a combination therapy. Whereas BMP-2 induces bone formation by committing mesenchymal stem cells towards the osteoblastic lineage, PTH could act upon these committed cells to prolong the matrix-synthesizing function. Furthermore, the anti-apoptotic effect of PTH could also have enhanced bone formation by expanding the osteoblast life span by counteracting the possible apoptotic effects of BMP-2 on osteoblasts.[20,29]

Unfortunately, further histological analysis (e.g. counting of the osteoblast number) of the mechanism underlying the anabolic effect in the combination therapy was impossible due to the woven aspect of the newly formed bone.
Compared to previous studies, the ectopic results obtained in our study corresponded with previous findings of PTH-mediated enhancement of ectopic BMP-induced bone formation in a collagen sponge.[8,9] In contrast to the clearly enhanced ectopic effect, no significant differences could be observed between a PTH/BMP-7 combination and PTH alone in a previous study.[30] This non-significant effect might be caused by their use of a less challenging partial thickness metaphysic defect model. Since the spontaneous regeneration response was capable of healing the non-treated defects as well, no significant effect of BMP-7 could be shown compared to the control group. Consequently, PTH enhanced both spontaneous and BMP-7 assisted healing response and no significant differences in bone formation were observed between the PTH/BMP-7 combination and PTH alone. In the critical sized defect model in this study, the normal bone regeneration response resulted in limited amounts of bone formation at the defect edges which was not significantly enhanced by PTH. However, bone regeneration was significantly stimulated by the BMP-2 releasing implants and PTH could act upon this to synergistically enhance the healing response.
In conclusion, this study clearly shows that BMP-2-induced osteogenesis can be enhanced by intermittent administration of PTH. Although PTH alone did not significantly improve bone formation, it can be beneficial for local bone regeneration in combination with BMP-2. Based on this study, PTH/BMP-2 combination therapy could be considered for the restoration of large bone defects in orthopedic surgery. However, due to the physiological and anatomical differences between humans and different animal species for bone regeneration, future studies in more relevant large animal models and clinical trials will be needed to maximize the clinical efficacy of PTH/BMP-2 combination therapies.[31, 32]

References

1. Wozney, J.M. Overview of bone morphogenetic proteins. Spine 27, S2, 2002.
2. Burkus, J.K., Transfeldt, E.E., Kitchel, S.H., Watkins, R.G., and Balderston, R.A. Clinical and radiographic outcomes of anterior lumbar interbody fusion using recombinant human bone morphogenetic protein-2. Spine 27, 2396, 2002.
3. Friedlaender, G.E., Perry, C.R., Cole, J.D., Cook, S.D., Cierny, G., Muschler, G.F., Zych, G.A., Calhoun, J.H., LaForte, A.J., and Yin, S. Osteogenic protein-1 (bone morphogenetic protein-7) in the treatment of tibial nonunions. J Bone Joint Surg Am 83-A Suppl 1, S151, 2001.
4. Govender, S., Csimma, C., Genant, H.K., Valentin-Opran, A., Amit, Y., Arbel, R., Aro, H., Atar, D., Bishay, M., Borner, M.G., Chiron, P., Choong, P., Cinats, J., Courtenay, B., Feibel, R., Geulette, B., Gravel, C., Haas, N., Raschke, M., Hammacher, E., van der Velde, D., Hardy, P., Holt, M., Josten, C., Ketterl, R.L., Lindeque, B., Lob, G., Mathevon, H., McCoy, G., Marsh, D., Miller, R., Munting, E., Oevre, S., Nordsletten, L., Patel, A., Pohl, A., Rennie, W., Reynders, P., Rommens, P.M., Rondia, J., Rossouw, W.C., Daneel, P.J., Ruff, S., Ruter, A., Santavirta, S., Schildhauer, T.A., Gekle, C., Schnettler, R., Segal, D., Seiler, H., Snowdowne, R.B., Stapert, J., Taglang, G., Verdonk, R., Vogels, L., Weckbach, A., Wentzensen, A., and Wisniewski, T. Recombinant human bone morphogenetic protein-2 for treatment of open tibial fractures: a prospective, controlled, randomized study of four hundred and fifty patients. J Bone Joint Surg Am 84-A, 2123, 2002.
5. Lotinun, S., Sibonga, J.D., and Turner, R.T. Differential effects of intermittent and continuous administration of parathyroid hormone on bone histomorphometry and gene expression. Endocrine 17, 29, 2002.

6. Qin, L., Raggatt, L.J., and Partridge, N.C. Parathyroid hormone: a double-edged sword for bone metabolism. Trends Endocrinol Metab 15, 60, 2004.
7. Neer, R.M., Arnaud, C.D., Zanchetta, J.R., Prince, R., Gaich, G.A., Reginster, J.Y., Hodsman, A.B., Eriksen, E.F., Ish-Shalom, S., Genant, H.K., Wang, O., and Mitlak, B.H. Effect of parathyroid hormone (1-34) on fractures and bone mineral density in postmenopausal women with osteoporosis. N Engl J Med 344, 1434, 2001.
8. Horiuchi, H., Saito, N., Kinoshita, T., Wakabayashi, S., Tsutsumimoto, T., Otsuru, S., and Takaoka, K. Enhancement of recombinant human bone morphogenetic protein-2 (rhBMP-2)-induced new bone formation by concurrent treatment with parathyroid hormone and a phosphodiesterase inhibitor, pentoxifylline. J Bone Miner Metab 22, 329, 2004.
9. Kabasawa, Y., Asahina, I., Gunji, A., and Omura, K. Administration of parathyroid hormone, prostaglandin E2, or 1-alpha,25-dihydroxyvitamin D3 restores the bone inductive activity of rhBMP-2 in aged rats. DNA Cell Biol 22, 541, 2003.
10. Kempen, D.H., Lu, L., Hefferan, T.E., Creemers, L.B., Maran, A., Classic, K.L., Dhert, W.J., and Yaszemski, M.J. Retention of *in vitro* and *in vivo* BMP-2 bioactivities in sustained delivery vehicles for bone tissue engineering. Biomaterials 29, 3245, 2008.
11. Kempen, D.H., Lu, L., Heijink, A., Hefferan, T.E., Creemers, L.B., Maran, A., Yaszemski, M.J., and Dhert, W.J. Effect of local sequential VEGF and BMP-2 delivery on ectopic and orthotopic bone regeneration. Biomaterials 30, 2816, 2009.
12. Kempen, D.H., Yaszemski, M.J., Heijink, A., Hefferan, T.E., Creemers, L.B., Britson, J., Maran, A., Classic, K.L., Dhert, W.J., and Lu, L. Non-invasive monitoring of BMP-2 retention and bone formation in composites for bone tissue engineering using SPECT/CT and scintillation probes. J Control Release 134, 169, 2009.
13. Wang, S., Lu, L., and Yaszemski, M.J. Bone-tissue-engineering material poly(propylene fumarate): correlation between molecular weight, chain dimensions, and physical properties. Biomacromolecules 7, 1976, 2006.
14. Oldham, J.B., Lu, L., Zhu, X., Porter, B.D., Hefferan, T.E., Larson, D.R., Currier, B.L., Mikos, A.G., and Yaszemski, M.J. Biological activity of rhBMP-2 released from PLGA microspheres. J Biomech Eng 122, 289, 2000.
15. Kempen, D.H., Kruyt, M.C., Lu, L., Wilson, C.E., Florschutz, A.V., Creemers, L.B., Yaszemski, M.J., and Dhert, W.J. Effect of autologous bone marrow stromal cell seeding and bone morphogenetic protein-2 delivery on ectopic bone formation in a microsphere/poly(propylene fumarate) composite. Tissue Eng Part A 15, 587, 2009.
16. Yamamoto, M., Tabata, Y., Hong, L., Miyamoto, S., Hashimoto, N., and Ikada, Y. Bone regeneration by transforming growth factor beta1 released from a biodegradable hydrogel. J Control Release 64, 133, 2000.
17. Yamamoto, M., Takahashi, Y., and Tabata, Y. Controlled release by biodegradable hydrogels enhances the ectopic bone formation of bone morphogenetic protein. Biomaterials 24, 4375, 2003.
18. Jorgensen, S.M., Demirkaya, O., and Ritman, E.L. Three-dimensional imaging of vasculature and parenchyma in intact rodent organs with X-ray micro-CT. Am J Physiol 275, H1103, 1998.
19. Dobnig, H., and Turner, R.T. Evidence that intermittent treatment with parathyroid hormone increases bone formation in adult rats by activation of bone lining cells. Endocrinology 136, 3632, 1995.
20. Jilka, R.L., Weinstein, R.S., Bellido, T., Roberson, P., Parfitt, A.M., and Manolagas, S.C. Increased bone formation by prevention of osteoblast apoptosis with parathyroid hormone. J Clin Invest 104, 439, 1999.
21. Leaffer, D., Sweeney, M., Kellerman, L.A., Avnur, Z., Krstenansky, J.L., Vickery, B.H., and Caulfield, J.P. Modulation of osteogenic cell ultrastructure by RS-23581, an analog of human parathyroid hormone (PTH)-related peptide-(1-34), and bovine PTH-(1-34). Endocrinology 136, 3624, 1995.
22. Onyia, J.E., Bidwell, J., Herring, J., Hulman, J., and Hock, J.M. *In vivo*, human parathyroid hormone fragment (hPTH 1-34) transiently stimulates immediate early response gene expression, but not proliferation, in trabecular bone cells of young rats. Bone 17, 479, 1995.
23. Alkhiary, Y.M., Gerstenfeld, L.C., Krall, E., Westmore, M., Sato, M., Mitlak, B.H., and Einhorn, T.A. Enhancement of experimental fracture-healing by systemic administration of recombinant human parathyroid hormone (PTH 1-34). J Bone Joint Surg Am 87, 731, 2005.
24. Seebach, C., Skripitz, R., Andreassen, T.T., and Aspenberg, P. Intermittent parathyroid hormone (1-34) enhances mechanical strength and density of new bone after distraction osteogenesis in rats. J Orthop Res 22, 472, 2004.

25. Skripitz, R., Andreassen, T.T., and Aspenberg, P. Parathyroid hormone (1-34) increases the density of rat cancellous bone in a bone chamber. A dose-response study. J Bone Joint Surg Br 82, 138, 2000.
26. Skripitz, R., Andreassen, T.T., and Aspenberg, P. Strong effect of PTH (1-34) on regenerating bone: a time sequence study in rats. Acta Orthop Scand 71, 619, 2000.
27. Wang, E.A., Rosen, V., D'Alessandro, J.S., Bauduy, M., Cordes, P., Harada, T., Israel, D.I., Hewick, R.M., Kerns, K.M., LaPan, P., and et al. Recombinant human bone morphogenetic protein induces bone formation. Proc Natl Acad Sci U S A 87, 2220, 1990.
28. Wozney, J.M., Rosen, V., Celeste, A.J., Mitsock, L.M., Whitters, M.J., Kriz, R.W., Hewick, R.M., and Wang, E.A. Novel regulators of bone formation: molecular clones and activities. Science 242, 1528, 1988.
29. Hay, E., Lemonnier, J., Fromigue, O., and Marie, P.J. Bone morphogenetic protein-2 promotes osteoblast apoptosis through a Smad-independent, protein kinase C-dependent signaling pathway. J Biol Chem 276, 29028, 2001.
30. Morgan, E.F., Mason, Z.D., Bishop, G., Davis, A.D., Wigner, N.A., Gerstenfeld, L.C., and Einhorn, T.A. Combined effects of recombinant human BMP-7 (rhBMP-7) and parathyroid hormone (1-34) in metaphyseal bone healing. Bone 43, 1031, 2008.
31. Aerssens, J., Boonen, S., Lowet, G., and Dequeker, J. Interspecies differences in bone composition, density, and quality: potential implications for *in vivo* bone research. Endocrinology 139, 663, 1998.
32. Seeherman, H., Li, R., and Wozney, J. A review of preclinical program development for evaluating injectable carriers for osteogenic factors. J Bone Joint Surg Am 85-A Suppl 3, 96, 2003.

13

General discussion and future perspectives

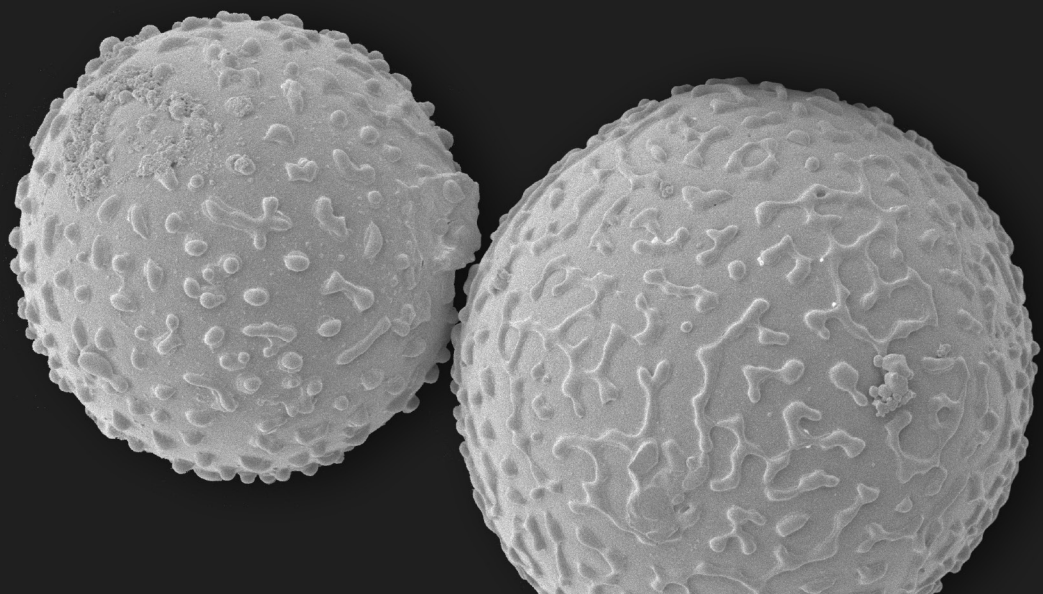

Growth factors and cytokines are crucial for the regulation of cell phenotype and thus are essential to guide tissue structure and function in bone regeneration strategies. The potential of growth factors in bone regeneration was already recognized with their discovery, as growth factor extracts from bone were able to induce ectopic bone formation upon implantation.[1,2] Since this osteoinductive activity was shown to be related to some of the BMPs, these growth factors started to dominate this field. Although the existence of BMPs was already discovered in the 1960s, translational research for clinical applications could not start until after the cloning of their respective genes, allowing for their mass production in the early 1990s. When the research project described in the current thesis started in 2001, the first clinical trials with BMPs had just been published.[3-11] Based on these results, BMP-7 obtained its humanitarian device exemption for long bone non-unions in October 2001 and BMP-2 its FDA pre-market approval for use in anterior lumbar interbody fusions in July 2002.[12,13] As clinical research progressed, additional FDA approvals for BMP-based products were obtained for intertransverse lumbar spinal fusion, posterolateral lumbar spine pseudoarthrosis, acute open tibial shaft fractures and maxillofacial sinus and alveolar ridge augmentations.[14-17] Apart from FDA-approved applications, off-label use has increased as well to an estimated 85% of procedures using BMPs.[18]

Despite more than a decade of clinical experience with BMPs, the results of many trials have been rather disappointing considering the impressive pre-clinical results in numerous animal models. Initially, the addition of BMP to unreamed intramedullary nail fixation in acute open tibial shaft fractures appeared more effective compared to unreamed nail fixation alone.[19] However, a recent large randomized clinical trial showed no additional effect of BMPs in open tibial fractures treated with reamed intramedullary nailing.[20] Furthermore, when they were applied in fracture non-unions, BMPs were not more effective compared to autograft.[19] Only in spinal fusion, BMPs seemed more effective compared to autograft bone in terms of spinal fusion which has resulted in a tremendous increase in their use from 0.7% to 25% of all spinal fusions from 2002 till 2006.[21,22] However, these industry-sponsored BMP-2 spinal fusion trials are currently under discussion due to possible study design bias, conflicts of interest, and underreporting of complications.[23,24] Moreover, in addition to the disappointing clinical effectivity of these BMP-based treatments, many serious complications associated with these new growth factor-based technologies have also emerged.[23,25]

Shortcomings of the current BMP-based treatments

The limited and heterogeneous evidence to support the clinical use of BMPs and increasing number of complications has several underlying causes that are partly related to the supraphysiologic dosages and use of inadequate delivery systems.[26-28] In current clinical applications, BMPs are delivered in collagen carriers at supraphysiologic dosages up to 40 mg.[29] To put this amount into perspective, 20,000 kg autograft bone would be required to obtain this single dose from bone matrix.[30] The collagen carrier used for clinical applications releases approximately 95% of these amounts within the first 14 days.[13,31-33] This is an enormous growth factor dose delivered in a very short time-frame, considering the slow up-regulation of BMPs in natural bone healing, which peaks at/after 21 days.[34-36] Furthermore, collagen sponges and powders by themselves function poorly as a graft material. During the FDA scientific discussion for approval of Osigraft in 2004, it was

already noticed that "healing of a critical size bone defect by collagen alone is unlikely" as "minimal bone formation is observed".[31] Overall, it seems that the current BMP-based treatments are characterized by inefficient use of the growth factor in insufficient delivery vehicles.

In addition to and indirectly resulting from the inefficient use of BMPs, many unwanted side effects have been noted in the course of the clinical trials. Some of these complications are directly related to the effects of BMPs on bone, such as uncontrolled bone formation or stimulated osteoclast activity resulting in osteolysis and graft subsidence.[25,37-40] Others are related to the multifaceted actions of BMPs, such as its induction of inflammation resulting in soft-tissue swelling, sterile cyst formation and radiculitis.[13,23,25,41-43]

Due to our limited knowledge of the pleiomorphic effects of BMPs, linking the possible side effects further away from the site of implantation to the growth factors still remains difficult. However, it is well known that BMPs are involved in many other processes throughout the body.[44] In the adult human being, BMP receptors are expressed in various organs including the brain, heart, pancreas, gastrointestinal tract, muscle, bone, kidneys and bladder, and BMPs have been shown to be involved in various processes and diseases, including for example Alzheimer, renal fibrosis, heart hypertrophy, diabetes, colorectal cancer and muscle dystrophy and osteoporosis. Although the initial biodistribution studies in animals showed a low systemic availability after its release from the implant, BMP exposure may be significant with the suprafysiologic human dosages considering an 82% recovery of an intravenously dose from the liver, lung, kidney and spleen within 1 minute after administration in animals.[13,45] Since BMPs can be considered as intrinsic stable proteins as they survived the original purification process from bone with removal of the mineral component with hydrochloric acid and processing in strong chaotrophic agents such as urea[46], many of the other organ systems expressing the BMP receptor may also be under the influence of the local BMP implants.

Indicative of these processes occurring away from the site of application has been the occurrence of several other adverse events that however could not be directly related to the BMP therapies yet. For example, there were 15 cancer events (12 different types of cancer) in 12 patients receiving 40 mg of BMP-2 (AMPLIFY™) for posterolateral fusion, as opposed to 5 cancer events in 5 patients in the control group receiving autograft.[47] Although the multiple cancer events in 2 patients were not taken into account, statistical analysis revealed a 94% probability that this may be product-related.[47] Therefore, future research should also further investigate these pleiomorphic effects since this information plays an essential role in obtaining more insight in possible adverse events and helps determine contraindications for future growth factor-based therapies in clinical applications.

Natural bone healing; a multifactorial and ill-described process

An increased understanding in the molecular coordination and cellular processes during natural bone healing may help to guide growth factor strategies for regenerative therapies. So far, we are only beginning to understand the regulation of bone healing. Investigation of the temporal and spatial growth factor expression during fracture healing and distraction osteogenesis has shown an abundance of growth factors and cytokines to

be involved in the inflammatory phase, soft or hard callus formation phases and remodeling phase of bone formation.[48,49] For some of the growth factors (e.g. IGF, TGF-β and PDGF), it has been possible to determine their local concentrations.[50,51] However, measuring the BMP concentrations at the tissue level still remains difficult due to the small quantities naturally produced and limited sensitivity of current assays.[50,51] Furthermore, the origin of the target cells, the molecular mechanisms involved in their chemotaxis and their moment of arrival in the fracture or distraction site are still not fully known. These are also important processes that may help decide the timing and release rate at which growth factors need to be delivered at a target site.
In addition to timing of growth factor release, it should be kept in mind that bone regeneration indeed is coordinated by multiple growth factors and cytokines, rather than one single factor such as BMP. The potency of orchestrated growth factor actions in bone regeneration was already demonstrated shortly after molecular cloning of BMPs by the fact that the amounts of recombinant BMP-2 required to induce *in vivo* bone formation were approximately 10 times higher compared to non-recombinant bovine bone extracts containing a mixture of proteins.[52,53] Also in *in vivo* studies described in this thesis many of the growth factor, cytokine and hormone combinations were more efficient compared to either of the proteins alone.[54-56] Whereas many of the molecular mechanisms involved in these growth factor interactions are already under investigation on a cellular level, translational research on their interactions at a tissue level is still in its infancy. Using composite delivery vehicles as presented in this thesis allowing for more complex sequential and adjustable release profiles will help to identify the effects of growth factor ratio, timing and release sequence of multiple growth factors and will help us increase our knowledge of the actions and interactions of growth factors in bone regeneration.

Growth factor delivery

Already shortly after their discovery, it was noticed that controlled local BMP delivery was essential to enhance their effect. In fracture models, the effect of percutaneous buffer-delivered growth factor injections remained limited to the first couple of days.[57,58] Although the implantation of protein extract from bone was sufficient to induce its ectopic regeneration, its reconstitution in a collagenous matrix enhanced its osteoinductive potential.[1]
In the course of pre-clinical studies evaluating the effective dose, it was noticed that not only the concentration but also the length of time that BMP was present at the implant site positively correlated with the rate of bone formation, the amount of bone formed and the density of the formed bone.[13] Consequently, controlled growth factor delivery has become an essential part of bone regeneration research. However, the ability to tailor *in vivo* BMP release from collagen was limited, as its release is independent of most collagen sponge characteristics.[59-61] Only an increase in crosslinking density of the collagen matrices allowed limited elongation of the BMP retention. However, above a certain crosslinking density, the osteoinductive capacity decreased as a result of impaired cell infiltration into the densely crosslinked matrix.[61-63]
Although the release profiles in the current treatments are obviously inappropriate, the optimal growth factor dose, release duration and required timing of release are still unknown. Few studies have characterized the *in vivo* growth factor release from delivery vehicles and its subsequent effect on bone formation (see "pharmacokinetics" section of chapter 2). Although optimizing these pharmacokinetic parameters is the first logical

step in improving growth factor therapies, this process will not be easy as many factors related to our interventions influence bone regeneration. Since alterations to the growth factors release rate often require changes to the scaffold structure or composition, these material changes will also influence bone formation. The use of composite formulation with polymer microspheres as growth factor delivery vehicles, as described in this thesis, may provide an important tool for the tailoring of growth factor release independent from the main scaffold properties. Whereas changes to the microsphere characteristics allow tailoring of the growth factor release, the main scaffold matrix component defining the overall structural and biochemical properties remain the same. As a result, differences in bone formation can be attributed more clearly to the growth factor pharmacokinetics. Since the microsphere properties dictated release, they may also be used the other way around. By keeping the microsphere characteristics and subsequent growth factor release the same, they may also help to compare extracellular matrix functions of different materials for bone regeneration. Overall, microsphere/biomaterial combinations are ideal candidates to further investigate the correlations between growth factor pharmacokinetics or material properties and bone formation.
To further optimize growth factor release and speed up carrier development, scientists should also make an effort to standardize their studies. Assessment and reporting of all scaffold characteristics and outcome parameters in a standardized way would facilitate future comparison of results from different studies. This includes reporting characteristics such a delivery vehicle dimensions, growth factor dosage and bone volume which will allow calculation of the bone volume per volume of scaffold or per microgram of the released growth factor to compare the osteoinductive capacity of the different formulations. Also the investigation of the growth factor release profiles is essential in these studies, as it provides more insight in local growth factor dosages over time. Through such a collaborative effort, it will eventually be possible to efficiently obtain more insight into the optimal growth factor pharmacokinetics for bone regeneration and the various effects related of our interventions.

Scaffolds as bone regeneration matrices

The therapeutic success of future bone regeneration strategies will also strongly depend on the appropriate local environment created by the scaffold matrix in addition to the scaffold's growth factor release properties. Despite the extensive use of collagen in (pre-) clinical BMP studies and various other clinical applications, the collagen sponges and powders as used until now provide minimal structural support and function poorly as a graft material.[31] Since cell behavior is determined by many biomaterial characteristics, such as biochemical composition, dimensionality or surface topography, it should also interact with the invading cells in such a way that it supports their adhesion, organization, proliferation, differentiation and extracellular matrix formation. Furthermore, cell and tissue fate will also be influenced by changes to the biomaterial upon implantation as a result of protein absorption, cellular actions or biodegradation. Since so many material factors influence the tissue regeneration process, choosing the appropriate biomaterial and designing a growth factor-delivering scaffold for clinical applications remains extremely difficult.
Optimization of all these scaffold parameters with the plethora of materials available and virtually endless number of possible combinations or blends will be an enormous task.

One of the ways to tackle this problem, is to make use of the introduction of emerging new high-throughput screening technologies such as microarrays.[64-66] Using this technology, over 2000 individual materials and material blends can be analyzed and compared *in vitro* for their potency to evoke cell responses such as adherence and proliferation. Subsequently, they allow rapid identification of optimal biocompatible and biomimetic substrates and help design material blends which capture the benefits of each individual material. This helps to efficiently guide material choices towards their implementation into translational research. In addition to these *in vitro* technologies, standardization of *in vivo* research may further allow identification of the optimal biomaterials as scaffolds. Eventually, this will accelerate delivery vehicle design for future clinical applications.

Conclusions

Overall, this thesis took a first step forward by highlighting the potential of polymers to control growth factor release at the target site. However, various aspects of bone regeneration still need to be addressed in order to make growth factor-based treatment for bone regeneration feasible and safe. The recent discussion on safety aspect of the current BMP-based therapies should warn clinicians to be reluctant in using current products in clinical applications. Perhaps the safety issues even may result in withdrawal of current BMP-based therapies with supraphysiologic dosages from the market. Due to a limited understanding of their biological actions and a too rapid marketing of new BMP-based therapies with inefficient growth factor application, insufficient delivery vehicles and serious product-related adverse events, growth factor-based bone regeneration is still under heavy pressure. However, considering their tremendous therapeutic potential, we should not abandon the possibility of applying growth factors in future clinical applications. The challenge facing researchers today is to optimize growth factor delivery, lowering the growth factor dosage and to create the appropriate local environment for bone regeneration within the delivery vehicle. Eventually, this will ensure that patients can safely benefit from these new bone regeneration strategies in future clinical applications. Although this sounds straightforward, this still is an enormous task considering the complexity bone formation itself and the influence of numerous aspects related to our interventions.

References

1. Sampath, T.K., and Reddi, A.H. Dissociative extraction and reconstitution of extracellular matrix components involved in local bone differentiation. Proc Natl Acad Sci U S A 78, 7599, 1981.
2. Urist, M.R. Bone: formation by autoinduction. Science 150, 893, 1965.
3. Boden, S.D., Zdeblick, T.A., Sandhu, H.S., and Heim, S.E. The use of rhBMP-2 in interbody fusion cages. Definitive evidence of osteoinduction in humans: a preliminary report. Spine (Phila Pa 1976) 25, 376, 2000.
4. Boyne, P.J., Marx, R.E., Nevins, M., Triplett, G., Lazaro, E., Lilly, L.C., Alder, M., and Nummikoski, P. A feasibility study evaluating rhBMP-2/absorbable collagen sponge for maxillary sinus floor augmentation. Int J Periodontics Restorative Dent 17, 11, 1997.
5. Cochran, D.L., Jones, A.A., Lilly, L.C., Fiorellini, J.P., and Howell, H. Evaluation of recombinant human bone morphogenetic protein-2 in oral applications including the use of endosseous implants: 3-year results of a pilot study in humans. J Periodontol 71, 1241, 2000.

6. Friedlaender, G.E., Perry, C.R., Cole, J.D., Cook, S.D., Cierny, G., Muschler, G.F., Zych, G.A., Calhoun, J.H., LaForte, A.J., and Yin, S. Osteogenic protein-1 (bone morphogenetic protein-7) in the treatment of tibial nonunions. J Bone Joint Surg Am 83-A Suppl 1, S151, 2001.
7. Geesink, R.G., Hoefnagels, N.H., and Bulstra, S.K. Osteogenic activity of OP-1 bone morphogenetic protein (BMP-7) in a human fibular defect. J Bone Joint Surg Br 81, 710, 1999.
8. Groeneveld, E.H., van den Bergh, J.P., Holzmann, P., ten Bruggenkate, C.M., Tuinzing, D.B., and Burger, E.H. Histomorphometrical analysis of bone formed in human maxillary sinus floor elevations grafted with OP-1 device, demineralized bone matrix or autogenous bone. Comparison with non-grafted sites in a series of case reports. Clin Oral Implants Res 10, 499, 1999.
9. Howell, T.H., Fiorellini, J., Jones, A., Alder, M., Nummikoski, P., Lazaro, M., Lilly, L., and Cochran, D. A feasibility study evaluating rhBMP-2/absorbable collagen sponge device for local alveolar ridge preservation or augmentation. Int J Periodontics Restorative Dent 17, 124, 1997.
10. Riedel, G.E., and Valentin-Opran, A. Clinical evaluation of rhBMP-2/ACS in orthopedic trauma: a progress report. Orthopedics 22, 663, 1999.
11. van den Bergh, J.P., ten Bruggenkate, C.M., Groeneveld, H.H., Burger, E.H., and Tuinzing, D.B. Recombinant human bone morphogenetic protein-7 in maxillary sinus floor elevation surgery in 3 patients compared to autogenous bone grafts. A clinical pilot study. J Clin Periodontol 27, 627, 2000.
12. United States Food and Drug Administration Humanitarian Device Exemption OP-1 for recalcitrant long bone nonunions (H010002). http://www.accessdata.fda.gov/cdrh_docs/pdf/H010002b.pdf, 2001.
13. United States Food and Drug Administration Premarket Approval Application INFUSE Bone Graft/LT-Cage Lumbar Tapered Fusion Device for anterior lumbar interbody fusion (P000058). http://www.accessdata.fda.gov/cdrh_docs/pdf/P000058b.pdf, 2002.
14. United States Food and Drug Administration Humanitarian Device Exemption OP-1 Putty for revision posterolateral (intertransverse) lumbar spinal fusion (H020008). http://www.accessdata.fda.gov/cdrh_docs/pdf2/H020008b.pdf, 2004.
15. United States Food and Drug Administration Premarket Approval Application INFUSE Bone Graft for acute, open tibial shaft fractures (P000054 & P050053). http://www.accessdata.fda.gov/cdrh_docs/pdf/P000054b.pdf, 2004.
16. United States Food and Drug Administration Premarket Approval Application INFUSE Bone Graft for sinus augmentations and localized alveolar ridge augmentations (P050053). http://www.accessdata.fda.gov/cdrh_docs/pdf5/P050053b.pdf, 2007.
17. United States Food and Drug Administration Humanitarian Device Exemption INFUSE/MASTERGRAFT Posterolateral revision device for symptomatic, posterolateral lumbar spine pseudarthrosis. http://www.accessdata.fda.gov/cdrh_docs/pdf4/H040004b.pdf, 2008.
18. Ong, K.L., Villarraga, M.L., Lau, E., Carreon, L.Y., Kurtz, S.M., and Glassman, S.D. Off-label use of bone morphogenetic proteins in the United States using administrative data. Spine 35, 1794, 2010.
19. Garrison, K.R., Shemilt, I., Donell, S., Ryder, J.J., Mugford, M., Harvey, I., Song, F., and Alt, V. Bone morphogenetic protein (BMP) for fracture healing in adults. Cochrane Database Syst Rev, CD006950, 2010.
20. Aro, H.T., Govender, S., Patel, A.D., Hernigou, P., Perera de Gregorio, A., Popescu, G.I., Golden, J.D., Christensen, J., and Valentin, A. Recombinant human bone morphogenetic protein-2: a randomized trial in open tibial fractures treated with reamed nail fixation. J Bone Joint Surg Am 93, 801, 2011.
21. Garrison, K.R., Donell, S., Ryder, J., Shemilt, I., Mugford, M., Harvey, I., and Song, F. Clinical effectiveness and cost-effectiveness of bone morphogenetic proteins in the non-healing of fractures and spinal fusion: a systematic review. Health Technol Assess 11, 1, 2007.
22. Cahill, K.S., Chi, J.H., Day, A., and Claus, E.B. Prevalence, complications, and hospital charges associated with use of bone-morphogenetic proteins in spinal fusion procedures. Jama 302, 58, 2009.
23. Carragee, E.J., Hurwitz, E.L., and Weiner, B.K. A critical review of recombinant human bone morphogenetic protein-2 trials in spinal surgery: emerging safety concerns and lessons learned. Spine J 11, 471, 2011.
24. Mirza, S.K. Commentary: Folly of FDA-approval studies for bone morphogenetic protein. Spine J 11, 495, 2011.
25. Benglis, D., Wang, M.Y., and Levi, A.D. A comprehensive review of the safety profile of bone morphogenetic protein in spine surgery. Neurosurgery 62, ONS423, 2008.

26. Baskin, D.S., Ryan, P., Sonntag, V., Westmark, R., and Widmayer, M.A. A prospective, randomized, controlled cervical fusion study using recombinant human bone morphogenetic protein-2 with the CORNERSTONE-SR allograft ring and the ATLANTIS anterior cervical plate. Spine (Phila Pa 1976) 28, 1219, 2003.
27. Boakye, M., Mummaneni, P.V., Garrett, M., Rodts, G., and Haid, R. Anterior cervical discectomy and fusion involving a polyetheretherketone spacer and bone morphogenetic protein. J Neurosurg Spine 2, 521, 2005.
28. Dickerman, R.D., Reynolds, A.S., Morgan, B.C., Tompkins, J., Cattorini, J., and Bennett, M. rh-BMP-2 can be used safely in the cervical spine: dose and containment are the keys! Spine J 7, 508, 2007.
29. Dimar, J.R., 2nd, Glassman, S.D., Burkus, J.K., Pryor, P.W., Hardacker, J.W., and Carreon, L.Y. Clinical and radiographic analysis of an optimized rhBMP-2 formulation as an autograft replacement in posterolateral lumbar spine arthrodesis. J Bone Joint Surg Am 91, 1377, 2009.
30. Seeherman, H., Wozney, J., and Li, R. Bone morphogenetic protein delivery systems. Spine 27, S16, 2002.
31. Committee for Medicinal Products for Human Use, E.M.A. scienfitic discussion for the approval of Osigraft. http://www.emea.europa.eu/humandocs/PDFs/EPAR/osigraft/039301en6.pdf, 2004.
32. Seeherman, H., Li, R., and Wozney, J. A review of preclinical program development for evaluating injectable carriers for osteogenic factors. J Bone Joint Surg Am 85-A Suppl 3, 96, 2003.
33. Uludag, H., D'Augusta, D., Palmer, R., Timony, G., and Wozney, J. Characterization of rhBMP-2 pharmacokinetics implanted with biomaterial carriers in the rat ectopic model. J Biomed Mater Res 46, 193, 1999.
34. Cho, T.J., Gerstenfeld, L.C., and Einhorn, T.A. Differential temporal expression of members of the transforming growth factor beta superfamily during murine fracture healing. J Bone Miner Res 17, 513, 2002.
35. Groeneveld, E.H., and Burger, E.H. Bone morphogenetic proteins in human bone regeneration. Eur J Endocrinol 142, 9, 2000.
36. Niikura, T., Hak, D.J., and Reddi, A.H. Global gene profiling reveals a downregulation of BMP gene expression in experimental atrophic nonunions compared to standard healing fractures. J Orthop Res 24, 1463, 2006.
37. Pradhan, B.B., Bae, H.W., Dawson, E.G., Patel, V.V., and Delamarter, R.B. Graft resorption with the use of bone morphogenetic protein: lessons from anterior lumbar interbody fusion using femoral ring allografts and recombinant human bone morphogenetic protein-2. Spine (Phila Pa 1976) 31, E277, 2006.
38. Vaidya, R., Carp, J., Sethi, A., Bartol, S., Craig, J., and Les, C.M. Complications of anterior cervical discectomy and fusion using recombinant human bone morphogenetic protein-2. Eur Spine J 16, 1257, 2007.
39. Vaidya, R., Weir, R., Sethi, A., Meisterling, S., Hakeos, W., and Wybo, C.D. Interbody fusion with allograft and rhBMP-2 leads to consistent fusion but early subsidence. J Bone Joint Surg Br 89, 342, 2007.
40. Helgeson, M.D., Lehman, R.A., Jr., Patzkowski, J.C., Dmitriev, A.E., Rosner, M.K., and Mack, A.W. Adjacent vertebral body osteolysis with bone morphogenetic protein use in transforaminal lumbar interbody fusion. Spine J 11, 507, 2011.
41. Dmitriev, A.E., Lehman, R.A., Jr., and Symes, A.J. Bone morphogenetic protein-2 and spinal arthrodesis: the basic science perspective on protein interaction with the nervous system. Spine J 11, 500, 2011.
42. Glassman, S.D., Gum, J.L., Crawford, C.H., 3rd, Shields, C.B., and Carreon, L.Y. Complications with recombinant human bone morphogenetic protein-2 in posterolateral spine fusion associated with a dural tear. Spine J 11, 522, 2011.
43. Poynton, A.R., and Lane, J.M. Safety profile for the clinical use of bone morphogenetic proteins in the spine. Spine (Phila Pa 1976) 27, S40, 2002.
44. Wagner, D.O., Sieber, C., Bhushan, R., Borgermann, J.H., Graf, D., and Knaus, P. BMPs: from bone to body morphogenetic proteins. Sci Signal 3, mr1, 2010.
45. United States Food and Drug Administration Summary Minutes, Meeting of the Orthopaedics and Rehabilitation Devices Advisory Panel, January 10, 2002. http://www.fda.gov/ohrms/dockets/ac/02/minutes/3828m1.pdf, 2002.
46. Wozney, J.M. Overview of bone morphogenetic proteins. Spine 27, S2, 2002.

47. United States Food and Drug Administration Executive Summary for P050036 Metronic's AMPLIFY rhBMP-2 matrix, Orthopaedic and Rehabilitation Devices Advisory Panel, July 27, 2010. http://www.fda.gov/downloads/AdvisoryCommittees/CommitteesMeetingMaterials/MedicalDevices/MedicalDevicesAdvisoryCommittee/OrthopaedicandRehabilitationDevicePanel/UCM220079.pdf, 2010.
48. Ai-Aql, Z.S., Alagl, A.S., Graves, D.T., Gerstenfeld, L.C., and Einhorn, T.A. Molecular mechanisms controlling bone formation during fracture healing and distraction osteogenesis. J Dent Res 87, 107, 2008.
49. Tsiridis, E., Upadhyay, N., and Giannoudis, P. Molecular aspects of fracture healing: which are the important molecules? Injury 38 Suppl 1, S11, 2007.
50. Giannoudis, P.V., Pountos, I., Morley, J., Perry, S., Tarkin, H.I., and Pape, H.C. Growth factor release following femoral nailing. Bone 42, 751, 2008.
51. Schmidmaier, G., Herrmann, S., Green, J., Weber, T., Scharfenberger, A., Haas, N.P., and Wildemann, B. Quantitative assessment of growth factors in reaming aspirate, iliac crest, and platelet preparation. Bone 39, 1156, 2006.
52. Wang, E.A., Rosen, V., Cordes, P., Hewick, R.M., Kriz, M.J., Luxenberg, D.P., Sibley, B.S., and Wozney, J.M. Purification and characterization of other distinct bone-inducing factors. Proc Natl Acad Sci U S A 85, 9484, 1988.
53. Wang, E.A., Rosen, V., D'Alessandro, J.S., Bauduy, M., Cordes, P., Harada, T., Israel, D.I., Hewick, R.M., Kerns, K.M., LaPan, P., and et al. Recombinant human bone morphogenetic protein induces bone formation. Proc Natl Acad Sci U S A 87, 2220, 1990.
54. Kempen, D.H., Creemers, L.B., Alblas, J., Lu, L., Verbout, A.J., Yaszemski, M.J., and Dhert, W.J. Growth factor interactions in bone regeneration. Tissue Eng Part B Rev 16, 551, 2010.
55. Luo, T., Zhang, W., Shi, B., Cheng, X., and Zhang, Y. Enhanced bone regeneration around dental implant with bone morphogenetic protein 2 gene and vascular endothelial growth factor protein delivery. Clin Oral Implants Res, 2011.
56. Ratanavaraporn, J., Furuya, H., Kohara, H., and Tabata, Y. Synergistic effects of the dual release of stromal cell-derived factor-1 and bone morphogenetic protein-2 from hydrogels on bone regeneration. Biomaterials 32, 2797, 2011.
57. Blokhuis, T.J., den Boer, F.C., Bramer, J.A., Jenner, J.M., Bakker, F.C., Patka, P., and Haarman, H.J. Biomechanical and histological aspects of fracture healing, stimulated with osteogenic protein-1. Biomaterials 22, 725, 2001.
58. den Boer, F.C., Bramer, J.A., Blokhuis, T.J., Van Soest, E.J., Jenner, J.M., Patka, P., Bakker, F.C., Burger, E.H., and Haarman, H.J. Effect of recombinant human osteogenic protein-1 on the healing of a freshly closed diaphyseal fracture. Bone 31, 158, 2002.
59. Friess, W., Uludag, H., Foskett, S., Biron, R., and Sargeant, C. Characterization of absorbable collagen sponges as rhBMP-2 carriers. Int J Pharm 187, 91, 1999.
60. Uludag, H., Friess, W., Williams, D., Porter, T., Timony, G., D'Augusta, D., Blake, C., Palmer, R., Biron, B., and Wozney, J. rhBMP-collagen sponges as osteoinductive devices: effects of *in vitro* sponge characteristics and protein pI on *in vivo* rhBMP pharmacokinetics. Ann N Y Acad Sci 875, 369, 1999.
61. Yamamoto, M., Takahashi, Y., and Tabata, Y. Controlled release by biodegradable hydrogels enhances the ectopic bone formation of bone morphogenetic protein. Biomaterials 24, 4375, 2003.
62. Yamamoto, M., Kato, K., and Ikada, Y. Effect of the structure of bone morphogenetic protein carriers on ectopic bone regeneration. Tissue Eng 2, 315, 1996.
63. Yamamoto, M., Tabata, Y., Hong, L., Miyamoto, S., Hashimoto, N., and Ikada, Y. Bone regeneration by transforming growth factor beta1 released from a biodegradable hydrogel. J Control Release 64, 133, 2000.
64. Hay, D.C., Pernagallo, S., Diaz-Mochon, J.J., Medine, C.N., Greenhough, S., Hannoun, Z., Schrader, J., Black, J.R., Fletcher, J., Dalgetty, D., Thompson, A.I., Newsome, P.N., Forbes, S.J., Ross, J.A., Bradley, M., and Iredale, J.P. Unbiased screening of polymer libraries to define novel substrates for functional hepatocytes with inducible drug metabolism. Stem Cell Res 6, 92, 2011.
65. Khan, F., Tare, R.S., Kanczler, J.M., Oreffo, R.O., and Bradley, M. Strategies for cell manipulation and skeletal tissue engineering using high-throughput polymer blend formulation and microarray techniques. Biomaterials 31, 2216, 2010.
66. Zhang, R., Liberski, A., Sanchez-Martin, R., and Bradley, M. Microarrays of over 2000 hydrogels--identification of substrates for cellular trapping and thermally triggered release. Biomaterials 30, 6193, 2009.

14

Summary

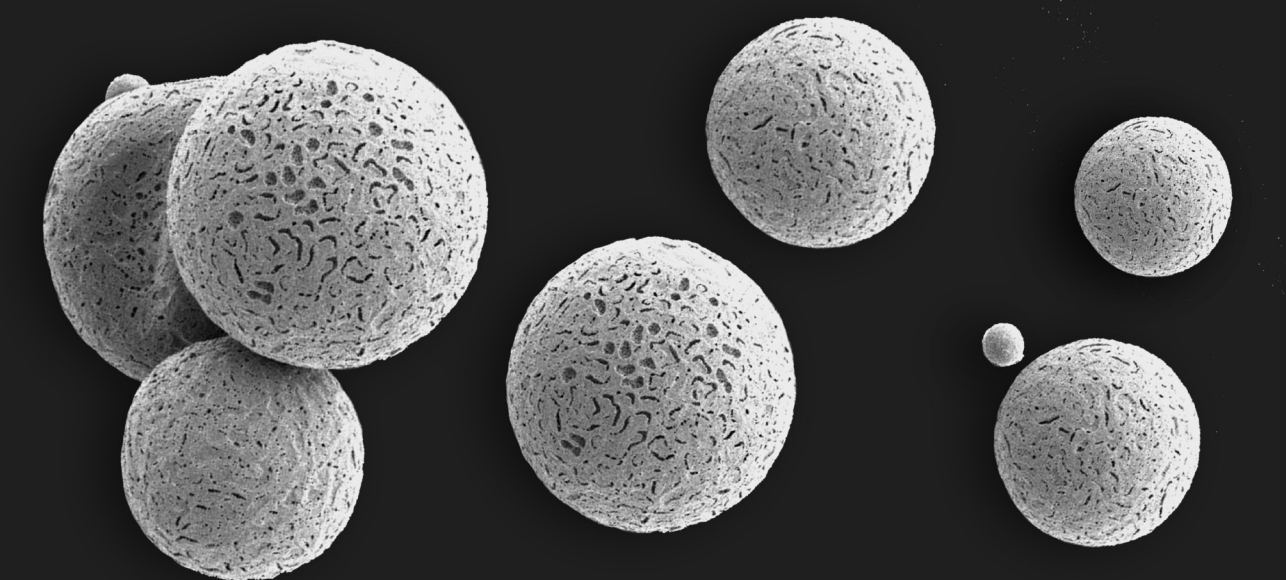

Summary

The field of bone tissue engineering provides a promising strategy to repair and regenerate lost bone tissue. The concept of bone tissue engineering is commonly based on 3 components and consists of 1) a three-dimensional matrix, 2) cells and 3) growth factors. The three dimensional scaffold plays a central role in the regenerative strategy since it can provide mechanical strength, a delivery matrix for growth factors and a framework for cell proliferation and bone tissue formation. The cells are responsible for the matrix deposition that precedes ossification and can be locally recruited after implantation or seeded onto the scaffold before implantation. Pivotal in bone regeneration will be the ability to deliver appropriate growth factors from the matrix in a controlled fashion to modulate cellular function and direct tissue formation towards bone. This chapter summarizes the studies that were performed for this thesis to integrate a delivery system and scaffold to improve the pharmacokinetic profile and biologic response of growth factors.

The studies in the first part concentrate on the development of a polymeric composite, which can serve as a delivery vehicle for growth factors and a scaffold for bone formation. Most scaffolds in this thesis are based on the cross-linkable, biodegradable polymer poly(propylene fumarate) (PPF). When combined with a cross-linker, PPF forms an injectable paste that can be polymerized into a mechanically strong scaffold. Due to the unfavorable conditions during scaffold polymerization, growth factors incorporated into the scaffold matrix during this reaction will likely lose their bioactivity. Although absorption of growth factors after scaffold manufacturing is possible, this method provides little possibilities to tailor the growth factor pharmacokinetics. Therefore, biodegradable polymer microspheres were incorporated into the scaffold and served as local delivery vehicles while maintaining injectability of the PPF paste. The microsphere matrix protects the proteins from destructive environmental conditions during te cross-linking reaction. In a pilot study, we first studied the effect of the incorporation of conventional poly(lactic-co-glycolic acid) (PLGA) microspheres into a PPF scaffold on the release profile of a model drug Texas red dextran and the compressive modulus of the scaffold matrix.[1] The resulting microsphere/PPF composite was capable of releasing a model drug in a sustained fashion over a prolonged period of time. Although the conventional PLGA microspheres could be physically entrapped in the PPF scaffold, the incorporation of the microspheres decreased the compressive modulus of the PPF scaffold.

To improve the immobilization of the microspheres and the composite's mechanical properties, new PPF and PPF/PLGA blend microspheres were developed (**chapters 2 and 3**). These microspheres could be covalently bound to the scaffold by cross-linking the carbon-carbon double bonds of PPF in the microspheres and the scaffold. During their development, the effects of various fabrication parameters on important microsphere properties such as morphology, size, drug entrapment efficiency and release were investigated. Overall, these studies showed that microsphere characteristics and release profiles could be modulated by varying the fabrication parameters and that all microsphere formulations degraded by a bulk degradation mechanism, with slower degradation as the PPF content in the blend increased. Identification of the effects of the fabrication parameters on microsphere characteristics did not only prove useful for the development of PPF/PLGA blend microspheres but could also be applied to adjust the microsphere characteristics from other synthetic polymeric materials.

The effects of PPF/PLGA microsphere incorporation on the mechanical properties of a PPF scaffold and drug release kinetics from the composite were studied in **chapter 4**. Pure PLGA and pure PPF microspheres were used for this study. Both microsphere/scaffold composites exhibited a sustained release of the model drug for at least 28 days and displayed a minimal burst release during the initial phase, as compared to drug release from microspheres alone. Scaffolds containing PPF microspheres were characterized by a significantly higher initial compressive modulus than those containing PLGA microspheres, which was attributed to the interfacial covalent bonding between PPF microspheres and the PPF matrix.

Since previous studies were done using the model drug Texas red dextran, the second part of this thesis focuses on the incorporation of the osteoinductive growth factor bone morphogenetic protein-2 (BMP-2) into PLGA microsphere/scaffold composite and evaluation of its growth factor release and bioactivity. At the time of designing the implants for this study, the information from literature to predict the *in vivo* release profile was limited. Therefore, a slow degrading PLGA with a lactic to glycolic acid ratio of 75:25 and a molecular weight of 62 kDa was used for the microsphere fabrication in an attempt to release BMP-2 for a prolonged period of time. To maximize the BMP-2 binding capacity of our microspheres, acid end-capped PLGA was used as this is known to increase the binding capacity of the polymer. These BMP-2-loaded PLGA microspheres were incorporated into a PPF scaffold and the composite's *in vitro* release and *in vivo* bone forming capacity was tested in an ectopic implantation site in goats (**chapter 5**). The composites were loaded with 3 different microsphere formulations (0, 0.08 or 8 µg BMP-2/mg microspheres) or impregnated with a BMP-2 solution and were combined with either plasma (no cells) or culture-expanded bone marrow stromal cells (BMSCs) in plasma. *In vitro* release showed that incorporation of BMP-2-loaded microspheres in the scaffold resulted in a more sustained *in vitro* release with a lower burst phase, as compared to BMP-2-impregnated scaffolds. *In vivo*, BMP-2-impregnated scaffolds and composites loaded with 0 and 0.08 µg BMP-2 per mg of microspheres failed to induce bone formation at a subcutaneous implantation site. However, ectopic bone formation was seen in the pores of the composites loaded with 8 µg BMP-2 per mg microspheres. This study clearly shows feasibility of bone induction by BMP-2 release from microspheres/scaffold composites, although the amount of bone in the composites was too low to be clinically significant. Moreover, peroperatively seeded autologous BMSCs on the composites had no significant effect on ectopic bone formation. Despite the low amount of bone in composites loaded with the high BMP-2 dose, several important observations were done during the work described in **chapter 5** which suggested that local *in vivo* BMP-2 concentrations might have been insufficient in the early phase of implantation to induce bone formation. *In vitro*, the composites released less than 2.5 % of the incorporated BMP-2 within the first 24 days. Furthermore, histological analysis of the implanted composites showed large amounts of non-resorbed PLGA in the PPF matrix after 9 weeks of implantation, which may indicate a large quantity of retained BMP-2. Also fluorochrome analysis showed a late onset of bone mineralization, which most likely occurred between 7 and 9 weeks. This might suggest insufficient BMP-2 concentrations in the early days of implantation to induce bone formation and mineralization. Overall, all three observations suggest BMP-2 release was too slow from these microspheres.

Despite the mechanical advantages of the newly developed PPF and PPF/PLGA blend

microspheres, we could not immediately start using them in further experiments due to the need for a faster BMP-2 release. Since addition of PPF to the microsphere matrix results in slower degradation (**chapter 4**), growth factor release is expected to slow down even further when PPF/PLGA blend microspheres with similar polymer characteristics as in **chapters 3 and 4** were used. To increase the growth factor release at early time-points, we tested a faster degrading 23 kDa PLGA with a lactic to glycolic acid ratio of 50:50. In addition, we also experimented with the faster degrading hydrogels based on gelatin.

The choice for these materials was based on their *in vitro* ability to retain a growth factor within their matrix. This *in vitro* characterization was carried out using phosphate buffered saline as frequently done in investigations of release kinetics. Although this provides valuable information on protein binding and release mechanisms, extrapolating the data to the *in vivo* situation is not possible due to differences between both environments. Apart from *in vitro* and *in vivo* hydrolysis of the polymer matrix, cellular actions accelerate implant degradation *in vivo*. Furthermore, serum proteins might enhance desorption of bound growth factors. Since these *in vivo* events are difficult to mimic *in vitro*, characterization of the *in vivo* release kinetics is essential for the optimization of growth factor delivery vehicles. Therefore, we explored methods to characterize the *in vivo* pharmacokinetic profile by using radioactively labeled growth factors and nuclear medicine techniques for their detection. This approach has been applied frequently by determining the remaining activity of the tracer at sacrifice and comparing this with the activity prior to implantation. However, this requires a large number of animals to obtain a detailed release profile of multiple types of implants to compare different composites. In **chapter 6**, we investigated a non-invasive screening method based on scintillation probes to quantify the pharmacokinetics of a radio-labeled growth factor. First the influence of the source-to-probe distance and counting rate linearity were characterized to optimize the accuracy of the measurement setup. Since the *in vivo* situation rarely allows perfect parallel positioning of the probes, we also determined the interference of multiple sources on the background signal at increasing deviations from parallel probe positioning. In the second part, the scintillation probe setup was validated in a rat subcutaneous implantation model using 4 different ^{125}I-BMP-2-loaded implants. Comparison of the non-invasive method to the post-sacrifice method showed a good correlation between the measurements at the 2 time-points included.

In **chapter 7**, the scintillation probe setup was compared to a high-resolution single photon emission computed tomography/X-ray computed tomography (SPECT/CT) scanner for small animals. Both the scintillation probe setup and the SPECT/CT provided detailed release profiles at an ectopic and femoral defect implantation site with a good correlation between the measurement setups and no significant differences between the non-invasive and *ex vivo* analysis after 8 weeks of follow up. The non-invasive µCT imaging showed the onset and extent of bone formation at both locations over time. Since growth factor release usually precedes bone formation, simultaneous non-invasive monitoring of both events in the same animal over a prolonged period of time provided valuable information on the role of the growth factor during bone regeneration. Overall, these chapters show that both the scintillation probe setup and the SPECT/CT could be reliably applied as non-invasive screening tool to determine the *in vivo* protein release profiles of different implants in the same animal.

After exploring methods to measure the *in vivo* pharmacokinetics of the composite, we proceeded to determine the effect of prolonged growth factor retention on the stability/ bioactivity of the protein. Since radioactivity is not indicative for the chemical integrity of the growth factor, *in vitro* and *in vivo* biological tests remain necessary to test its biological actions and stability upon release. **Chapter 8** assessed both the *in vitro* and *in vivo* release and bioactivity of BMP-2 from 4 different sustained delivery vehicles over time. The delivery vehicles consisted of 1) a gelatin hydrogel, 2) PLGA microspheres embedded in a gelatin hydrogel, 3) PLGA microspheres embedded in a PPF scaffold and 4) PLGA microspheres embedded in a PPF scaffold surrounded by a gelatin hydrogel. *In vitro*, all 4 delivery vehicles released the BMP-2 in a sustained fashion over a 12-week period. Loss of bioactivity was found for BMP-2 released from gelatin implants after 6 weeks, while the BMP-2 released from the other implants continued to show bioactivity over the full 12-week period. Upon implantation, the release profile of the scaffold changed significantly. Although all scaffolds showed bone induction after 6 and 12 weeks of subcutaneous implantation in rats, ectopic BMP-2 osteoinductive capacity varied significantly among the delivery vehicles. Incorporation of BMP-2-loaded PLGA microspheres in the hydrophobic solid PPF matrix enhanced bone formation the most extensively.

The previous chapters describe the development of a composite polymer biomaterial and prolonged BMP-2 release with retention of growth factor bioactivity. However, bone regeneration involves a large number of growth factors and cytokines for its regulation which all interact to coordinate bone tissue formation. Therefore, the third section of this thesis focuses on the application of combinations of growth factors in bone regeneration. First, **chapter 9** provides an overview of the literature on the application of growth factor combinations in translational bone regeneration studies. Overall, many of these growth factors interact during bone formation, which results in an enhancement or inhibition of the regeneration process. Despite the limited number of studies, synergistic and additive effects are associated with most growth factor combinations, which highlight their tremendous potential for future clinical applications.

Two growth factor combinations gained our particular interest. The first combination consisted of vascular endothelial growth factor (VEGF) and BMPs. VEGF is a potent angiogenic growth factor, which induces vessel formation from the pre-existing vascular network. These vessels are crucial for sufficient nutrient supply and invasion of cells during bone repair. Given the importance of VEGF during osteogenesis, the combined release of BMP-2 and VEGF was studied in **chapter 10**. To mimic the natural VEGF and BMP-2 expression profile during normal bone formation, a composite consisting of BMP-2-loaded PLGA microspheres embedded in a PPF scaffold surrounded by a VEGF-loaded gelatin hydrogel was designed to sequentially deliver both growth factors with a rapid VEGF release in the first 2 weeks and a more sustained BMP-2 release over the full 8 week period. Upon ectopic implantation in rats, the local release of VEGF and BMP-2 was able to enhance angiogenesis and osteogenesis, respectively. Their combined delivery significantly increased bone formation compared to BMP-2 alone. Although the trend in orthotopic osteogenesis was similar to the effects in ectopic osteogenesis, here the combination of growth factors was not able to significantly enhance bone formation compared to an equal dose of BMP-2 alone.

The second combination that appears promising in bone regeneration is parathyroid hormone with BMPs. PTH is one of the major systemic regulators of bone metabolism and its anabolic properties after intermittent subcutaneous administration have made it particularly appealing for the treatment of patients with osteoporosis. In **chapter 11**, we explored the effect of local BMP-2 release in combination with intermittent subcutaneous PTH administration. As expected, BMP-2 alone was capable of inducing ectopic bone formation and almost complete healing of a femoral defect in rats. Despite its effect on bone mineral density of the rest of the skeleton (measured in the humerus and vertebra), intermittent PTH administration alone had no significant effect on bone formation in the ectopic and orthotopic implants. However, in combination with BMP-2, intermittent PTH administration significantly enhanced bone mineral density and bone volume in the composites at both implantation sites. This study clearly shows that a combination of systemically administered PTH in combination with a BMP-2 releasing construct also has great potential to enhance the local bone regeneration.

Overall, this thesis clearly highlights the potential of polymeric composites as growth factor delivering scaffolds for bone regeneration. It shows that polymeric microspheres can be used to locally deliver growth factors from the composite while maintaining their bioactivity. The diversity of physicochemical properties of polymers allows tailoring of the growth factor release profile from the delivery vehicle and the creation of a construct capable of releasing two growth factors independent from each other. These features provide the research community with excellent tools to identify the optimal amounts, ratio, timing and release sequence of various growth factors and will help optimizing the bone regeneration process to ensure consistent success for future clinical applications.

References

1. Kempen, D.H.R., Kim, C.W., Lu, L., Dhert, W.J.A., Currier, B.L., and Yaszemski, M.J. Controlled release from poly(lactic-co-glycolic acid) microspheres embedded in an injectable, biodegradable scaffold for bone tissue engineering. Materials Science Forum, 3151, 2003.

15

Nederlandse samenvatting

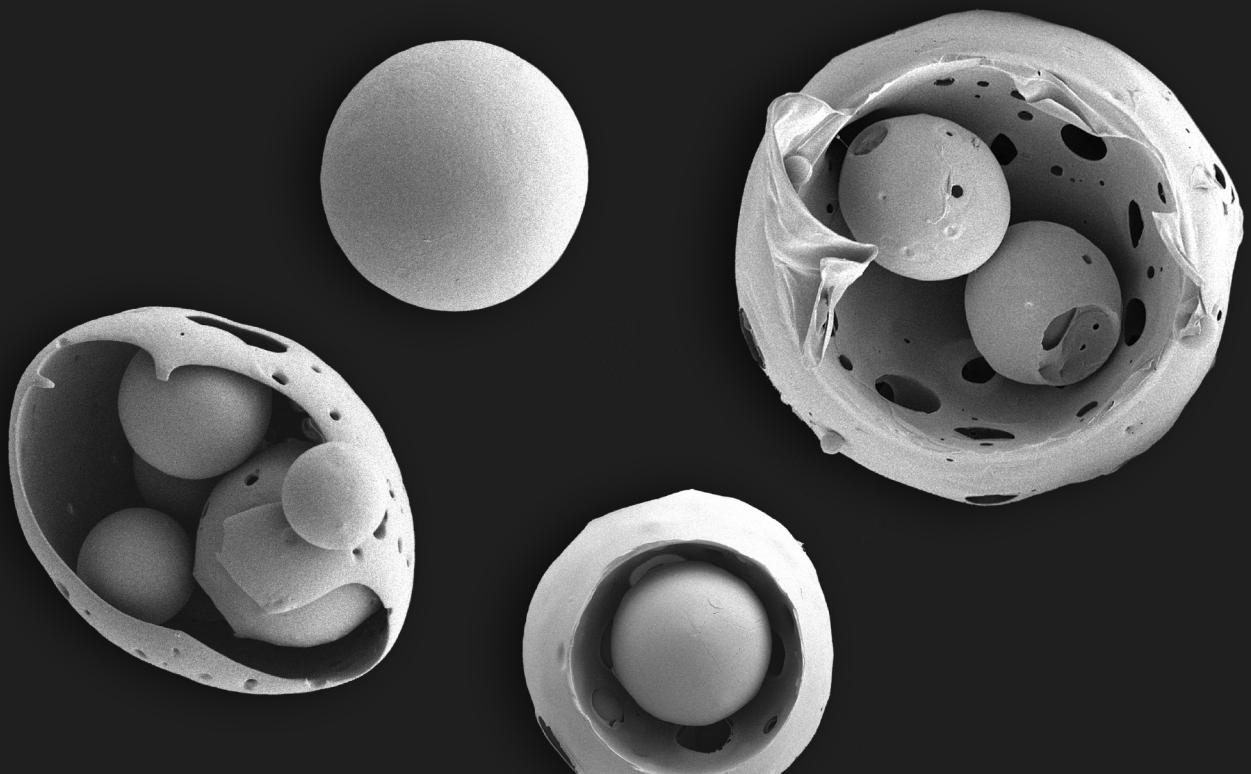

Samenvatting

Bot heeft, in tegenstelling tot verschillende andere typen weefsel, een zeer goed regeneratief vermogen. De meeste botbreuken of kleine botdefecten genezen dan ook zonder probleem bij een adequate behandeling. Slechts in enkele gevallen geneest een botbreuk of botdefect niet. Dit kan veroorzaakt worden door een inadequaat verlopend genezingsproces bijvoorbeeld door onvoldoende immobilisatie van de fractuurdelen of lokale doorbloedingsproblemen. Het kan echter ook zijn, dat er een botdefect is ontstaan, dat simpelweg te groot is om door een normaal verlopend genezingsproces overbrugd te worden. In dit soort gevallen wordt gebruik gemaakt van bottransplantaties om het regeneratieproces te stimuleren. Lichaamseigen bot wordt het meest frequent gebruikt aangezien dit alle drie de botsimulerende elementen bevat, namelijk: 1) een matrix die de botvorming geleid, 2) de cellen die bot vormen, 3) groeifactoren die botvorming stimuleren. Omdat lichaamseigen bot maar in beperkte mate kan worden weggenomen, wordt daarnaast gebruik gemaakt van donorbot van de botbank. Het voordeel van donorbot is, dat dit in grotere mate beschikbaar is. Het is echter niet zo goed als lichaamseigen bot en kan resulteren in overdracht van ziekten. Vanwege deze nadelen wordt binnen de regeneratieve geneeskunde gezocht naar alternatieven om botgenezing te stimuleren.

Bij de ontwikkeling van alternatieven voor bottransplantaties wordt gebruik gemaakt van de drie elementen die een rol spelen bij botgenezing. Biomaterialen spelen hierbij een centrale en multifunctionele rol, aangezien deze het botdefect opvullen en de mechanische stabiliteit bieden. Tevens moeten biomaterialen botvorming faciliteren en biologisch afbreekbaar zijn, zodat het lichaam ze kan vervangen door bot. Vanuit de matrix kunnen lokaal groeifactoren worden afgegeven, die bij botregeneratie betrokken zijn. Botvormende cellen kunnen op het materiaal worden gezaaid of lokaal worden gerekruteerd en zullen uiteindelijk het materiaal vervangen in lichaamseigen bot. Cruciaal in dit proces is echter een juiste afgifte van groeifactoren, die de cellulaire processen zo coördineren, dat het gevormde weefsel ook uiteindelijk bot wordt. De studies in dit proefschrift zijn erop gericht om een afgiftesysteem voor groeifactoren te integreren in een biomateriaal voor botregeneratie, zodat de afgifte van groeifactoren en hiermee gepaard gaande botvorming gereguleerd kunnen worden.

Het eerste deel van dit proefschrift richt zich op het ontwikkelen van een biomateriaal, dat botvorming faciliteert en waaruit groeifactoren gecontroleerd kunnen worden afgegeven. De meeste matrices in dit proefschrift zijn gebaseerd op het polymeer poly(propylene fumarate) (PPF). Dit polymeer kan worden gemengd met een crosslinker, waardoor het injecteerbaar wordt. De verschillende PPF moleculen worden door middel van een chemische reactie door de crosslinker onderling verbonden, waardoor de injecteerbare pasta uithardt tot een mechanisch sterke matrix. Omdat deze chemische reactie nadelige gevolgen kan hebben voor de biologische activiteit van groeifactoren, kunnen deze niet direct in de matrix worden geïncorporeerd. Derhalve worden de groeifactoren eerst geladen in micropartikels van ongeveer 2 tot 200 µm groot, die de groeifactoren beschermen tegen de nadelige gevolgen van de chemische reactie. Na toevoeging van de micropartikels aan de PPF pasta blijft deze injecteerbaar en door verschillende soorten micropartikels toe te voegen kan de afgifte van groeifactoren worden gevarieerd. In een eerste studie zijn conventionele micropartikels van polymelkzuur (PLGA) gebruikt. Deze studie toont aan dat deze micropartikels gemakkelijk kunnen worden geïncorporeerd

in de PPF matrix en dat ze in staat zijn een molecuul (Texas red dextran) met de grootte van een groeifactor geleidelijk af te geven gedurende minimaal 28 dagen. Het nadeel van deze conventionele micropartikels is echter, dat ze de mechanische aspecten van het biomateriaal beïnvloeden waardoor dit minder sterk wordt.

Om de immobilisatie van de micropartikels te verbeteren en het verlies in sterkte van de matrix te beperken, wordt de ontwikkeling van nieuwe PPF bevattende micropartikels in **hoofdstuk 2 en 3** beschreven. Deze micropartikels kunnen covalent worden gefixeerd in een PPF matrix door crosslinks tussen de PPF moleculen in de micropartikels en het biomateriaal. Tijdens de ontwikkeling van deze micropartikels zijn verschillende parameters in het fabricageproces gevarieerd om hun effect op aspecten als morfologie en grootte van de micropartikels te bekijken. Tevens is het effect op de efficiëntie van het incorporeren van Texas red dextran en de afgifte ervan bestudeerd. Beide hoofdstukken laten zien hoe de verschillende micropartikelaspecten en de daarmee samenhangende afgifteprofielen kunnen worden gevarieerd. Doordat PPF langzamer wordt afgebroken dan PLGA, resulteert toevoeging van PPF in een langzamere degeneratie van de micropartikels. In **hoofdstuk 4** wordt het effect van deze nieuwe PPF micropartikels op de mechanische aspecten van een PPF matrix en de afgifte van Texas red dextran vanuit het biomateriaal beschreven. Hierbij zijn de PPF micropartikels vergeleken met de conventionele PLGA micropartikels. Het molecuul Texas red dextran is vanuit de micropartikels in de biomaterialen gedurende een periode van minimaal 28 dagen afgegeven, waarbij het biomateriaal de initiële snelle afgifte van de micropartikels zelf reduceert. Hierdoor is de afgifte gelijkmatiger. De biomaterialen, die PPF micropartikels bevatten, hebben een significant hogere compressiemodulus vergeleken met de conventionele PLGA micropartikels. Deze verbetering wordt toegeschreven aan de mogelijkheid tot covalente bindingen tussen de PPF micropartikels en het PPF biomateriaal.

Nadat de ontwikkeling van de micropartikels en hun incorporatie in een PPF biomateriaal met Texas red dextran was bestudeerd, is in het tweede deel van dit proefschrift de groeifactor bone morphogenetic protein-2 (BMP-2) geïncorporeerd. Deze groeifactor is in staat botvorming te induceren en komt bij fractuur genezing normaliter tot expressie gedurende enkele weken. Daarom wordt in **hoofdstuk 5** gestreefd om BMP-2 vertraagd af te geven gedurende een periode van enkele weken. Omdat ten tijde van deze studie de BMP-2 afgifte uit de micropartikels slecht voorspelbaar was, is gekozen om de groeifactor te incorporeren in PLGA micropartikels. Hierover is enige informatie in de literatuur beschikbaar. Er is gekozen voor een langzaam afbrekende PLGA met een lactide-glycolide ratio van 75:25 en een molecuul gewicht van 62 kDa. Tevens is gekozen voor een PLGA met zo veel mogelijk carboxylgroepen om de bindingscapaciteit van PLGA voor BMP te vergroten en de afgifteduur te verlengen tot enkele weken. Er zijn drie soorten micropartikels gefabriceerd met een lading van 0, 0.08 en 8 µg BMP-2/mg micropartikels. Deze partikels zijn geïncorporeerd in een PPF biomateriaal. Vervolgens is de *in vitro* (buiten een lichaam) afgifte van BMP-2 uit het materiaal bestudeerd en is de *in vivo* (in een lichaam) botvormende capaciteit bestudeerd na onderhuidse implantatie in geiten. Aangezien dit een locatie is waar normaal gesproken geen botvorming plaatsvindt, is al het bot, dat onderhuids is gevormd, het gevolg van de interventie. Van de geïmplanteerde biomaterialen is een deel bezaaid met stromale beenmergcellen en het andere deel getest zonder cellen. In vergelijking met PPF matrices, die geïmpregneerd waren met BMP-2, toonden de matrices met micropartikels een langzamere en geleidelijkere afgifte van

BMP-2. Na verwijdering van de onderhuidse implantaten was er geen botvorming zichtbaar in de geïmpregneerde en 0 of 0.08 µg/mg micropartikels bevattende matrices. In de PPF matrices met de hoogste dosering BMP-2 (8 µg/mg micropartikels) was wel een kleine hoeveelheid bot gevormd. Hoewel deze hoeveelheid bot te klein is voor klinische toepassingen, toonde deze studie wel het voordeel van de BMP-2 geladen micropartikels in het biomateriaal ten opzichte van BMP-2 geïmpregneerde PPF matrices aan. Daarnaast is aangetoond, dat de stromale beenmergcellen op de matrices geen toegevoegd effect hadden op botvorming. Naast deze conclusies waren er ook aanwijzingen in deze studie dat de BMP-2 afgifte vanuit de micropartikel bevattende PPF matrices misschien wel te langzaam verliep. *In vitro* werd maar 2.5 % van de totale hoeveelheid groeifactor afgegeven gedurende de eerste 24 dagen. Ook tijdens de histologische analyse van de 9-weken geïmplanteerde matrices waren nog grote hoeveelheden PLGA zichtbaar, die nog niet geresorbeerd waren en derhalve nog BMP-2 konden bevatten. Analyse van de toegediende fluorochromen toonde aan, dat de aanvang van botvorming erg laat was en waarschijnlijk pas plaats heeft gevonden tussen week 7 en 9. Deze late aanvang kan het gevolg zijn van een te langzame BMP-2 afgifte, waardoor de concentratie BMP-2 te laag is gebleven om bot te kunnen induceren in de vroege fase na implantatie.

Om de afgifte van BMP-2 uit het biomateriaal te versnellen is in de vervolgstudies geëxperimenteerd met sneller biologisch afbreekbare polymeren. Hiervoor is gebruik gemaakt van PLGA met een lactide-glycolide ratio van 50:50 en een molecuul gewicht van 23 kDa en een hydrogel van gelatine. Door een snellere afbraak van het materiaal zal de groeifactor, die erin zit, waarschijnlijk sneller vrijkomen. Helaas was het niet direct mogelijk de nieuw ontwikkelde PPF bevattende micropartikels te gaan gebruiken, omdat in **hoofdstuk 3** al is aangetoond, dat toevoeging van PPF zal leiden tot een langzamere afbraak van de micropartikels. Hierdoor zal de afgifte van BMP-2 waarschijnlijk eerder verder vertraagd worden dan versneld. Omdat al deze materiaalkeuzes gebaseerd zijn op eerdere *in vitro* resultaten, was het ook noodzakelijk om meer inzicht te krijgen in de snelheid waarmee een groeifactor daadwerkelijk wordt afgegeven na implantatie. In de vorige studies is de afgifte in een reageerbuisje met een fysiologische zoutoplossing bekeken. Echter, dit is niet te vergelijken met *in vivo* waarbij bijvoorbeeld cellen kunnen helpen bij de afbraak van het polymeer of lichaamseiwitten kunnen helpen bij het versneld vrijkomen van de groeifactor. Omdat dit soort processen niet *in vitro* zijn na te bootsen, is gezocht naar een methode om de *in vivo* afgifte te kunnen meten. Vooralsnog is de enige methode die in de literatuur beschreven is, het radioactief labelen van groeifactoren. Door radioactiviteit te correleren aan de hoeveelheid groeifactor en deze voor en na implantatie te meten, kan de hoeveelheid afgegeven groeifactor worden berekend. In het verleden is dit meerdere malen gedaan, waarbij het proefdier echter werd opgeofferd. Om een gedetailleerd afgiftepatroon met meerdere tijdspunten te verkrijgen, zijn veel meetpunten nodig. Omdat dit een groot aantal proefdieren zou vergen, is in **hoofdstuk 6** een niet-invasieve methode getest, waarbij radioactiviteit gemeten wordt met een scintillatie detector. Allereerst is *in vitro* bepaald op welke afstand de detectoren van de radioactieve bron dienen te worden geplaatst en met welke hoeveelheid radioactiviteit een groeifactor moet worden gelabeld. Omdat meerdere implantaten in hetzelfde proefdier kunnen worden geplaatst, is ook gekeken of de nabijheid van een andere radioactieve bron de meting van een implantaat kan verstoren indien de detectoren niet parallel zijn geplaatst. Uiteindelijk werd de *in vivo* toepasbaarheid van de meetopstelling gevalideerd door vier verschillende ^{125}I-BMP-2 geladen implantaten onderhuids bij een

rat in te brengen. Tijdens deze validatie van de meetopzet was het mogelijk om de ^{125}I-BMP-2 afgifte uit de implantaten te bepalen. Daarbij was er een goede correlatie tussen de niet-invasief verrichte metingen en metingen verricht met de in het verleden gebruikte methode op 2 tijdstippen.

In **hoofdstuk 7** is de meetopzet met scintillatie detector vergeleken met een hoog resolutie SPECT/CT (single photon emission computed tomography/X-ray computed tomography) scanner. Dit keer werd één implantaat onderhuids geplaatst en een ander implantaat in een femur (bovenbeen) defect. Het was wederom mogelijk met beide methoden het afgifteprofiel van ^{125}I-BMP-2 te bepalen en er was wederom een goede correlatie tussen de metingen bepaald met SPECT/CT en scintillatie detectoren. Omdat de botvorming in gang wordt gezet door de afgegeven groeifactor, gaven de opeenvolgende CT scans een goed beeld van de hoeveelheid bot, die over de 8 weken periode werd gevormd. Uiteindelijk kan worden geconcludeerd, dat de meetopzet met de scintillatie detectoren en de SPECT/CT betrouwbare methoden zijn om de afgifte van radioactief gelabelde groeifactoren uit een biomateriaal voor botregeneratie te bepalen.

Door middel van een radioactief label kan een *in vivo* afgifteprofiel worden gemeten. Omdat dit geen informatie geeft over de bioactiviteit van de groeifactor na afgifte, wordt in **hoofdstuk 8** de meting van *in vitro* en *in vivo* bioactiviteit van BMP-2 beschreven, nadat deze is vrijgekomen uit een biomateriaal. Er zijn vier soorten materialen getest: 1) een gelatine hydrogel, 2) PLGA micropartikelen in een gelatine hydrogel, 3) PLGA micropartikels in een PPF matrix, 4) PLGA micropartikels in een PPF matrix omringd door een gelatine hydrogel. *In vitro* was de snelheid, waarmee BMP-2 vrijkwam, verschillend. Gedurende 12 weken werd de bioactiviteit van de vrijgekomen groeifactor bepaald, waarbij alleen na 6 weken een reductie in activiteit kon worden gemeten bij BMP-2 afkomstig uit gelatine hydrogels. Bij de overige materialen bleef BMP-2 activiteit aantoonbaar gedurende de volledige 12 weken. Om de *in vivo* activiteit te meten werden de materialen onderhuids geïmplanteerd in ratten. Bij het meten van de *in vivo* afgifte veranderde het afgifteprofiel volledig, waarbij de groeifactor sneller werd afgegeven ten opzichte van *in vitro*. Hoewel er in alle materialen bot werd gevormd, verschilde de hoeveelheid bot in de vier materialen significant. De afgifte van BMP-2 uit PLGA micropartikels in een PPF matrix resulteerde in de grootste hoeveelheid nieuw gevormd bot.

In tegenstelling tot de vorige studies waarbij één enkele groeifactor is afgegeven, wordt botvorming normaliter gereguleerd door een grote hoeveelheid groeifactoren en cytokines. Daarom is het effect van combinaties van groeifactoren op botvorming onderzocht en beschreven in het derde deel van dit proefschrift. De eerder opgedane kennis over de BMP-2 afgifte uit verschillende materialen was een goede basis om een biomateriaal met complexer afgifteprofiel voor 2 groeifactoren te ontwikkelen. Hieraan voorafgaand is eerst een literatuurstudie gedaan naar het effect van combinaties van groeifactoren op botvorming. **Hoofdstuk 9** geeft een overzicht van de geteste groeifactor combinaties in translationele botregeneratie studies. Ondanks een beperkt aantal studies in de literatuur, resulteerde de combinatie in de meeste gevallen in een additief of synergetisch effect ten opzichte van de groeifactoren apart. Slechts in enkele gevallen was het effect van de combinatie niet significant of remmend. Van de verschillende geteste combinaties zijn 2 interessante combinaties gekozen, die nader zijn bestudeerd.

De eerste combinatie is vascular endothelial growth factor (VEGF) en BMPs. VEGF stimuleert de vorming van capillairen uit bestaande vaten. Deze nieuwe vaten zijn cruciaal voor de ingroei van cellen en de aanvoer van voedingsstoffen tijdens de botvorming. Gezien het belang van vroege vaatvorming tijdens botvorming, is de combinatie BMP-2 en VEGF onderzocht en in **hoofdstuk 10** beschreven. Om de natuurlijke expressie van deze groeifactoren tijdens botvorming na te bootsen, zijn BMP-2 geladen micropartikels geïncorporeerd in PPF, welke vervolgens zijn omringd door een VEGF geladen gelatine hydrogel. De implantaten zijn onderhuids en in het femurdefect in ratten ingebracht gedurende 8 weken. Het bleek dat tijdens het meten van de afgifteprofielen, VEGF snel vrij kwam uit het biomateriaal tijdens de eerste 2 weken, terwijl daarnaast BMP-2 gedurende de volle 8 weken werd afgegeven. Dit resulteerde in stimulatie van vaat- en botvorming in respectievelijk de VEGF en BMP-2 bevattende onderhuidse implantaten. Tevens was er meer botvorming in de implantaten die beide groeifactoren bevatten ten opzichte van implantaten met alleen BMP-2. Ondanks dat de trend in de femurdefecten hetzelfde was, bleek de hoeveelheid bot in de defecten met de VEGF en BMP-2 bevattende implantaten niet significant meer te zijn dan die met alleen BMP-2.

Een tweede interessante combinatie is parathyroid hormoon (PTH) met BMPs. PTH is één van de belangrijkste systemische regulatoren van het bot metabolisme. Vanwege de anabolische effecten van intermitterende PTH toediening op bot wordt dit hormoon momenteel gebruikt voor de behandeling van patiënten met ernstige osteoporose. Omdat PTH ook mogelijk de door BMPs gestimuleerde botvorming kan bevorderen, wordt deze combinatie in **hoofdstuk 11** beschreven. De BMP bevattende biomaterialen zijn wederom onderhuids en in femurdefecten in ratten geïmplanteerd. PTH is dagelijks eenmalig subcutaan toegediend. Zoals verwacht, resulteerde de locale BMP-2 afgifte in onderhuidse botvorming en bijna volledige genezing van de femurdefecten. Ondanks dat de totale botdichtheid (gemeten in de wervelkolom en humerus) toenam, was PTH op zichzelf niet in staat om subcutane botvorming te initiëren en had het geen significant effect op de botgroei in de femurdefecten. Echter in combinatie met BMP-2 resulteerde het intermitterend toegediende PTH in significant grotere botdichtheid en groter botvolume in zowel de subcutane implantaten als de femurdefecten.

Alles bij elkaar tonen de resultaten van het proefschrift aan dat polymeren veelbelovend zijn voor de locale afgifte van groeifactoren in botregeneratie. De van polymeer vervaardigde micropartikels zijn in staat een groeifactor lokaal af te geven gedurende een langere periode waarbij de bioactiviteit van de groeifactor behouden blijft. Daarnaast biedt de grote variëteit in polymeren de mogelijkheid om het afgifteprofiel van groeifactoren te veranderen. Door polymeren met verschillende bindingseigenschappen van groeifactoren te combineren is het zelfs mogelijk om een biomateriaal te creëren, waaruit twee groeifactoren met een verschillende snelheid vrijkomen. Aangezien er nog weinig bekend is over de effecten van groeifactorcombinaties op botregeneratie, zijn dit soort samengestelde biomaterialen uitermate geschikt om hier verder onderzoek naar te doen. Door de polymeereigenschappen te variëren kunnen verschillende afgifteprofielen worden vergeleken. Dit zal helpen de ideale timing, ratio en volgorde van de gecombineerde groeifactorafgifte te bepalen waardoor uiteindelijk efficiënter gebruik kan worden gemaakt van groeifactoren in toekomstige klinische toepassingen.

Acknowledgements

I would like to thank my (co-)promotors Wouter Dhert, Michael Yaszemski, Laura Creemers and Lichun Lu. You opened the worlds of science and orthopedic research for me. I would not have been able to do this without your advice. Thank you for your guidance and support from the early stage of this research project as a medical student, as well as providing the opportunity to pursue my PhD and orthopedic residency through the Agiko program. Your encouragements and criticism have helped to improve the quality of the research and has enriched my growth as a student towards scientist.

This thesis could not have been written without the help and support of many people. I would like to express my deep gratitude for their help with this project. Especially the following people have contributed, directly or indirectly, to great extend to this thesis:

Jacqueline Alblas
Al Amundson
Patricia Beighley
Jason Britson
Julie Burgess
Prof. René Castelein
Jon Charlesworth
Kelly Classic
Prof. Bradford Currier
Mahrokh Dadsetan
Teresa Decklever
Diyar Delawi
Anthony Florschutz
Patricia Friedrich
James Greutzmacher
Theresa Hefferan
Andras Heijink
Yvonne van der Helm
James Herrick
Teresa Hoff
Esmaiel Jabbari
Bradley Kemp
Choll Kim
Jinku Kim
Moyo Kruyt
Rodney Landsworth
Dirk Larson
Avudaiappan Maran
Prof. Cumhur Öner
Larry Peterson
Mattie van Rijen
Prof. Erik Ritman
Prof. Daniël Saris
Suzanne Segovis
Kris Shogren
James Tarara
Prof. Abraham Verbout
Andrew Verknocken
Sylvia Visser
Shanfeng Wang
Paul Westers
Clayton Wilson
Xun Zhu

my fellow PhD-students,

my parents in law, the Ankringa family

my parents and brothers Pieter and Steven. Thank you for your endless support and the opportunity to pursue my dreams.

and last, but not least, Nynke! Thank you for your love, support and tremendous patience for putting up with me and my laptop during all these years. Without you, I would not have been able to finish this thesis.

Curriculum Vitae

The author of this thesis was born on April 12, 1978 in Delft, The Netherlands. In 1996 he graduated from high school (VWO, Sint Stanislas College, Delft) and started to study medicine at the University of Utrecht. In 2000, he joined two research projects as a student at the department of orthopaedics (supervisor: prof. dr. W.J.A. Dhert and dr. L.B. Creemers) of the University Medical Center Utrecht. Before starting his rotations, he joined the 'Tissue Engineering and Polymeric Biomaterials Laboratory' (supervisors: prof. dr. M.J. Yaszemski and dr. L.Lu) at the department of orthopedic surgery of the Mayo Clinic for 6 months in 2001 and started studying growth factor release from polymer composites for bone regeneration. After receiving his Medical Degree in 2003, he started working at the department of orthopedic Surgery (head: dr. W.J. Willems) of the Onze Lieve Vrouwe Gasthuis. During this year, he wrote a proposal for an AGIKO scholarship which was granted by ZonMW and allowed him to continue his research work in 2004 at the orthopaedic departments of the UMC Utrecht and Mayo Clinic. In October 2007 he started his surgical training at the Deventer Hospital (head: dr. M. Eeftinck Schattenkerk) as part of his orthopaedic training. He continued his orthopaedic residency working for 1 year at the OLVG and the Antonius Hospital (head: dr. M.R. Veen). He is currently working as a resident at the University Medical Center Utrecht (head: prof. dr. D.B.F. Saris) after which he will return to the OLVG to complete his orthopaedic residency in 2013.